UNIVERSITY OF SOUTHAMPTON

FACULTY OF NATURAL AND ENVIRONMENTAL SCIENCES

School of Ocean and Earth Science

Volume 1 of 1

MICROBIAL COMMUNITIES IN SINKING AND SUSPENDED PARTICLES AND THEIR INFLUENCE ON THE OCEANIC BIOLOGICAL CARBON PUMP

by

Manon T Duret

Thesis for the degree of Doctor of Philosophy

October 2018

Manon T Duret

MICROBIAL COMMUNITIES IN SINKING AND SUSPENDED PARTICLES AND THEIR INFLUENCE ON THE OCEANIC BIOLOGICAL CARBON PUMP

Supervised by:

Dr. Phyllis Lam, Prof. Richard Lampitt, Prof. Thomas Bibby

Je dédie ce travail à ma mère pour son amour et soutien inconditionnel qui m'ont toujours poussé à depasser mes limites.

Merci de croire en moi Maman. Je t'aime.

ABSTRACT

UNIVERSITY OF SOUTHAMPTON
FACULTY OF NATURAL AND ENVIRONMENTAL SCIENCES
School of Ocean and Earth Science
Thesis for the degree of Doctor of Philosophy

MICROBIAL COMMUNITIES IN SINKING AND SUSPENDED PARTICLES AND THEIR INFLUENCE ON THE OCEANIC BIOLOGICAL CARBON PUMP

Manon T Duret

Export of photosynthetically produced organic matter, from the sunlit to the dark ocean, in the form of sinking particles represents the major mechanism of the biological carbon pump that removes CO_2 from the atmosphere. Most of the organic matter bound in sinking particles undergoes microbial remineralisation while traversing the water column, thereby causing CO_2 and inorganic nutrients to be released. Increasing evidence indicates that most remineralisation does not occur directly on sinking particles, but rather on suspended particles and dissolved organic matter resulting from their disaggregation and solubilisation. Most particulate organic carbon in the mesopelagic ocean is bound to suspended particles, which represent a major substrate for heterotrophic organisms. Despite their crucial importance, suspended particles and their associated microbial communities have been largely overlooked in favour to sinking particles. This thesis presents the first comparison of diversity and functionalities between microbial communities associated with suspended and sinking particles.

Using amplicon sequencing of small-subunit ribosomal RNA genes on particles collected with a marine snow catcher deployed in the Southern Ocean, this thesis demonstrates that prokaryotic communities associated with suspended and sinking particles differ significantly. Particle-associated remineralising bacteria showed a clear preference for either particle-type likely relating to differential organic matter composition. Suspended particles from the upper-mesopelagic were predominately composed of prymnesiophytes and soft-tissue animals, while more efficient carbon export from diatoms was indicated by their prevalence in sinking particles. Eukaryotic sequences associated with suspended and sinking particles were largely dominated by heterotrophic protists, highlighting their major contribution to particulate organic matter remineralisation in the upper-mesopelagic.

Finally, remineralisation activities, as well as nitrogen and sulphur cycling, were investigated by comparing metatranscriptomes of various particle-types collected in the North Atlantic. Free-living, small sinking and small suspended particle-associated microbes appeared most active in the remineralisation of simple organic compounds, while large suspended particles acted as the main venue of complex organic matter remineralisation. Additionally, actively expressed genes related to anaerobic processes in small particles corroborate recent postulations that marine particles may serve as oxygen-deficient microniches, and hence, may be key to redox cycling of elements in the ocean.

Overall, this dissertation highlights differences between suspended and sinking particles as well as their potential biogeochemical implications in the ocean and provides further insights into constraints shaping the oceanic biological carbon pump.

Table of contents

List of tables

List of figures

List of equations

List of appendices

Declaration of authorship

I, Manon Tiphaine Duret, declare that this thesis and the work presented in it are my own and has been generated by me as the result of my own original research.

MICROBIAL COMMUNITIES IN SINKING AND SUSPENDED PARTICLES

AND THEIR INFLUENCE ON THE OCEANIC BIOLOGICAL CARBON PUMP

I confirm that:

1. This work was done wholly or mainly while in candidature for a research degree at this University;
2. Where any part of this thesis has previously been submitted for a degree or any other qualification at this University or any other institution, this has been clearly stated;
3. Where I have consulted the published work of others, this is always clearly attributed;
4. Where I have quoted from the work of others, the source is always given. With the exception of such quotations, this thesis is entirely my own work;
5. I have acknowledged all main sources of help;
6. Where the thesis is based on work done by myself jointly with others, I have made clear exactly what was done by others and what I have contributed myself;
7. Part of this work have been published as:

   Duret, M. T., Lampitt, R. S. and Lam, P. (2018), Prokaryotic Niche Partitioning Between Suspended and Sinking Marine Particles. Environmental Microbiology Reports. doi:10.1111/1758-2229.12692

Signed: ...18 October 2018.....

Date: .....

Acknowledgements

Scientific Support

First and foremost, I would like to sincerely thank my principal supervisor and advisor, Dr. Phyllis Lam, for her continuous scientific support of my PhD research and other projects. I would also like to acknowledge her patience, her motivation, and her knowledge and enthusiasm for the marine microbial world. Her guidance has helped me to become a better scientist and to achieve this thesis.

I would like to thank Prof. Richard Lampitt for making my first research cruises some of the most enjoyable moments of my life, as well as for his precious scientific advice and his passion for marine particles. I would also like to thank Dr. Tom Bibby for his assistance in the formation of this work. I would also like to thank Dr. Adrian Martin who, as my panel chair, has offered me comfort and valuable advice over the course of my PhD.

I would like to give a special thanks to Dr. Jessika Füessel for offering me her scientific support and inputs when I needed. These really helped me move my thinking and research forward.

I would like to thank Dr. Alison Baylay for her help with the sequencing of my samples, her patience and her help. I would also like to thank Dr. Cynthia Dumousseaud for her help with the nutrients and dissolved organic nitrogen measurement analysis.

I would like to thank Dr. Anna Belcher, Chelsey Baker and Dr. Emma Cavan for their valuable help with the marine snow catcher deployment and sampling.

I would like to thank Dr. Marc Chapman, Dr. Sam Haldenby and Dr. Maria Pachiadaki for their inputs in the bioinformatics processing of my dataset.

Finally, I would like to thank everybody else who has helped me form this thesis.

Personal Support

It is a difficult task to list the people that have accompanied me in this journey in order of importance. Therefore, I would first like to state that you have all played a big role at some point, in many ways and in different aspects.

Pour commencer, je voudrais remercier ma maman et mes sœurs adorées, Anne-Flore et Chloé, pour leur soutien moral. Merci d'être toujours derrière moi quelle que soient les circonstances – je vous remercie du fond du cœur. Merci à toi Anne-Flore pour avoir

toujours été à mon écoute et pour m'avoir crié dessus quand j'en avais besoin. Tu avais raison. Je voudrais aussi remercier ma magnifique nièce Maxine. Merci à toi Chloé pour ta rationalité (et ton irrationalité) qui a toujours été très réconfortante. Malgré la distance, nous sommes devenues plus proches. Rock et Roll.

Je tiens à remercier ma grande amie, Dr. Poukette, que j'ai rencontré grâce à notre amour commun du plankton, même si ce n'est pas très malin de sa part. Elle avec ses satellites et moi avec mes acides nucléiques, nous formons le couple océanographique parfait.

Je voudrais aussi remercier mon ami d'enfance Clément, qui malgré le fait qu'il n'ait jamais bien compris ce que je faisais, m'a toujours soutenue inconditionnellement. Tes cartes postales hilarantes sont toujours d'un grand réconfort.

I would like to thank the people of the Office (164/25) – Cat, Dave, Rachael, and James (in alphabetical order). I could not have chosen better people to share an office with, and to become best friends with.
Cat (santéesque) and Rachael (xylophonesque) – thank you for your immense support and help with literally everything PhD (and non-PhD) related.
James – thank you for being such a caring person. I cannot thank you enough for the support you have provided me when I needed it the most.
Dave – **Hey Dave.**
I would also like to thank all the other people of the office for being really cool: Alanoud, Cristian and Sam (the OGs), as well as Callum, Roche and Sarah.

I would then like to especially thank Kyle for a lot of reasons. I want to thank him for being such a massive PL, a great scientist and housemate, and also for the many enthusiastic discussions we have shared about the origin of life, santé-euh, *Emiliania huxleyi*, sloth following their dreams, faecal pellets, Rupaul's dragrace, the remineralisation of organic matter and doge. He has also provided me with invaluable support. Now and forever, I am grateful to have you as my great friend, but also as my fellow researcher.

I would like to especially thanks Dr. Tom[esha] Chalk and Elwyn for opening their home and for being amazing human beings. It is an absolute pleasure to live with you two, and I have no intention of leaving. Thank you also for letting me dye your hair at the P-Palace.

Tali, I am very grateful to have met you, and you are my BFF.

I would like to thank the entire NOCS PhD and scientific community where I have met amazing people. Especially Maarten because he is funny, I love him and he likes Vitas. I would like to give a special thanks to my particle buddy Anna who is the ideal partner at sea. I would like to thank again Jessika for the chats and coffees, and for being there for

me until the end. Merci encore à Cynthia pour nos pauses café et nos papotages. I would like to thank Lucie and Chris for being amazing people. I would also like to thank the following people (without a particular order) that I have had the chance to meet in NOCS: Rob, Lisette, Erik, Luca, Matthias, Elena, Stu, Helen, Jaimie, Gavin, Tali, Sev, Vlad, Chelsey.

Finally, I would like to thank again Phyllis for offering me support in many other aspects than science, as well as my previous supervisors Ginny Edgcomb, Maria Pachiadaki, Dorothée Vincent and Alice Delegrange for being inspiring mentors and amazing woman scientists.

Financial Support

The work carried during this PhD was supported by the University of Southampton, the Graduate School of the National Oceanography Centre of Southampton and the National Environmental Research Council.

Abbreviations

AOA	Ammonia-oxidising archaea
AOB	Ammonia-oxidising bacteria
BCP	Biological carbon pump
CARD-FISH	Fluorescent catalysed reporter deposition in situ hybridisation
CCA	Canonical correspondence analysis
CO_2	Carbon dioxide
CTD	Conductivity-temperature-depth sensors
DCM	Deep chlorophyll maximum
DMS	Dimethylsulphide
DMSO	Dimethyl-sulphoxide
DMSP	Dimethylsulphoniopropionate
DNA	desoxyribonucleic acid
DNRA	Dissimilatory nitrate/nitrite reduction to ammonium
DOC	Dissolved organic carbon
DOM	Dissolved organic matter
FL	Free-living
HMW	High molecular-weight
HS_2^-	Sulphide
LMW	Low molecular-weight
MCP	Microbial carbon pump
MLD	Mixed layer depth
mRNA	Messenger RNA
MSC	Marine snow catcher
N_2	Dinitrogen gas
N_2O	Nitrous oxide
ncRNA	Non-coding RNA
NH_3	Ammonia
NH_4^+	Ammonium

NMDS	Non-parametric multidimensional scaling
NO	Nitric oxide
NO_2^-	Nitrite
NO_3^-	Nitrate
NOB	Nitrite oxidising bacteria
OMZ	Oxygen minimum zone
OTU	Operational taxonomic unit
PA	Particle-associated
PAP	Porcupine Abyssal Plain
PERMANOVA	Permutational multivariate analyses of variance
POC	Particulate organic matter
POM	Particulate organic matter
PON	Particulate organic nitrogen
POP	Particulate organic phosphorus
RNA	Ribonucleic acid
rRNA	Ribosomal RNA
RT-qPCR	Reverse transcription quantitative PCR
SIMPER	Similarity percentage analysis
SK10	Sinking particles > 10 µm
SO_3^{2-}	Sulphite
SO_4^{2-}	Sulphate
SS0.22	Suspended particles 0.22 – 10 µm
SS10	Suspended particles 10 – 100 µm
SS100	Suspended particles > 100 µm
TEP	Transparent exopolymer polysaccharide

Chapter 1: Introduction

1.1 Oceanic biological carbon pump

1.1.1 Overview of the oceanic carbon pump

The ocean has absorbed ~ 50 % of anthropogenic carbon dioxide (pCO_2) released in the atmosphere since the beginning of the industrial era (Sabine et al., 2004) and is currently taking up 2 Gt of carbon per year (Siegenthaler and Sarmiento, 1993), thereby buffering the Earth's climate and reducing the effect of increasing anthropogenic carbon emissions. Oceanic carbon uptake is facilitated by three distinct components: one physical and two biological. The former – known as the solubility pump, refers to the dissolution of CO_2 in surface waters and its subsequent transport to depth via thermohaline circulation. The solubility pump relies on the formation of cold, saline water in high latitudes (Volk and Hoffert, 1985). Stored CO_2 will eventually outgas again once the water parcel it was dissolved into upwells to the surface in warmer climatic conditions. Flux of CO_2 between ocean and atmosphere in time-scales of decades to several centuries is primarily driven by the solubility pump (Siegenthaler and Sarmiento, 1993).

In contrast, the biological carbon pump (BCP) is crucial when considering time-scales of centuries to millennia, as carbon stored through this mechanism has a much longer residence time in the ocean (Sarmiento and Gruber, 2006). The BCP corresponds to the production of biogenic carbon from atmospheric pCO_2 via phytoplankton photosynthesis, which then sinks out of surface waters to be sequestrated at depth (Fig. 1.1A). Two thirds of the carbon gradient existing in oceanic water columns is attributed to the BCP (Passow and Carlson, 2012).

The BCP is further subcategorised into two components: (i) the soft tissue pump, corresponding to the organic carbon generated by photosynthesis, and (ii) the carbonate pump whereby calcium carbonate ($CaCO_3$) is produced in the form of phytoplanktonic

mineral shells (Volk and Hoffert, 1985). The soft tissue pump exports ~ 10 times more carbon than the carbonate pump (Sarmiento et al., 2002), however mineral shells have the ability to ballast organic matter to depth (Klaas and Archer, 2002).

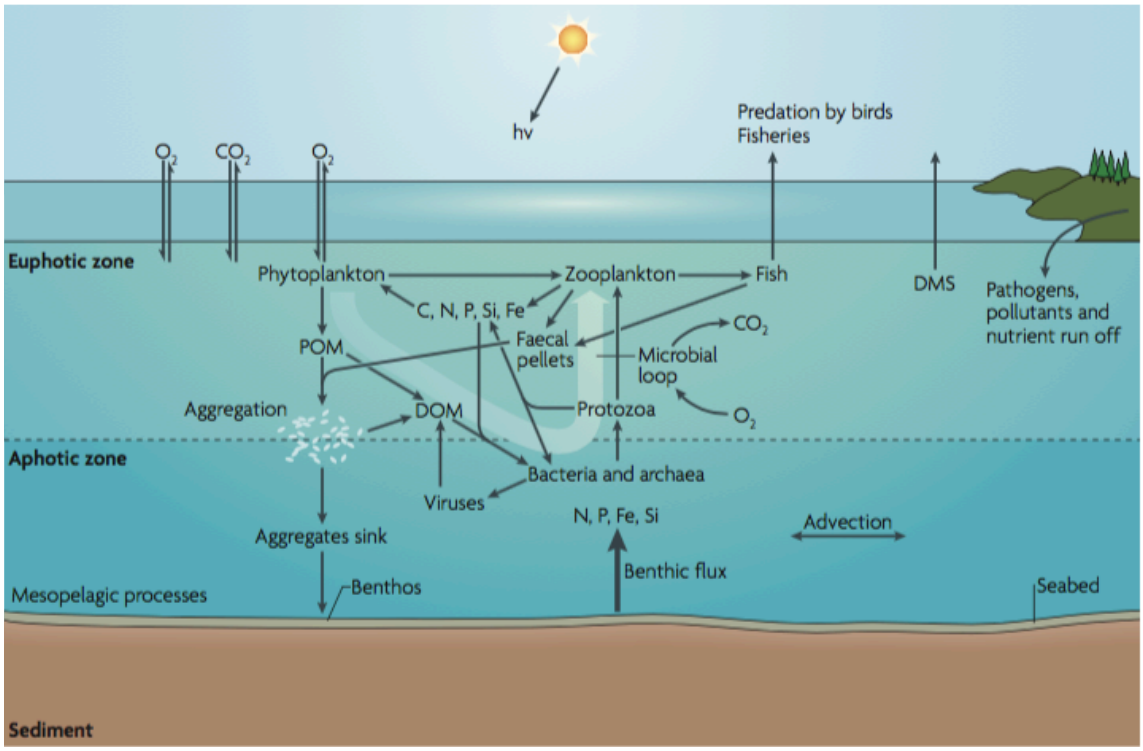

Figure 1.1A. Microbial structuring of marine ecosystems (from Azam and Malfatti, 2007). POM is generated by photosynthetic activity of phytoplankton in the euphotic zone (sunlit part of the ocean, generally ~ 0 to 100 m). A large portion of this organic matter becomes DOM via the activity of extracellular enzymes and is taken up almost entirely by bacteria as well as protists. Most of this DOM is remineralised (i.e., transformed into nutrients and CO_2) while a fraction is reintroduced into the classical marine food-web by microzooplankton grazing. DMS: dimethylsulfide; hv: light.

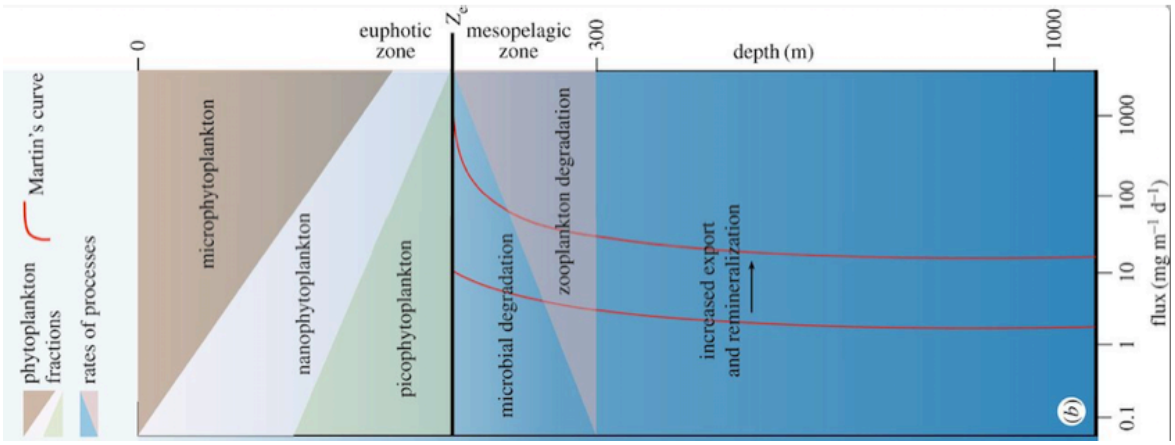

Figure 1.1B. Representation of the oceanic biological carbon pump (from Benoiston et al., 2017). Processes affecting the decrease of sinking particles flux are represented with area span reflecting the relative importance of phytoplankton fractions or processes rate.

1.1.2 The biological carbon pump

Inorganic atmospheric carbon is dissolved in surface waters and fixed into organic matter by photosynthetic organisms, using mostly inorganic nutrients as substrate within the euphotic zone, where light levels are sufficient to support photosynthesis (generally 0 to ~ 100 m) (Reinfelder, 2011). Due to its high turnover rates, phytoplankton is responsible for ~45 % of global primary production, although it only represents 1 % of the land's photosynthetic biomass (Field et al., 1998). The organic matter produced by phytoplankton can be in the form of (i) particulate organic matter (POM) as biomass (living phytoplanktonic cells) and (ii) dissolved organic matter (DOM) released as secretions (Fig. 1.1A). POM and DOM are operationally differentiated by size – POM being traditionally defined as anything retained on a 0.2 µm pore-size filter (Verdugo et al., 2004).

This primary production forms the base of all oceanic life. It is the base of marine food-webs and can follow different trophic routes, including the classic phytoplankton-copepod-fish (Ryther, 1969) and the microbial loop (Pomeroy, 1974). The microbial loop reintroduces DOM and inorganic nutrients into the classical food-web by incorporating them into microbial biomass that can be subsequently consumed by larger organism. Marine microbes include unicellular organisms (phytoplankton or photosynthetic microbes, heterotrophic protists, bacteria, archaea and fungi) and viruses. Within the microbial loop, phytoplanktonic biomass can be grazed on by microzooplankton (20 – 200 µm hetero- and mixotrophic protists) or nanozooplankton (2 – 20 µm) depending on prey cell-size. Phytoplankton can also be lysed by viruses (Suttle, 2005) and the organic matter produced by lysis can be consumed by heterotrophic prokaryotes (Azam and Hodson, 1977) and/or small protists, which in turn can sustain larger organisms. Alternatively, phytoplankton cells can also become inactive due to nutrient and light-limitation (Azam et al., 1983). These processes, and every interaction along the food-web, lead to a change in nature and composition of organic matter and is responsible for the production of DOM and POM different from the original phytoplanktonic biomass (e.g., phytodetrital aggregates, faecal pellets). Microbes dominate several trophic levels and are major actors

in the complex interactions taking place between members of marine ecosystems (Azam and Malfatti, 2007).

Part of the organic matter produced will be consumed and remineralised (transformed back into CO_2 and inorganic nutrients) in the euphotic zone by heterotrophic organisms, thereby supporting recycled primary production – as opposed to new primary production supported by upwelled nutrients and nitrogen fixation by diazotrophs (Dugdale and Goering, 1967). The rest of the organic matter will be exported to the mesopelagic zone, where light levels are insufficient to support photosynthesis (~ > 100 - 1000 m) (Ducklow et al., 2001; Volk and Hoffert, 1985). This exported organic matter is the motor of the biological carbon pump which annually removes more than 10 billion tons of carbon from the euphotic zone (Buesseler and Boyd, 2009). The microbial carbon pump (MCP) is a complementary mechanism to the classic BCP and corresponds to microbial production of recalcitrant DOM (DOM with lifetime > 100 years) from labile organic matter throughout the water column (Jiao et al., 2010). The MCP is estimated to store ~ 0.4 % of the annual primary production (Legendre et al., 2015).

This organic matter can be exported from the euphotic to the mesopelagic zone via three processes (Fig. 1.2):

(i) The export of POM, which can vary substantially in size, ranging from phytoplankton single-cell to aggregates > 500 µm or marine snow.
(ii) The export of organic matter as a result of physical vertical mixing of the water column, caused for instance by winds.
(iii) The diel migration of mesozooplankton (metazoans such as copepods), which graze in the euphotic zone and release POM (faecal pellets) and DOM in the mesopelagic zone and throughout their journey (Steinberg et al., 2000).

The main channel for the export of organic matter to the mesopelagic is the sinking of particles out of the euphotic zone. It is the focus of this introductory chapter.

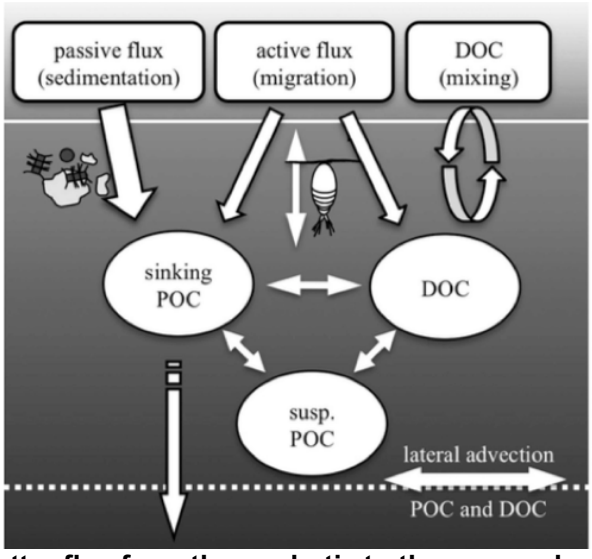

Figure 1.2. Organic matter flux from the euphotic to the mesopelagic zone (from Arístegui et al., 2009). Three interconnected pools of organic carbon are indicated: dissolved organic carbon (DOC), sinking particulate organic carbon (sinking POC) and suspended particulate organic carbon (susp. POC). DOC and POC are susceptible to lateral transport. The flux of carbon from the epipelagic to the dark ocean can be caused by passive sedimentation of POC, vertical mixing of DOC, or active transport of DOC and POC mediated by migrant zooplankton. The euphotic zone is represented above the full line, the mesopelagic zone between the full and dashed lines and the bathypelagic zone below the dashed line.

1.1.3 Particle remineralisation

Depending on the attenuation depth or remineralisation length scale, which is the depth reached by sinking particles, carbon will be sequestrated for different periods of time (Kwon et al., 2009). From the carbon sinking out of the euphotic zone, referred to as export flux, only a fraction will leave the mesopelagic zone and reach the deep sea (~ 2000 m), referred to as sequestration flux. The sequestration flux leads to carbon sequestration time > 100 years (Passow and Carlson, 2012). The sequestration flux is largely determined by particle attenuation, which is in turn primarily influenced by the remineralisation processes occurring in the mesopelagic ocean. The BCP is quite inefficient as there is an exponential attenuation of particle flux with depth (Martin et al., 1987) (Fig. 1.1B). Depending on the oceanic region (Henson et al., 2012; Buesseler et al., 2007b), only ~ 5 to 25 % of primary production is exported out of the euphotic zone (De La Rocha and Passow, 2007) and even less reaches the deep sea (Francois et al., 2002).

Therefore, around 97 % of the primary production is remineralised (Turner, 2015). Most of this remineralisation occurs in the euphotic and upper-mesopelagic zones.

POM production defines the strength of the BCP (Guidi et al., 2009), while the efficiency of the BCP is mainly influenced by the activities and structure of heterotrophic communities (including zooplankton and heterotrophic microbes) below the euphotic zone. Although the quantity of POM processed by heterotrophic members varies widely between oceanic regions (Ducklow et al., 2001), heterotrophic microbes have been measured (Cho and Azam, 1988; Kiørboe and Jackson, 2001; Smith et al., 1992; Collins et al., 2015; Karl et al., 1988) and modelled (Buesseler et al., 2007b; Anderson and Tang, 2010) to be responsible for most POM remineralisation compared to zooplankton. For instance, at the Porcupine Abyssal Plain (PAP) site, heterotrophic prokaryotes were estimated to remineralise 70 to 90 % of POM, while mesozooplankton were estimated to process ~ 50 % of sinking particles (by causing their disaggregation, see section 1.3.5) (Giering et al., 2014). Both members carry different direct and/or indirect roles in remineralisation processes (Fig. 1.3).

Sinking particles can be remineralised by a combination of the following pathways (Fig. 1.4) (Collins et al., 2015):

(i) Direct respiration of POM by microbial communities associated with sinking particles, leading to release of CO_2 and inorganic nutrients.
(ii) Solubilisation of POM into DOM by sinking particle-associated microbial communities and mesozooplankton mechanical disaggregation, which is subsequently respired by free-living microbial communities.
(iii) Disaggregation of sinking particles into suspended particles, which can then be:
    a. Respired by microbial communities associated with suspended particles and/or,

b. Solubilised into DOM by suspended particle-associated communities or mesozooplankton, which is subsequently respired by free-living microbial communities.

These biological processes, coupled with abiotic processes, are responsible for dynamic exchanges between sinking and suspended POM and DOM pools, thereby shaping organic matter availability in the ocean.

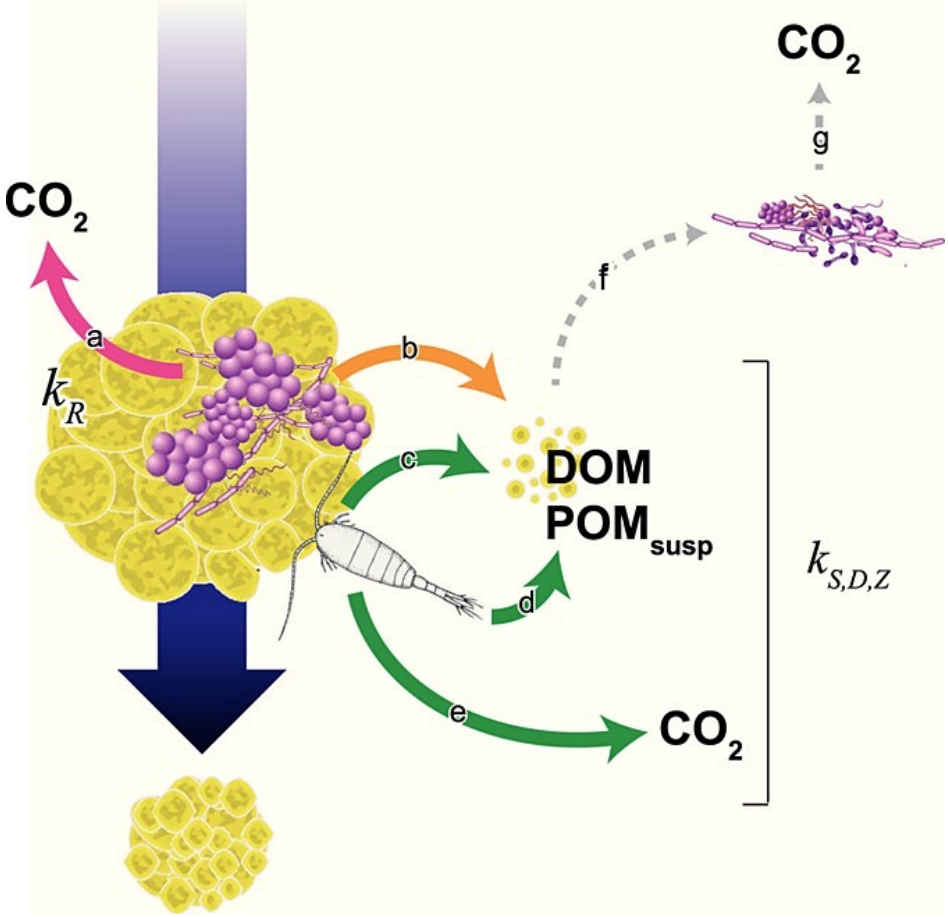

Figure 1.3. Schematic of major processes removing sinking particles in the mesopelagic ocean (from Collins et al., 2015). k are rate constants (d^{-1}) attributed to the various sinking particle attenuation processes presented by the arrows. Arrow a (magenta): respiration of sinking particles by sinking particle-associated heterotrophic bacteria. Arrow b (orange): enzymatic solubilization or mechanical disaggregation of sinking particle-associated bacteria. This process transfers organic matter to dissolved and/or suspended phases in surrounding waters, where free-living bacterial communities (arrows f and g, dashed) can metabolize it. Arrows c–e (green): particle flux attenuation processes attributable to mesozooplankton, including (arrow c) mechanical disaggregation (sloppy feeding), (arrow d) egestion or excretion, or (arrow e) direct respiration of material to CO_2. Disaggregation and excretion can transfer particle material to the DOM and/or suspended phases; egestion of smaller faecal pellets can also transfer material to the suspended organic matter pool.

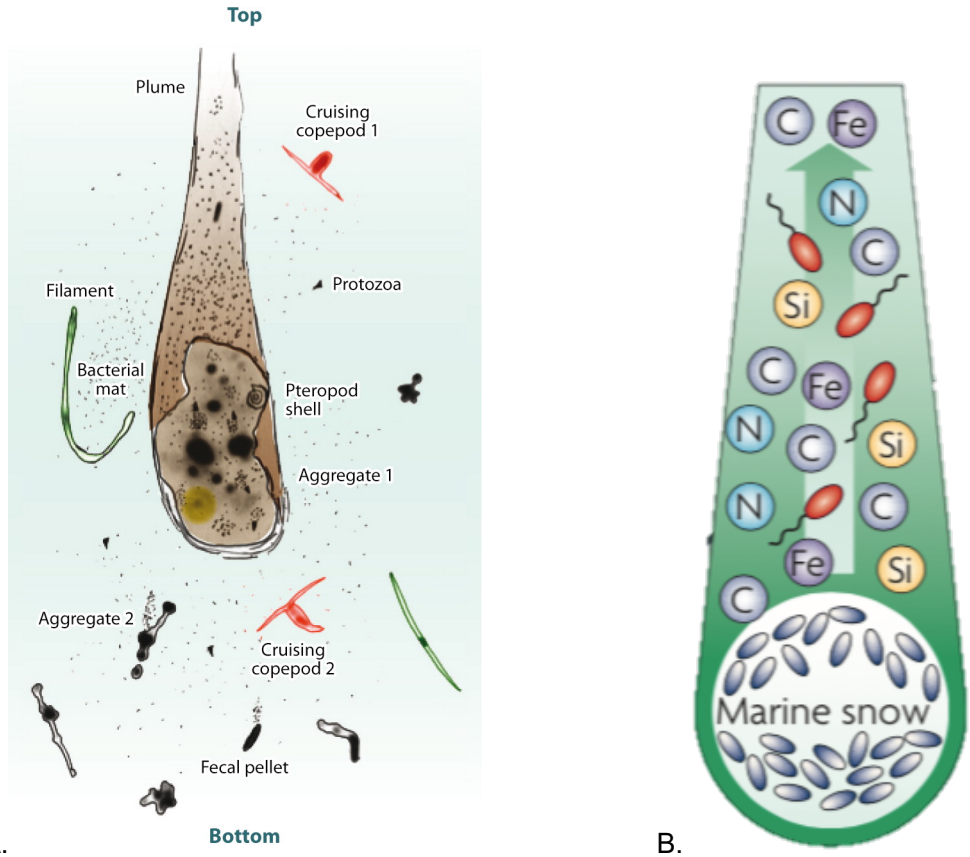

Figure 1.4A. Modified image of a sinking aggregate (from Stemmann and Boss, 2012).

Figure 1.4B. Conceptual vision of microbial communities associated with marine snow (from Azam and Malfatti, 2007). Marine snow is highly colonised by bacteria, presumably because it is formed from pre-colonised surface particles transporting elements including carbon, nitrogen, phosphorus, iron and silica into the ocean's interior. The high hydrolytic enzyme activities of bacteria convert POM into suspended DOM forming a plume. Free-living bacteria that are attracted to such DOM-rich hot spots respire organic carbon to CO_2 and their biomass production feeds into the pelagic food-web.

1.2 Marine particles overview

1.2.1 Operational definition

Particles are operationally defined as anything retained on a 0.2, 0.45 or 0.7 µm pore-size filter – the latter especially used as nominal pore-size for GF/F filter which is commonly used to quantify particulate organic carbon (POC) and particulate organic nitrogen (PON). Therefore, the size-range of particles spans from submicron scales (Wells and Goldberg, 1994) to macroscopic scales (µm to cm) (Alldredge and Silver, 1988) and particles exist in a continuous size-spectrum (Verdugo et al., 2004) (Fig. 1.5).

Nonetheless, particles have been historically subcategorised into macroparticles or marine snow (> 500 µm, visible with the naked eye), microparticles (500 – 1 µm) and submicron particles (1 – 0.1 µm) (Simon et al., 2002). Hence, particles can be composed of a wide variety of components, ranging from giant viruses to mammalian carcasses (Andersen et al., 2016).

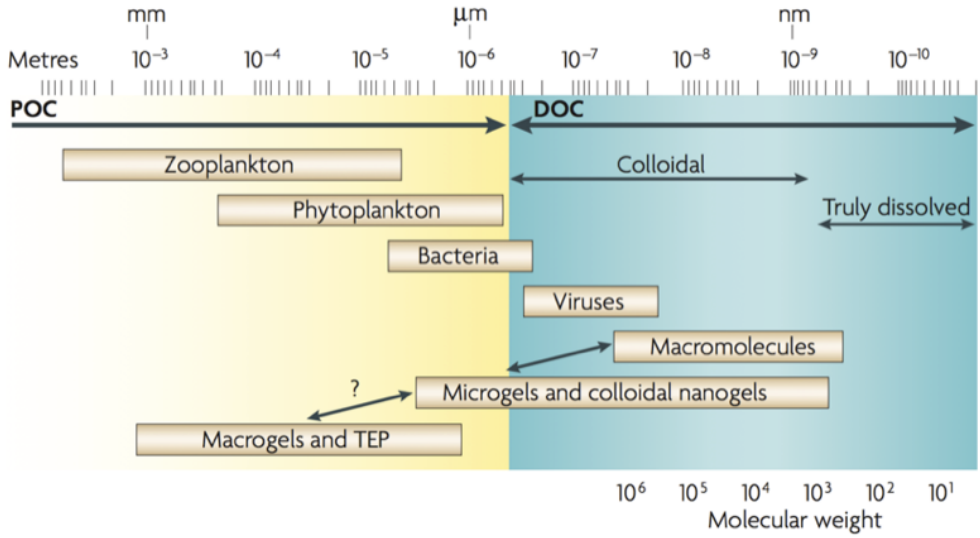

Figure 1.5. Size-range of organic matter (from Azam and Malfatti, 2007). The full-size range of organic matter is shown, from monomers, polymers, colloids and gel particles to traditional particles (divided into POC and DOC). These organic nutrient pools form an intricate three-dimensional architecture of polymers, colloids, gel particles and large aggregates. The organic matter architecture provides the spatial context within which microbes interact with each other and with the environment.

1.2.2 Particle composition and variability

Particle components include, but are not limited to, a combination and/or aggregation of various materials such as mesozooplankton faecal pellets, living and non-living phytoplanktonic cells and fragments, empty larvacean houses and live microbial cells (Alldredge and Silver, 1988; Simon et al., 2002; Stemmann and Boss, 2012). Along with their size, the morphology of particles can vary widely (Fig. 1.6).

Mesozooplankton faecal pellets are a repackaged and condensed form of smaller materials (e.g., phytoplankton cells, dinoflagellates) as they are surrounded by a

membrane (Ebersbach et al., 2011), thereby providing them enhanced protection against remineralisation.

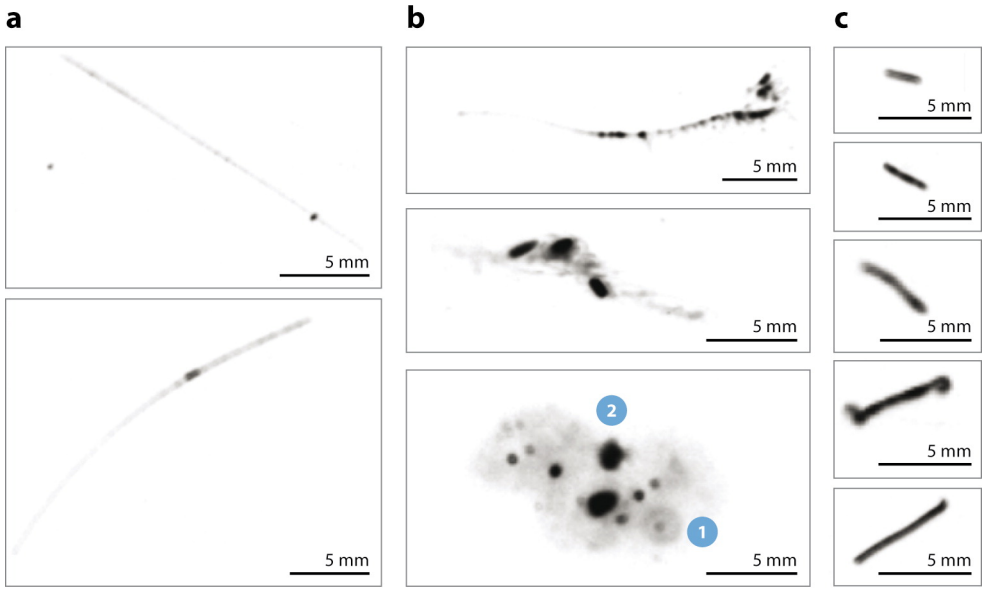

Figure 1.6. Examples of 3D holographic photograph of particles (from Stemmann and Boss, 2012). (a) Elongated particles, possibly diatom chains. (b) Different types of aggregates (1, radiolarian organism; 2, small opaque particles embedded in the aggregate matrix). (c) cylindrical particles possibly consisting of mesozooplankton faecal pellets.

Marine snow describes large aggregates (≥ 500 µm) of different kinds of materials, including those listed above. They are entities containing materials that are bound together by transparent exopolymer polysaccharides (TEP) (Alldredge et al., 1993). TEP are sticky carbon-rich molecules ranging from 1 to 100 µm in size and are a key driver of POM export to the mesopelagic ocean as they are the matrix forming most aggregates (Mari et al., 2017). They are produced by phytoplankton and bacteria, and can be found at high concentrations in oceanic waters (Passow et al., 2001).

Although most particle components originate, directly or indirectly (Fig. 1.1A), from phytoplankton primary production in the euphotic zone, some can derive from prokaryotic chemolithoautotrophic production. Chemolithoautotrophs use reduced inorganic compounds as an energy source and CO_2 as carbon source for the production of biomass (Anantharaman et al., 2013). They are considered of particular importance as a source of labile organic matter in meso- and bathypelagic waters (> 1000 m) (Arístegui et al., 2009). Nonetheless, little is known regarding their factual contribution to POM production in the

ocean, and especially in the euphotic zone as most studies have been conducted in the dark ocean.

Particle composition depends primarily on the structure of phytoplankton community in the euphotic zone (e.g., dominated by diatoms or prymnesiophytes), which itself is influenced by the oceanic region and season (Turner, 2015). The physiological state of the phytoplankton community also influences particle composition, with senescent phytoplankton cells and those in exponential growth producing drastically different organic matter (Bjornsen, 1988; Biddanda and Benner, 1997; Buchan et al., 2014). Particle composition also varies with sampling depth (Sheridan et al., 2002).

1.2.3 Chemical composition

Particles are composed of a heterogeneous mix of chemical components of different nature depending on their origin:

(i) Biogenic corresponding to materials of organic origin.

(ii) Authigenic corresponding to inorganic materials, which can be:

   a. Produced by certain phytoplankton for the construction of mineral shells, such as coccoliths ($CaCO_3$) synthesised by coccolithophores and opals (silicate) synthesised by diatoms (Reinfelder, 2011). When contained in particles, this material serves as ballast (Turner, 2015).
   b. Originated from coastal runoff by lateral transport (Jeandel et al., 2015).
   c. Originated from aeolian dust deposition in oceanic region under the influence of desert winds (Iversen and Ploug, 2010).

POM is constituted by a wide range of organic molecules including particulate organic carbon (POC), particulate organic nitrogen (PON), particulate organic phosphorus (POP) and other minor elements. The organic compounds included in POM may exist in the form of proteins, polysaccharides, fatty acids and nucleic acids. The former two are the main contributors to POM, especially in the euphotic zone (Teeling et al., 2012; Hwang and

Druffel, 2003; Fernandez et al., 1992; Van Rijssel et al., 2000). In addition, POM also consists of hundreds of different chemical compounds that remain largely uncharacterised (Moran et al., 2016).

1.3 Sinking and suspended particles

1.3.1 Categorisation by sinking velocity

Other than by their composition, particles can be categorised by their sinking velocity. They can be theoretically subdivided into two categories (Lam and Marchal, 2015):

(i) Sinking particles, which constitute most of the POM flux to the deep ocean. They are rare out of the euphotic zone as they have relatively short residence times in the water column.
(ii) Suspended particles, which bound the majority of organic carbon in the ocean and have long residence times (months to years).

Although this dual classification is a simplification, it complies with the current operational definition and sampling methodologies used to collect sinking and suspended particles (McDonnell et al., 2015b).

Stokes' law defines the sinking velocity of a particle in water. It is derived from the buoyancy force and the viscous drag of a particle. It is proportional to the size and density of particles (Lam and Marchal, 2015) and increases in warmer water (Bach et al., 2012).

Suspended particles are defined by a state of neutral buoyancy. Sinking velocity of marine snow aggregates ranges from 10 to 1000 m d^{-1} (Armstrong et al., 2002; Alldredge and Silver, 1988) and from 30 to 1500 m d^{-1} for faecal pellets, depending on the mesozooplankton species (Atkinson et al., 2001; Giesecke et al., 2010). Sinking velocity of particles increases if they contain mineral ballast (Ploug et al., 2008; Iversen and Ploug, 2010).

1.3.2 Carbon content and role as substrate

The concentration of sinking particles at a certain depth (C) is linked with the downward particle flux (F) and their sinking rate (w), by F= C * w (McDonnell et al., 2015a). Regardless of oceanic region, the POC concentration of sinking particles diminishes with depth, most times exponentially (Martin et al., 1987), as particles are remineralised thereby resulting in attenuation of the particle flux (Fig. 1.1B). In comparison, POC concentration of suspended particles is relatively constant with depth and at one to two orders of magnitude higher than that of sinking particles (Bacon et al., 1985; Riley et al., 2012; Baker et al., 2017; Cavan et al., 2017; Giering et al., 2014; Verdugo et al., 2004; Bishop et al., 1977; Baltar et al., 2009, 2010).

The downward flux of POC from the euphotic zone has been estimated to be insufficient to satisfy the carbon demand of heterotrophic organisms in the mesopelagic (Boyd et al., 1999; Reinthaler et al., 2006; Steinberg et al., 2008; Baltar et al., 2009). Additionally, low microbial respiration rates have been measured on sinking particles from the mesopelagic of different oceanic regions (Belcher et al., 2016b, 2016a; Cavan et al., 2017). In the mesopelagic zone, suspended particles have been suggested as a complementary organic carbon substrate to sinking particles for microbes (Baltar et al., 2009, 2010; Arístegui et al., 2009), and also for metazoans (Gloeckler et al., 2017). This is in agreement with deep water oxygen deficits associated with suspended particles (Bochdansky et al., 2010). In the subtropical northeast Atlantic, suspended particles accounted for up to 60 % of carbon demand in the upper-mesopelagic (Alonso-González et al., 2009).

1.3.3 Organic matter composition

The two most important components of sinking particles are marine snow (Shanks and Trent, 1980) and mesozooplankton faecal pellets (Turner, 2015). They are generally the main constituents of the particle flux leading to the rapid export of POM from the euphotic

zone (Ebersbach and Trull, 2008). Conversely, most suspended particles result from the fragmentation of sinking particles (Lam and Marchal, 2015) (Fig. 1.2). They may also be the product of self-assembled DOM and small POM – either laterally or vertically advected and from autotrophic *in situ* production – into buoyant microgels by adsorption on TEP (Baltar et al., 2010).

Although they are interconnected, suspended and sinking particles can have entirely different chemical signatures and compositions. In the North Pacific, suspended particles contained lipid biomarkers derived from phytoplankton and mesozooplankton, whereas sinking particles primarily contained lipids derived from mesozooplankton (Wakeham and Lee, 1989). Similarly, in the mesopelagic of the Mediterranean Sea, sinking and suspended particles presented radically different amino acid and pigment compositions (Abramson et al., 2010). These differences translate to the variability of the organic matter composition and lability present within suspended and sinking particles, as well as the necessity to better characterise the origins and evolution of organic matter in the two types of particle with depth.

1.3.4 Bioavailability

Lability is a measure of the biological availability of the organic matter. The bioavailability decreases as the lability decreases and the recalcitrance increases. Labile organic matter has lower carbon to nitrogen ratios (C/N) than recalcitrant organic matter, as nitrogen is preferentially consumed (Anderson and Sarmiento, 1994). The lability hence decreases as organic matter ages and with complexity of the chemical structure.

Theoretically, as suspended particles have a longer residence time in the water column than sinking particles, the latter should contain more labile organic matter than the former (Buesseler et al., 2007a; Wakeham et al., 2009; Riley et al., 2012). Small particles ($\leq 10^2$ µm) are generally as considered suspended while larger particles ($10^{2\text{-}4}$ µm) are considered to be sinking (Verdugo et al., 2004). Particle-size has been shown to be proportional to the lability of the organic matter they contain (Walker et al., 2016). For

these two reasons, suspended particles should contain more recalcitrant organic matter than sinking particles. However, based on existing observations, this theoretical principle does not hold true.

In the mesopelagic of the Eastern Tropical North Pacific Ocean, organic matter in suspended particles was more labile than in sinking particles (Druffel et al., 1998; Wakeham and Canuel, 1988; Repeta and Gagosian, 1984; Karl and Knauer, 1984). Furthermore, another study taking place in the same oceanic region found organic matter in suspended particles to be more labile than organic matter in sinking particles within the euphotic zone, while the opposite was true in the upper-mesopelagic (Sheridan et al., 2002). In the mesopelagic of the Mediterranean Sea, suspended particles were found to contain more labile compounds than sinking particles originated from fresh phytoplanktonic material (Abramson et al., 2010). This is likely due to the fact that particle dynamics are under the influence of many abiotic and biotic components.

More studies are needed to characterise the organic matter lability in other oceanic regions, as well as the evolution of C/N ratio with depth in order to understand the discrepancy between theoretical assumptions and measurements. It is noteworthy to mention that the above-mentioned studies are based on the assumption that suspended particles are smaller than sinking particles. This is not always the case as other parameters can influence the sinking velocity of particles (Lam and Marchal, 2015). The above-mentioned studies suggest that labile suspended particles in the mesopelagic originate from the disaggregation of rapidly sinking fresh material aggregates such as marine snow.

1.3.5 Particle dynamics

Sinking particles can be divided into two functional types: (i) fast-sinking particles, such as faecal pellets and ballasted marine snow, which do not interact much with the suspended particle pool, and (ii) slow-sinking aggregates, such as marine snow composed of fresh

algal materials, which actively participate in exchanges with the suspended particle pool (Ebersbach et al., 2011).

The amount of exchange between sinking and suspended particles therefore depends on the nature of sinking particles and subsequent particle dynamics between the two particle-pools (Lam and Marchal, 2015). Particle dynamics impact exchanges between sinking and suspended particles, their remineralisation and subsequently their chemical composition. Such processes can be:

(i) Abiotic, such as Brownian motion, laminar and turbulent shear which are caused by water movements.
(ii) Biotic, mainly led by heterotrophic members of the ecosystem.

When leading to the aggregation of particles, abiotic processes are referred to as physical coagulation. They cause particles of different sizes to collide together and form larger aggregates with higher sinking speeds (Burd and Jackson, 2009). The efficiency of this process depends on the velocity of particle collision and particle stickiness, which is directly related to original particles TEP concentration (Mari et al., 2017). Particle coagulation can also lead to formation of suspended particles by adsorption of DOM on TEP forming buoyant microgels. These processes can also lead to the disaggregation of sinking particles into smaller suspended particles (Burd and Jackson, 2009).

Biotic processes involved in particle dynamics are more complex than abiotic processes as they involve a wide range of organisms and interactions. Mesozooplankton and heterotrophic microbes are the main actors of biotic processes and play complementary roles in particle disaggregation/aggregation processes. Biotic aggregation processes occur from the ingestion of POM by mesozooplankton and its repackaging into faecal pellets (≥ 50 µm) (Stamieszkin et al., 2017). Microzooplankton can also lead to the formation of minipellets (3 – 50 µm) (Gowing and Silver, 1985), which also leads to creation of faster sinking particles.

Biotic disaggregation processes are mainly carried out by mesozooplankton (Strom et al., 1997) and microzooplankton (Poulsen and Iversen, 2008) feeding behaviours. Microzooplankton predate on bacteria associated with particles (Ploug and Grossart, 2000) while mesozooplankton can feed directly on sinking aggregates or on associated microzooplankton, thereby causing the release of DOM and smaller suspended particles (Fig. 1.3). This process is known as sloppy feeding. It has also been suggested that mesozooplankton purposefully break-down large sinking particles into suspended particles in order to promote bacterial colonisation, and thus enhance particles nutritional value. This process is known as microbial gardening (Mayor et al., 2014). Other heterotrophic microbes (bacteria and picozooplankton) remineralising activities can also lead to particle disaggregation.

The extent of sinking particle disaggregation caused by heterotrophic microbes is unknown. Nonetheless, it is ultimately these organisms that are responsible for most of the final remineralisation steps which are the release of CO_2 and inorganic nutrients (Cho and Azam, 1988; Kiørboe and Jackson, 2001; Smith et al., 1992; Collins et al., 2015). Bacteria have indeed been modelled to respire > 70 % of POC (Buesseler et al., 2007b; Anderson and Tang, 2010; Giering et al., 2014) while microzooplankton have been measured to respire up to 50 % of POC in sinking particles (Poulsen and Iversen, 2008). Viruses also play a major role in oceanic carbon cycling (Weinbauer et al., 2011). Recent work has also highlighted the importance of archaea in the remineralisation of POM (Orsi et al., 2015). Heterotrophic microbes play major roles in the regulation of the BCP efficiency (Guidi et al., 2016).

1.4 Microbial communities associated with particles

1.4.1 Particles as microbial hotspots

Marine particles are intensively colonised by all kinds of microbes (Fig. 1.4A). As such they have been referred to as microbial hotspots in the ocean (Hagström et al., 1979;

Fuhrman and Azam, 1982; Cole et al., 1988). This is caused by nutrient concentrations of particles being up to 3 orders of magnitude higher than in surrounding bulk seawater (Blackburn and Fenchel, 1999). Microbial cells associated with particles are up to 800 times more abundant than in the surrounding environment (Simon et al., 2002; and reference therein). Because there is an easily identifiable distinction between microbes associated with particles and those in the surrounding seawater, studies have historically investigated particle-associated (PA) versus free-living (FL) microbial communities.

FL microbial cells exhibit a variety of differences with PA microbes, including a distinct morphology than PA cells, which are generally larger than FL cells (Caron et al., 1982; Malfatti et al., 2010; Malfatti and Azam, 2010). However, the main distinction between PA and FL microbes resides in their abilities to degrade and uptake organic matter substrates. PA microbes are able to process POM by releasing hydrolytic enzymes leading to its breakdown into DOM (Ziervogel et al., 2010; Baltar et al., 2017; Arnosti, 2011; Steen et al., 2010; Arnosti and Steen, 2013), which can subsequently be transported into the cell. Conversely, FL microbes are unable to breakdown POM into DOM, and therefore rely on readily available DOM sources (Ziervogel and Arnosti, 2008). PA microbes catalyse more DOM production than they can uptake (Fig. 1.3). This phenomenon might be related to the increase of single-cell enzymatic activities upon particle-attachment (Grossart et al., 2007). It causes the formation of a plume of highly concentrated DOM around the particle (Fig. 1.4B) (Shanks and Trent, 1979; Smith et al., 1992), which is enhanced by sinking motions (Kiørboe et al., 2002). This plume is colonised by chemosensory and motile FL microbes (Stocker et al., 2008; Kiørboe and Jackson, 2001).

PA microbes are presumably more metabolically active than FL microbes (Crump et al., 1999, 1998; Ghiglione et al., 2007; Grossart et al., 2007; Ploug et al., 1999; D'Ambrosio et al., 2014) and also present differential metabolic capabilities. PA communities possess metabolic pathways for the degradation of complex polysaccharides (Cottrell and Kirchman, 2000; Lyons and Dobbs, 2012; Buchan et al., 2014), such as chitin (Fontanez

et al., 2015) fatty acids and lipids (Orsi et al., 2015). Expectedly, PA microbes have enhanced capabilities for particle colonisation (Orsi et al., 2015; Ganesh et al., 2014, 2015; Smith et al., 2013) such as surface-attachment that includes biofilm formation (Dang and Lovell, 2016) and quorum sensing (Krupke et al., 2016; Gram et al., 2002). Quorum sensing is a signalling mechanism used by bacteria within a same population, for instance colonising the same particle, to regulate their gene expression in response to fluctuations in cell density (Servinsky et al., 2015). Like FL, PA microbes possess genes related to chemotaxis and motility (Yawata et al., 2016). Furthermore, PA microbes generally possess larger genomes encoding for more versatile metabolic capabilities compared to FL microbes (Yawata et al., 2014). FL cell genomes are often more streamlined and include genes encoding for metabolic and regulatory functions that allow them to thrive under oligotrophic conditions (Polz et al., 2006).

FL and PA microbes exhibit different potential regarding biogeochemical functions. Large particles such as marine snow can provide anaerobic microenvironments, even within oxygenated waters (Alldredge and Cohen, 1987; Bianchi et al., 2018). Therefore, PA microbes are more likely to perform anaerobic processes such as sulphate reduction (SO_4^{2-}) and nitrate reduction (NO_3^-), while FL microbes do not appear to carry these traits in oxygenated waters (Ganesh et al., 2014, 2015; Smith et al., 2013). Such differences are an outcome of differential taxonomic composition between PA and FL microbial communities.

1.4.2 Microbial communities associated with particles

The literature presented in this section is based on knowledge gathered from particles sampled from size-fractionated filtration of bulk seawater, containing a mixture of suspended and sinking particles, or from sinking particles sampled with sediment traps (see Chapter 2 – part 2.1).

1.4.2.1 Heterotrophic prokaryotic members

PA prokaryotic communities have been characterised in a variety of environments including oxygen minimum zones (OMZ) (Suter et al., 2018; Ganesh et al., 2014), coastal ecosystems (Simon et al., 2014), estuarine environments (Crump et al., 1999), inland seas (Crespo et al., 2013), ocean trenches (Eloe et al., 2010), open oceans (Allen et al., 2012) and lakes (Shi et al., 2018), as well as during phytoplankton blooms (Teeling et al., 2012). They generally show enrichments in *Bacteroidetes*, *Vibrionales*, *Alteromonadales* and *Oceanospirillales* (*Gammaproteobacteria*), *Rhodobacterales* (*Alphaproteobacteria*), *Planctomycetes*; *Actinobacteria*, *Deltaproteobacteria*, *Campylobacterales* (*Epsilonproteobacteria*), and *Verrucomicrobia* taxa.

Different prokaryotic groups have been observed to selectively colonise particles depending on the particle-size. Microbial communities associated with particles of different sizes consistently exhibit different prokaryotic members (e.g., > 30 µm [Fuchsman et al., 2011], > 20 µm [Salazar et al., 2016], > 8 µm [Milici et al., 2016], > 3 µm [Orsi et al., 2015; Milici et al., 2016], > 1.6 µm [Ganesh et al., 2014] and > 0.8 µm [Salazar et al., 2016]). The diversity of filter pore-sizes used in these studies highlight the lack of consensus regarding the optimal pore-size to use to collect of PA microbial communities.

Bacterial communities associated with three particle size-fractions from the Arctic Ocean, classified as sinking aggregates (> 60 µm), suspended particles (1 – 60 µm) and FL bacteria (1 – 0.22 µm), differed significantly, although they were all dominated by *Gammaproteobacteria*, *Bacteroidetes* and *Alphaproteobacteria* (Kellogg and Deming, 2009). It is noteworthy that the differentiation between suspended and sinking particles was solely based on particle-size. In the Eastern Tropical North Pacific OMZ, a study investigating microbial communities, divided into large PA (> 30 µm), PA (1.6 – 30 µm) and FL (0.2 – 1.6 µm), found that surface-colonisers belonging to *Gammaproteobacteria* (*Vibrio* spp., *Pseudomonas* spp. and *Alteromonas* spp.) were more enriched in the large PA fraction (Ganesh et al., 2015). Similarly, in a freshwater lake, Shi et al. (2018)

observed that large aggregates (> 120 µm) were enriched in *Cytophagia* and *Alphaproteobacteria*, while small particles (3 – 36 µm) and FL fractions (0.2 – 3 µm) were more similar to each other and distinct from communities associated with large aggregates.

While most archaea are FL, the marine euryarchaeal group II (MGII) has recently been shown to possess traits required for surface adhesion and degradation of polymers such as proteins and fatty acids (Zhang et al., 2015). Additionally, PA and FL MGII archaea have been observed to be physiologically distinct, with PA representatives exhibiting increased capacities for surface adhesion and the catabolism of high molecular-weight (HMW) organic compounds compared to FL representatives (Orsi et al., 2015).

The evolution of PA community structure with depth is dictated by environmental conditions at depth as well as particle-type (Pelve et al., 2017). There is consensus that heterotrophic bacterial colonisation of sinking particles occurs in the euphotic zone and PA community subsequent structure in the mesopelagic results from the evolution of that initial euphotic community rather than from successive colonisations occurring as the particles sink (Delong et al., 1993; Lecleir et al., 2014; Thiele et al., 2015). Conversely, high particle-attachment and -detachment rates, as well as chemotaxis abilities of PA bacterial strains have been experimentally observed (Kiørboe et al., 2002). Furthermore, model of PA bacterial community evolution has shown that particles are first colonised by opportunistic taxa possessing capabilities to rapidly degrade POM, before being progressively outcompeted by secondary consumers. These secondary consumers cannot degrade complex POM and feed on smaller by-product molecules released by primary consumers (Datta et al., 2016). For these reasons, a general model of sinking particle colonisation seems challenging, and more environmental studies are needed.

1.4.2.2 Protist members

Protist cell-sizes span over 5 orders of magnitude, ranging from < 1 µm (chlorophyte *Ostreococcus* sp.) to 10 cm (radiolarian colony). Protists exhibit a plethora of

morphologies, behaviours and nutritional modes (Caron et al., 2012; Caron, 2017), thereby critically influencing the ecology and chemistry of marine ecosystems (Worden et al., 2015). Although their nutritional behaviours exist in a continuum, protists are generally considered to be either: (i) autotrophic (using inorganic matter or light as energy source); (ii) heterotrophic (using organic matter as energy source) or (iii) mixotrophic (able to use a combination of inorganic matter or light as well as organic matter as an energy source) (Stoecker et al., 2017).

Phototrophic protists represent most of the surface ocean phytoplankton biomass and are therefore mainly defining the BCP strength (Guidi et al., 2009). Furthermore, heterotrophic and mixotrophic protists feed on sinking particles containing POM produced by phytoplankton (Calbet and Landry, 2004; Steinberg and Landry, 2017; Schmoker et al., 2013; Sherr and Sherr, 2002; Taylor, 1982; Lampitt et al., 1993; Caron et al., 1986), thereby also affecting the BCP efficiency. Heterotrophic protists, by lengthening the food-web, lead to organic carbon loss from the particulate to the dissolved pool (Pomeroy and Wiebe, 1988) as well as to the suspended particle pool (Steinberg et al., 2008). Although the specifics are still unknown, there is a strong association between certain heterotrophic protists, such as *Radiolaria* and the alveolate parasites *Syndiniales*, with carbon export in oligotrophic oceans (Guidi et al., 2016).

PA bacterivorous protists influence PA bacterial communities in a variety of ways. As they predate on PA bacteria, protists lead to formation of bacterial biofilms on particles as a mean of protection (Seiler et al., 2017). They can also control growth and vertical distribution of certain bacterial populations by specifically grazing on them (Anderson et al., 2013; Pernthaler, 2005).

Protist communities recovered in large size-fractions are generally enriched in dinoflagellates, ciliates, *Retaria* (including *Rhizaria*) and *Stramenopiles* (including diatoms) in various oceanic regions such as the open ocean (Fontanez et al., 2015; Allen et al., 2012), OMZs (Duret et al., 2015; Parris et al., 2014) and estuaries (Smith et al., 2013).

Such enrichments can reflect either the cell-size of living protists, the attachment or association of protists on particles or phytodetrital components of particles.

1.4.2.3 Viruses

Within the euphotic zone, viruses lead to the loss of 2 to 3 % of phytoplankton POM to DOM (Suttle, 1994) (Fig. 1.1) thereby influencing the BCP efficiency either positively or negatively (Rhodes and Martin, 2010; Weinbauer et al., 2011; Needham et al., 2017). Viral infection triggers cell lysis and the release of labile DOM, which can be subsequently remineralised to inorganic nutrients fuelling recycled primary production. This phenomenon is referred to as the viral shunt (Suttle, 2005). Viruses can also induce the termination of phytoplankton blooms (Bratbak et al., 1991) thereby also influencing the BCP strength.

Marine snow aggregates have been described as viral factories, as has been shown on artificial macro-aggregates (Bettarel et al., 2016) and viruses, such as Mimivirus, are enriched in PA compared to FL size-fractions (Allen et al., 2012). By specifically infecting certain microbial groups, virus play a major role in structuring PA microbial communities (Brum et al., 2015; Suttle, 2007).

1.5 Thesis objectives and outline

1.5.1 Objectives

Previous studies on marine particles have been heavily biased towards sinking particles despite the importance of suspended particles in the ocean, particularly in mesopelagic ecosystems. Unlike sinking particles, they are very poorly characterised in terms of their chemical composition and their associated microbial communities. Additionally, dynamics connecting the two particle-pools together as well as the exact role of suspended particles in the BCP and long-term carbon storage remain to be elucidated.

Additionally, microbial communities associated with these two particle-types have been disproportionally studied. Very little is known regarding suspended particle-associated microbial communities. Furthermore, the only literature differentiating communities associated with suspended and sinking particles is based on size-fractionation of bulk seawater, which uses particle-size as discriminant. This is inaccurate to distinguish suspended and sinking particles, as sinking velocity is also a factor of particle composition (such as mineral and lipid content) rather than simply of particle-size. For these reasons, the composition and functionalities of microbial communities associated with suspended particles remain largely unknown.

This thesis tests the hypothesis that microbial communities associated with suspended particles are different from those associated with sinking particles. More precisely, this thesis addresses the following questions:

Chapter 3: Are prokaryotic communities associated with suspended and sinking particles different? If so what are the likely contributing factors to such distribution, and what are the implications on organic matter cycling?

Chapter 4: What are the eukaryotic contributions to particle export from the surface to mesopelagic ocean? Specifically:

- Which phytoplankton taxa are the most efficient in carbon export?
- What metazoan and phytoplankton taxa influence sinking and suspended particles in the mesopelagic?
- Are heterotrophic protists residing on mesopelagic sinking and suspended particles different? If so, how does their distribution impact organic matter remineralisation and particle attenuation?

Chapter 5: Are there functional differences between sinking and suspended particle-associated microbial communities with respect to:

- Carbon remineralisation?
- Biogeochemical cycling of other key elements, such as nitrogen and sulphur?

1.5.2 Outline

The introductory chapter reports our current knowledge regarding the biological carbon pump and associated remineralisation processes, particle dynamics between suspended and sinking particles and particle-associated microbial communities. It highlights gaps in our knowledge that need to be closed to accurately understand the ties of the oceanic biological carbon pump.

Chapter 2 provides an overview of available sampling techniques, including the method applied to collect samples to investigate differences between suspended and sinking particle-associated microbial communities for this thesis work. This chapter also includes an examination of method limitations.

Chapters 3 and 4 establish differences between taxonomical structure of microbial communities associated with suspended and sinking particles. Potential impacts on the biological carbon pump and particle dynamics are suggested based on enriched taxa and available literature regarding their physiology and biogeochemical functions. Samples for both chapters were collected at two depths of four sites in the Scotia Sea (Southern Ocean) using a marine snow catcher. Chapter 3 investigates differences between prokaryotic communities associated with suspended and sinking particles ≥ 10 µm using 16S rRNA gene amplicon sequencing. Chapter 4 examines differences between eukaryotic communities associated with ≥ 10 µm and 0.22 – 10 µm suspended particles, and ≥ 10 µm sinking particles using 18S rRNA gene amplicon sequencing.

Chapter 5 establishes differences between remineralisation activities and associated nitrogen and sulphur cycling mediated by microbial communities associated with suspended and sinking particles. The meaning of such differences regarding the biological carbon pump and particle dynamics, as well as oceanic nitrogen and sulphur cycling, are analysed. This chapter investigates functional differences using metatranscriptomic sequencing. Large (≥ 10 µm) and small (0.22 – 10 µm) suspended and sinking particles were collected at four depths at the Porcupine Abyssal Plain site in the North Atlantic.

Finally, chapter 6 offers a synthesis of key findings from chapters 3, 4 and 5. This chapter explores limitations of this thesis, reports work in progress and suggests future experiments to further investigate the role of suspended particle-associated microbial communities.

This thesis is written in a three-papers format. As such, elements presented in chapters 1 and 2 might be repeated in chapters 3, 4 and 5. These chapters contain supplementary information regarding specifics of the different chapters and are presented in annexes.

Chapter 2: Key methodologies and study sites

2.1 Sampling particle-associated microbial communities in the environment

2.1.1 Methodologies and limitations

Studies investigating molecular ecology of particle-associated (PA) and free-living (FL) microbial communities commonly use size-fractionated filtration of seawater. The following section provides a description of methodologies commonly used to target PA microbial communities and discuss some limitations of each technique.

2.1.1.1 Size-fractionated filtration of bulk seawater

Size-fractionated filtration of biomass from seawater is the most commonly used methodology to collect PA bacterial communities, as it isolates FL from PA communities. This method has been used since the dawn of molecular biology tools development (Fuhrman et al., 1988) and has provided crucial information for our understanding of oceanic microbial ecology.

Seawater is most commonly collected with Niskin bottles attached to a conductivity, temperature and depth (CTD) rosette unit. Following collection, bulk seawater is passed through an inline series of filters with decreasing pore-size. Microbes collected on the largest pore-size filter (ranging from 1.6 to 30 µm), referred to as the prefilter, are considered PA. Microbes collected on the smallest pore-size filter (typically 0.2 µm, but recently 0.1 µm) are considered FL. There are several limitations to this sampling methodology.

Firstly, there is a lack of consensus regarding the pore-size used to collect particles (e.g., 30 µm for Fuchsman et al., 2011; 3 µm for Orsi et al., 2015; and 1.6 µm for Ganesh et al., 2014), which makes inter-study comparison difficult.

Secondly, this method does not offer an accurate separation between fractions as it is influenced by the volume filtered. The larger the volume filtered, the more biomass will be retained on the prefilter, resulting in the retention of smaller particles (with a size inferior to the prefilter pore-size) and FL microbes. Padilla et al. (2015) showed that there are drastic changes in the prefilter community associated with small variations of the filtered volume. Furthermore, pressure applied on particles during their passage through tubing forced by a pump leads to particle-breakage and the collection of genetic material from PA microbes on downstream filters. Additionally, the amount of material collected on filters is influenced by particle concentration in the seawater. Both parameters are difficult to quantify and render inter-study comparison more difficult.

Thirdly, and with regards to separation between suspended and sinking PA microbial communities, bulk seawater collected with a Niskin bottle contains a mixture of suspended and sinking particles in unknown proportions. Therefore, it is impossible to access specific information about suspended and sinking PA microbial communities with this method. Although particle-size has been used as a discriminant to separate suspended from sinking particles in size-fractionated filtration (e.g., Kellogg and Deming, 2009), particle velocity is not purely a function of particle-size (Iversen and Ploug, 2010), as particle-shape and density also impact sinking behaviours (Lam and Marchal, 2015).

2.1.1.2 Sediment traps

Sinking particles have been sampled using sediment traps for several decades (Berger, 1971) and the collected data have undeniably contributed to enhance our understanding of the biological carbon pump (Martin et al., 1987).

Sediment traps are designed to intercept sinking particles during their transit downwards and accurately represent an integration of sinking particles over the time period they are left open, typically days to several months. Traps are usually filled with preservatives such as formalin to prevent particle degradation (McDonnell et al., 2015b).

Particles collected in sediment traps tend to aggregate, thereby preventing particles to be preserved in their original forms. Furthermore, the extended deployment times and fixation methods render these particles unsuitable for the investigation of microbial activities (metatranscriptomics, metaproteomics, enzymatic rates measurements) as it is difficult to understand how they affect PA microbial community composition and activities. Nevertheless, this sampling tool (e.g., Pelve et al., 2017), as well as its modifications, such as gel traps (e.g., Thiele et al., 2015), have been used to sample sinking PA communities.

2.1.1.3 Manual particle-picking

Picking of single particles has been used to collect relatively intact marine snow aggregates (> 0.5 mm) for bacterial PA community investigation (e.g., Delong et al., 1993). Although this method is delicate enough to not drastically disturb aggregate-associated communities, it offers a very limited resolution as only a few large aggregates can be sampled at a time.

2.1.2 Marine snow catcher: accurate sampling of suspended and sinking particles

The marine snow catcher (MSC) is a large volume water-sampler (100 L) of 1.5 m height composed of (i) an upper section (93 L) that is detachable from a (ii) bottom section (7 L) (Lampitt et al., 1993; Riley et al., 2012) (Fig. 2.1A). Two large openings allow water and particles to enter the device as it is lowered open through the water column from the ship's winch system. The large openings (30 cm) are designed to reduce water turbulence

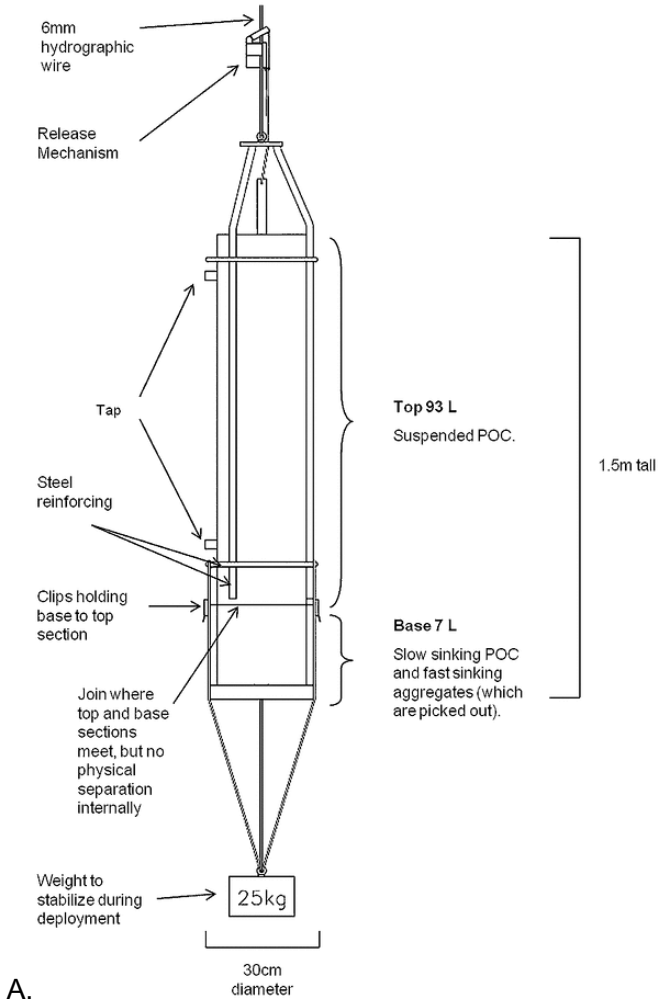

A.

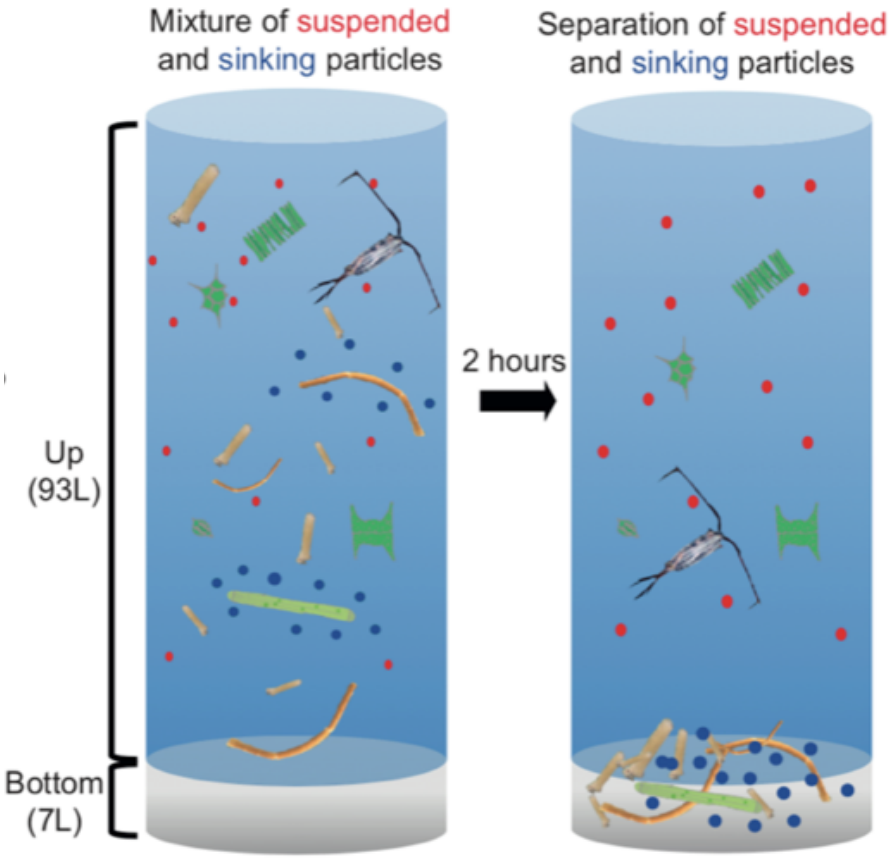

B.

Figure 2.1A. Characteristics of the marine snow catcher (from Riley et al., 2012).
Figure 2.1B. Conceptual vision of the marine snow catcher.

thereby limiting particle breakage. The MSC is closed at the desired depth by a mechanical messenger and recovered. Once recovered, the MSC is left on deck for two hours prior to sampling, in order for sinking particles to sediment at the bottom of the MSC while suspended particles remain in suspension in the upper part (Fig. 2.1B). Theoretically, particles sinking at a velocity ≥ 24m d^{-1} (MSC height/settling time = 200 cm/2 hours) are considered sinking, and particles sinking at lower velocities are considered suspended.

After this settling time, the upper part of the MSC is sampled for suspended particles. Once the upper part is fully and gently drained, the MSC is disassembled and the bottom part is sampled for sinking particles.

This sampling method was used for this thesis work to collect suspended and sinking particles. Microbial communities associated with the two particle-types were investigated using molecular tools, which are discreetly described in each chapter.

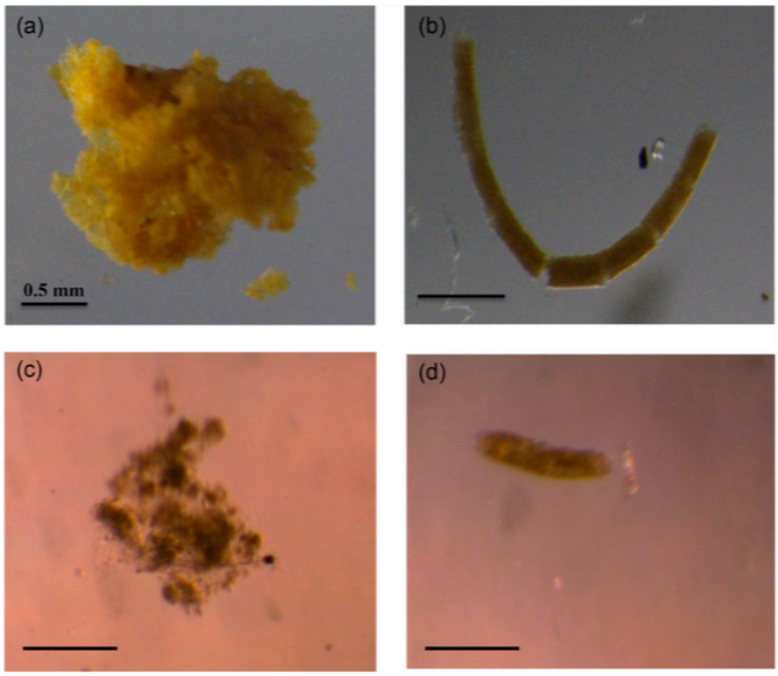

Figure 2.2. Particle images of sinking particles from the Southern Ocean and PAP (from Cavan et al., 2016). Images a and b: Particles collected in the Southern Ocean; images c and d depict particles samples at PAP.

2.2 Sampling sites

Particles were collected from two distinct oceanic regions using the MSC (Fig. 2.3). The MSC was deployed at four sites in the Scotia Sea (Southern Ocean) during austral summer 2014, and at the Porcupine Abyssal Plain (PAP) in the northeast Atlantic during spring 2015.

Both sampling sites differ regarding their productivity and ecosystem structure, especially in terms of mesozooplankton (Cavan et al., 2016) and carbon export characteristics (Henson et al., 2012). The Scotia Sea and PAP both exhibit high productivity periods, with PAP being the overall more productive region while the Scotia Sea has the greatest range of primary production levels (Cavan et al., 2016). During bloom periods, slow-sinking particles are the key component of POC flux at PAP while it is fast-sinking particles that prevails in the Scotia Sea (Baker et al., 2017). Additionally, the morphology of sinking aggregates from both sites is different (Fig. 2.2).

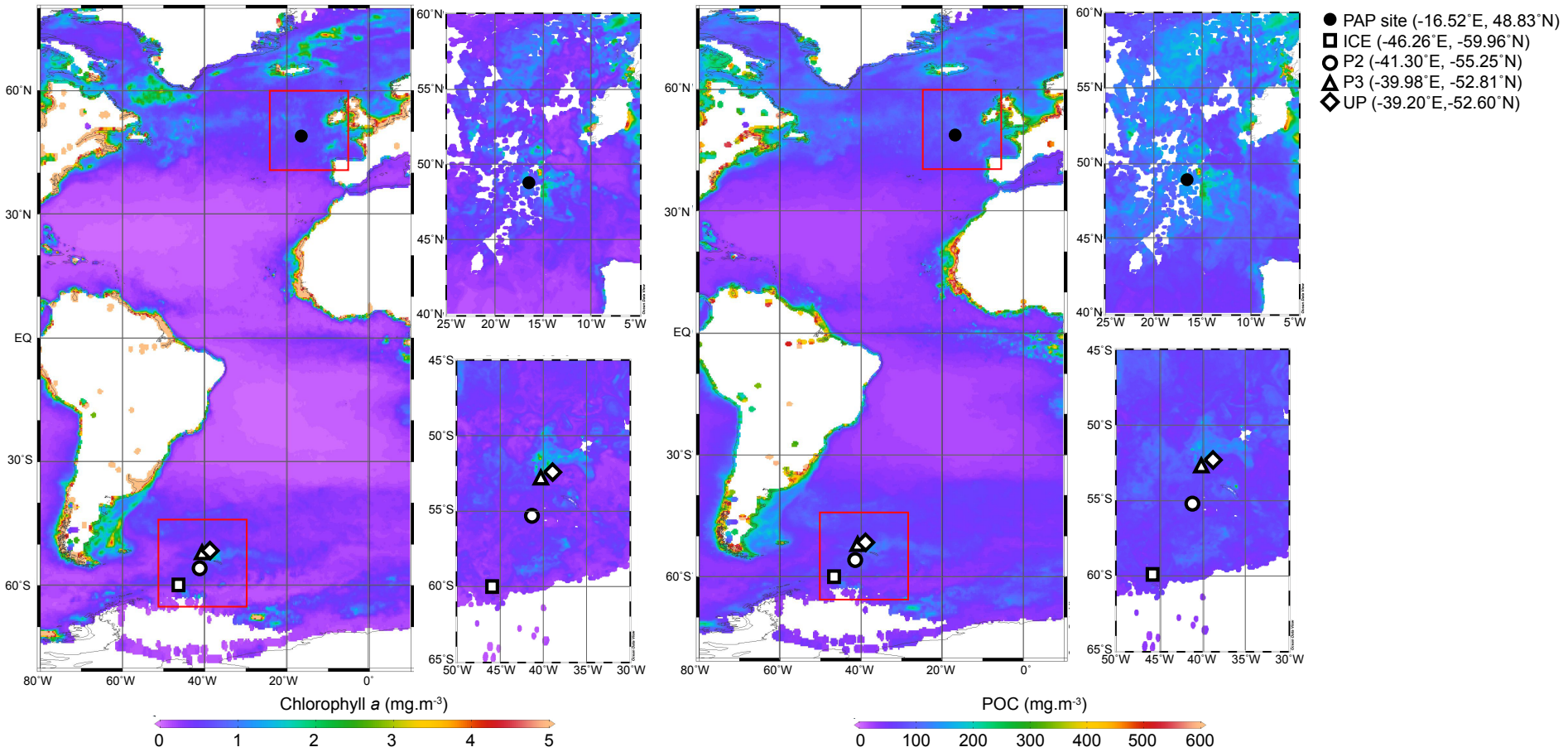

Figure 2.3. Surface chlorophyll *a* and particulate organic carbon sampling maps. These maps were constructed on Ocean Data View using data from NASA Ocean Color 9 km resolution level 3 browser. The chlorophyll *a* data (mg m^{-3}) was corrected with the OCx algorithm and the POC data (mg m^{-3}) was corrected by D. Stramski 2007 method (version 443/555). Data for JCR304 are the 32-day composition (17/11/2014-18/12/2014) and the DY032 are the 8 day composite (26/06/2015-03/07/2015). The overall map corresponds to the annual composite for the year 2015.

Chapter 3: Prokaryotic niche partitioning between suspended and sinking marine particles

This chapter has been published in *Environmental Microbiology Reports* as:

Prokaryotic niche partitioning between suspended and sinking marine particles

Manon T Duret[1]*, Richard S Lampitt[2], Phyllis Lam[1]

[1]Ocean and Earth Science, University of Southampton

[2]National Oceanography Centre Southampton

PL, MTD and RSL designed the study. MTD collected and analysed samples, conducted data analysis and wrote the manuscript. PL assisted in the manuscript preparation. RSL provided feedback on the manuscript.

Article DOI: 10.1111/1758-2229.12692

3.1 Abstract

Suspended particles are a major organic carbon substrate for heterotrophic microorganisms in the mesopelagic ocean (~ 100 – 1000 m). Nonetheless, microbial communities associated with these particles have been overlooked compared to sinking particles, the latter being the main carbon transporters of the oceanic biological carbon pump.

This study is the first to differentiate prokaryotic communities associated with suspended and sinking particles, collected with a marine snow catcher at four environmentally distinct stations in the Scotia Sea. Amplicon sequencing of the 16S rRNA gene revealed distinct prokaryotic communities associated with the two particle-types in the mixed layer (0 – 100 m) and upper-mesopelagic zone, presenting on average 42.5 ± 15.2 % dissimilarity.

Although ubiquitous remineralising taxa were present within both particle-types, gammaproteobacterial *Pseudomonadales* and *Vibrionales*, and alphaproteobacterial *Rhodobacterales* preferred sinking particles while *Flavobacteriales* (*Bacteroidetes*) favoured suspended particles. We propose that the niche-partitioning observed in this oceanic region could be driven by properties of organic matter found within the two particle-types: K-strategists, specialised in the degradation of complex organic compounds, thrived on semi-labile suspended particles while generalists r-strategists were adapted to the transient nature of sinking particles.

Differences between the two particle-associated communities were more pronounced in the mesopelagic zone than in the surface mixed layer. This likely reflects greater exchanges between particle-pools caused by more dynamic mixing in the surface ocean.

3.2 Introduction

The oceanic biological carbon pump annually removes ~ a third of anthropogenic atmospheric carbon dioxide (pCO_2) (Sabine et al., 2004) via the export of organic carbon produced by phytoplankton in the euphotic zone (sunlit part of the ocean) towards the deep ocean. Sinking particles are responsible for the rapid export of particulate organic matter (POM) into the mesopelagic (base of euphotic zone to ~ 1000 m) (Turner, 2015). The two major components of sinking particles are marine snow and faecal pellets (Ebersbach and Trull, 2008; Belcher et al., 2016). Marine snow are aggregates ≥ 500 µm (Shanks and Trent, 1980) that embed various materials such as microbial cells and various phytodetrital materials (Alldredge and Silver, 1988; Simon et al., 2002) bound together by transparent exopolymer polysaccharides (Alldredge et al., 1993). Faecal pellets can be produced by mesozooplankton (Stamieszkin et al., 2017) or microzooplankton (Gowing and Silver, 1985). They are a compacted form of organic matter that is more resistant to remineralisation than marine snow owing to their density and surrounding membrane (Ebersbach et al., 2011).

The depth reached by sinking particles is a key factor in oceanic carbon sequestration (Kwon et al., 2009) – the deeper they export POM, the longer it will be removed from atmosphere-surface ocean reservoirs (Passow and Carlson, 2012). Only 5 to 25 % of particles produced in the euphotic zone reach the mesopelagic zone (De La Rocha and Passow, 2007; Buesseler and Boyd, 2009) and even less reach the deep ocean (Francois et al., 2002). This is owing to POM remineralisation occurring as particle sink, most of which takes place in the euphotic and upper-mesopelagic, leading to the release of CO_2 and dissolved inorganic nutrients. This process is responsible for the decrease in efficiency of the biological carbon pump (De La Rocha and Passow, 2007). Remineralisation processes also lead to the release of dissolved organic matter (DOM) in a plume and the disaggregation of sinking particles into suspended particles (Collins et al., 2015). Mesozooplankton, through their feeding behaviours such as sloppy feeding

(Lampitt et al., 1993), are responsible for most of sinking particle disaggregation (Giering et al., 2014) and the release of DOM (Strom et al., 1997). Complementary to these processes, final steps of remineralisation are mostly carried out by microbial communities (Cho and Azam, 1988; Smith et al., 1992; Kiørboe and Jackson, 2001) that are either associated with particles or free-living in the water column and feeding on released DOM.

Prokaryotic communities associated with particles generally show higher concentrations, growth rates, enzymatic activities and metabolic diversity than their free-living counterparts (Grossart et al., 2007; Ganesh et al., 2014; Satinsky et al., 2014; Dang and Lovell, 2016). The two microbial communities are phylogenetically distinct. *Bacteroidetes*; *Vibrionales*, *Alteromonadales* and *Oceanospirillales* (*Gammaproteobacteria*); *Rhodobacterales* (*Alphaproteobacteria*); *Planctomycetes*; *Actinobacteria*; *Deltaproteobacteria*; *Campylobacterales* (*Epsilonproteobacteria*); and *Verrucomicrobia* are generally enriched in particle-associated communities (Delong et al., 1993; Crespo et al., 2013; Bižić-Ionescu et al., 2014; Lecleir et al., 2014; López-Pérez et al., 2016; Mestre et al., 2017). These taxa have adaptive capabilities for surface-attachment and enhanced abilities to assimilate and dissimilate single-carbon compounds and to degrade polysaccharides (Cottrell and Kirchman, 2000; Lyons and Dobbs, 2012; Fontanez et al., 2015). Particle-associated microbes are key actors in remineralisation processes as they are also typically detected during peaks of organic matter production such as phytoplankton blooms (Bauer et al., 2006; McCarren et al., 2010; Buchan et al., 2014) and oil spills (Mason et al., 2012).

While the concentration of particulate organic carbon (POC) in sinking particles decreases exponentially with depth (Martin et al., 1987; Francois et al., 2002), the concomitant POC concentration in suspended particles remains constant at ~ one to two orders of magnitude higher (Bishop et al., 1977; Bacon et al., 1985; Verdugo et al., 2004; Riley et al., 2012; Seitz et al., 2016). As the POC flux to the mesopelagic is not high enough to meet organic carbon demand of heterotrophs therein (Boyd et al., 1999; Steinberg et al., 2008; Baltar et al., 2009), suspended particles have been considered as a major organic

carbon substrate for both microbes (Arístegui et al., 2009; Baltar et al., 2009, 2010) and metazoans (Gloeckler et al., 2017).

Sinking particles, as main transporters of POM to depth, are the starting point of remineralisation processes. On the other hand, suspended particles are a major POM substrate for mesopelagic heterotrophs. For these reasons, sinking and suspended particles have different ecological roles with regards to microbes in the ocean. No studies to date have investigated distinctions between microbial communities associated with suspended and sinking particles. It therefore remains unknown whether the two particle-types harbour different microbial communities, with hence possibly different genetic make-ups and metabolic potentials. Such differences would affect our understanding of factors regulating the biological carbon pump efficiency.

Methodologies traditionally used to sample particle-associated microbial communities are not suitable to collect the two particle-types separately. They collect either solely sinking particles or bulk seston containing a mixture of sinking and suspended particles in unknown proportions. These techniques include:

(i) Direct particle-picking, biased towards larger-sized visible aggregates (Delong et al., 1993).
(ii) Sediment and gel traps for the collection of sinking particles (Lecleir et al., 2014; Fontanez et al., 2015).
(iii) *In situ* size-fractionated filtration with underwater submersible pumps collecting both suspended and sinking particles (McDonnell et al., 2015).
(iv) The most commonly used size-fractionated filtration of bulk seawater collected with Niskin bottles collecting both suspended and sinking particles (Bižić-Ionescu et al., 2014).

The main variable considered by these methods is particle-size, as sinking particles are generally considered larger than suspended particles (Verdugo et al., 2004). However, the sole use of particle-size as discriminant is accurate as other parameters, such as particle-

shape (Lam and Marchal, 2015) and mineral content (Ploug et al., 2008) also influence particle sinking velocity. Sinking velocity is the most objective parameter differentiating between sinking and suspended particles. The marine snow catcher (MSC) (Lampitt et al., 1993) is a 95 L gentle water-sampler using sinking velocity for the separate collection of the two particle-types from a same water sample (Riley et al., 2012). After retrieval from the desired depth, the MSC is left undisturbed on the ship's deck for two hours to allow sinking particles to sediment at the bottom of the sampler while suspended particles remain in suspension in the upper part (Fig. 2.1).

This study compares the diversity and structure of prokaryotic communities associated with suspended and sinking particles collected with an MSC deployed in the mixed layer (10 m below the deep chlorophyll maximum [DCM]) and in the upper-mesopelagic (110 m below the DCM). Amplicon sequencing of the V4 region of 16S rRNA encoding gene was used to characterise particle-associated communities sampled at four stations of contrasting nutrient and productivity regimes in the Scotia Sea (Southern Ocean) (Fig. 2.3 and Annex A1) during the austral summer 2014. These stations included two low-productivity stations – ICE at the marginal ice edge and P2 in a high-nutrient-low-chlorophyll region – and two more productive stations – P3 in an iron-enriched region and UP in an upwelling region (Table 3.1). We hypothesise that; (i) suspended and sinking particles harbour different prokaryotic communities and (ii) specific factors, such as particle organic matter composition, contribute to such variability.

3.3 Results

3.3.1 Amplicon sequencing results

A total of 6,979,982 V4 16S rDNA paired-ends reads were recovered from particle-associated communities (≥ 10 µm), and 247,354 sequences from free-living communities (0.22 – 10 µm). Although, free-living communities are not the focus of this study, they are presented here as a reference for the surrounding water column prokaryotic community.

After sequence trimming, pairing, merging and removal of chloroplast rDNA sequences, 1,638,059 sequences remained in particle-associated libraries with an average length of 460 bp (74,126 ± 118,652 sequences/library). Differences between the number of sequences per library was largely caused by unequal proportions of chloroplastic rDNA (median of 75 and 77 % for suspended and sinking particle-associated libraries respectively). Suspended particle-associated communities were sequenced to greater depths than sinking particle-associated communities (Annex A2). In order to allow an unbiased comparison of communities associated with suspended and sinking particles ≥ 10 µm, libraries were rarefied following different strategies depending on the analysis performed (see 3.6).

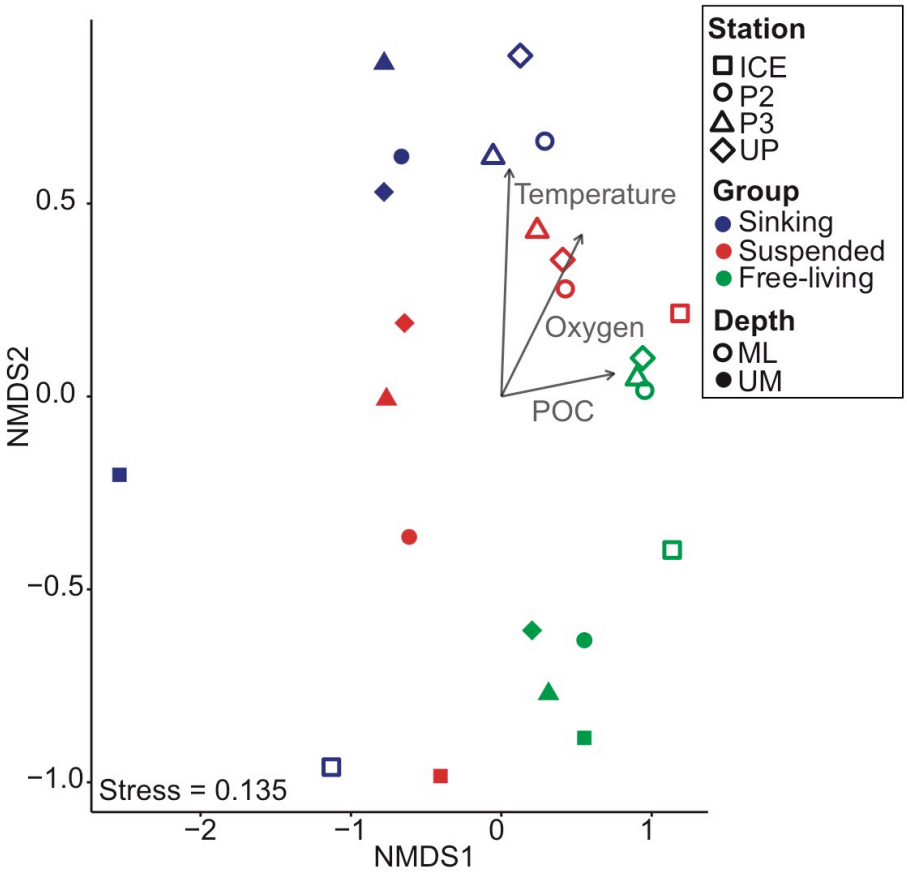

Figure 3.1. Non-metric multidimensional scaling plot of OTU composition. NMDS was calculated with Bray-Curtis distance of the rarefied dataset. The significance of environmental parameters (oxygen, fluorescence and POC concentrations and temperature) was tested using a PERMANOVA ($p < 0.05$). Significant environmental parameters are displayed and their respective arrow length is proportional to the community structure variability they explain. ML = mixed layer, UM = upper-mesopelagic.

Table 3.1. Sampling stations description and associated hydrochemical variables. Mean chlorophyll *a* concentration corresponds to the average of values measured above the mixed layer depth as a proxy for productivity. HNLC= High Nutrient Low Chlorophyll; PFZ = Polar Front Zone; AAZ = Antarctic zone; SS = suspended; SK = sinking.

Latitude (˚N)	Longitude (˚E)	Station	Station description	Mean chlorophyll *a* (µg L^{-1})	Depth (m)	Potential temperature (˚C)	Salinity	Oxygen (µM)	Particle-type	POC (µg L^{-1})
-59.9624	-46.1597	ICE	On the Antarctic continental ice edge.	0.40	60	-1.06	34.2	333.6	SS	75.7
									SK	2.5
					160	-0.76	34.4	253.6	SS	32.2
									SK	10.3
-55.2484	-41.264	P2	HNLC zone.	0.37	55	0.18	33.8	348.9	SS	124.6
									SK	14.1
					155	0.84	34.2	246.4	SS	38.6
									SK	2.7
-52.8121	-39.9724	P3	Iron fertilized zone, near South Georgia continental margin.	1.90	70	1.87	33.9	334.0	SS	124.2
									SK	5.6
					170	1.52	34.3	222.3	SS	31.4
									SK	3.9
-52.6018	-39.1994	UP	Upwelling station in proximity to P3, in frontal system PFZ and AAZ.	1.23	70	1.99	33.9	335.2	SS	92.2
									SK	22.5
					170	1.50	34.3	222.3	SS	45.8
									SK	9.1

3.3.2 Community structure analysis

A non-parametric multidimensional scaling (NMDS) analysis based on Bray Curtis dissimilarity distance of OTU (operational taxonomic unit) relative abundances (Fig. 3.1) revealed a clear distinction between suspended particle-associated, sinking particle-associated and free-living communities. Suspended and sinking particle-associated communities and free-living communities formed distinct loose clusters in the mixed layer and the upper-mesopelagic. An unweighted pair group method with arithmetic means (UPGMA) tree at a 70% cut-off (Fig. 3.2) corroborated these observations showing similar clustering patterns at both sampling depths. The average dissimilarity between suspended and sinking particle-associated communities was higher in the upper-mesopelagic (48.1 ± 12.9 %) than in the mixed layer (36.8 ± 15.3 %), except at UP (Annex A3-A). A permutational multivariate analysis of variance (PERMANOVA) (Annex A4-A) revealed that community-type (suspended or sinking particle-associated, or free-living) was a strong predictor of variability, explaining 27 % of OTU composition against 15 and 20 % attributed to the sample origin (station and depth) ($p < 0.05$).

Every station had > 50 % dissimilarity compared to any other, and samples collected at ICE exhibited the highest dissimilarity (~ 70 % in the mixed layer and ~ 80 % in the upper-mesopelagic) (Annex A3-B). Accordingly, communities sampled at ICE clustered individually from other stations (Fig. 3.1 and 3.2). Furthermore, a higher dissimilarity was observed between communities in the upper-mesopelagic (69.7 ± 12.8 %) than in the mixed layer (63.1 ± 14.9 %) at all stations. A PERMANOVA analysis of environmental parameters (Annex A4-B) revealed that variation in temperature, oxygen concentration and POC concentration (Table 3.1) altogether predicted 43 % of the OTU composition ($p < 0.05$).

A total of 8,156 OTU were represented in this dataset with 139 OTU representing 75% of the overall sequences. The proportion of OTU shared between sinking and suspended particle-associated communities was low in the mixed layer (13.7 ± 4.6 %) and upper-

mesopelagic (16.0 ± 2.2 %) (Fig. 3.3 and Annex A5), although they represented a large proportion of the sequences in all samples. Furthermore, the proportion of sequences affiliated with OTU shared between suspended (83.8 ± 14.5 %) and sinking particle-associated communities (74.0 ± 13.2 %) was higher in the mixed layer than in the upper-mesopelagic (77.0 ± 11.3 % and 65.5 ± 21.1 % respectively). Sinking particle-associated communities had a higher proportion of unique OTU (absent from their suspended particle counterpart and free-living communities) at both depths, which consisted of 25.0 ± 18.4 % of total OTU (representing 31.0 ± 9.6 % of sequences). Suspended particle-associated communities shared more sequences with free-living communities (85.0 ± 11.8 %) than did sinking particle communities in the mixed layer (57.3 ± 23.8 %) and in the upper-mesopelagic (75.5 ± 8.3 % versus 64.5 ± 14.2 % respectively). The alpha-diversity indices, Shannon's and Pielou's, as well as the unbiased number of OTU (Annex A6) were higher for sinking particle-associated communities in the mixed layer. On the other hand, they were higher for suspended particle-associated communities in the upper-mesopelagic. Higher values indicate a higher OTU richness and evenness.

3.3.3 Microbial community composition

Despite variability inherent to sampled stations, disparities between suspended and sinking particle-associated were regardless apparent at both depths, and even at lower taxonomic levels.

Proteobacteria and *Bacteroidetes* were the two most abundant phyla, respectively representing 65.8 ± 13.4 % and 22.6 ± 12.2 % of the overall dataset (Annex A7-A). In the upper-mesopelagic, the former was significantly enriched in sinking particle-associated communities while the latter was enriched in suspended particle-associated communities (Kruskall-Wallis test [KW], $p < 0.05$). At the same depth, the phyla *Crenarchaeota* and *Planctomycetes* were more abundant in suspended particles while *Fibrobacteres* was more abundant in sinking particles. In the mixed layer and upper-mesopelagic, the phyla

Firmicutes and *Actinobacteria* were more abundant in sinking particles while archaeal phylum *Euryarchaeota* was more abundant in suspended particles.

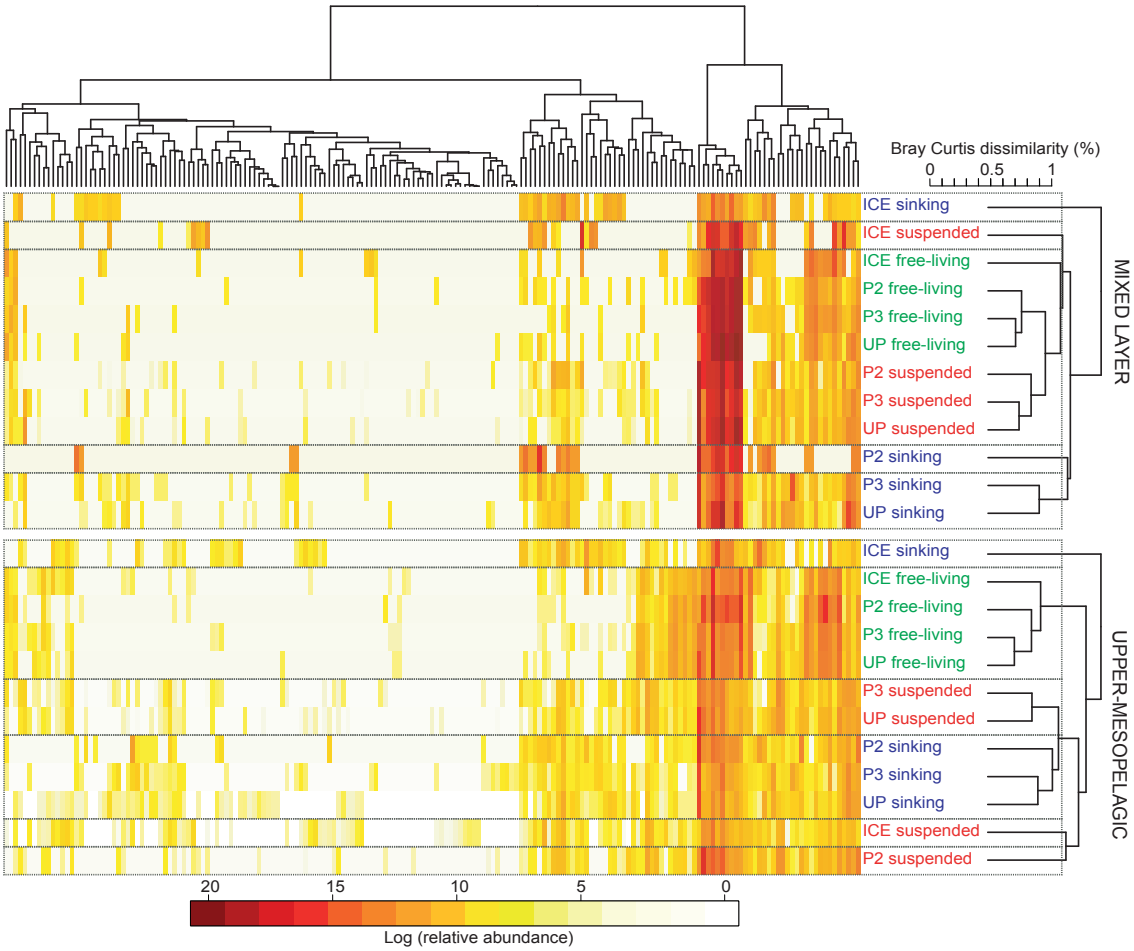

Figure 3.2. Heatmap of taxonomic family composition and similarity clustering (following page). The heatmap represents log (relative abundance) of the fifty most abundant taxonomic families from the rarefied dataset. The similarity tree was calculated with an unweighted pair group method with arithmetic mean based on Bray-Curtis distance of the rarefied dataset.

With regards to the taxonomic class level (Annex A7-B), *Flavobacteria* and *Saprospirae* (*Bacteroidetes*); *Deltaproteobacteria*; *Thermoplasmata* (*Euryarchaeota*) and *Thaumarchaeota* (*Crenarchaeota*); AB16 (SAR406), OM190 (*Planctomycetes*) and BS119 relatives; as well as *Acidobacteria* were in significantly higher proportion in suspended than in sinking particle-associated communities in the upper-mesopelagic (KW, $p < 0.05$) (Table 3.2). On the other hand, *Gammaproteobacteria* sequences were significantly more abundant in sinking particles (KW, $p < 0.05$). Although not significantly, taxonomic classes *Alphaproteobacteria*, *Bacilli* (*Firmicutes*) and *Cytophagia* (*Bacteroidetes*) appeared more abundant within sinking particle-associated communities.

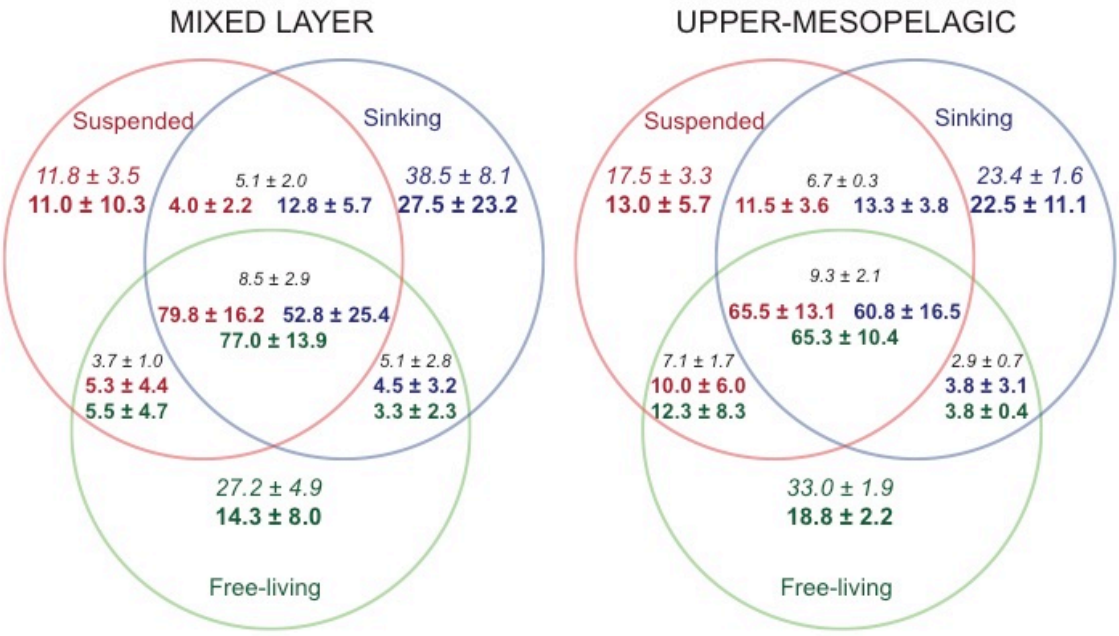

Figure 3.3. Venn diagrams of average proportions of shared/unique OTU and affiliated sequences. The proportions of shared/unique OTU were calculated on the rarefied dataset and correspond to average values from all stations. Detailed numbers for each station are presented in Annex A5. Numbers in non-bold black font are the average number of shared OTU normalised to the total number of OTU. Numbers in non-bold coloured font (red for suspended particles, blue for sinking particles and green for free-living) are the average number of unique OTU normalised to the total number of OTU. Number in bold coloured font are the relative abundance of sequences affiliated with shared/unique OTU.

In the mixed layer, only *Bacilli* and *Betaproteobacteria* sequences were significantly enriched in sinking particle-associated communities (KW, $p < 0.05$). No other constant and/or significant patterns in the mixed layer were observed across stations.

At lower taxonomic levels (order in Fig. 3.4 and family in Fig. 3.2), compositional differences between suspended and sinking particle-associated communities were also more evident in the upper-mesopelagic than in the mixed layer. A similarity percentage analysis (SIMPER) revealed that the family composition of suspended and sinking particle-associated communities was more dissimilar in the upper-mesopelagic than in the mixed layer, except at UP (Annex A8-A). Furthermore, higher numbers of taxa explained the dissimilarity observed between suspended and sinking particle-associated communities in the upper-mesopelagic than in the mixed layer. With regards to the 50

most abundant taxonomic orders, 31 presented identical enrichment patterns across particle-associated communities sampled at every station in the upper-mesopelagic (19 within suspended and 12 within sinking particles), while only 10 presented similar enrichment patterns in the mixed layer (1 within suspended and 9 within sinking particles).

Table 3.2. Relative abundances of taxonomic classes in suspended and sinking particle-associated communities. The overall 30 most abundant taxonomical classes are presented. Significant statistical differences between the two particle-types were assessed with a Kruskall-Wallis test. Significant differences ($p < 0.05$) are highlighted with an asterisk (*) and the highest relative abundances with bold font.

	MIXED LAYER			UPPER-MESOPELAGIC		
	p-value	Sinking	Suspended	p-value	Sinking	Suspended
Gammaproteobacteria	0.69	44.4%	55.3%	0.03*	**59.5%**	29.8%
Flavobacteria	0.89	22.3%	23.5%	0.03*	13.1%	**34.3%**
Alphaproteobacteria	1	16.8%	16.4%	0.49	7.5%	4.2%
Deltaproteobacteria	0.89	0.9%	0.5%	0.03*	1.7%	**10.3%**
Unaffiliated	0.2	4.1%	1.8%	0.11	1.0%	1.8%
Bacilli	0.03*	**4.5%**	0.2%	0.11	3.4%	1.2%
Thermoplasmata	0.69	0.1%	0.2%	0.03*	0.6%	**2.2%**
Verrucomicrobia	0.89	1.7%	0.3%	0.89	3.8%	2.2%
Cytophagia	0.06	0.6%	0.3%	0.69	3.1%	2.1%
Betaproteobacteria	0.03*	**1.5%**	0.3%	0.89	1.1%	1.9%
AB16	0.46	0.0%	0.0%	0.03*	0.2%	**0.7%**
Saprospirae	0.2	0.7%	0.2%	0.03*	0.3%	**2.8%**
Pedospharae	1	0.0%	0.0%	0.03*	0.2%	**0.5%**
Actinobacteria	0.2	1.2%	0.6%	0.06	1.3%	0.3%
Acidimicrobia	1	0.0%	0.0%	0.2	0.3%	0.4%
Planctomycetia	0.77	0.1%	0.2%	0.2	0.4%	0.9%
OM190	0.19	0.0%	0.0%	0.03*	0.1%	**1.3%**
Fibrobacteria	0.66	0.0%	0.0%	0.2	0.6%	0.4%
Opituta	1	0.2%	0.1%	0.03*	0.0%	0.2%
SAR202	NA	0.0%	0.0%	0.89	0.1%	0.0%
Thaumarchaeota	NA	0.0%	0.0%	0.03*	0.0%	**0.2%**
Clostridia	0.11	0.4%	0.0%	0.49	0.3%	0.2%
Bacteroidia	0.41	0.2%	0.0%	0.69	0.3%	0.2%
Phycisphaera	1	0.1%	0.0%	0.11	0.1%	0.3%
Epsilonproteobacteria	0.87	0.0%	0.0%	0.36	0.5%	0.1%
SHAB590	0.45	0.0%	0.0%	0.46	0.1%	0.3%
BS119	0.19	0.0%	0.0%	0.03*	0.0%	**0.2%**
Sphingobacteria	1	0.0%	0.0%	0.2	0.0%	0.1%
Halobacteria	0.45	0.0%	0.0%	1	0.1%	0.1%

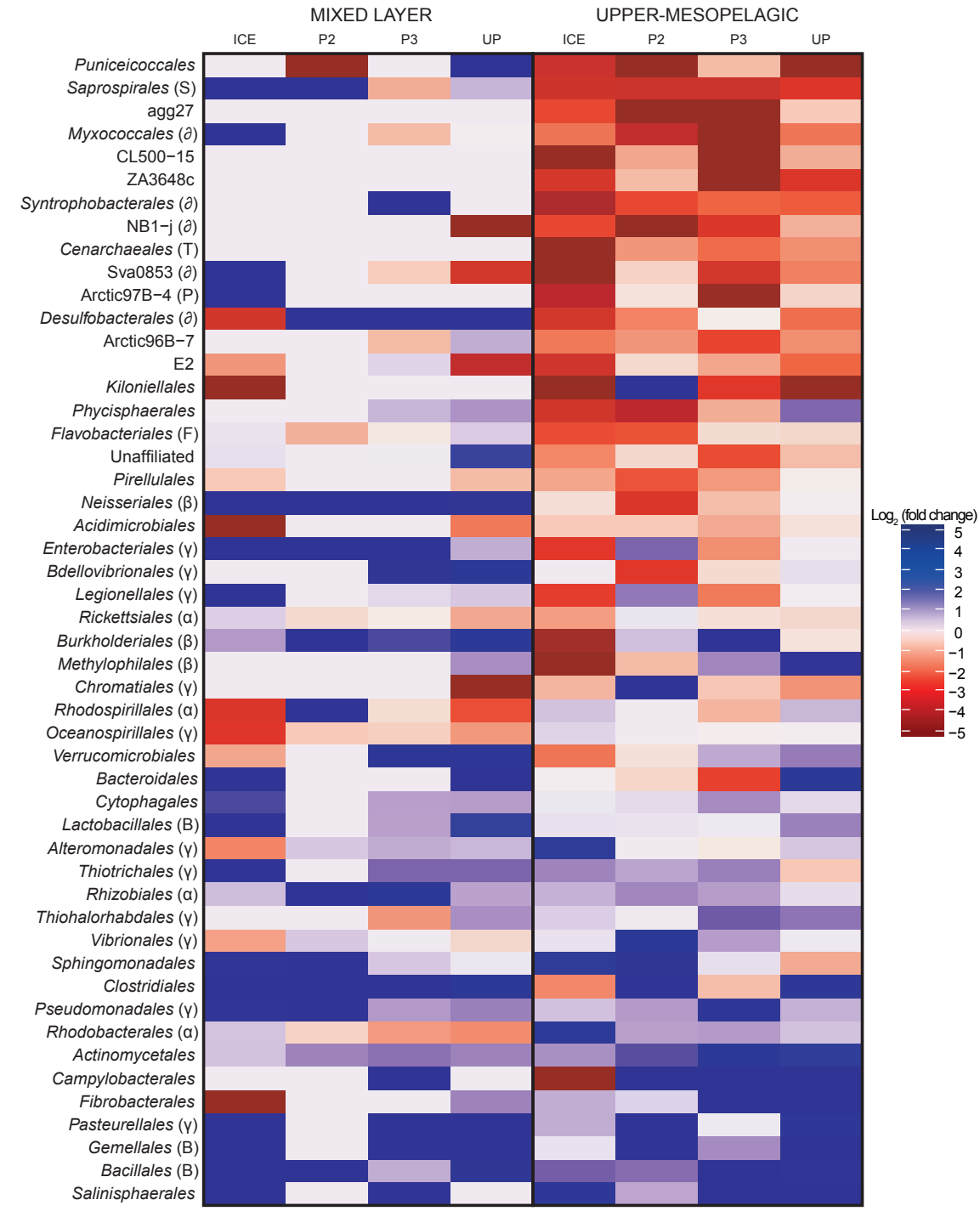

Figure 3.4. Enrichment of taxonomic orders in suspended and sinking particle-associated communities. The $\log_2$ (fold change) was calculated for the 50 most abundant taxonomic orders and is based on their relative abundance within sinking and suspended particle-associated communities (see Equation 1). Negative values (red) correspond to an enrichment in suspended particles and positive values (blue) in sinking particles. The legend values of 5/-5 correspond to Inf/-Inf, i.e., showing the absolute absence of an order in a sample compared to its counterpart. Indicated between parentheses are the families belonging to the following classes: α = *Alphaproteobacteria*; β = *Betaproteobacteria*; δ = *Deltaproteobacteria*, γ = *Gammaproteobacteria*; B = *Bacilli*, F = *Flavobacteria*; P = Pedospharae; S = *Saprospirae*; T = *Thaumarchaeota*.

At the taxonomic order level (order in Fig. 3.4), suspended particle-associated communities were enriched in; *Bacteroidetes* (including *Saprospirales* and *Flavobacteriales*), *Planctomycetes* (*Planctomycetales*, *Pirellulales* and OM190 relatives), *Euryarchaeota* (*Cenarchaeales*) and *Crenarchaeota* (*Thermoplasmata*, E2), as well as in several orders from *Deltaproteobacteria* (*Spirobacillales*, *Myxococcales*, *Syntrophobacterales*, *Desulfobacterales*, and PB19, NB1-j and Sva0853 relatives), and from *Verrucomicrobia* (*Puneiceicoccales*, *Pedosphaerae*), the betaproteobacterial *Neisserales*, the actinomicrobial *Acidimicrobiales*, and the SAR406 relatives (ZA3648c and Arctic96B-7) in the upper-mesopelagic. On the other hand, sinking particle-associated communities were enriched in *Gammaproteobacteria* (including *Pseudomonadales*, *Vibrionales*, *Pasteurellales* and *Salinisphaerales*), *Alphaproteobacteria* (*Rhodobacterales* and *Rhizobiales*), *Firmicutes* (*Bacillales*, *Gemellales* and *Lactobacillales*) and *Actinobacteria* (*Actinomycetales*), as well as the *Bacteroidetes* order *Cytophagales* and the *Fibrobacteres* order *Fibrobacterales* in the upper-mesopelagic.

In the mixed layer, only the gammaproteobacterial *Oceanospirillales* was enriched within suspended particle-associated communities. Conversely, *Gammaproteobacteria* (*Pseudomonadales* and *Enterobacteriales*), *Betaproteobacteria* (*Burkholderiales* and *Neisseriales*), *Alphaproteobacteria* (*Sphingomonadales* and *Rhizobiales*) and *Firmicutes* (*Bacillales*, *Clostridiales* and *Gemellales*) orders, as well as the *Actinobacteria* order *Actinomycetales* was enriched within sinking particle-associated communities.

3.4 Discussion

This study is the first to compare microbial communities associated with suspended and sinking particles using next-generation amplicon sequencing of the V4 16S rRNA genes. Our results reveal previously undiscovered differences between the two prokaryotic communities and clear differences between suspended and sinking particle-associated communities in terms of structure and diversity. Taxa collectively known as particle-associated were found significantly enriched in either suspended or sinking particles.

Although significant at both depths, prokaryotic niche partitioning observed between the two particle-associated communities was more evident in the upper-mesopelagic than in the mixed layer.

3.4.1 Suspended and sinking particles niche partitioning

Regardless of site-to-site differences, particle-type was the factor explaining most of community composition variability, with suspended and sinking particle-associated communities displaying enrichments in specific taxa. Members of *Gammaproteobacteria*, alphaproteobacterial *Rhodobacterales* and *Bacteroidetes* are ubiquitous heterotrophic members of oceanic bacterial communities, which bloom in association with phytoplankton populations (Buchan et al., 2014). These common particle-associated taxa (Delong et al., 1993; Crespo et al., 2013; Bižić-Ionescu et al., 2014; Lecleir et al., 2014; Fontanez et al., 2015; López-Pérez et al., 2016) were significantly enriched in either suspended or sinking particle-associated communities.

In the upper-mesopelagic, sinking particle-associated communities were significantly enriched in *Gammaproteobacteria* (including *Pseudomonadales*, *Vibrionales* and *Pasteurellales*), *Alphaproteobacteria* (*Rhodobacterales* and *Rhizobiales*), *Actinobacteria* and *Firmicutes*. Gammaproteobacterial *Pseudomonadales* and *Vibrionales* (Pinhassi and Berman, 2003; Allers et al., 2007; Mason et al., 2012; Stewart et al., 2012; Logue et al., 2015; Liu et al., 2017), as well as members of Rhodobacterales, including Rhodobacteraceae (Buchan et al., 2005; Brinkhoff et al., 2008; Mayali et al., 2015), are generalist copiotrophs exhibiting surface-attachment capabilities (e.g., biolfim formation, pili, non-specific extracellular polymers and proteins). Their versatile metabolic capabilities allow them to utilise a wide spectrum of phytoplankton-derived organic matter substrates, ranging from monocyclic to aromatic compounds (labile to more refractory compounds) (Sperling et al., 2017). They respond rapidly to enrichments of organic matter, both in dissolved and particulate forms, in their environment owing to their sensory chemotaxis systems and motility abilities. They are commonly considered as primary colonisers of

marine particles which initiate the process of remineralisation (Dang and Lovell, 2016). Microbial communities associated with sinking particles are thought to be relatively stable with depth. Recent reports indicate that colonising communities at depth most likely originate from the euphotic zone, which are modified as the particle sinks, as opposed to resulting from a succession of colonisers (Thiele et al., 2015).

Chemotaxis, motility and surface attachment capabilities as well as acute competition strategies would allow these taxa to rapidly sense, colonise and consume POM in sinking particles. Subsequently, their ability to degrade low- to high-molecular-weight (LMW to HMW) organic compounds would allow them to degrade the transient composition of organic matter within sinking particles as they sink and become increasingly refractory. Furthermore, their aptitude to produce antimicrobial secondary metabolites and quorum sensing signalling molecules coupled with biofim forming strategies (Givskov et al., 1997; Whitehead et al., 2001; Gram et al., 2002; Buchan et al., 2005; Thomas et al., 2008; Dang and Lovell, 2016) could allow them to regulate specific traits (such as motility loss, exoenzyme production) to enhance their competiveness in order to exploit the ecological niche constituted by sinking particles.

On the other hand, the phylum *Bacteroidetes* (including *Flavobacteriales* and *Saprospirales*), *Planctomycetes* (*Planctomycetales* and *Pirellulales*), *Deltaproteobacteria* (*Desulfobacterales* and *Myxococcales*) and *Verrucomicrobia* were significantly enriched within suspended particle-associated communities in the upper-mesopelagic. *Planctomycetes* and *Verrucomicrobia* have been reported to have abilities for surface-attachment, such as on detrital aggregates (Delong et al., 1993; Crump et al., 1999), and for biopolymers degradation (García-Martínez et al., 2002; Woebken et al., 2007). *Flavobacteria* also have adaptations for surface-attachment (Gómez-Pereira et al., 2012). These taxa are typically associated with the decaying phase of phytoplankton blooms (Buchan et al., 2014) and are considered secondary particle colonisers (Dang and Lovell, 2016). Unlike their counterparts on sinking particles, *Flavobacteria* appears to be specialised in the degradation of complex and HMW organic compounds (Bauer et al.,

2006; Williams et al., 2013; Kabisch et al., 2014). Accordingly, unlike *Roseobacter* whose genomes are abundant in ABC transporters (specialised in the uptake of LMW compounds) encoding genes, *Flavobacteria* genomes are abundant in genes encoding for TonB dependent-transporters that are active in the uptake of HMW molecules (Tang et al., 2012).

Reintjes et al. (2017) has shown both *in vivo* and *in vitro* that *Bacteroidetes* members are able to assimilate large polysaccharides in their periplasmic space, where subsequent hydrolysis to LMW and cell-uptake takes place. This "selfish" hydrolysis strategy leads to a reduction of diffusive loss to the cell surroundings. This uptake mechanism is more efficient than the one traditionally assumed to take place on sinking particles, by which hydrolytic exoenzymes released by the associated heterotrophic community leads to the formation of a plume enriched in dissolved organic matter consumed by free-living communities (Smith et al., 1992; Kiørboe and Jackson, 2001). If relevant to other members of the suspended particle-associated community, this restrictive strategy of organic matter consumption could be an ecological indicator of the differential nature of organic substrate present within suspended and sinking particles. Whereby, suspended particle-associated communities specialise in energy-efficient hydrolytic pathways to consume semi-labile organic matter, while competitive colonisers in sinking particles rapidly adapt to the transient nature of organic matter, ranging from labile to refractory as the particle sinks.

Although suspended and sinking particle-associated communities share features, their structure and diversity also varied among sampled stations driven by environmental factors like temperature, particulate organic carbon and chlorophyll *a* concentrations. UP and P3 are characterised by higher primary production levels than P2 and ICE owing to their influence by South Georgia continental margin that upwells nutrients into surface waters (Atkinson et al., 2001). Samples from ICE, located on the marginal ice zone of the Antarctic continent, were strong outliers. Melting ice provides nutrients-rich cold and salty brines to the surface layer that are responsible for shaping prokaryotic communities.

These communities are generally dominated by psychrophilic bacteria adapted to sub-zero temperatures and high-salinity conditions (Brown and Bowman, 2001).

3.4.2 Organic matter as a driver for life strategy

Most *Gammaproteobacteria* members (Lauro et al., 2009; McCarren et al., 2010) and *Rhodobacterales* (Dang and Lovell, 2016) are primary coloniser r-strategists – they grow rapidly to competitively exploit transient sources of organic matter. At the other end of the spectrum, *Bacteroidetes* are secondary coloniser K-strategists, specialised in the degradation of complex HMW organic compounds (Bauer et al., 2006). The differential metabolic capabilities of r- and K-strategists is enabled by their distinct genomic repertoires (Lauro et al., 2009). The two life strategies have been previously applied to explain variability of free-living microbes in stable oligotrophic environments versus in transient nutrient-rich environments (Giovannoni et al., 2014). We propose that a similar theory could be applied to particle-associated communities in order to explain enrichments of r-strategists on sinking particles and K-strategists on suspended particles. The niche differentiation between ubiquitous heterotrophic bacteria in suspended and sinking particles may be driven by the differential nature of organic matter available within the two particle-pools in the Scotia Sea.

Heterotrophic bacteria differ in their ability to degrade organic matter, which is why modifications in phytoplankton composition lead to a succession in associated bacterial community (Pinhassi et al., 2004; Teeling et al., 2012). Furthermore, as the phytoplankton bloom ages, the composition of organic matter produced changes; starting from labile LMW compounds at early stages (e.g., amino acids, carbohydrates), to HMW compounds at later stages (e.g., nucleic acids, polysaccharides) (Buchan et al., 2014). Accordingly, inexperimental and environmental settings of organic matter enrichments, alteromonads are first detected closely followed by *Rhodobacterales* and prior to being eventually outcompeted by *Flavobacteria*, as the organic matter lability decreases (*in situ* – e.g., Fuchs et al., 2000; Sheik et al., 2014 – and *in vitro* – e.g., Yamada et al., 2016). This

suggests that suspended particles in the upper-mesopelagic contained a higher proportion of semi-labile organic matter, which would be favourable for K-strategists. Meanwhile, r-strategists would colonise sinking particles in the euphotic zone, where organic matter is relatively fresh, and would subsequently modify their metabolism as the particle sinks alongside changing in organic matter composition. Although organic matter quality is likely to be a major determining factor upon the selection of r-/K-strategists in particle-associated communities, other intrinsic capabilities may also add to the selection process (such as hydrolytic abilities, biofilm formation, quorum sensing mechanisms, chemotaxis sensitivity and motility speed).

3.4.3 Differential particle dynamics with depth

Differences observed between suspended and sinking particle-associated communities were more pronounced in the upper-mesopelagic than in the mixed layer. Within the mixed layer, a plethora of biotic and abiotic processes take place, including; microbial remineralisation (leading to the release of dissolved organic matter – e.g., Carlson, 2002 – and particulate organic matter – e.g., Turner, 2015), zooplankton feeding activities (Giering et al., 2014) and turbulent mixing. These processes lead to continuous aggregation and disaggregation of particles, altering their sizes and other physochemical properties (Burd and Jackson, 2009). Particle dynamic processes linking suspended and sinking particle-pools together are more intense in the mixed layer than in the upper-mesopelagic (Lam and Marchal, 2015). The higher proportion of taxa showing an enrichment in either particle-type in the upper-mesopelagic than in the mixed layer corroborates the higher connectivity between the two particle-types. Adding to the higher connectivity of particle pools, inherent physiological traits of heterotrophic bacteria could also reduce differences between prokaryotic communities associated with either particle-type. For instance, motility of marine heterotrophic microbes is enhanced in highly productive environments (Dang and Lovell, 2016), such as within the mixed layer.

3.5 Conclusion

While typical ubiquitous particle-associated remineralising taxa were expectedly found in our samples, suspended and sinking particle-associated communities were not identical. In the upper-mesopelagic, the niche partitioning of heterotrophic taxa likely reflects a different life strategy imposed by the composition of organic matter available within the two particle-pools. K-strategists would exploit more refractory compounds bound to suspended particles, while r-strategists would benefit from their broad hydrolytic capabilities to degrade the transient composition of organic compounds in sinking particles. In the mixed layer, continuous dynamic biotic and abiotic processes alter particles, which leads to a higher connectivity between the two particle-associated communities.

While sinking particles are primarily responsible for the rapid delivery of labile particulate organic carbon to the upper-mesopelagic, suspended particles constitute the majority of marine particulate organic carbon in the ocean and support most of the microbial carbon respiration in the mesopelagic (Baltar et al., 2009, 2010). This correlates with extremely low respiration rates measured on sinking particles at the same stations (~ 5.19 ng C h^{-1} $particle^{-1}$) (Belcher et al., 2016). Consequently, suspended and sinking particle-associated communities are likely to play different roles in biological carbon pump. As most suspended particles come from the disaggregation of sinking particles, their associated microbial communities coupled with free-living communities undertake final remineralisation steps leading to most of CO_2 production (Collins et al., 2015), thereby reducing the biological carbon pump efficiency. Further investigations are required to uncover metabolic pathways active in carbon remineralisation as well as their rates of occurrence within the two particle-types in order to provide more information on how organic carbon is remineralised in the ocean.

3.6 Experimental procedures

3.6.1 Sampling stations and particle collection

Sampling took place during the austral summer 2014 (15 November – 17 December) on-board the RRS James Clark Ross (cruise JR304). Four stations of contrasting nutrient regimes and productivity in the Scotia Sea were sampled, including two low-productivity stations – ICE at the marginal ice edge and P2 in a high-nutrient-low-chlorophyll region – and two more productive stations – P3 in an iron-enriched region and UP in an upwelling region (Table 3.1). Surface chlorophyll *a* data represented on the map (Fig. 2.3) was constructed with the Ocean Data View software (https://odv.awi.de) using the mean values for December 2014 collected by the MODIS satellite (http://oceancolor.gsfc.nasa.gov/cgi/l3).

Particles were collected with a marine snow catcher (MSC) (Fig. 2.1) deployed in the mixed layer (10m below the deep chlorophyll maximum [DCM]) and the upper-mesopelagic (110m below the DCM) within ~ 30 minutes of each other, the former depth usually corresponding to a peak in particle abundance (Lampitt et al., 1993; Belcher et al., 2016). The deep chlorophyll maximum was defined by using fluorescence profiles from the conductivity-temperature-depth sensors (CTD Seabird 9Plus with SBE32 carousel) cast, at most, 4 hours prior to the MSC deployment (Annex A1). Temperature, oxygen concentration and chlorophyll *a* concentration based on fluorescence measurements were obtained from CTD casts, and particulate organic carbon concentrations were measured from samples collected with the MSC as measured by Belcher et al. (2016).

Suspended and sinking particles were collected from the upper part and the base of the MSC respectively. Sinking particles are here defined as the particles that have sunk to the base of the MSC bottom after standing on deck for 2 hours (average sinking speed ≥ 12 m d^{-1}) and include both slow- and fast-sinking particles (Riley et al., 2012). Particles remaining buoyant in the upper part of the MSC are considered suspended. Microbial

communities associated with suspended particles were sampled by sequentially filtering ~10 L of seawater collected from the upper part of the MSC through; (i) a 100 µm pore-size nylon filter (47 mm diameter, Millipore), (ii) a 10 µm pore-size polycarbonate membrane filter (47 mm diameter, Millipore), and (iii) a 0.22 µm pore-size Sterivex cartridge filter (Millipore) driven by a peristaltic pump. Microbial communities associated with sinking particles were collected by gravity-filtering ~1.5 L of seawater from the bottom part of the MSC onto a 10 µm pore-size polycarbonate membrane filter. Both filtering steps were performed in under 1 hour, and filters were subsequently incubated with RNAlater (Ambion™, Thermo Fisher Scientific) for 12 hours at 4˚C, prior to being stored at -80˚C until further processing onshore. All equipment used for sampling procedures were cleaned in RNaseZap (Ambion™, Thermo Fisher Scientific) and rinsed with Milli-Q water prior to sampling.

3.6.2 DNA extraction, amplification and sequencing

Nucleic acids were recovered from the filters using a ToTALLY RNA kit (Ambion™, Thermo Fisher Scientific) followed by a DNA extraction step as described in Lam et al. (2011) – though only DNA extracts were considered in this study. Extracted DNA was further purified with a Wizard DNA clean-up system (Promega) following the manufacturer's recommendations.

Prior to amplification, the DNA extracted from 100 and 10 µm pore-size filters of suspended particles were pooled together to allow comparison with 10 µm pore-size filters collected from sinking particles, and hence consider particles ≥ 10 µm. DNA extracts from both filters were pooled in equal volumes in order to preserve the signal ratios and avoid distortion of the community structure on suspended particles ≥ 10 µm and were used as a template for PCR amplification.

Amplicon sequencing of prokaryotic 16S rDNA V4 region was performed according to Herbold et al. (2015). The primer set Pro341F (5'-CCTACGGGNBGCASCAG-3') and Pro805R (5'-GACTACNVGGGTATCTAATCC-3'; 464 bp) (Takahashi et al., 2014), and

proofreading polymerase Kapa HiFi HotStart (Kapa Biosystems), including overhang adapters (respectively 5'-TCGTCGGCAGCGTCAGATGTGTATAAGAGACAG and 5'-GTCTCGTGGGCTCGGAGATGTGTATAAGAGACAG), were used at first for a 25-cycle PCR. Amplicons were subsequently used as templates for a 10-cycle index PCR for the overhangs to be linked to Illumina sequencing adapters and indices (Nextera XT Index Primer 1 [i7] and Primer 2 [i5]) for downstream sequencing. As one sample (UP station sinking particle in the mixed layer) had a total amount of extracted DNA less than 12.5 ng, a nested PCR approach was applied with an additional amplification using the universal 16S rDNA primers set, 27F (5'-AGAGTTTGGATCMTGGCTCAG-3') and 1492R (5'-ACCTTGTTACGACTT-3'; 1,465bp) prior to the two-step PCR procedure described above. This procedure did not change the profile of the communities as evidenced by Annex A9-A and A9-B, including the nested PCR sample from this study along with other samples collected during the same cruise that were amplified using the same method. After each PCR round, amplicons were purified with the Agencourt AMPure XP PCR clean-up kit (Beckman Coulter) following manufacturer's recommendations. The quality of purified amplicons was assessed with a DNA7500 Kit read on a 2100 BioAnalyser (Agilent Technologies), and the quantity measured with a Qubit dsDNA High-Sensitivity assay kit (Invitrogen™, Thermo Fisher Scientific).

Purified amplicons were pooled at equimolar concentrations (4 nM each) for the library preparation using a Nextera XT DNA kit (Illumina) following manufacturer's recommendations and included 5 % PhiX. Finally, the amplicons were sequenced with an Illumina MiSeq sequencing system (M02946, Illumina) using a MiSeq Reagent 600-cycle Kit v3 (Illumina).

3.6.3 Bioinformatics

The sequence data has been submitted to the GenBank under accession number SUB2922837. Raw sequences were demultiplexed and their adapter sequences trimmed using the MiSeq Control software (v 2.5.0.5, Ilumina) directly after sequencing. The quality

of demultiplexed raw read pairs was checked with FastQC (v 0.11.4; Babraham Bioinformatics). Forward and reverse reads were merged with the PANDAseq assembler software (v 2.8) (Masella et al., 2012) using the default parameters (simple Bayesian algorithm for assembly) and a maximum read length of 500 bp and Phred33 quality score of 0.8. OTU clustering was subsequently performed under QIIME (MacQIIME v 1.9.1_20150604) (Caporaso et al., 2010) after all libraries were compiled into a single FASTA file using the *multiple_split_libraries_fastq.py* function. Clustering was performed using the open reference function *pick_open_reference_otus.py* using default parameters (UCLUST algorithm for OTU picking) using a minimum sequence identity of 97% against the 16S rRNA Silva database (v 128) (Quast et al., 2013). Singleton OTU and sequences affiliated with chloroplastic rDNA were removed from this dataset.

3.6.4 Data analyses

The non-parametric multidimensional scaling (NMDS) analysis and the unweighted pair group method with arithmetic mean (UPGMA) tree were based on the Bray Curtis dissimilarity distance of OTU relative abundance compositions. The significance of factors influencing the communities OTU composition was investigated with permutational multivariate analyses of variance (PERMANOVA). Similarity percentage analysis (SIMPER) was used to investigate average differences between community compositions within each station at the family level. α-diversity was estimated using Shannon's and Pielou's indices as well as the unbiased number of OTU. The significance of relative abundance differences between particle-associated communities was investigated using a Kruskall-Wallis test (KW, $p < 0.05$).

Enrichment was calculated based on the $\log_2$ (fold change) of taxonomic order relative abundance differences between sinking and suspended particle-associated communities in the rarefied dataset. It was calculated using the following equation:

$$Enrichment = \log_2\left(\frac{RA_{sinking}}{RA_{suspended}}\right)$$

Equation 3.1. Taxa enrichment in sinking versus suspended particles.

With $RA_{sinking}$ as the relative abundance of the taxa in sinking particle-associated community at one depth and $RA_{suspended}$ as the relative abundance of the same taxa in suspended particle-associated community at the same depth.

Statistical analyses were performed with the R statistics software (http://www.r-project.org) using the *vegan* package. In order to retain as many sequences as possible given differences in sequencing depths, different rarefaction strategies were used depending on the analyses performed. For the calculation of SIMPER and the proportions of shared/unique OTU, the dataset was rarefied to the smallest library size in a considered station (n = 9,716 sequences for ICE; 6,460 for P2; 17,654 for P3 and 15,404 for UP). Multivariate analyses comparing samples from all stations (NMDS, UPGMA, PERMANOVA and α-diversity) were performed on the dataset rarefied to the smallest library size (n = 2,613 sequences/library). The taxonomic composition of communities at various levels is based on the relative abundance of the non-rarefied dataset.

Chapter 4: Eukaryotic contribution to suspended and sinking particles and potential influence on the oceanic biological carbon pump

This chapter is in preparation for submission to *Limnology and Oceanography Letters* as:

Eukaryotic contribution to suspended and sinking particles and potential influence on the oceanic biological carbon pump

Manon T Duret[1]*, Richard S Lampitt[2], Phyllis Lam[1]

[1]Ocean and Earth Science, University of Southampton

[2]National Oceanography Centre Southampton

PL, MTD and RSL designed the study. MTD collected and analysed samples, conducted data analysis and wrote the manuscript. PL assisted in the manuscript preparation. RSL provided feedback on the manuscript.

4.1 Abstract

Suspended marine particles contain most of the particulate organic matter in the ocean thereby providing an organic substrate for heterotrophs, and especially those in the mesopelagic. Conversely, sinking particles are major contributors to the carbon flux defining the strength of the biological carbon pump.

This study is the first to investigate the distribution of eukaryotic communities among sinking and suspended particles using amplicon 18S rRNA gene sequencing on particles collected in the mixed layer and upper-mesopelagic of the Scotia Sea (Southern Ocean). We investigated the influence of phytoplankton and metazoans on particulate organic matter flux from the mixed layer to the mesopelagic and on suspended particles in the upper-mesopelagic as well as the distribution of hetero/mixotrophic protists between both particle-types.

Chain-forming diatoms constituted most of phytoplankton sequences recovered in sinking particles collected in the upper-mesopelagic, while prymnesiophytes constituted most sequences from suspended particles. This suggests that diatom-enriched aggregates are more efficient in the transfer of carbon to the mesopelagic when compared to prymnesiophyte-enriched aggregates, which are likely to break down into suspended particles. While copepods were most influential on sinking particles, soft-tissue animals appeared to contribute to suspended particle composition in the upper-mesopelagic. Finally, mesopelagic hetero/mixotrophic protist communities associated with the two particle-types differed. Further work is needed to decipher their exact role in particle attenuation and, hence, the regulation of the biological carbon pump efficiency.

4.2 Introduction

The oceanic biological carbon pump (BCP) corresponds to the processes by which the organic matter produced by phytoplankton photosynthesis in the epipelagic ocean (~ < 100 m) is exported to depth, thereby sequestrating atmospheric carbon in the mesopelagic (~ 100 to 1000 m) and deeper ocean (Turner, 2015). This downward export of organic matter removes more than 10 billion tons of carbon from the epipelagic each year (Buesseler and Boyd, 2009), corresponding to 5 to 25% of photosynthetic primary production reaching the mesopelagic (De La Rocha and Passow, 2007). Most of this carbon flux occurs in the form of particulate organic matter (POM). This POM consists of a combination of different materials such as faecal pellets, living and non-living microbial cells and fragments, as well as empty larvacean houses, all of which can be included into large aggregated entities (marine snow). The nature of sinking particles depends largely on the structure of phytoplankton community (Lin et al., 2017; Korb et al., 2012), as well as the heterotrophic community members, including mesozooplankton (> 200 µm) (Steinberg and Landry, 2017) and heterotrophic microbes (prokaryotic members and unicellular eukaryotes, also known as protists) (Worden et al., 2015).

Heterotrophic communities alter the BCP efficiency, either; (i) negatively by leading to a decrease in carbon export caused by remineralisation processes, which release carbon dioxide (CO_2) and dissolved organic matter (DOM) (Cho and Azam, 1988; Kiørboe and Jackson, 2001; Smith et al., 1992; Collins et al., 2015; Steinberg et al., 2008) or (ii) positively by enhancing particle export to depth. Mesozooplankton can lead to an increase of particle export by grazing on phytoplankton cells, thereby repackaging them into larger particles as faecal pellets (≥ 50 µm depending on the species) (Stamieszkin et al., 2017), which subsequently sink faster (Ebersbach et al., 2011; Atkinson et al., 2001; Giesecke et al., 2010). Furthermore, vertical migration of mesozooplankton may also lead to active transfer of organic matter from one depth to another as they feed on POM at the surface and release faecal pellets and DOM at greater depths (Steinberg et al., 2000).

Conversely, they also consume sinking particles by sloppy feeding, thereby causing the release of DOM (Strom et al., 1997) and their breakage into smaller particles that may remain in suspension in the water column (De La Rocha and Passow, 2007). The proportion of suspended particles originating from the disaggregation of sinking particles is currently unknown (Lam and Marchal, 2015), as it is governed by abiotic processes as well as other biotic processes such as the feeding behaviours of micro- and nanozooplankton (protists 20 – 200 µm and 2 – 20 µm respectively) (Poulsen and Iversen, 2008; Ploug and Grossart, 2000).

There is an enrichment of heterotrophic protists, such as flagellates and ciliates, on large sinking particles relative to the surrounding waters (Simon et al., 2002), even in the bathypelagic ocean (~ > 1000 m) (Bochdansky et al., 2017). Furthermore, micro- and nanozooplankton consume ~ 60 % of the daily phytoplankton primary production (Calbet and Landry, 2004; Schmoker et al., 2013) and can produce “minipellets” (3 – 50 µm faecal pellets) (Gowing and Silver, 1985), which can also contribute to POM export to the mesopelagic if dense enough. Nonetheless, as they consume phytoplankton primary production, they allow organic matter to enter the microbial loop thereby lengthening the “food chain”, which results in greater carbon losses (Pomeroy and Wiebe, 1988). In other words, they can consequently reduce the efficiency of the BCP. Although there have been studies focusing on differences between various sizes of freely suspended and particle-associated protists communities (e.g., cut-off at 30 µm [Duret et al., 2015; Bochdansky et al., 2017], 1.6 µm [Parris et al., 2014]) remain largely understudied, especially their heterotrophic members (Caron et al., 2017; Edgcomb, 2016).

The consumption of particles by heterotrophs leads to a decrease in the concentration of sinking particles with depth (Martin et al., 1987; Francois et al., 2002). On the other hand, the quantity of suspended particles remains constant with depth, with a POC concentration at ~ two or more orders of magnitude higher than that of sinking particles (Bacon et al., 1985; Riley et al., 2012; Baker et al., 2017; Cavan et al., 2017; Giering et al., 2014; Verdugo et al., 2004; Bishop et al., 1977). Especially in the mesopelagic,

suspended particles are major substrates of organic carbon for heterotrophic microbes (Baltar et al., 2009, 2010; Herndl and Reinthaler, 2013) and micronekton (fish, cephalopods and crustaceans) (Gloeckler et al., 2017). Like sinking particles, they are hotspots for microbial activity and diversity (Bochdansky et al., 2010). However, most studies on particle-associated microbial communities thus far have focused on sinking particles, and primarily, on their prokaryotic members. The main reason behind this knowledge gap is the difficulty to sample suspended particles separately from sinking particles.

Conventional sampling methodologies used for marine microbial communities are unable to distinguish between suspended and sinking particles as they either collect; (i) a mixture of both particle-types in unknown proportions (e.g, size-fractionated filtration of seawater), or (ii) mainly large sinking particles (e.g., sediment traps) (McDonnell et al., 2015). The marine snow catcher (MSC) (Lampitt et al., 1993) is a large water-sampler that uses sinking velocity to differentiate suspended from sinking particles originating from the same water sample. After its retrieval from the desired depth, the MSC is left undisturbed on the ship's deck for two hours. This period allows sinking particles to sediment at the bottom of the sampler (MSCB) while suspended particles remain in suspension in the upper part (MSCU) (Fig. 2.1). Water samples are collected from the MSCU followed by the MSCB, and both are subsequently size-fractionated to further separate collected particles into size-classes. A parallel study conducted in the Scotia Sea (Southern Ocean) has already found distinct prokaryotic communities associated with sinking and suspended particles collected with the MSC (Chapter 3). Notably, common remineralising taxa *Pseudomonadales*, *Vibrionales* and *Rhodobacterales* were found enriched within sinking particles, while Bacteroidetes were enriched within suspended particles. Furthermore, a study performed in the northeast Atlantic Ocean has uncovered differences in the active eukaryotic communities collected from the MSCU and MSCB (Chapter 5).

High-throughput amplicon sequencing of the V4 18S rRNA encoding gene was used to investigate the composition and structure of particle-associated protist communities using

the MSC. Suspended and sinking particles were collected at two depths of four stations of contrasting productivity regimes in the Scotia Sea during austral summer 2014. The objective of this study is to determine the eukaryotic contributions to suspended and sinking particles. More specifically; (i) which phytoplankton taxa are the most efficient in particulate carbon export to the mesopelagic, (ii) what metazoan and phytoplankton taxa influence sinking and suspended particles in the upper-mesopelagic, (iii) are mesopelagic heterotrophic and mixotrophic protists residing on the two particle-types different, and if so, (iv) how does their distribution affect sinking particle attenuation.

4.3 Material and methods

4.3.1 Study site

Sampling took place during austral summer 2014 (15 November – 12 December) on-board the RRS James Clark Ross (cruise JR304). In the Scotia Sea, four stations of contrasting nutrient regimes and surface productivity were sampled, including two low-productivity stations – ICE (-59.9624˚N, -46.1597˚E) and P2 (-55.2484˚N, -41.2640˚E) – and two more productive stations – P3 (-52.8121˚N, -39.9724˚E) and UP (-52.06018˚N, -39.1994˚E) (Table 3.1). Surface chlorophyll *a* data is presented on a map constructed with the Ocean Data View software (https://odv.awi.de) using the mean values for December 2014 collected by the MODIS satellite (http://oceancolor.gsfc.nasa.gov/cgi/l3) (Fig. 2.3).

4.3.2 Hydrographic settings

The two less productive stations were located on the Antarctic continental ice-edge (ICE) and in a high nutrient low chlorophyll zone (P2), whereas the two more productive stations were located in an iron fertilised zone from South Georgia continental margin (P3) and in an upwelling zone at the frontal system of polar front zone and the Antarctic zone (UP) (Fig. 2.3). P3 and UP were in close vicinity and showed higher chlorophyll *a* concentrations (average of 1.90 and 1.23 µg L^{-1} in the mixed layer, respectively), while

ICE and P2 were further apart and had lower surface chlorophyll *a* concentrations (respectively 0.37 and 0 40 µg L^{-1}) (Table 3.1). There was a sharp temperature decrease between the mixed layer depth and the upper-mesopelagic (10 m and 100 m below the DCM) at all stations except ICE, at which the surface temperature was low (< -1˚C) due to freshly melted ice.

4.3.3 Particle sampling

Particles were collected with an MSC (Fig. 2.1) deployed in the mixed layer (10 m below the deep chlorophyll maximum [DCM]) and in the upper-mesopelagic (110 m below the DCM) within ~ 30 minutes of each other. The base of the mixed layer usually corresponded to a peak in particle abundance in this region (Belcher et al., 2016). The DCM was defined by using fluorescence profiles taken during the conductivity-temperature-depth (CTD Seabird 9Plus with SBE32 carousel) cast maximum 4 hours prior to the MSC deployment (Annex A1). Temperature, oxygen concentration and chlorophyll *a* concentration based on fluorescence measurements were obtained from CTD casts, and particulate organic carbon (POC) concentrations were measured from samples collected with the MSC (Table 3.1) and measured as described by Belcher et al. (2016).

Suspended and sinking particles were collected from the upper part (MSCU) and the bottom part of the MSC (MSCB) respectively (Fig. 2.1). Sinking particles are defined here as the particles that have sunk to the MSCB after 2 hours (average sinking velocity ≥ 12 $m.d^{-1}$) and include both slow- and fast-sinking particles (Riley et al., 2012). Particles remaining in suspension in the MSCU are considered suspended. Both sinking and suspended particles consisted of a mixture of single free-living cells and cells associated with particles or aggregates. For all stations, POC concentrations were higher in suspended particles, and within the mixed layer depth compared to the upper-mesopelagic (Table 3.1).

Suspended particles were sampled by sequentially filtering ~ 10 L of seawater collected from the MSCU through; i) a 100 µm pore-size nylon filter (47 mm diameter, Millipore), ii)

a 10 µm pore-size polycarbonate membrane filter (47 mm diameter, Millipore), and iii) a 0.22 µm pore-size Sterivex cartridge filter (Millipore) driven by a peristaltic pump. Sinking particles were collected by gravity filtering ~ 1.5 L of seawater collected from the MSCB onto 10 µm pore-size polycarbonate membrane filter. Both filtering steps were performed in under 1 hour, and filters were subsequently incubated with RNAlater (Ambion™, Thermo Fisher Scientific) for 12 hours at 4˚C, prior to being stored at -80˚C until further processing onshore. All equipment used for sampling procedures was cleaned in RNaseZap (Ambion™, Thermo Fisher Scientific) and rinsed with Milli-Q water prior to sampling.

Four particle fractions were collected in total at each station and each depth: (i) suspended particles 0.22 – 10 µm (referred to as SS0.22), (ii) 10 – 100 µm (SS10), and (iii) ≥ 100 µm (SS100), as well as (iv) sinking particles ≥ 10 µm (SK10).

4.3.4 DNA extraction and sequencing

Nucleic acids were recovered from the filters using a ToTALLY RNA kit (Ambion™, Thermo Fisher Scientific) followed by a DNA extraction step as described in Lam et al. (2011) – though only DNA extracts were considered in this study. Extracted DNA was further purified with a Wizard DNA clean-up system (Promega) following manufacturer's recommendations.

Amplicon sequencing of eukaryotic 18S rDNA V4 region was performed according to Hadziavdic et al. (2014). The primer set F-574 (5'-GCGGTAATTCCAGCTCCAA-3') and TAReukREV3 (5'-TTGGCAAATGCTTTCGC-3'; 378 bp), including overhang adapters (respectively 5'-TCGTCGGCAGCGTCAGATGTGTATAAGAGACAG-3' and 5'-GTCTCGTGGGCTCGGAGATGTGTATAAGAGACAG-3'), and the proofreading polymerase Kapa HiFi HotStart (Kapa Biosystems) was used for a first 25-cycle PCR. Amplicons were subsequently used as templates for a 10-cycle index PCR for the overhangs to be linked to Illumina sequencing adapters and indices (Nextera XT Index Primer 1 [i7] and Primer 2 [i5]) for downstream sequencing. For the samples showing a

total amount of extracted DNA less than 12.5 ng (ICE SS10 mixed layer, UP and P3 SS100 upper-mesopelagic), a nested PCR approach was applied, including an additional amplification with the universal 18S rDNA primers set prior to the two-step PCR described above. This procedure caused little variation the OTU composition and structure of microbial communities, as evidenced by Annex A9-A and A9-B showing prokaryotic communities amplified using the same nested PCR approach for 16S rDNA amplicon sequencing. After each PCR round, amplicons were purified with the Agencourt AMPure XP PCR clean-up kit (Beckman Coulter) following manufacturer's recommendations. The quality of purified amplicons was assessed with a DNA7500 Kit read on a 2100 BioAnalyser (Agilent Technologies), and the quantity measured with a Qubit dsDNA High-Sensitivity assay kit (Invitrogen™, Thermo Fisher Scientific).

Purified amplicons were pooled at equimolar concentrations (4 nM each) for the library preparation using a Nextera XT DNA kit (Illumina) following manufacturer's recommendations and included 5 % PhiX. Finally, the amplicons were sequenced with an Illumina MiSeq sequencing system (M02946, Illumina) using a MiSeq Reagent 600-cycle Kit v3 (Illumina).

4.3.5 Bioinformatics

The sequence data are to be submitted to the GenBank database under an accession number to be determined. Raw sequences were demultiplexed and their adapter sequences trimmed using the MiSeq Control software (v2.5.0.5, Ilumina) directly after sequencing. The quality of demultiplexed raw read pairs was checked with FastQC (v 0.11.4; Babraham Bioinformatics). Forward and reverse reads were merged with the PANDAseq assembler software (v 2.8) (Masella et al., 2012) using the default parameters (simple Bayesian algorithm for assembly) and a maximum read length of 500 bp and Phred33 quality score of 0.8. OTU clustering was subsequently performed under QIIME (MacQIIME v 1.9.1_20150604) (Caporaso et al., 2010) after all libraries were compiled into a single FASTA file using the *multiple_split_libraries_fastq.py* function. Clustering was

performed using the open reference function *pick_open_reference_otus.py* using default parameters (UCLUST algorithm for OTU picking) using a minimum sequence identity of 97% against the 16S rRNA Silva database (v 128) (Quast et al., 2013). Singleton OTU were discarded.

4.3.6 Statistical analyses

The canonical correspondence analysis (CCA) and permutational multivariate analyses of variance (PERMANOVA) were performed on the rarefied dataset and were used to investigate the significance of environmental (Table 3.1) and inherent sampling factors responsible for the composition variability. The similarity percent analysis (SIMPER) were based on the Bray Curtis dissimilarity distance of the OTU composition and were used to investigate the differences between communities associated with the different particle-types.

Based on taxonomic affiliation and/or physiological information on taxa, OTU were divided into three categories for individual analyses and subsequent discussions: phytoplankton, metazoans and heterotrophic protists, which would also include mixotrophs. The abundances presented are relative to the total number of sequences or OTU present within the particle-type and category considered.

Taxa enrichments relative to SK10 in the mixed layer were calculated according to the following equation:

$$Enrichment = \log_2\left(\frac{RA_{\,sample\ UM}}{RA_{\,SK10\ ML}}\right)$$

Equation 4.1. Taxa enrichment in upper-mesopelagic sampled compared to sinking particle samples in the mixed layer.

With $RA_{\,SK10\ ML}$ as the relative abundance of the taxa in SK10 mixed layer and $RA_{\,sample\ UM}$ as the relative abundance of the same taxa in the sample being compared in the upper-mesopelagic. Therefore, negative values indicate an enrichment within SK10 mixed layer while positive values indicate an enrichment within the compared sample.

Analyses were performed with the R statistics software (http://www.r-project.org), using features of the *vegan* package. Statistical analyses were performed on the dataset rarefied to the smallest library size, either at a considered station and depth or overall, depending on the analysis performed. For the calculation of SIMPER and the proportions of shared/unique OTU, the dataset was rarefied to the smallest library size in a considered station (n = 16,127 sequences for ICE; 29,119 for P2; 6,055 for P3 and 28,937 for UP). Multivariate analyses comparing samples from all stations (CCA and PERMANOVA) were performed on the dataset rarefied to the smallest library size (n = 3,976 sequences/library). The taxonomic composition of communities at various levels is based on the relative abundance of the non-rarefied dataset.

4.4 Results and discussion

4.4.1 Sequencing results

A total of 2,517,165 V4 18S rDNA paired-ends reads were recovered from all four particle-types (suspended particles 0.22 – 10 µm [SS0.22], 10 – 100 µm [SS10], and ≥ 100 µm [SS100], as well as sinking particles ≥ 10 µm [SK10]). After sequence trimming, pairing and merging, and removal of metazoan sequences, a total of 1,533,266 sequences remained with an average length of 450 bp (29,852 ± 22,428 sequences/library) (Annex B1). At both depths (mixed layer and upper-mesopelagic), there was a higher proportion of *Metazoa* affiliated sequences in SK10 and SS100, except at ICE, while a higher proportion of phytoplankton sequences was observed in SS0.22 and SS10 in the mixed layer (Annex B2).

4.4.2 Environmental community structuring

The CCA analysis based on protist OTU composition (Fig. 4.1) revealed a clear separation between stations, as well as between mixed layer and upper-mesopelagic samples considering each station individually. A PERMANOVA analysis calculated for

phototrophic and hetero-/mixotrophic members of the protist communities (Annex B3-A and B3-B) revealed that every environmental parameter tested (oxygen, fluorescence and POC concentrations, and temperature) as well as particle-type (SK10, SS100, SS10 and SS0.22) were significant predictors of OTU composition ($p < 0.05$), with the latter explaining ~ 18 % of observed variability.

Similar to prokaryotic communities collected in identical particle-types (Chapter 3), protist communities collected at ICE were the most dissimilar compared to those collected at other stations (P2, P3 and UP) (average Bray Curtis distance of 70.3 versus 56.3 % respectively) (Fig. 4.2). This is due to the unique conditions present at ICE, located on the Antarctic continental ice edge (Fig. 2.3), compared to the other stations not influenced by melting-ice runoff (Atkinson et al., 2001). These conditions include negative temperatures (Chen and Laws, 2017) and high concentrations of macro- (Garrison et al., 2005) and micronutrients release (such as iron and vitamin B_{12}) (Sedwick and Ditullio, 1997; Taylor and Sullivan, 2008) that could influence autotrophic and heterotrophic protist community structure.

4.4.3 Particle flux components and influence on suspended particles in the mesopelagic ocean

Particle collection in the mixed layer and upper-mesopelagic were conducted within a limited time frame (~ 30 min), which therefore does not consider the time lapse potentially existing between primary production and POM export from the mixed layer (Buesseler, 1998). However, comparing the phytoplankton and metazoan taxonomic composition in sinking particles collected within the mixed layer with those collected in the upper-mesopelagic could serve as a proxy for particle flux composition. Phytoplankton detritus and mesozooplankton faecal pellets were indeed the two main components of sinking particles at the sampled stations over the same sampling period (Belcher et al., 2016). Furthermore, comparing the taxonomic composition of sinking particles in the mixed layer to suspended particles in the upper-mesopelagic can, to some extent, inform us on

particle dynamics and the influence of sinking particle disaggregation on suspended particles composition (Lam and Marchal, 2015).

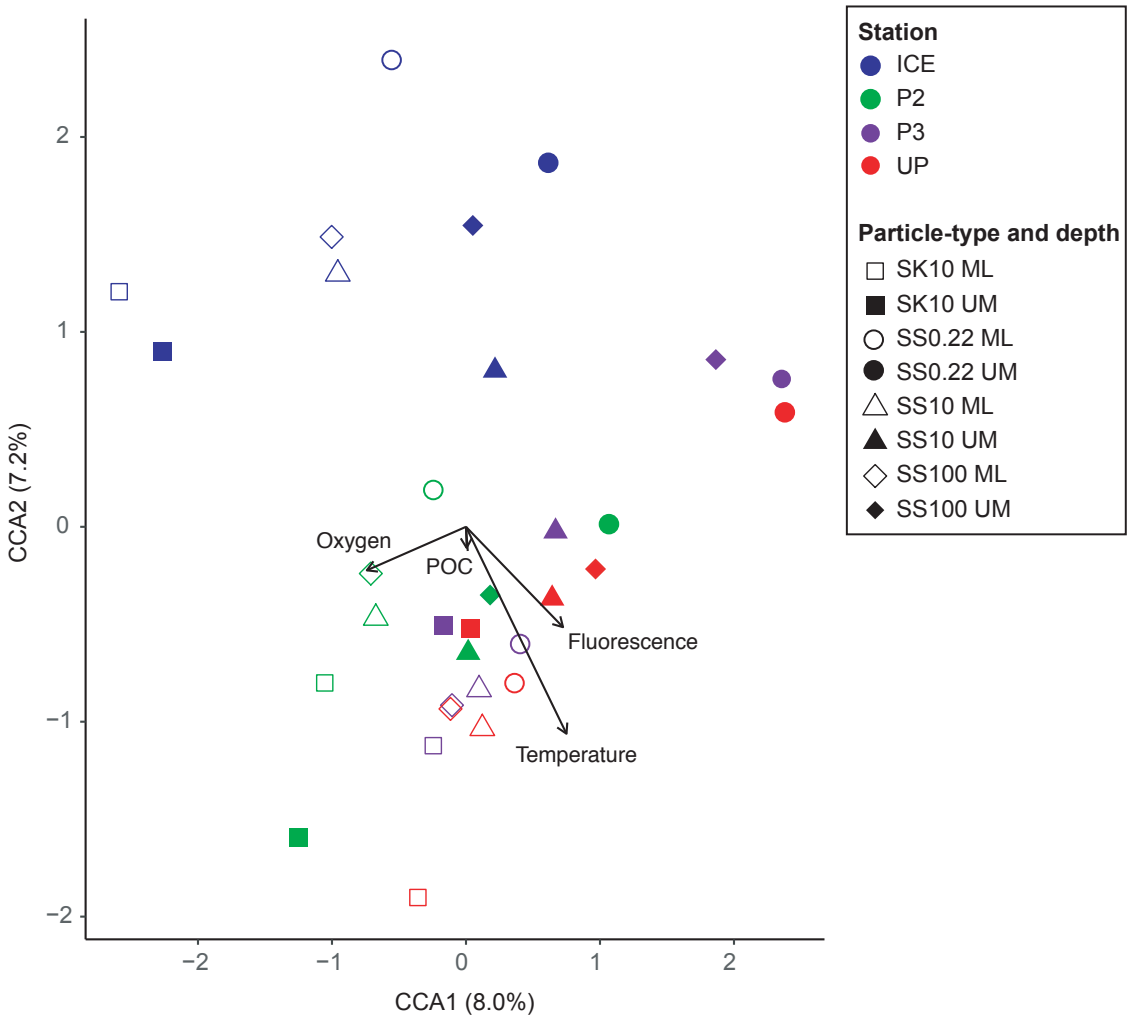

Figure 4.1. Canonical correspondence analysis plot of protist-affiliated OTU composition. The CCA was calculated on the rarefied dataset. The significance of environmental parameters (oxygen, fluorescence, POC concentrations and temperature) was tested with a PERMANOVA ($p < 0.05$). Significant environmental parameters are displayed and their respective arrow length is proportional to the variability in community structure explain. ML = mixed layer, UM = upper-mesopelagic; SS0.22 = suspended particles 0.22 – 10 µm; SS10 = suspended particles 10 – 100 µm; SS100 = suspended particles ≥ 100 µm; (SS100), SK10 = sinking particles ≥ 10 µm.

4.4.3.1 Phytoplankton components of the particle flux

4.4.3.1.1 Surface phytoplankton communities

Expectedly, phytoplankton communities (≥ 10 µm) collected in the mixed layer differed largely between stations, owing to differential nutrient regimes (Fig 4.3A and Annex B4-A).

P2 was largely dominated by the prymnesiophyte *Phaeocystis* (representing 83.3 % of phytoplankton sequences of SK10 in the mixed layer). *Phaeocystis antarctica* has been reported to form large blooms in the Southern Ocean (Zoccarato et al., 2016; Arrigo, 1999) as well as within sea-ice (Brown and Bowman, 2001).

Table 4.1. Proportion of OTU and affiliated sequences shared between particle-types. The proportions of phytoplankton and metazoan shared/unique OTU were calculated on the rarefied dataset. Table A displays values for phytoplankton communities and table B for metazoan communities. ML = mixed layer, UM = upper-mesopelagic; SS0.22 = suspended particles 0.22 – 10 µm; SS10 = suspended particles 10 – 100 µm; SS100 = suspended particles ≥ 100 µm; (SS100), SK10 = sinking particles ≥ 10 µm; OTU = % OTU shared; seq = % affiliated sequences.

			ICE		P2		P3		UP	
			OTU	seq	OTU	seq	OTU	seq	OTU	seq
A	**SK10 ML with**	**SK10 UM**	12.8	32.0	22.6	89.6	20.9	82.3	25.8	89.4
	SK10 ML with	**SS100 UM**	23.7	80.8	25.0	82.6	10.5	100.0	25.4	72.9
		SS10 UM	25.5	76.9	29.4	82.8	19.5	92.9	37.5	88.7
		SS0.22 UM	17.1	72.9	16.0	77.9	15.4	71.4	19.5	73.0
	SS ML with	**SS100 UM**	29.0	57.6	35.7	12.9	21.3	0.3	26.9	17.1
		SS10 UM		14.8		3.3		2.1		5.3
		SS0.22 UM		42.0		4.2		0.7		1.5
B	**SK10 ML with**	**SK10 UM**	4.5	90.7	20.4	99.4	31.0	72.8	22.3	87.0
	SK10 ML with	**SS100 UM**	10.0	2.9	11.0	96.9	5.8	80.2	23.7	99.5

While diatom sequences represented only 15.6 % of SK10 phytoplankton sequences in the mixed layer at P2, they averaged at 69.6 ± 9.7 % in ICE, P3 and UP. The polar centric diatom families *Coscinodiscophyceae* and *Mediophyceae* represented most of the sequences, the former being more abundant at ICE (34.0 versus 12.0 % respectively) and the latter at P2 and P3 (11.9 versus 42.5 % respectively). *Actinocyclus* and *Corethron* were the dominant diatoms at ICE (34.0 %). Conversely, *Chaeotoceros* (13.8 %) along with unidentified members of the *Mediophyceae* family (27.5 %) were the dominating species at P3 and UP. *Coscinodiscophyceae* and *Mediophyceae* diatoms have been consistently reported in polar waters (Zoccarato et al., 2016; Rodríguez-Marconi et al., 2015; Poulton et al., 2010). Particularly, *Actinocyclus* (*Coscinodiscophyceae*) and *Chaetoceros* (*Mediophyceae*) have been frequently detected in polar waters naturally enriched in iron (Georges et al., 2014; Rembauville et al., 2016). This is in agreement with the environmental conditions at respective stations, as P2 is located in a high-nutrient-low-

chlorophyll region (Fig. 2.3 and Table 3.1) unlike ICE, P3 and UP which benefit from various iron inputs. While phytoplankton communities at ICE can use the high concentrations of iron originating from melted sea-ice (Sedwick and Ditullio, 1997; Taylor and Sullivan, 2008), P3 and UP benefit from enriched upwelled waters at the South Georgia continental margin (Atkinson et al., 2001).

4.4.3.1.2 Sinking phytoplankton taxa

In the upper-mesopelagic, phytoplankton sequences in SK10 were less abundant relative to the mixed layer (Annex B2) and both communities exhibited differences in terms of their structure and diversity (Fig 4.3A, Fig. 4.4 and Annex B4-A).

Mediophyceae diatoms, mostly represented by *Chaetoceros*, represented 41.5 ± 13.0 % of phytoplankton sequences collected in the SK10 fraction in the upper-mesopelagic of every station, while *Coscinodiscophyceae* were mostly absent except at P2 where they represented 13.0 % of phytoplankton sequences. This implies that few *Actinocyclus* cells (*Coscinodiscophyceae*) sunk out from the mixed layer at ICE, and that most *Chaetoceros* were exported to the upper-mesopelagic at all stations. This apparent differential export is in agreement with literature on carbon export owing to different diatom groups (Leblanc et al., 2018). The fast-growing *Chaetoceros* has been correlated with high carbon export to depth, while the opposite is true for *Actinocyclus* that has been negatively correlated with POC export (Tréguer et al., 2018). *Actinocyclus* has a large biovolume (Lin et al., 2017), but unlike *Chaetoceros*, it is not chain forming (e.g., Poulton et al., 2010) thereby leading to a reduction of its sinking velocity (Bannon and Campbell, 2017). This could explain why it did not contribute as much as *Chaetoceros* to carbon export to the mesopelagic. Furthermore, the presence of *Chaetoceros* in SK10 fractions agrees with the observed presence of chain-forming centric diatoms in sinking particles collected at the same depths and sampling period with light microscopy (Belcher et al., 2016)

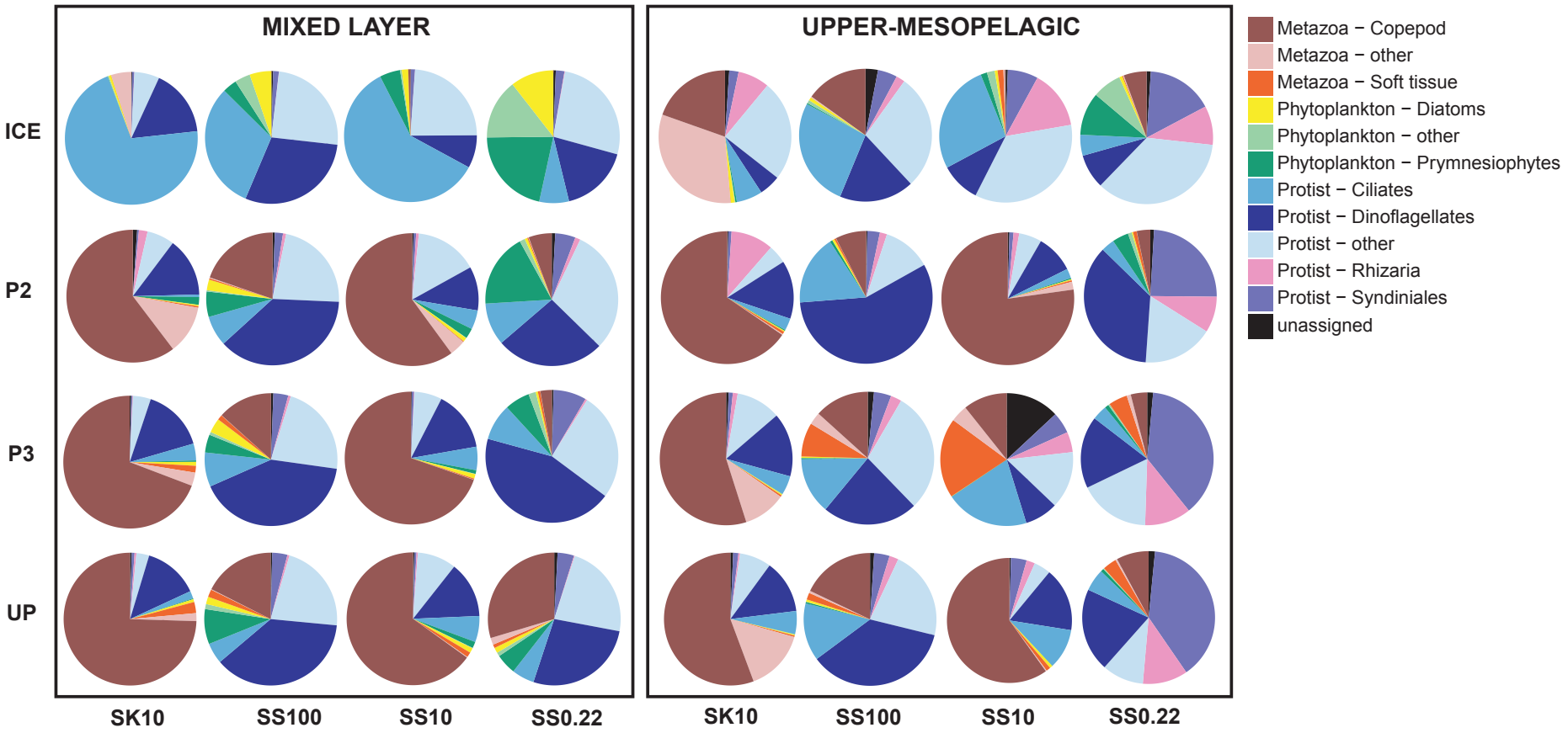

Figure 4.2. Total eukaryotic community composition. Pie charts were constructed with the relative abundance of selected taxa in the rarefied dataset. Sequences were subcategorised into *Metazoa* (copepod, soft-tissue animal and others), phytoplankton (diatom, prymnesiophyte and others), other protists (ciliates, dinoflagellates, *Rhizaria*, *Syndinales* and others) and non-affiliated eukaryotes. SS0.22 = suspended particles 0.22 – 10 µm; SS10 = suspended particles 10 – 100 µm; SS100 = suspended particles ≥ 100 µm; (SS100), SK10 = sinking particles ≥ 10 µm.

A.

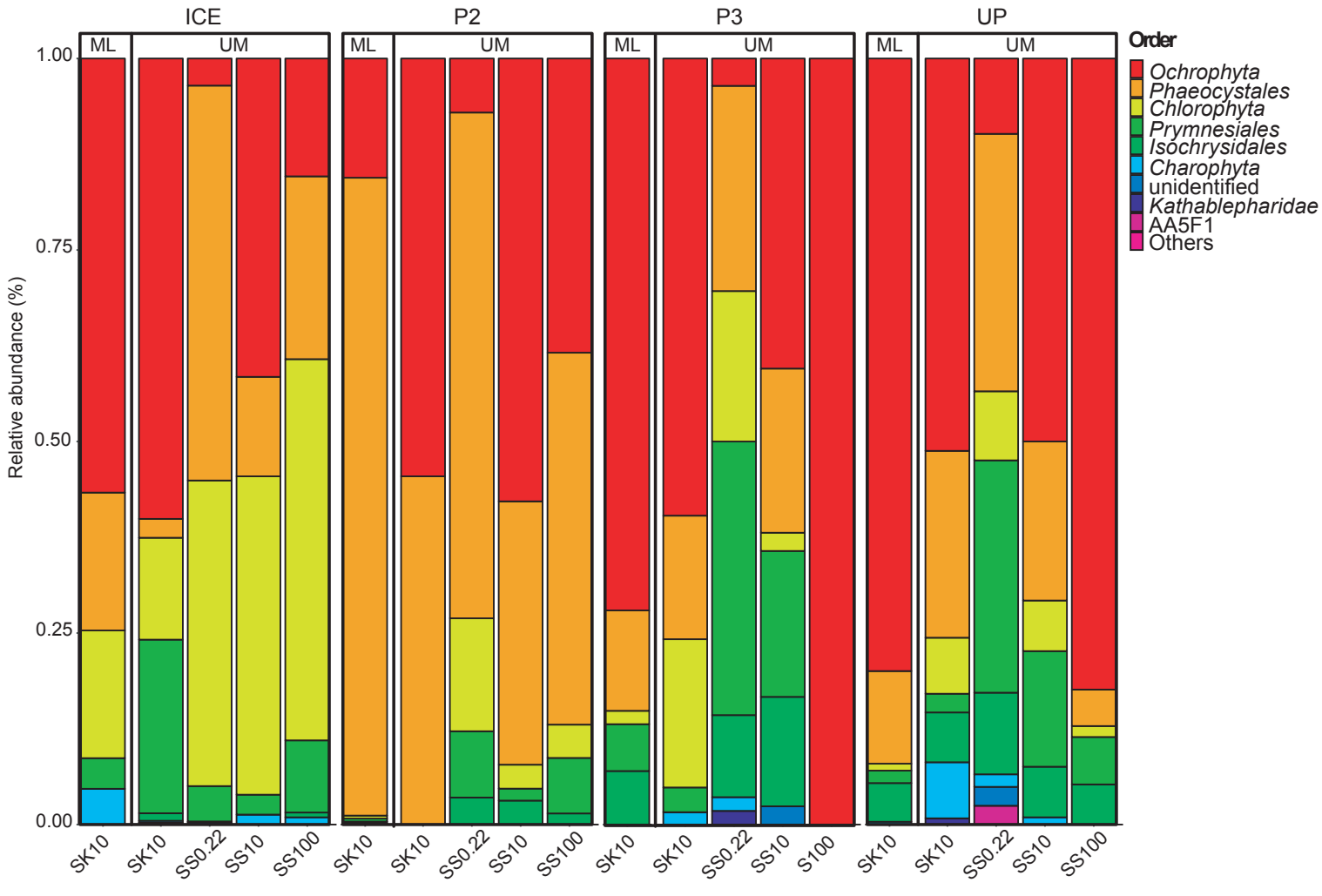
ICE
P2
P3
UP
ML
UM
Relative abundance (%)
1.00
0.75
0.50
0.25
0.00
SK10
SS0.22
SS10
SS100
S100
Order
Ochrophyta
Phaeocystales
Chlorophyta
Prymnesiales
Isochrysidales
Charophyta
unidentified
Kathablepharidae
AA5F1
Others

B.

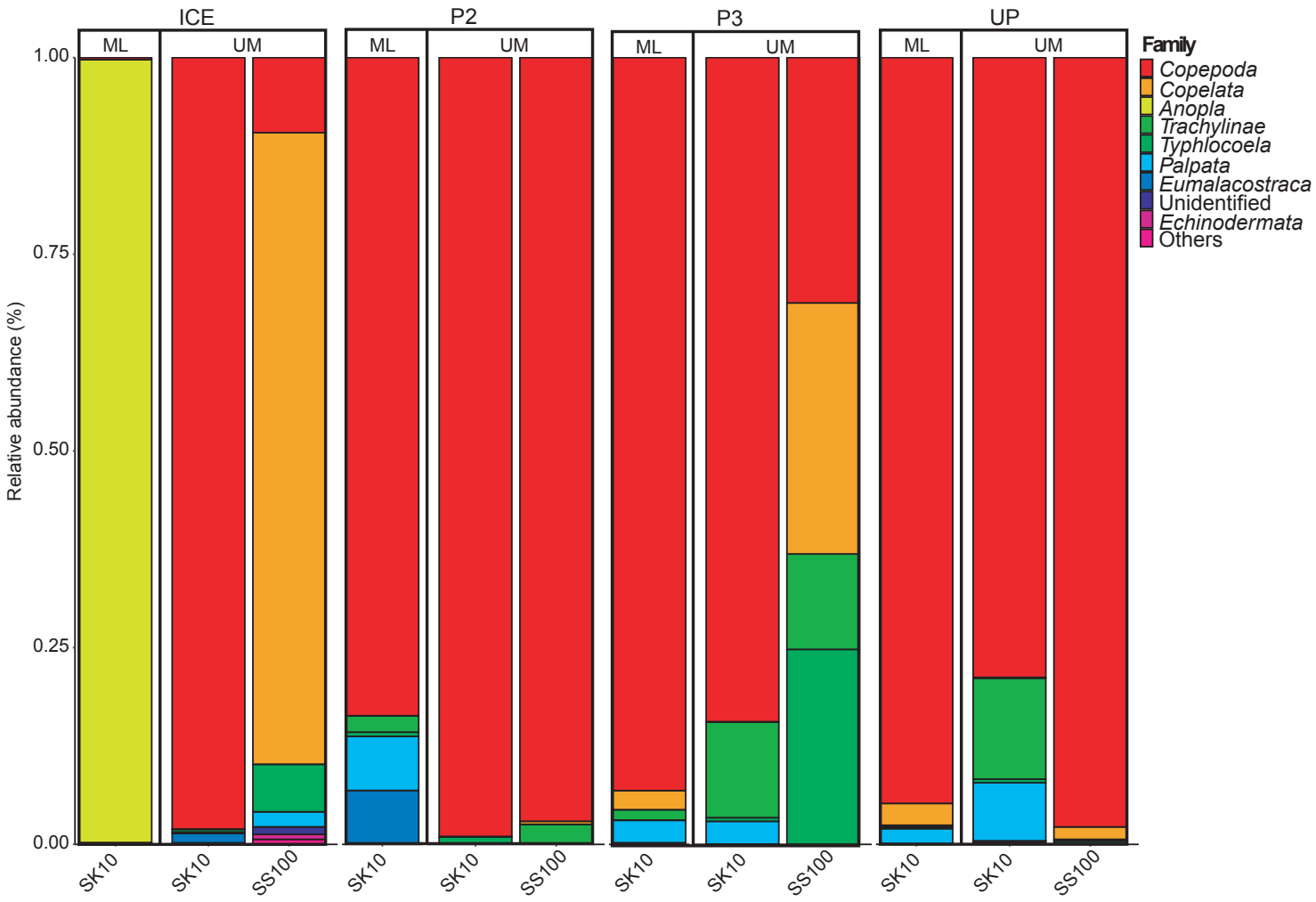
ICE
P2
P3
UP
ML
UM
Relative abundance (%)
1.00
0.75
0.50
0.25
0.00
SK10
SS100
Family
Copepoda
Copelata
Anopla
Trachylinae
Typhlocoela
Palpata
Eumalacostraca
Unidentified
Echinodermata
Others

C.

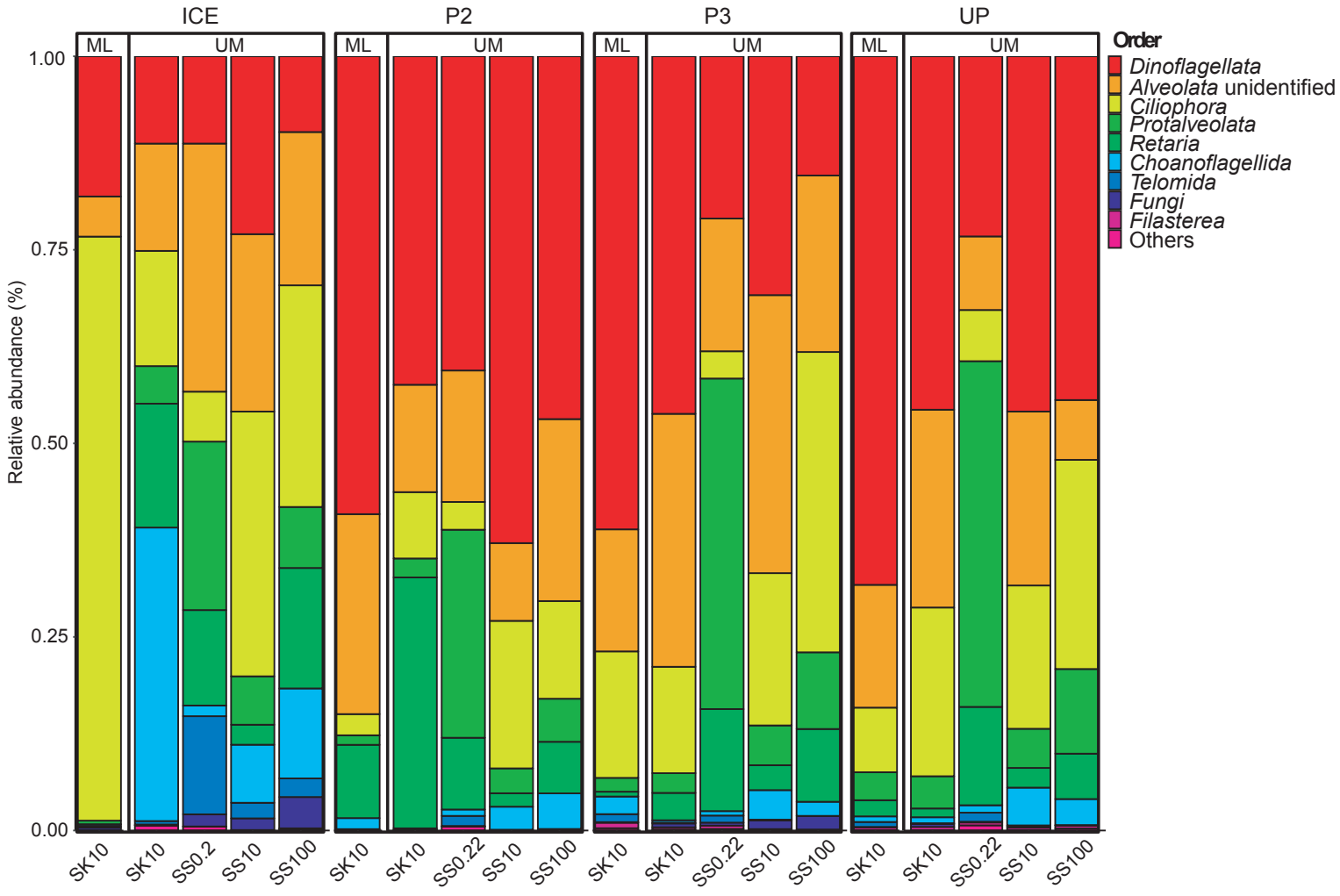
ICE
P2
P3
UP
ML
UM
Relative abundance (%)
1.00
0.75
0.50
0.25
0.00
SK10
SS0.2
SS0.22
SS10
SS100
Order
Dinoflagellata
Alveolata unidentified
Ciliophora
Protalveolata
Retaria
Choanoflagellida
Telomida
Fungi
Filasterea
Others

Figure 4.3. Taxonomic composition of phytoplankton, metazoan and hetero/mixotrophic protist communities (previous three pages). Panel A shows the taxonomic order composition of phytoplankton communities, panel B the taxonomic class composition of metazoan communities and panel C the taxonomical order composition of hetero/mixotrophic protist communities. ML = mixed layer, UM = upper-mesopelagic.

Aggregates and faecal pellets that are ballasted by biogenic minerals, such as opals produced by diatoms, sink significantly faster than those that are not (Ploug et al., 2008; Klaas and Archer, 2002). As they sink faster, these particles are less affected by increased remineralisation processes in the upper-mesopelagic (Martin et al., 1987), and therefore sink deeper and lead to more efficient long-term carbon sequestration (Kwon et al., 2009). This is one reason why diatoms are assumed as efficient carbon transporter to the deep ocean (Jin. et al., 2006), while non-ballasted phytoplankton taxa are not as efficient (Armstrong et al., 2002).

Fewer sequences belonging to the prymnesiophyte *Phaeocystis* were retrieved in SK10 in the upper-mesopelagic compared to the mixed layer at P2 (45.5 %). This implies that despite its abundance in the mixed layer, this taxon is not as efficient as diatoms for carbon export to the deep ocean, and hence for long-term carbon sequestration. Instead, *Phaeocystis* was observed primarily in the small-suspended fraction (SS0.22) of the upper-mesopelagic, thereby suggesting that although they contribute to the POM flux out of the euphotic zone, *Phaeocystis*-enriched aggregates are unlikely to sink to greater depths. *Phaeocystis* has previously been reported as a key component of POC export in polar waters (DiTullio et al., 2000), as they have the ability to form aggregates and sink rapidly out of the mixed layer (Arrigo, 1999). However, this phytoplankton appeared to contribute little to carbon transfer efficiency, especially compared to its diatom counterparts, as observed elsewhere in Antarctic waters (Lin et al., 2017). The rapid export of *Phaeocystis* out of the euphotic zone is related to their enhanced production of transparent exopolymer polysaccharides (TEP) (Passow et al., 2001). There is an increase of *Phaeocystis* TEP production when the colony starts to die (Hong et al., 1997). However, TEP-enriched aggregates have a reduced density which, if they are not

ballasted enough by minerals such as opals produced by diatoms (Mari et al., 2017), have a reduced sinking velocity or can even be buoyant (Eberlein et al., 1985). This further agrees with the enrichment of *Phaeocystis* in suspended particles in the upper-mesopelagic.

At P2, P3 and UP, 87.1 ± 3.4 % of sequences collected in SK10 in the upper-mesopelagic were affiliated with OTU shared with SK10 in the mixed layer (representing 23.1 % ± 2.0 % of OTU diversity in the upper-mesopelagic) while at ICE only 32.0 % of sequences belonged to OTU shared between SK10 at both depths (12.8 % of OTU) (Table 3.1). Additionally, 91.9 ± 5.2 % of SK10 sequences in the upper-mesopelagic (11.8 ± 0.8 % of OTU) were shared with all suspended particle size-fractions. This suggests that in the upper-mesopelagic the influence of other contributors on the composition of sinking particles is limited. Such influences could be; (i) the export of small sinking particles from the surface (< 10 µm) (Dall'Olmo and Mork, 2014), which would have not been sampled here, (ii) time decoupling between primary production in the mixed-layer and organic matter export to the mesopelagic (Buesseler, 1998), (iii) presence of low-light adapted phytoplankton in the upper-mesopelagic (Jacques, 1983) and/or (iv) lateral export of sinking particles from adjacent mesopelagic water masses.

4.4.3.1.3 Influences on suspended particles in the upper-mesopelagic

In the upper-mesopelagic, suspended particles 10 – 100 µm (SS10) and > 100 µm (SS100) were largely dominated by prymnesiophytes (32.4 ± 18.9 %), mostly represented by *Phaeocystis*, and by diatoms (55.6 ± 24.7 %) mainly belonging to *Proboscia* (*Coscinodiscophyceae*) at P3, *Thalassionema* (*Fragilariophyceae*) at UP, and unidentified members of *Mediophyceae* at ICE and P2 (Fig 4.3A and Annex B4-A). *Phaeocystis* dominated suspended particles 0.22 – 10 µm (SS0.22) at all stations (44.5 ± 15.4 %). Every suspended particle size-fraction in the upper-mesopelagic at ICE comprised high proportions of chlorophyte sequences (36.8 ± 14.0 %).

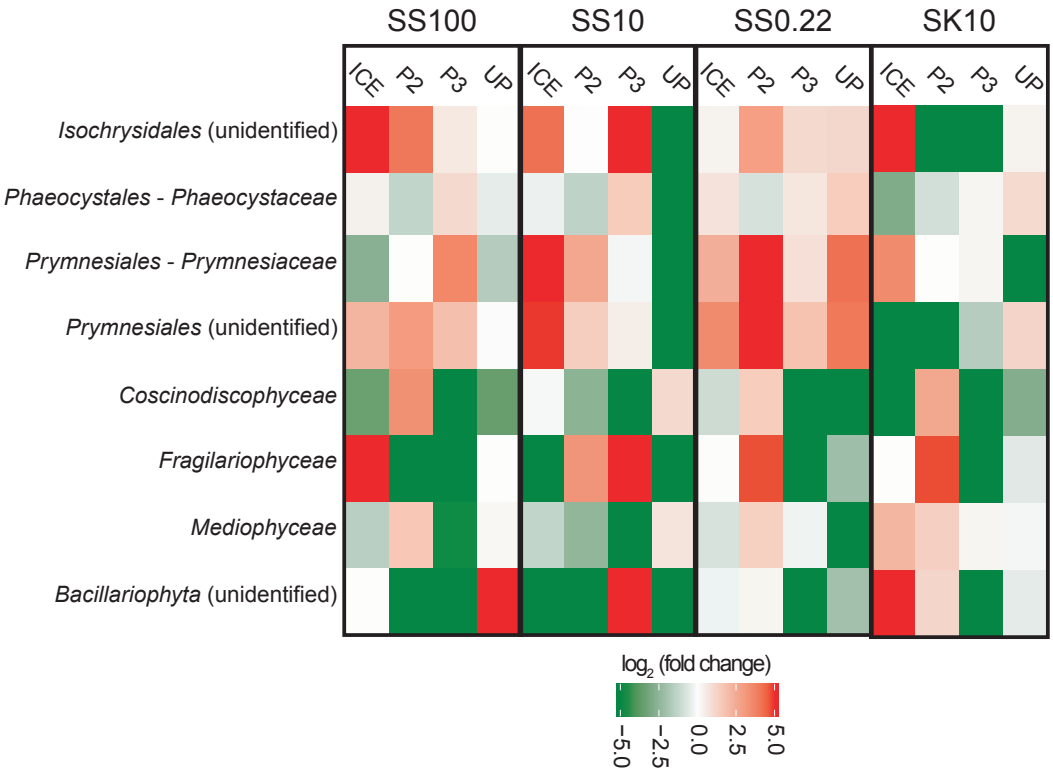

Figure 4.4. Enrichment of phytoplankton taxonomic families in sinking and suspended particles in the upper-mesopelagic. The relative abundance of taxa in sinking particles from the mixed layer was used as the base in order to look at sinking particle export and sinking particle disaggregation in the upper-mesopelagic. Enrichments were calculated using Equation 4.1 on the rarefied dataset. Negative values (green) indicate an enrichment within SK10 mixed layer and positive values (red) indicate an enrichment within the compared sample in the upper-mesopelagic.

Altogether, suspended particle size-fractions in the upper-mesopelagic contained 81.1 ± 8.6 % of sequences affiliated with OTU shared with SK10 from the mixed layer (representing 22.0 ± 6.9 % of OTU). The highest difference with SK10 in the mixed layer was observed with SS10 (Table 4.1). Prymnesiophytes and chlorophytes were particularly enriched in every suspended particle size-fractions in the upper-mesopelagic compared to SK10 in the mixed layer (Fig. 4.4). Conversely, suspended particle size-fractions in the mixed layer altogether shared 28.2 ± 5.2 % of OTU with those in the upper-mesopelagic. These OTU represented 38.1 ± 17.7 % of phytoplankton sequences in suspended particle size-fractions at ICE and 5.3 ± 5.5 % at the other stations.

Suspended particles in the mesopelagic can originate from; (i) the disaggregation of sinking particles, through the action of biotic and abiotic processes (Lam and Marchal,

2015), (ii) from chemolithoautotrophic primary production in the mesopelagic (Arístegui et al., 2009), and also (iii) from vertical mixing or lateral transport, which lead to the introduction of suspended material from adjacent water masses (Baltar et al., 2009). As only photosynthetic primary producers are considered here, and therefore should originate from the surface mixed layer, the composition of suspended particles in the upper-mesopelagic is a result of either; (i) disaggregation of sinking particles from the mixed layer and/or (ii) vertical mixing within the sunlit mixed layer.

Regarding sinking particles disaggregation, the enrichment of prymnesiophytes, and more particularly of *Phaeocystis*, in every suspended particle size-fractions coupled with the enrichment of diatoms in sinking particles in the upper-mesopelagic, further supports the differential particle dynamics between prymnesiophyte-enriched and diatom-enriched aggregates. On one hand, prymnesiophyte-enriched aggregates sinking from the mixed layer are more likely to break down into suspended particles in the upper-mesopelagic, while on the other hand, diatom-enriched aggregates are more likely to sink faster and deeper into the ocean, helped by their larger cell-size and mineral ballast. This is similar to the observed influence of phytoplankton community structure on phytoplankton-dominated POC export characteristics (Giering et al., 2017). The higher proportion of diversity shared between suspended particles in the mixed layer and those in the upper-mesopelagic at ICE compared to other stations suggests a higher influence of vertical mixing that leads to the intrusion of surface suspended particles deeper in the water column. This is concurrent with the influence of Antarctic continental ice edge melted runoffs at this station (Atkinson et al., 2001).

4.4.3.2 Zooplankton components of the particle flux

The diversity of sequences collected in SK10 in the mixed layer was similar to that of the upper-mesopelagic with 87.5 ± 9.6 % of metazoan sequences belonging to 19.6 ± 9.6 % of OTU shared between the two particle-types (Table 4.1). Nonetheless, the compositional structure of metazoan sequences from both particle-types was different (Fig. 4.3B and

Annex B4-B). Except at ICE in the mixed layer, SK10 samples were dominated by copepod sequences (90.4 ± 5.1 %), which were mostly affiliated with *Calanoida* (67.6 ± 6.7 %) and *Cyclopoida* (20.9 ± 6.0 %). This agrees with results from Belcher et al. (2016) showing that calanoid faecal pellets represented more than half of sinking POC flux. POC export dominated by mesozooplankton faecal pellets generally leads to limited connectivity between sinking and suspended particle pools in the mesopelagic. Faecal pellets are indeed more resistant to remineralisation compared to phytoplankton-dominated aggregates as they have higher densities and are surrounded by a protective membrane (Abramson et al., 2010). Beside their role in repackaging surface primary production into faecal pellets (Turner, 2015), mesozooplankton are also responsible for the breakage of sinking particles, for instance by sloppy feeding (Steinberg and Landry, 2017), which contributes to the creation of smaller suspended particles thereby connecting the two particle-pools together (Lam and Marchal, 2015).

In the upper-mesopelagic, sequences retrieved from SS100 and SK10 at ICE and P3 showed slightly increased differences compared to those from P2 and UP (Table 4.1). While SK10 at ICE and P3 were dominated by copepod sequences (> 80.0 %), SS100 at ICE was dominated by sequences that belonged to the tunicate family *Oikopleuridae*, and by sequences belonging to *Oikopleuridae* and to the ctenophore class *Typhlocoela*, and cnidarian class *Trachylinae* at P3. This suggests that different roles are played by mesozooplankton taxa in sinking and suspended particle-pools within the mesopelagic ocean.

The main limitations of these results are that; (i) living copepods could have swam towards the bottom of the MSC to feed on sinking particles within the time frame of particle settling (2 hours), which would subsequently have reduced their detection in suspended particles (i.e., in the upper part of the MSC), and (ii) it is difficult to determine the exact nature of detected DNA. DNA collected in various particle-types could therefore indicate; (i) the presence of the organisms themselves while alive (such as copepods) or (ii) fragments of shredded or dead body parts (antennas, broken shells), as well as (iii)

residual genetic material present in faecal pellets. Nonetheless, these results indicate that while copepods are more influential on sinking particles, by either their faecal pellets or their feeding behaviours, the soft-bodied *Oikopleuridae*, *Typhlocoela* and *Trachylinae* are more influential on suspended particles. Suspended particles could represent an organic substrate for these animals, such as suggested in the central North Pacific (Gloeckler et al., 2017). Additionally, their soft-tissue structures and/or secretions could actually be a major component of suspended particles themselves, as a binder for smaller particles and DOM, similar to empty larvacean houses, without reaching densities high enough to sink as is sometimes observed (Simon et al., 2002).

In complement to the increasingly applied environmental DNA approach to determine marine animal populations (e.g., mesozooplankton) (Djurhuus et al., 2018), 18S rRNA gene amplicon sequences of suspended and sinking particles could be a complementary tool to classic microscopy, usually focusing on sinking particles, to determine the constitution and metazoan contribution to the two particle-pools.

4.4.4 Heterotrophic protists colonising particles in the upper-mesopelagic

Heterotrophic protists sequences were more abundant in SS0.22 and SS10, than in SK10 and SS100 both in the mixed layer and upper-mesopelagic, representing on average 56.1 ± 25.5 % of total sequences (Annex B2). Such high contribution to total sequences suggests the importance of heterotrophic communities in structuring of microbial ecosystems by their abundance and trophic modes (Worden et al., 2015; Stoecker et al., 2017; Sherr and Sherr, 2002), especially in polar environments (Caron et al., 2016; Korb et al., 2012).

Specific OTU were abundant in heterotrophic communities depending on sampled station and depth, likely influenced by differential inherent environmental conditions (Fig. 4.1), although the OTU composition was mainly driven by particle-type, representing 18.4 % of OTU variability ($p < 0.05$) (Annex B3-B). heterotrophic communities in the mixed layer

were on average 43.2 ± 15.1 % dissimilar compared to 58.5 ± 14.9 % in the upper-mesopelagic (Annex B5). Every particle-type in the upper-mesopelagic was on average 66.6 ± 13.6 % dissimilar to SK10 in the mixed layer. This agrees with literature showing that heterotrophic assemblages from the surface and those from the mesopelagic and deeper are different (Zoccarato et al., 2016; López-García et al., 2002; Pernice et al., 2015, 2014; Edgcomb et al., 2011; Duret et al., 2015; Orsi et al., 2012).

heterotrophic communities in the mesopelagic ocean and below remain largely unknown (Edgcomb, 2016; Caron et al., 2017), and especially so in the Southern Ocean. Furthermore, most POC flux attenuation, and therefore remineralisation, typically occurs within the upper-mesopelagic (Martin et al., 1987). The following section will focus on differences between different particle-types collected in the upper-mesopelagic.

As little as 5.9 ± 1.1 % of heterotrophic OTU were shared among every particle-type in the upper-mesopelagic (Annex B6), although sequences affiliated with them represented 68.8 ± 19.7 % of samples. This is consistent with the hyper-dominance of a few core taxa observed in planktonic ecosystems (de Vargas et al., 2015). Nonetheless, each particle-type presented unique diversity (i.e., OTU absent from other particle-types in the upper-mesopelagic at a same station) with SS0.22 and SK10 heterotrophic communities exhibiting the highest proportion of unique OTU (60.7 ± 1.6 % and 40.8 ± 5.9 %) and affiliated sequences (12.5 ± 3.3 % and 6.4 ± 2.2 % respectively). These rare taxa are reservoirs that would likely become dominant in the event of abrupt environmental changes, given the right conditions (Sogin et al., 2006; Huber et al., 2007). Therefore, their higher representation in SK10 and SS0.22 could mark the presence of more transient conditions associated with these two particle-types. This also agrees with the presence of prokaryotic opportunist r-strategists in sinking particles from the same stations (Chapter 3).

Alveolata were the most abundant taxa among all samples (Fig. 4.2), representing 84.7 ± 13.0 % of heterotrophic sequences. While *Dinoflagellata* sequences were relatively

abundant in all particle-types (37.5 ± 18.3 %), *Protalveolata* sequences were most abundant in SS0.22 (34.0 ± 9.9 % versus 5.7 ± 2.6 % in other particle-types) and *Ciliophora* sequences in SS100, SS10 and SK10 (21.5 ± 8.7 % versus 5.0 ± 1.5 % in SS0.22) (Fig. 4.3C and Annex B4-C).

The distribution of dinoflagellates appeared to be governed more by sampled station rather than by particle-type, with *Gymnodiniales* (mainly represented by the species *Gyrodinium*) detected in all particle-types at P2 and UP, and along with *Dinophysiales* at P2. *Gyrodinium* cells (10 to 100 µm) are able to feed on phytoplankton cells much bigger than themselves, such as diatoms (Sherr and Sherr, 2007), and thus have been negatively correlated with POC export in the Southern Ocean owing to their grazing activities (Cassar et al., 2015; Lin et al., 2017).

Ciliophora sequences were mainly represented by *Choreotrichia* in SS10 and SK10 and by *Oligotrichia* in SS100, both of which have been detected abundantly in other mesopelagic sites (Grattepanche et al., 2016; Capriulo et al., 2002). These predators are generally respectively > 100 and > 40 µm and are important actors of top-down controls of microbial communities (Caron et al., 2012). In addition, *Oligotrichia* is a major mixotrophic protist group, which has the ability to sequester chloroplasts from their phytoplankton prey (kleptoplastidy) and can therefore participate in primary production when light conditions allow it (Stoecker et al., 2017).

While it should be taken into consideration that the detection of certain groups in specific particle size-fractions might have been simply caused by cell-size of their members, certain enrichments appeared to have been led by ecological preferences. Other than due to their size distribution, their slightly higher detection in SS100 could also be the result of their grazing activities on larger cells and phytodetrital aggregates. Comparatively, *Dinophysis* (40 – 100 µm), belonging to *Dinophysiales*, is an obligate mixotroph that requires light to grow (Stoecker et al., 2017). The detection of this taxa in the upper-

mesopelagic could indicate either that they sank as part of detrital sinking aggregates or that they were vertically entrained from surface waters.

For instance, *Choanoflagellata* (*Holozoa*) sequences were well represented at ICE in SK10, SS10 and SS100 (14.6 ± 13.9 %), and mostly belonged to *Diaphanoeca* of the family *Stephanoecidae*. These generally 3 – 10 µm heterotrophs are bacterivorous flagellates (Kirchman, 2008) that are regularly detected in polar waters (Georges et al., 2014; Smith et al., 2011). They are notorious predators in these regions (Marchant, 1985). The detection of these nanoflagellates on larger particle size-fractions suggests an active colonisation of sinking and suspended particles > 100 µm at ICE. Alternatively, these choanoflagellates are capable of forming colonies (Thomsen et al., 1991). Therefore, their capture in particles ≥ 10 µm could also reflect the presence of colonies.

As a result of their high growth and ingestion rates (Garzio et al., 2013), heterotrophic protists are efficient in the top-down control of phytoplankton communities and lead to enhanced loss of carbon to the dissolved pool by elongating the food chain (Pomeroy and Wiebe, 1988). They are responsible for the reduction of POC flux as they consume sinking particles and have been reported to be negatively correlated with POC export in Antarctic waters (Lin et al., 2017). The enrichment of specific groups belonging to these broad heterotrophic taxa suggests that suspended and sinking particles offer particular ecological conditions favoured by these groups, such as the chemical composition of POM and/or availability of their bacterial prey. Prey populations can shape the distribution of their predators (Anderson et al., 2013; Sherr and Sherr, 2002). Consequently, the distribution of specific prokaryotic remineralising taxa in suspended and sinking particles observed at the same sites (Chapter 3) could be partly responsible for the distribution of their own bacterivorous predators.

Protalveolata sequences, which were abundant in SS0.22, were mainly represented by *Syndiniales* (group II) that are notorious widespread marine parasites (< 2 µm). They can affect a wide variety of hosts, ranging from dinoflagellates to ciliates as well animals, that

they obligatorily kill upon infection (Guillou et al., 2008). Their preferential detection in SS0.22 suggests that these parasites were affecting mainly hosts < 10 µm rather than larger cells.

The second overall most abundant heterotrophic taxonomic class was *Rhizaria* (8.5 ± 7.5 %) with sequences affiliated with the order *Retaria* more represented in SS100, SK10 and SS0.22. Rhizarians are typically large cells (20 to 600 µm) that are globally abundant in mesopelagic waters, where they represent most of the planktonic biomass (Biard et al., 2016). They mainly are heterotrophs that are capable of feeding on copepods (Swanberg and Caron, 1991) thereby playing important roles as predators of larger microbial cells in the mesopelagic (Stoecker et al., 2017). Affiliated *Rhizaria* sequences in SS100 and SK10 were dominated by RAD-III, while they were dominated by RAD-II and RAD-III in SS0.22. Both groups are radiolarians, closely related to *Acantharea* (Not et al., 2007). These organisms make fragile mineral structures made out of silica or calcium carbonate (Caron et al., 2012). Additionally, *Acantharea* members can produce reproductive cysts (200 µm to 1 mm) covered in mineral shells, which can themselves contribute to POC export (Decelle et al., 2013). The detection of RAD-II and RAD-III in SS0.22 could originate from fragments of the mineral structure of cells or cysts, or from reproductive flagellated cells (2 – 3 µm) originated from ruptured cysts.

4.5 Conclusion

This study provides the first insights into eukaryotic contribution to suspended and sinking particle-pools, as well as their comparison between the mixed layer and upper-mesopelagic. In addition, it provides further data on the poorly characterised protist community of the mesopelagic Southern Ocean.

Diatoms dominated the phytoplankton composition of sinking aggregates collected in the mixed layer at all sites under the influence of iron enrichment. The chain-forming genus *Chaetoceros* appeared to contribute efficiently to carbon flux out of the mixed layer to the

upper-mesopelagic, likely aided by their silicate frustules. These opals act as ballast that cause aggregates to sink faster and deeper into the dark ocean, thereby leading to longer-term carbon sequestration.

On the other hand, prymnesiophyte-enriched aggregates, which predominated at the high-nutrients-low-chlorophyll zone, seemed more easily broken down into suspended particles in the upper-mesopelagic. In other words, prymnesiophyte are less efficient in mediating the biological carbon pump as their transfer efficiency to the mesopelagic was low compared to their diatom counterparts, even when they dominated surface phytoplankton community. In correlation, suspended particles in the upper-mesopelagic appeared to originate from the disaggregation of prymnesiophyte-enriched aggregates.

In the upper-mesopelagic, copepods, either by their feeding behaviour or the production of dense faecal pellets, were more influential on sinking particles while soft-tissue organisms either preferred feeding on suspended particles or their soft tissue became part of suspended components. This highlights the potential use of environmental DNA as a proxy and a complementary approach to classic microscopy observations for the study of the composition of suspended and sinking particles in the ocean.

Heterotrophic and mixotrophic protists contributed the most to eukaryotic community composition in the upper-mesopelagic, thereby suggesting their importance in remineralisation processes and subsequent carbon flux attenuation at this depth. Sinking and suspended particles were enriched in specific heterotrophic and mixotrophic protist groups. Apart from their size distribution, this suggests differential ecological conditions favoured by these groups, such as chemical composition of organic matter and prey population availability. Predator-prey relationship specificities, organic matter requirements as well as quantification of these heterotrophic protist groups are required to further understand their effect on suspended and sinking particles, as well as to decipher their roles in the biological carbon pump.

Chapter 5: Functional differences in suspended and sinking particle-associated microbial activities revealed by metatranscriptomics

This chapter in preparation for submission to *Frontiers in Marine Science* as:

Functional differences in suspended and sinking particle associated microbial activities revealed by metatranscriptomics

Manon T Duret[1]*, Richard S Lampitt[2], Phyllis Lam[1]

[1]Ocean and Earth Science, University of Southampton

[2]National Oceanography Centre Southampton

PL, MTD and RSL designed the study. MTD collected and analysed samples, conducted data analysis and wrote the manuscript. PL assisted in the manuscript preparation. RSL provided feedback on the manuscript.

5.1 Abstract

Sinking particles are major vehicles for particulate organic carbon flux to the deep sea, and thereby define the strength of the biological carbon pump. However, most of the particulate organic carbon in the oceans is bound to suspended particles. This is the first study to investigate organic carbon remineralisation and associated activities, with regards to nitrogen and sulphur cycling, on suspended and sinking particles separately. Metatranscriptomic data revealed a clear distribution of functionalities among small and large suspended and sinking particles collected from the Porcupine Abyssal Plain (North Atlantic).

Our data provide further evidence that, rather than directly taking place on sinking particles, most microbial remineralisation processes affecting the biological carbon pump efficiency are performed by; (i) microbes associated with small particles, likely resulting from the disaggregation of large sinking particles, and (ii) by free-living communities in the water column. Furthermore, microbes associated with large suspended aggregates showed an increased ability to degrade refractory carbohydrates compared to those associated with large sinking aggregates. This pattern was particularly pronounced below the mixed layer depth.

Microbial communities associated with small particles expressed genes involved in sulphur oxidation and chemolithoautotrophic carbon fixation pathways, suggesting their role as carriers of chemolithoautotrophy. Additionally, transcripts associated with sulphur reduction and denitrification pathways were present with small size-fractions, suggesting the possibility of active anaerobic remineralisation occurring in small particles, and thereby the presence of highly reduced conditions.

5.2 Introduction

Sinking particles are key players of the oceanic biological carbon pump (BCP) that removes ~ a third of anthropogenic atmospheric carbon dioxide (pCO_2) every year from the surface ocean (Sabine et al., 2004). They contribute to the transport of particulate organic matter (POM) produced by photosynthesis in the euphotic (0 – ~ 100 m) towards the mesopelagic ocean (~ 100 – 1000 m) (De La Rocha and Passow, 2007). As they sink, these particles constitute an organic matter substrate for heterotrophs thriving in the mesopelagic zone. As they consume it, this POM is recycled into CO_2 and inorganic nutrients that are released in surrounding waters (Ploug and Grossart, 2000). Microbial communities are the main actors of this organic matter remineralisation (Collins et al., 2015). They have been estimated to be responsible for > 70 % of remineralisation processes (Buesseler et al., 2007; Giering et al., 2014; Karl et al., 1988). Microbial remineralisation processes of sinking particles can be either:

(i) Directly carried out by sinking particle-associated microbial communities.

(ii) Indirectly by free-living microbial communities consuming *a posteriori* dissolved organic matter (DOM) released from POM solubilisation and hydrolysis enzymatic activities of microbes associated with sinking particles (Cho and Azam, 1988; Kiørboe and Jackson, 2001; Smith et al., 1992) and/or by mesozooplankton sloppy feeding (Strom et al., 1997).

(iii) Indirectly by microbial communities associated with suspended particles originating from the disaggregation of sinking particles caused by heterotrophs feeding behaviours and abiotic processes (Lam and Marchal, 2015).

Due to remineralisation processes, there is an attenuation of the downward flux of particulate organic carbon (POC) with depth that is related to an overall decrease of sinking particles concentration (Martin et al., 1987). Conversely, the concentration of POC in suspended particles remains approximately constant with depth at ~ one to two orders of magnitude higher than that of sinking particles (Bacon et al., 1985; Verdugo et al.,

2004; Bishop et al., 1977; Riley et al., 2012), reaching up to 1218 μm L^{-1} in the Porcupine Abyssal Plain site (PAP) (Baker et al., 2017). Being the largest pool of available POC in the ocean, suspended particles are key organic carbon substrates for heterotrophic microbes compared to sinking particles, which are, comparatively, a rare occurrence in the mesopelagic (Arístegui et al., 2009).

The low microbial respiration rates measured on fast-sinking particles (Belcher et al., 2016b, 2016a) coupled with higher rates measured on slow-sinking particles (Cavan et al., 2017) imply that both particle-types exhibit differential organic carbon composition, and hence, that differential remineralisation pathways must be carried out by the residential particle-associated microbial communities. Suspended and sinking particles have indeed different characteristics regarding their chemical composition (Karl et al., 1984; Bishop et al., 1977; Sheridan et al., 2002; Druffel et al., 1998; Abramson et al., 2010). For these reasons, both particle-types should be colonised by microbial inhabitants specialised in the degradation of their constitutive organic compounds. Metabarcoding studies conducted in the Scotia Sea (Southern Ocean) support this view and implicated a niche partitioning of heterotrophic microbial communities between suspended and sinking particles (Chapter 3 and Chapter 4). Notably, ubiquitous prokaryotic remineralising taxa *Pseudomonadales*, *Vibrionales* and *Rhodobacterales* were enriched within sinking particles, while *Bacteroidetes* was enriched within suspended particles. These apparent preferences might be the result of different chemical composition combined with the differential abilities of particle-associated heterotrophs to degrade organic matter bound to suspended and sinking particles. However, the above postulations are solely based on genomic and physiological information available for known members of these remineralising taxa. No study to date has investigated the biogeochemical functions of microbial communities associated with suspended and sinking particles.

This study interrogates differences between microbial communities, using metatranscriptomics, collected within sinking and suspended particles sampled during the spring bloom season at four depths of the productive Porcupine Abyssal Plain located in

the North Atlantic (Fig. 2.3). Active microbial diversity and their various metabolisms – especially relevant to organic matter remineralisation and production as well as associated nitrogen and sulphur metabolisms – in the two particle-types are examined in order to decipher how they impact particle dynamics, and hence the efficiency of the BCP.

5.3 Material and methods

5.3.1 Sampling stations, hydrographic parameters and particle collection

Sampling took place during spring 2015 (24 June - 2 July) at the PAP observatory site (49˚N, 16.5˚W) in the northeast Atlantic (Fig. 2.3) on-board the RRS Discovery (cruise DY032). Temperature, salinity, oxygen concentration, photosynthetically active radiation (PAR), beam transmission and chlorophyll *a* concentration determined by fluorescence were measured with sensors on a conductivity-temperature-depth (CTD) unit (Seabird 9Plus with SBE32 carousel) (Fig. 5.1A). Vertical profiles of the data obtained by CTD casts at the closest time to particle sampling were used to determine sampling depths.

Suspended and sinking particles were collected with a marine snow catcher (MSC) (Fig. 2.1) deployed at 28 m (within the mixed layer depth [MLD]), 70 m (below the MLD), 128 m (upper mesopelagic) and 500 m (mid-mesopelagic). Sinking particles, defined as particles that sunk to the base of the MSC after 2 hours (average sinking speed ≥ 12 m d^{-1}), were collected from the bottom part of the MSC. They comprise slow- and fast-sinking particles (Riley et al., 2012). Suspended particles were collected from the upper part of the MSC and are defined as particles that remained in suspension after 2 hours.

Samples were collected from the CTD and MSC deployments for measurement of nutrients. Unfiltered 15 mL water samples were collected and immediately frozen at –20˚C for onshore macronutrient measurements (nitrate, nitrite, phosphate and silicate). Concentrations were determined using a QuAAtro autoanalyser (Seal Analytical) following standard protocols (Hansen and Koroleff, 1983). Unfiltered 10 mL water samples were collected for immediate on-board ammonium measurements using the fluorescence

method described in Holmes et al. (1999), modified by Taylor et al. (2007). Particulate organic carbon (POC) concentrations of the suspended particles and of the combined fast- and slow-sinking particles (collected from the bottom part of the MSC) were measured by collecting 1 L from the upper and bottom part of the MSC respectively and were determined as described by Belcher et al. (2016a). This paper present and discuss POC concentration of fast-sinking particles while values for suspended particles were generated for this study (A. Belcher, pers. comm.).

5.3.2 Particle-associated microbial communities RNA sampling, extraction, amplification and sequencing

Microbial communities associated with suspended and sinking particles were sampled from ~ 7 L of seawater collected from the upper and bottom parts of the MSC respectively. Using a peristaltic pump, seawater samples were sequentially filtered through; (i) a 100 µm pore-size nylon filter (47 mm diameter, Millipore), (ii) a 10 µm pore-size polycarbonate membrane filter (47 mm diameter, Millipore), and (iii) a 0.22 µm pore-size Sterivex cartridge filter (Millipore). All the filtering steps were performed in under 30 minutes. Filters were then immediately incubated with RNAlater (Ambion™, Thermo Fisher Scientific) for 12 hours at 4˚C, prior to being stored at -80˚C until further processing onshore.

Following the manufacturers' instructions, the RNA was extracted from 100 and 10 µm individual filters using a ToTALLY RNA kit (Ambion™, Thermo Fisher Scientific), and RNA from 0.22 µm filters was extracted using a prior cell lysis step performed within the cartridge following a method described in Lam et al. (2011). A Turbo DNase kit (Ambion™, Thermo Fisher Scientific) was used to remove the remaining DNA, and an RNeasy MinElute Cleanup kit (Qiagen™) was used for further purification and concentration of RNA extracts. The concentration of the RNA extracts was assessed with a Qubit BR RNA assay kit (Invitrogen™, Thermo Fisher Scientific), and their integrity was assessed with the RNA Nano 6000 Assay kit read on a 2100 BioAnalyser (Agilent Technologies).

For each of the suspended and sinking particle samples, the RNA extracted from the 100 and 10 µm pore-size filters were pooled in equimolar quantities to form the large particles size-fraction (≥ 10 µm), whereas the RNA extracted from the 0.22 µm pore-size filters represented the small particle fraction (0.22 – 10 µm). Thus, particles were divided into large sinking (LSK) and small sinking (SSK) size-fractions, and large suspended (LSS) and small suspended (SSS) size-fractions. Please note that SSS and SSK may also have included the free-living fraction, but they are referred to as small particle size-fractions henceforth.

Subsequently, the pooled extract was diluted with RNase-free pure water to a volume of 9 µL. As the concentration of RNA extracts from the 100 and 10 µm pore-size filters for both particle-types at 500 m were undetectable (< 20 ng), equal volumes of the extracts from the two pore-size filters were pooled (i.e., 4.5 µL from both size-fractions). The RNA extracts were used as template for the ScriptSeq™ v2 RNA-Seq library preparation kit (Epicentre, Illumina) following the manufacturer's instructions. No rRNA removal step was performed prior to the library preparation in order to reduce the overall loss of RNA from the samples. Briefly, the RNA was fragmented into < 300 bp sequences, which were used as template for an RT-PCR. The synthesised cDNA was purified using an RNeasy MinElute Cleanup kit, and the fragments were indexed and amplified with 15 cycles of PCR. The generated amplicons were purified with Agencourt AMPure XP kit (Beckman Coulter). Prior to sequencing, the quality of the cDNA amplicons was assessed using a DNA7500 Kit read (Agilent Technologies), and the quantity measured with a Qubit dsDNA high sensitivity assay kit (Invitrogen™, Thermo Fisher Scientific). Amplicon solutions were diluted to 4 nM dsDNA, and subsequently pooled in equimolar proportions for sequencing. The dsDNA was transformed to ssDNA, and 1% PhiX was used as a control. The paired-end sequencing was carried out on an Illumina MiSeq sequencing system (M02946, Illumina) using a MiSeq Reagent 600-cycle Kit v3 (Illumina).

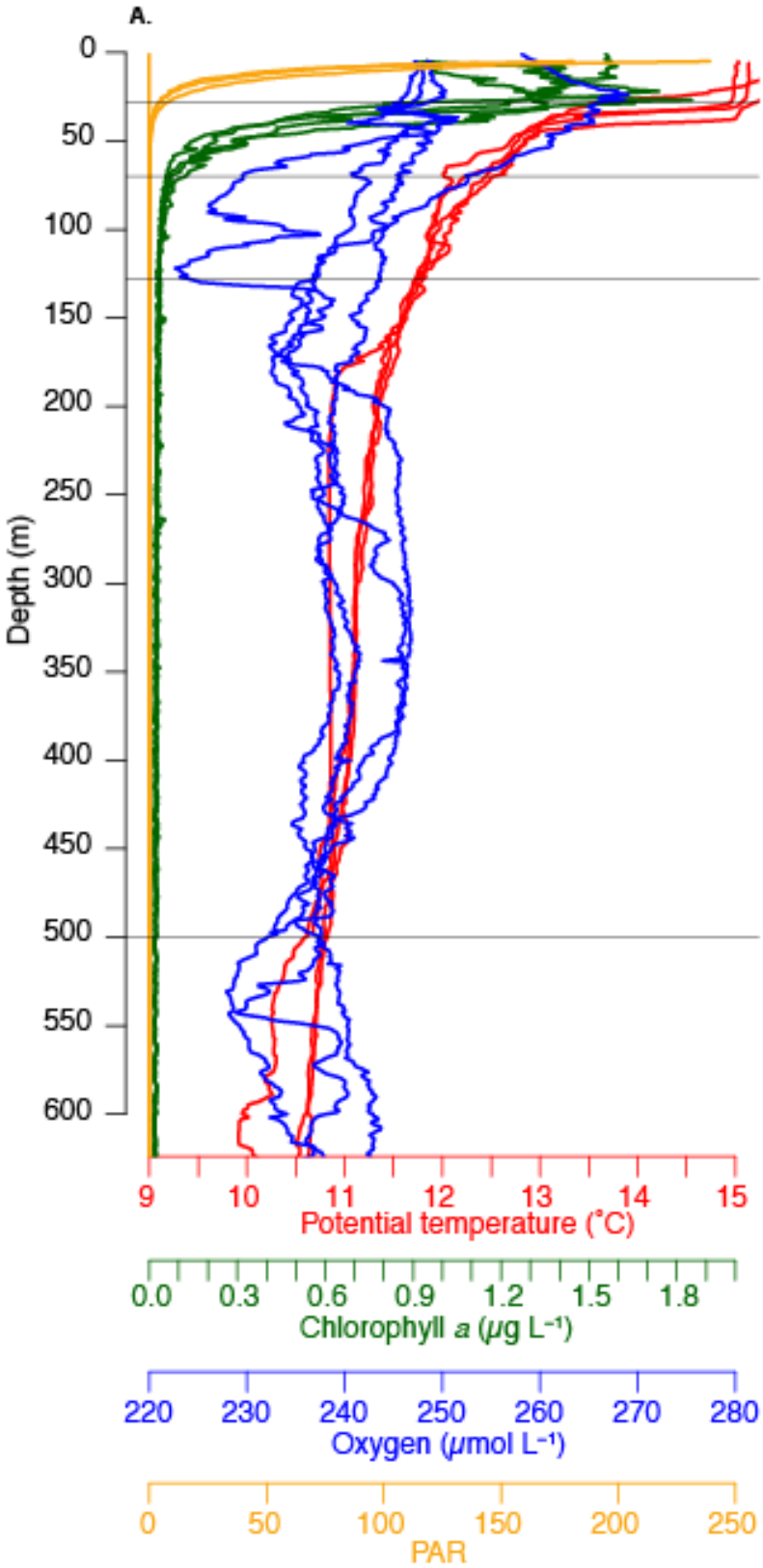

Figure 5.1. Environmental parameters profiles (this page and following two pages). A: environmental parameters (potential temperature, oxygen and chlorophyll *a* concentrations, and PAR) from CTD measurements; B: ammonium; C: nitrate; D: nitrite; E: POC; F: silicate; G: phosphate concentrations from Niskin bottles (black circles), MSC upper-part (red diamonds) and MSC bottom-part samples (blue diamonds). POC concentrations are indicated for suspended (red), slow sinking (blue), and fast-sinking (purple) from MSC samples.

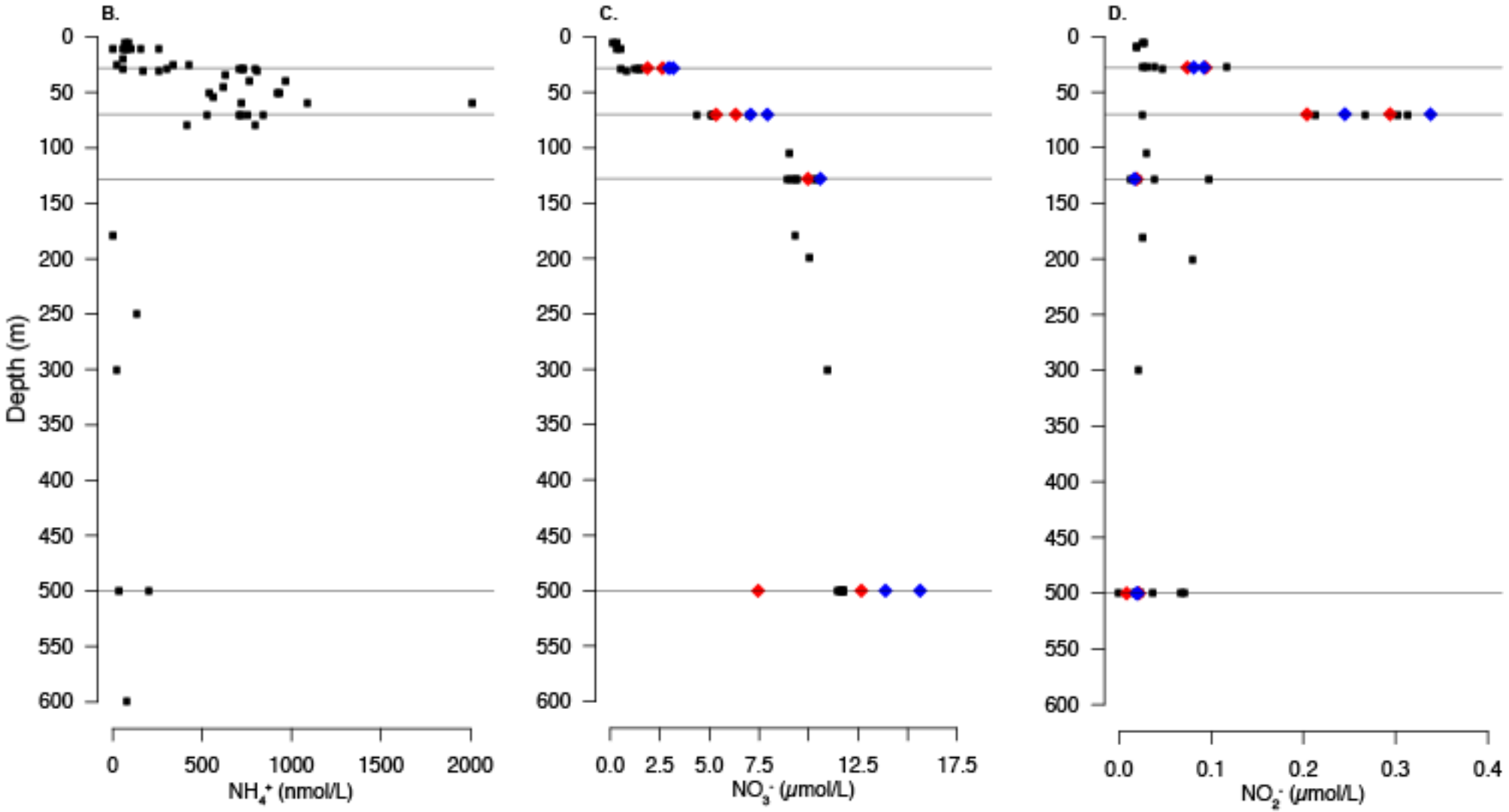
B.
C.
D.
Depth (m)
0
50
100
150
200
250
300
350
400
450
500
550
600
0
500
1000
1500
2000
NH4+ (nmol/L)
0.0
2.5
5.0
7.5
12.5
17.5
NO3- (µmol/L)
0.0
0.1
0.2
0.3
0.4
NO2- (µmol/L)

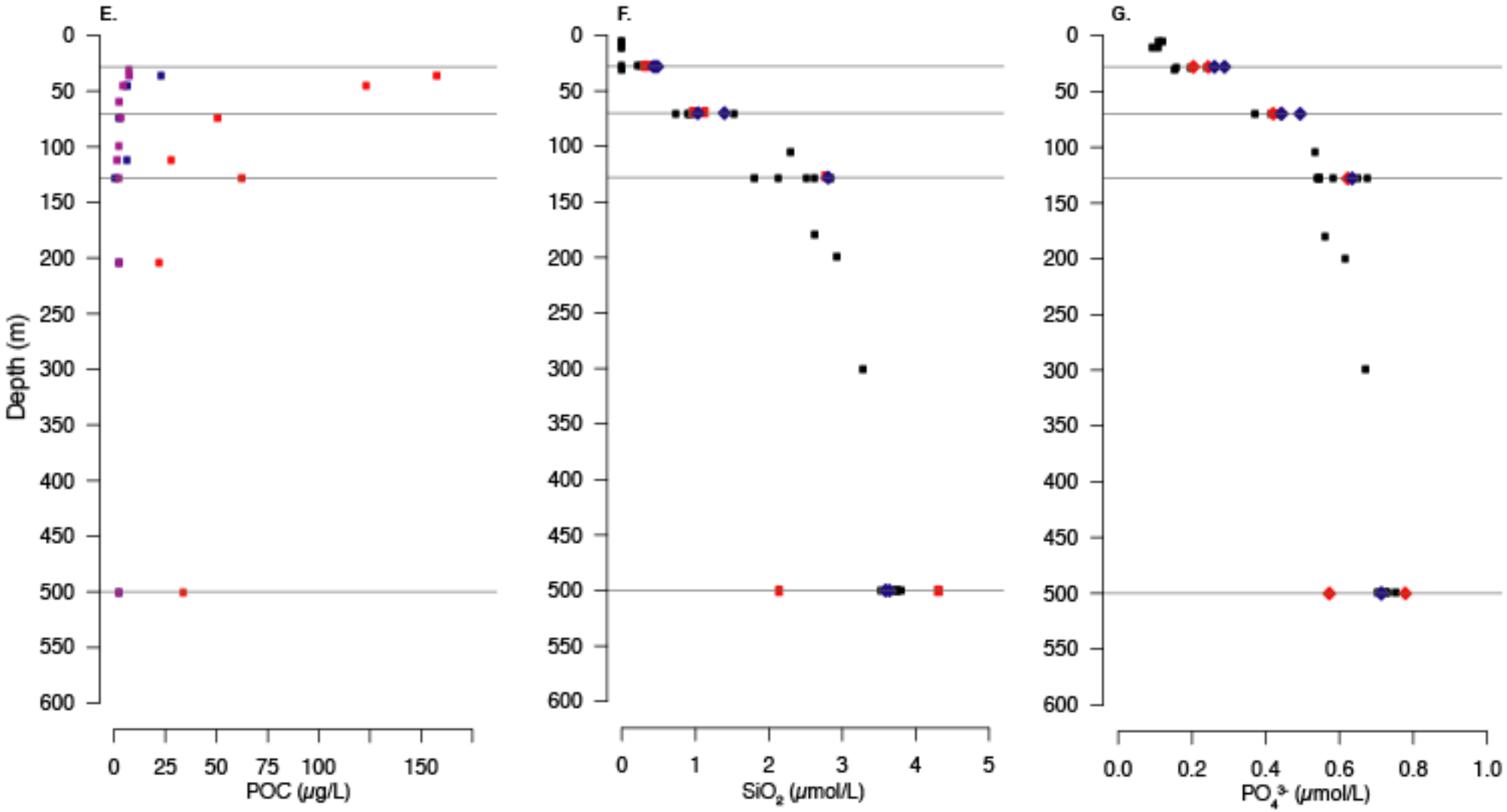
E.
F.
G.
Depth (m)
0
50
100
150
200
250
300
350
400
450
500
550
600
0 25 50 75 100 150
POC (µg/L)
0 1 2 3 4 5
SiO2 (µmol/L)
0.0 0.2 0.4 0.6 0.8 1.0
PO4 3- (µmol/L)

5.3.3 Bioinformatics and data analyses

The initial quality control of raw data generated was performed with FastQC (v 0.11.5; Babraham Bioinformatics) and followed by a trimming step to remove adaptors and poor quality (< Phred score 20) and short (<20 bp) reads using Trim Galore (v 0.4.4; Babraham Bioinformatics). SortMeRNA (v 2.1; Bonsai Bioinformatics) was used to isolate messenger RNA (mRNA) from ribosomal RNA (rRNA) and non-coding RNA (ncRNA) using the Silva rRNA database (v 119) (Quast et al., 2013) and the Rfam ncRNA database (11.0) (Burge et al., 2013). The resulting mRNA forward and reverse sequences were merged using FLASH (v 1.2.11) (Magoč and Salzberg, 2011) using default parameters as well as no minimum overlap and a maximum overlap of 300 bp.

Both assembled and non-assembled sequences were fed to the MG-RAST server (Wilke et al., 2016) in December 2016 and were used in the MG-RAST metatranscriptome pipeline (Meyer et al., 2008). Briefly, sequences were further quality checked and trimmed, genes were called and sequences were assembled through FragGeneScan, amino acids sequences were clustered at 90% identity with uclust. Using sBLAST similarity search, each protein sequence cluster was matched against a database. Transcripts were searched against the NCBI Reference Database (RefSeq) (Agarwala et al., 2017) using an e-value of 10^{-5} and a minimum identity of 60 % applied to the representative hit algorithm for taxonomical annotations. Transcripts were also annotated on their ontology and gene affiliation with the Subsystems reference database (SEED) (Overbeek et al., 2014). Sequence data will be available publicly from the MG-RAST server under an accession number to be determined. Individual transcripts of interest were manually curated, and a section of the SAMSA pipeline v 1.0 (Westreich et al., 2016) was used to access information on the transcripts at various taxonomical species level.

Statistical analyses were performed with the R statistics software (http://www.r-project.org), using the *vegan* package. The non-parametric multidimensional scaling (NMDS) analysis and the unweighted pair group method with arithmetic mean (UPGMA)

tree were based on the Bray Curtis distance of the relative abundance of transcripts in the rarefied dataset. The significance of factors influencing the sample composition was investigated with permutational multivariate analyses of variance (PERMANOVA). Similarity percentage analysis (SIMPER) was used to investigate average differences between samples composition at the transcript level. Unique and shared transcripts, as well as alpha-diversity indices were calculated on the rarefied dataset.

5.4 Results and discussion

5.4.1 Biogeochemical settings

Sampling was carried out during the spring bloom at PAP (Fig. 2.3), and during which the hydrographic structure of the water column remained relatively unchanged (Fig. 5.1A). The mixed layer depth stayed relatively stable at ca. 26 – 32 m (Belcher et al., 2016a), therefore justifying depths sampled for this study: 28 m for the mixed layer depth (MLD), 70 m for below the MLD, and 128 m and 500 m representing the upper- and mid-mesopelagic respectively.

In accordance to previous observations (Painter et al., 2010), water column concentrations of macronutrients (nitrate, phosphate and silicate) increased with depth, reaching up to ~10, ~1 and ~4 μM respectively below the MLD (Fig. 5.1B). Ammonium and nitrite maxima were observed beneath the MLD at ~ 1500 and ~ 400 nM respectively, indicative of active remineralisation (ammonification) and nitrification that are typical at these depths, particularly after productive spring blooms. Nutrient measurements obtained from seawater collected in the upper and bottom parts of the MSC were generally consistent with measurements from the water column, despite being slightly higher in the upper part of the MSC.

Particulate organic carbon (POC) concentrations of every particle-types decreased with depth (Fig. 5.1C), roughly following the Martin's curve (Martin et al., 1987). Suspended particles showed the highest POC concentrations (68.5 $\pm$ 48.5 μg L^{-1}) compared to fast-

sinking (4.0 ± 2.1 µg L^{-1}) and slow-sinking particles (6.6 ± 7.0 µg L^{-1}), consistent with what has been previously observed in this area (Riley et al., 2012). Both slow-sinking and suspended particles showed subsurface maxima within or below the MLD (~ 30 – 60 m), which was however not the case for fast-sinking particles. This suggests that the latter were being respired to CO_2 and/or fragmented as they sank, thereby leading to the accumulation of organic carbon in the form of suspended and slow-sinking particles (Baker et al., 2017). Fast-sinking particles were dominantly composed of phytodetrital aggregates (representing up to 96 % of the POC flux composition), although faecal pellets increased in proportion with depth (66 % at 500 m) (Belcher et al., 2016a).

5.4.2 Sequencing results overview

A total of 22,171,821 quality checked and trimmed cDNA sequences were recovered from the samples, of which 12,498,571 corresponded to a combination of rRNA and ncRNA, the latter representing a minor proportion of sequences. Therefore, 9,673,250 mRNA sequences were retained for annotation with MG-RAST (Annex C1). mRNA sequences represented a higher proportion of total RNA sequences at 128 and 500 m (30 ± 13 %) compared to 28 and 70 m (58 ± 26 %) for all four particle-types, i.e., small and large suspended particles (SSS and LSS respectively) collected from the upper MSC, and small and large sinking particles (SSK and LSK respectively) collected from the bottom MSC, with a size cut-off at 10 µm. On average, small particle size-fractions (SSS and SSK) contained a lower proportion of mRNA sequences (32 ± 26 %) than large particle size-fractions (LSK and LSS) (56 ± 17 %). This indicates a higher proportion of rRNA, which in turn suggests higher levels of active protein manufacturing and consequently growth within small particle size -fractions.

A total of 3,065,156 mRNA sequences were taxonomically affiliated using the NCBI Reference Database (RefSeq), while 1,290,887 sequences were annotated on their functional identity and ontology with the Subsystems reference database (SEED). More reads from small particle size-fractions were annotated (56 ± 8 % for RefSeq and 28 ± 5

% for SEED) compared to large particles size-fractions (19 ± 4 % and 6 ± 1 % respectively). This is consistent with higher proportions of unclassified protein-coding sequences generally recovered from large size-fractions (Allen et al., 2013; Smith et al., 2013; Ganesh et al., 2014; Fontanez et al., 2015). Additionally, the current version of MG-RAST has limited abilities to predict eukaryotic encoding regions (Wilke et al., 2016), and the active microbial community composition of large particle size-fractions had higher proportions of eukaryotic sequences.

5.4.3 Taxonomic affiliation of active community

A non-parametric multidimensional scaling (NMDS) analysis based on Bray-Curtis dissimilarity of taxonomical transcript composition from RefSeq affiliations (Fig. 5.2A) showed a clear separation between small and large particle-associated active microbial communities, with an overall dissimilarity of 55.8 ± 6.4 % considering all depths. Among them, small particle-associated communities (SSS and SSK) showed higher composition dissimilarity (34.2 ± 14.7 %) than large particle-associated communities (LSS and LSK) (24.5 ± 6.7 %; Annex C2-A). Regardless of depth, particle-size (SSK versus LSK, SSS versus LSS) seemed to be a greater factor driving community variability compared to particle-types (SSK versus SSS, LSK versus LSS). Consistently, particle-size explained significantly more compositional differences than particle-type (Annex C3-A).

Similar to 16S rDNA-based diversity analysis at the Scotia Sea (Chapter 3), active suspended and sinking particle-associated communities were more differentiated in the mid-mesopelagic than in the mixed layer. These depth-patterns could be representative of stronger particle dynamics and exchanges (connecting suspended and sinking particle-pools together) within the mixed layer, as maintained by surface wind mixing. These dynamic processes of aggregation and disaggregation of particles (Lam and Marchal, 2015) could explain the peak in POC concentration of suspended particles at 128 m (Fig. 5.1C), as large sinking particles break down into suspended particles. Consequently, a

higher connectivity resulted between communities associated with large particles at this depth. This also highlights that particle dynamics varies depending on particle-size.

Large particle-associated active communities had the highest proportion of unique taxonomical families (6.3 ± 1.7 %) and affiliated sequences (0.07 ± 0.02 %) compared to small particle-associated communities at all depths (2.9 ± 0.7 % and 0.02 ± 0.01 % respectively) (Annex C4-A). Nonetheless, the structure of microbial communities in each particle-type was largely different, for both eukaryotes (Annex C5-A) and prokaryotes (Annex C5-B). As anticipated, more sequences were affiliated with *Eukaryota* in large (31.5 ± 7.7 %) than in small particle size-fractions (5.7 ± 3.4 %). On the other hand, small particle size-fractions (79.5 ± 7.1 %) were dominated by *Bacteria* and *Archaea* sequences (against 54.6 ± 8.9 % in large particle size-fractions). Except for SSS (9.9 ± 4.0 %), viral sequences were well represented in all particle-types (15.8 ± 4.8 %) and mostly belonged to the *Microviridae* family, related to *Mimivirus* (Raoult, 2004). Mimivirus is a single-stranded giant DNA icosahedral lytic virus that affects important marine bacterial taxa, such as *Bacteroidetes* (Krupovic and Forterre, 2011), as well as various protist and phytoplankton taxa (Monier et al., 2008).

Eukaryotic sequences were dominated by multicellular organisms, including the phyla *Arthropoda*, *Nematoda* and *Chordata*, which altogether represented 12.8 ± 3.9 % of large particle size-fractions (LSS and LSK). The most abundant protist sequences belonged to diatoms and *Apicomplexa* representing 3.9 ± 1.4 % of large particle size-fractions. Diatom sequences were dominated by the taxonomic class *Coscinodiscophyceae* that were most represented in LSK than LSS, in which they showed a decrease with depth (Fig. 5.3A). *Coscinodiscophyceae* is a recurrent diatom group at the PAP site in this season (Smythe-Wright et al., 2010). Its presence is also consistent with the dominance by phytodetrital material of sinking particle flux with at this period (Belcher et al., 2016a). On the other hand, *Apicomplexa* sequences were dominated by the taxonomic class *Aconoidasida*. These alveolates are obligate parasites that cause the mortality of other protist as well as

metazoans (Edgcomb, 2016; Janouškovec et al., 2015), thereby playing an important role in the regulation of marine food-webs and biogeochemical cycles (Worden et al., 2015).

Large particle size-fractions were enriched in sequences belonging to choanoflagellates, especially at 28 and 128 m, where they represented up to 11.1 % of sequences. These bacterivorous nanoflagellates (< 10 µm) (Kirchman, 2008) were also found associated with suspended and sinking particles ≥ 10 µm in the mesopelagic of the Scotia Sea (Chapter 3). Due to their small cell-size, their occurrence in large particle size-fractions suggests an active colonisation of large particles by choanoflagellates in order to consume associated bacterial communities, similar to what has been observed previously on large aggregates (Lampitt et al., 1993; Ploug and Grossart, 2000). Alternatively, their presence could also reflect the presence of colonies (Thomsen et al., 1991).

Most abundant bacterial sequences belonged to *Proteobacteria*, *Bacteroidetes* and *Firmicutes*, which respectively represented 32.2 ± 16.1 %, 8.8 ± 4.6 % and 7.1 ± 7.8 % of overall sequences. *Proteobacteria* sequences were more abundant within small (51.0 ± 5.7 %) than large particle size-fractions (23.2 ± 10.0 %), while *Firmicutes* sequences were more abundant within large (12.2 ± 8.8 %) than small particle size-fractions (3.0 ± 1.4 %) (Fig. 5.3B). Within *Proteobacteria*, most dominant taxonomical orders were *Alteromonadales*, *Vibrionales* and *Pseudomonadales*. Additionally, these three gammaproteobacterial groups were more abundant within SSK (23.0 ± 10.4 %) than SSS (5.7 ± 0.7 %). The presence of these true particle-associated taxa (Ganesh et al., 2015; Fontanez et al., 2015) in the small particle-fractions indicate that they collected actual small particles and associated microbes, although they would have inadvertently also collected free-living microbes. Taxonomical orders *Rickettsiales*, *Rhodobacterales* and *Rhizobiales* were more abundant within small than large particle size-fractions. These gamma- and alpha-proteobacterial taxa are known opportunist copiotrophs (living in nutrient-rich environment) that exhibit surface-attachment capabilities allowing them to colonise particles and to degrade a wide spectrum of organic matter, as observed in many

different oceanic regions (Pinhassi and Berman, 2003; Allers et al., 2007; Mason et al., 2012; Stewart et al., 2012; Logue et al., 2015; Liu et al., 2017; Buchan et al., 2005; Brinkhoff et al., 2008; Mayali et al., 2015; Sperling et al., 2017). They have been found preferentially attached to sinking particles ≥ 10 µm in the Scotia Sea (Chapter 3). Conversely, *Bacteroidetes* classes *Flavobacteria* and *Cytophagia*, respectively represented by *Flavobacteriales* and *Cytophagales* in our samples, did not show evident preferences for either particle-type. These secondary particle colonisers (Gómez-Pereira et al., 2012; Dang and Lovell, 2016; Datta et al., 2016) are often associated with the decay phase of phytoplanktonic blooms as they specialise in the degradation of complex organic matter (Bauer et al., 2006; Williams et al., 2013; Kabisch et al., 2014). This is in contrast with results from the Scotia Sea (Chapter 3), where *Flavobacteria* members were enriched within suspended particles ≥ 10 µm. Such differences might reflect more dynamic particle exchanges and other strategies for particle remineralisation occurring at PAP, which represents an organic richer environment, especially following the spring bloom.

With respect to *Firmicutes*, the order *Clostridiales* was more abundant in large (9.8 ± 7.9 %) than small particle size-fractions (1.2 ± 0.6 %). *Firmicutes* are known to colonise large particles (Mestre et al., 2017) and are also generally associated with oxygen limited to anoxic environments (Wright et al., 2012; Crump et al., 2007). This is congruent with the reduction of oxygen concentration measured from the periphery to the centre of large sinking particles, although they did not reach anoxia (Belcher et al., 2016a).

Archaeal sequences were abundant in small particle-fractions, except at 28 m, and were mainly represented by *Thaumarchaeota* (8.7 ± 6.2 %) of which 6.8 ± 4.7 % belonged to *Nitrosopumilales*. These are chemolithoautotrophic ammonia-oxidising archaea (AOA) that play an important role in marine biogeochemical cycles (Stahl and de la Torre, 2012).

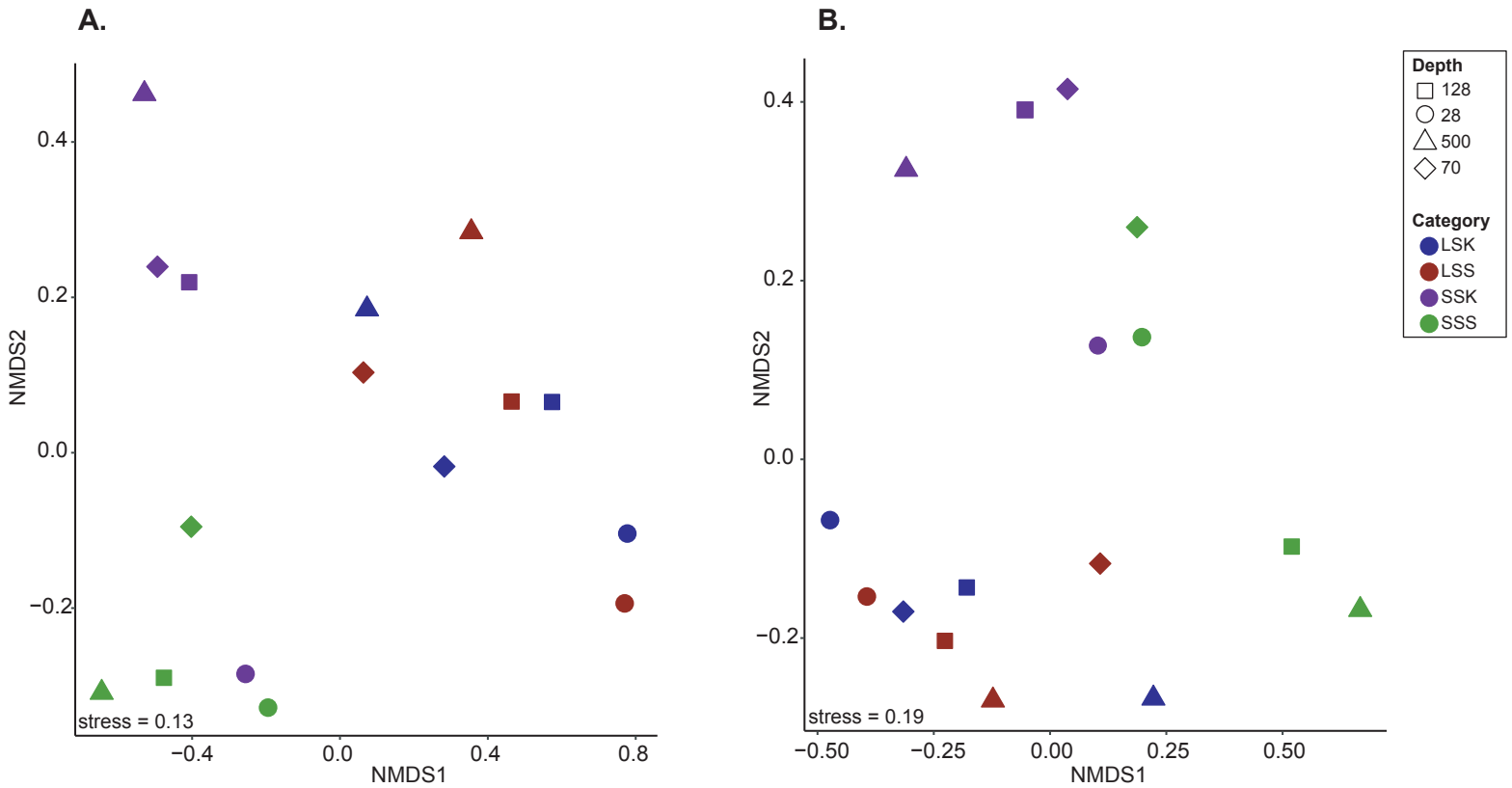

Figure 5.2. Non-metric multidimensional scaling plots of transcript composition. The NMDS was calculated with Bray-Curtis distance of the rarefied dataset. Panel A shows the NMDS based on taxonomic affiliations from Refseq and panel B based on functional annotations from SEED. LSK = large sinking particles (≥ 10 µm); LSS = large suspended particles; SSK = small sinking particles (0.22 – 10 µm); SSS = small suspended particles.

Figure 5.3. Taxonomic class composition (following two pages). Panel A shows the taxonomic affiliation of eukaryotic sequences and panel B of prokaryotic sequences. The category "Others" corresponds to the pooled abundance of remaining less abundant classes. LSK = large sinking particles (≥ 10 µm); LSS = large suspended particles; SSK = small sinking particles (0.22 – 10 µm); SSS = small suspended particles.

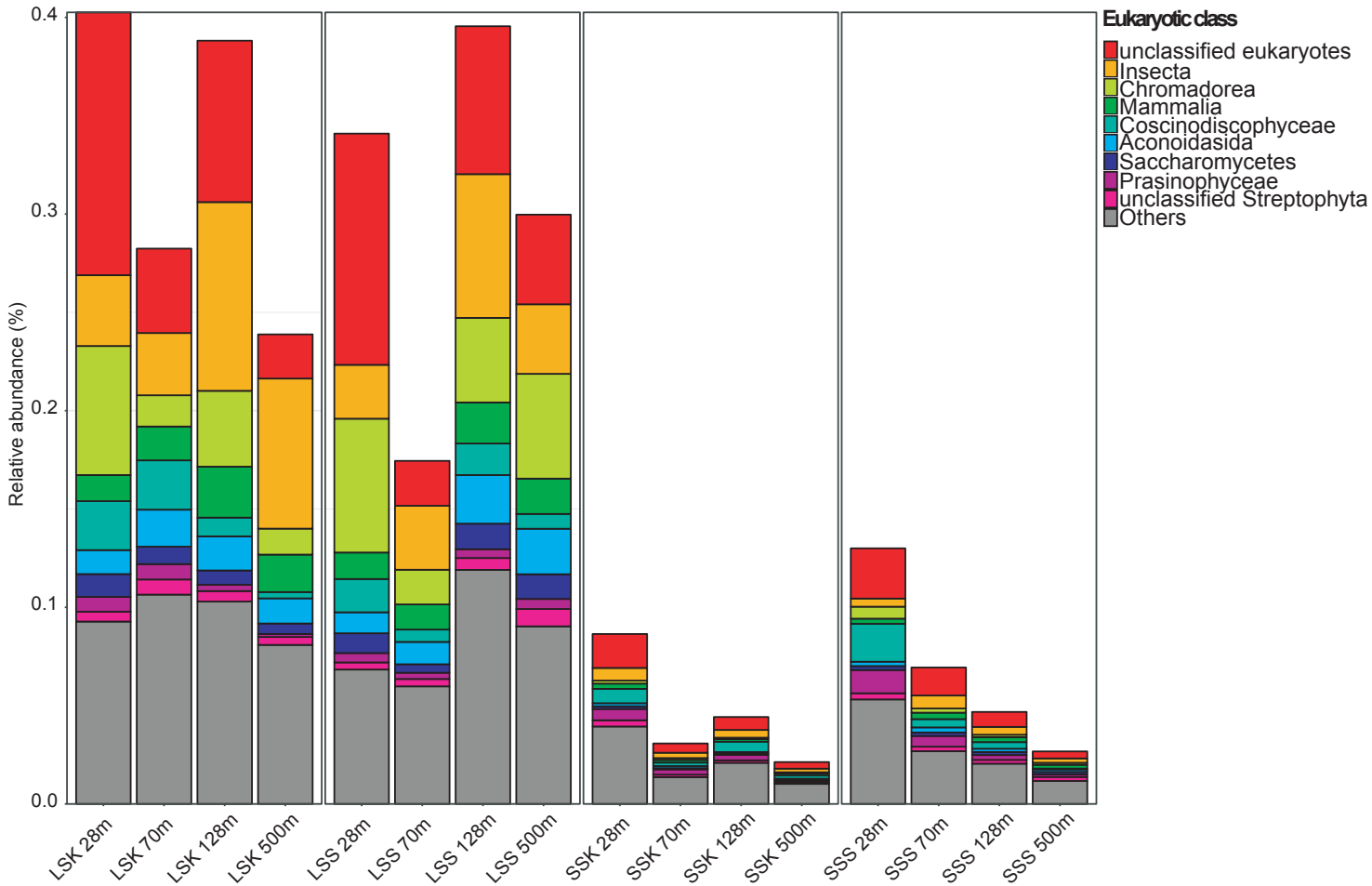
Relative abundance (%)
0.4
0.3
0.2
0.1
0.0
LSK 28m
LSK 70m
LSK 128m
LSK 500m
LSS 28m
LSS 70m
LSS 128m
LSS 500m
SSK 28m
SSK 70m
SSK 128m
SSK 500m
SSS 28m
SSS 70m
SSS 128m
SSS 500m
Eukaryotic class
unclassified eukaryotes
Insecta
Chromadorea
Mammalia
Coscinodiscophyceae
Aconoidasida
Saccharomycetes
Prasinophyceae
unclassified Streptophyta
Others

A.

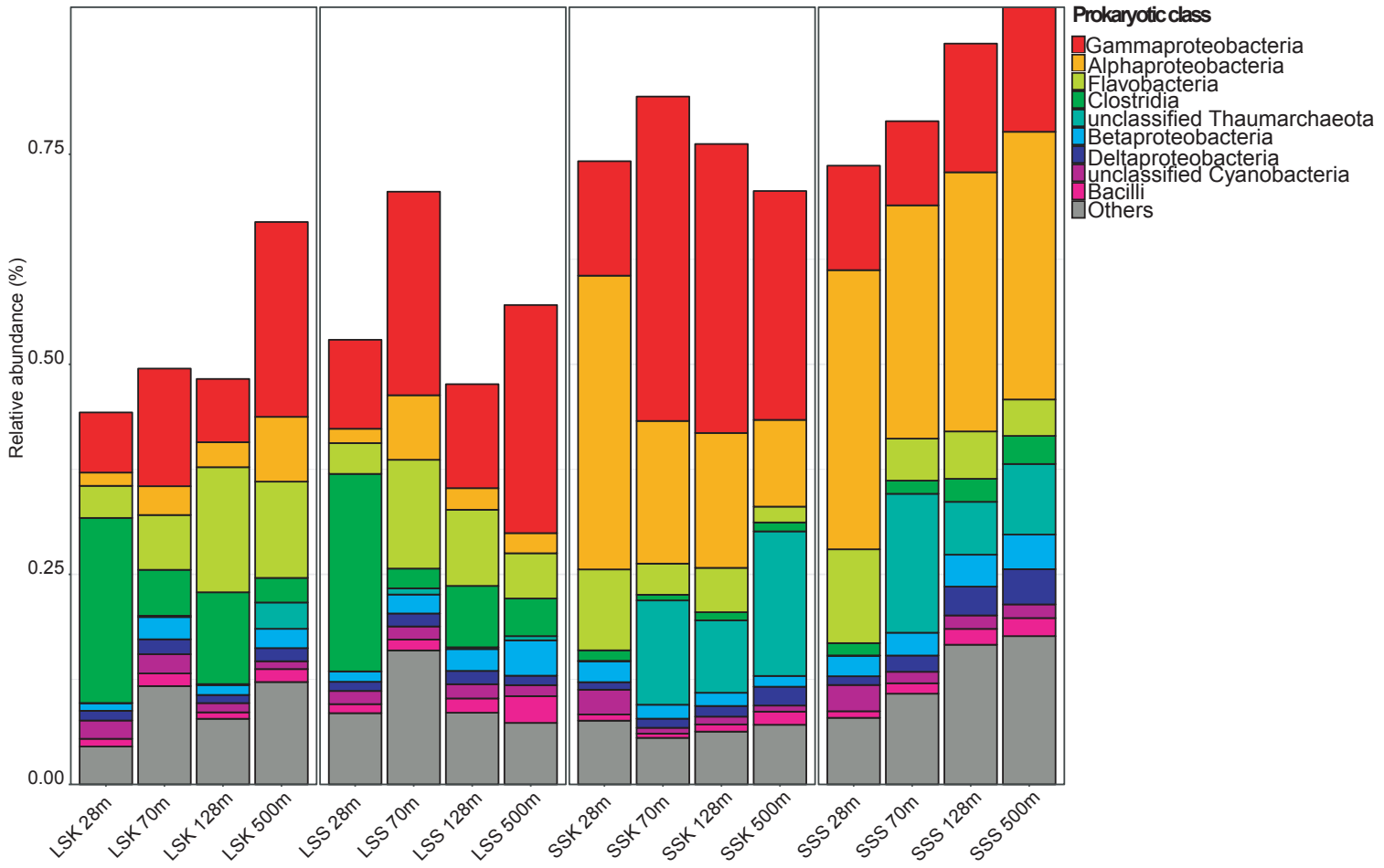
Prokaryotic class
Gammaproteobacteria
Alphaproteobacteria
Flavobacteria
Clostridia
unclassified Thaumarchaeota
Betaproteobacteria
Deltaproteobacteria
unclassified Cyanobacteria
Bacilli
Others
Relative abundance (%)
0.00
0.25
0.50
0.75
LSK 28m
LSK 70m
LSK 128m
LSK 500m
LSS 28m
LSS 70m
LSS 128m
LSS 500m
SSK 28m
SSK 70m
SSK 128m
SSK 500m
SSS 28m
SSS 70m
SSS 128m
SSS 500m

B.

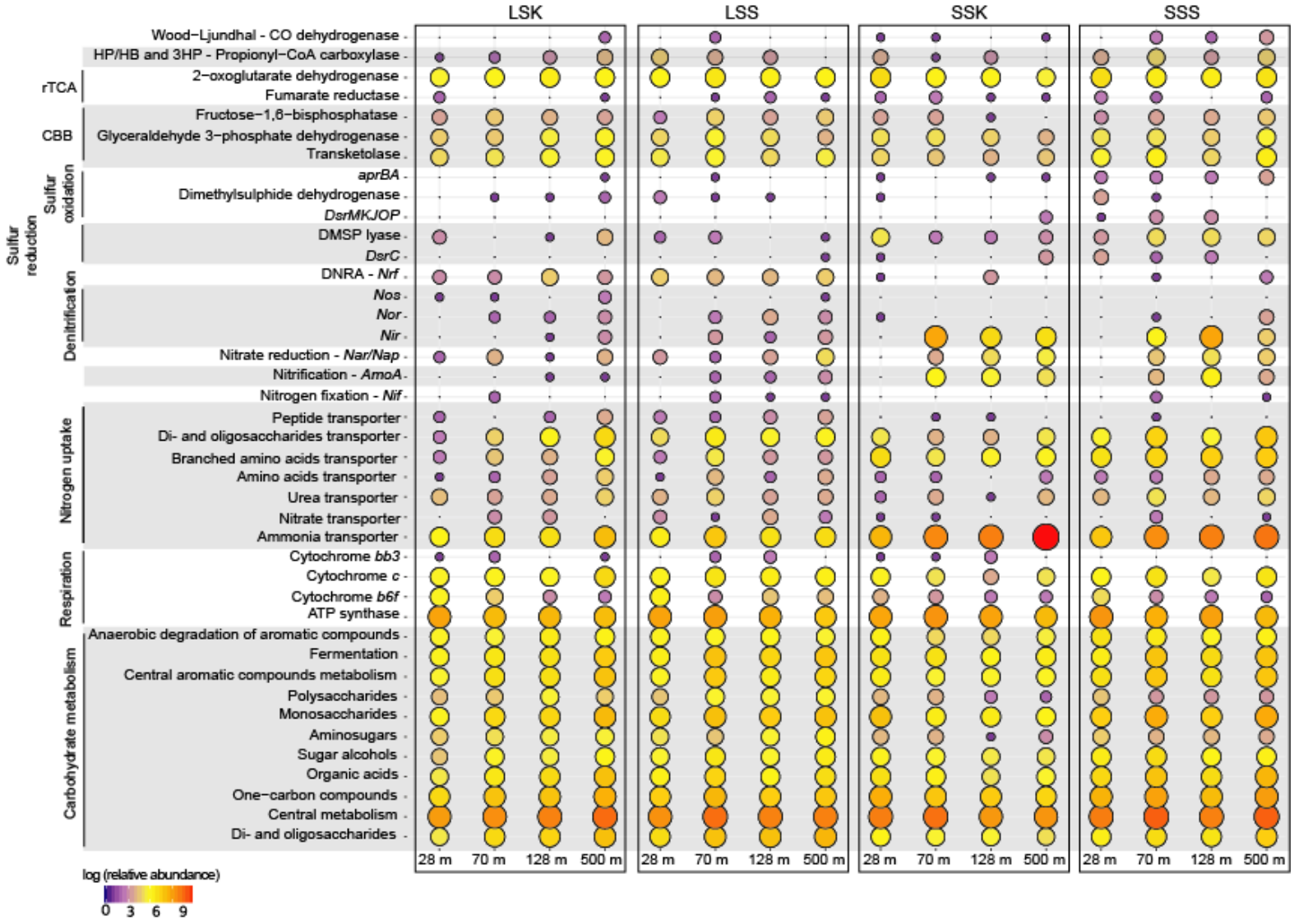
LSK
LSS
SSK
SSS
Wood−Ljundhal - CO dehydrogenase
HP/HB and 3HP - Propionyl−CoA carboxylase
rTCA
2−oxoglutarate dehydrogenase
Fumarate reductase
CBB
Fructose−1,6−bisphosphatase
Glyceraldehyde 3−phosphate dehydrogenase
Transketolase
Sulfur oxidation
aprBA
Dimethylsulphide dehydrogenase
DsrMKJOP
Sulfur reduction
DMSP lyase
DsrC
DNRA - Nrf
Denitrification
Nos
Nor
Nir
Nitrate reduction - Nar/Nap
Nitrification - AmoA
Nitrogen fixation - Nif
Nitrogen uptake
Peptide transporter
Di- and oligosaccharides transporter
Branched amino acids transporter
Amino acids transporter
Urea transporter
Nitrate transporter
Ammonia transporter
Respiration
Cytochrome bb3
Cytochrome c
Cytochrome b6f
ATP synthase
Carbohydrate metabolism
Anaerobic degradation of aromatic compounds
Fermentation
Central aromatic compounds metabolism
Polysaccharides
Monosaccharides
Aminosugars
Sugar alcohols
Organic acids
One−carbon compounds
Central metabolism
Di- and oligosaccharides
28 m
70 m
128 m
500 m
log (relative abundance)
0 3 6 9

Figure 5.4. Bubble plot of expression from genes of interest (previous page). The bubble plot represents the log (relative abundance) of the rarefied dataset and focuses on a selection of genes of interest from each metabolism discussed. Large bubbles in red indicate higher abundances than small bubbles in bue. A detailed list of genes of interest is presented in Annex C7.

5.4.4 Functional annotations

5.4.4.1 Ontology overview

Similar to taxonomic analyses presented above, NMDS analysis based on Bray-Curtis dissimilarity of the functional transcript composition annotated with SEED also revealed a clear separation between communities depending on particle-size rather than particle-type (Fig. 5.2B and Annex C3-B), with an overall dissimilarity between communities averaging at 44.9 $\pm$ 5.1 % (Annex C2-B). Additionally, differences between SSK and SSS were greater than differences between LSK and LSS. Consequently, this suggests that disparities in activity observed among particle-types are directly related to taxonomical composition of active microbial communities.

None of the environmental parameters measured within the MSC, including nutrients, oxygen, POC and chlorophyll *a* concentrations, and temperature and salinity, were found to have a significant effect on overall transcript composition of samples ($p < 0.05$; Annex C3-B). Therefore, variations in transcript composition with depth most likely reflects different particle dynamics.

Opposite trends were observed in the two alpha-diversity indices calculated (Pielou's and Shannon's) (Annex C6) for both size-fractions of sinking particles, with LSK showing an increase with depth while SSK showed a decrease. Similarly, in suspended particles, maxima were found below the MLD for LSS, which coincided with the minima for SSS. This could reflect continuous exchanges between both size-fractions of a same particle-type with depth, with functional diversity increasing as organic matter availability and lability decreases, and as organic matter complexity increases.

The ten most abundant transcripts represented on average 46.3 ± 13.9 % of sequences per sample and belonged to different ontology categories depending on particle size-fraction and type, as well as sampling depth. For instance, photosynthesis related genes (encoding for photosystem I and II proteins) were within the top ten most expressed genes within the MLD regardless of the sample.

Phages and prophages metabolism was the most abundant level 1 category of the SEED classification (Overbeek et al., 2014) in every sample (33.3 ± 12.9 %), with highest abundances found in LSK (42.7 ± 12.2 %) and lowest in SSS (18.2 ± 7.5 %). Among these, the most expressed genes were related to capsid protein synthesis and phage replication. These results are consistent with literature suggesting large particles and aggregates to be viral hotspots (Allen et al., 2012). When occurring below the euphotic zone, active viral replication and subsequent microbial cells lysis is responsible for the release of dissolved organic matter (Bettarel et al., 2016), thereby attenuating the efficiency of carbon export into the deep ocean (Suttle, 2007; Worden et al., 2015).

The following most expressed genes belonged to *Protein metabolism* (10.1 ± 2.6 %), *Carbohydrates metabolism* (6.1 ± 2.0 %) and *Amino acids metabolism* (4.6 ± 2.0 %) that represented similar proportions in every samples. *Virulence and disease defence metabolism* transcripts were relatively more abundant within small particles (6.6 ± 4.5 %) than large particle size-fractions (1.7 ± 0.7 %).

Transcripts belonging to the *Protein metabolism* were mainly involved in bacterial biosynthesis of large and small subunits of ribosomes. These transcripts were more expressed in small (2.8 ± 1.4 %) than in large particle size-fractions (1.9 ± 0.5 %). This is in agreement with the high proportion of rRNA recovered and of RNA polymerase expressed within small rather particle size-fractions, thereby implying relatively more active growth compared to communities associated with large particles. Within the *Carbohydrates metabolism* category, the highest expression came from genes related to the central carbohydrate metabolism (glycoxylate bypass, pyruvate metabolism and Krebs

cycle) while *Amino acids metabolism* was mainly represented by genes related to biosynthesis of methionine, glutamine and branched amino acid chains. Finally, *Virulence and disease defence metabolism* was mainly represented by genes involved in the resistance to antibiotics and toxic compounds, as well as by genes encoding for *Staphylococcus* adhesins that were more abundant in small (5.8 ± 4.6 %) than large particle size-fractions (0.1 ± 0.1 %). This is congruent with higher abundances of transcripts affiliated with *Staphylococcus* prophages in small (2.0 ± 1.1 %) rather than in large particle size-fractions (0.5 ± 0.2 %). *Staphylococcus* has been previously observed in small limnic and marine particles (Bižić-Ionescu et al., 2014; Yung et al., 2016).

On average, only 23.6 ± 0.6 % of transcripts were shared among every samples at a given depth, with a slightly higher proportion shared between large (52.2 ± 1.9 %) than small particle size-fractions (45.8 ± 2.6 %), except at 28 m (Annex C4-B). Nonetheless, these shared transcripts represented the majority of sequences in every samples (89.6 ± 6.1 %). Howbeit, large particle size-fractions had higher proportions of unique transcripts (18.4 ± 4.0 %) and affiliated sequences (3.3 ± 1.0 %) compared to small particle size-fractions at most depths (11.6 ± 3.8 % and 1.7 ± 1.1 % respectively). Most unique transcripts were related to *Carbohydrates metabolism*, and more precisely, to genes encoding for enzymes active in the utilisation of various saccharides (including aminosugars, organic acids, sugar alcohols, etc.) and CO_2 fixation pathways.

The data presented below was manually curated from SEED ontology and functional annotations and was subsequently reorganised into categories and sub-categories (Fig. 5.4). A simplified summary of this data is presented in Annex C7.

5.4.5 Carbohydrates catabolism and respiration pathways: insights into carbon remineralisation

5.4.5.1 Carbohydrates catabolism

Large particle size-fractions shared the highest expression of genes encoding for enzymes involved in the degradation of; (i) amino-sugars (mainly N-acetylglucosamine or chitin), (ii) di- and oligosaccharides (lactose, galactose, maltose and maltodextrin), (iii) polysaccharides (glycerol, glycogen), (iv) monosaccharides (deoxyribose, deoxynucleoside, mannose and L-rhamnose), and (v) general glycoside hydrolases. The expression of these genes increased with depth, sometimes reaching a peak below the MLD (e.g., polysaccharides degradation) which is consistent with the peak in ammonia concentration and our understanding of most intense remineralisation at these depths (Martin, 1987).

Expression of genes encoding for di- and oligosaccharide degradation and carbon storage regulation was particularly high in LSS. In addition, genes involved in the degradation of complex aromatic carbohydrate molecules were more expressed in large than in small particle size-fractions and showed an increase in expression with depth. Notably, genes encoding for enzymes degrading phenylacetyl-CoA and biphenyl as well as genes active in the central metabolism of aromatic intermediates (protocatechuate branch of beta-ketoadipate and homogentisate pathways) were more expressed in both LSK and LSS.

Expression of genes involved in fermentation processes (utilisation of mixed acids, and production of acetone, butanol and ethanol) and in anaerobic carbon remineralisation were detected in all samples, and particularly in large particle size-fractions, with a peak in expression observed in LSS below the MLD replaced by a peak in SSS at the depth below. Meanwhile, genes encoding for toluene 4-monooxygenae (T4MO), active in the degradation of toluene, were highly and only expressed in LSS samples.

In comparison, small particle size-fractions usually showed highest expressions for genes encoding for enzymes involved in the processing and degradation of small organic compounds. Examples include genes encoding for enzymes active in; (i) central carbohydrate metabolism (glyoxylate bypass, pyruvate metabolism, dehydrogenase complexes, glycolysis and gluconeogenesis), (ii) one-carbon metabolism (mainly serine-glyoxylate cycle), and the degradation of (iii) organic acids (propionate-CoA to succinate and propionyl-CoA to succinyl-CoA modules) and (iv) sugar alcohols (glycerol, glycerol-3-phosphate, inositol and mannitol). Furthermore, the expression of these genes increased with depth.

The processing and utilisation of small organics by microbes in small particle size-fractions was further supported by highest expressions of genes encoding for transporters for tricarboxylate (organic acid). Genes encoding for ABC transporters, involved in the transport of low molecular weight (LMW) compounds, were highly expressed in SSS. Nevertheless, this is not to say that microbial communities in small particle size-fractions did not use more complex organics as genes encoding for Ton and Tol transporters, involved in the transport of high molecular weight (HMW) compounds, were highly expressed in SSK. Similarly, those involved in peripheral pathways for the degradation of aromatic compounds (phenylalkanoic acid, biphenyl and phenylpropanoid compound) were more expressed in SSS, aside from below the MLD where LSS showed the highest expression of these genes. Small particle size-fractions exhibited further differences below the MLD (128 and 500 m), as genes involved in carbon storage regulation were more expressed in SSK, while those involved in monosaccharides degradation were more expressed in SSS.

5.4.5.2 Respiration pathways

Genes encoding for ATP synthases (1.1 ± 0.3 %) were overall the most abundant respiration related expressed genes and showed a clear decrease with depth. As these enzymes are responsible for the oxidation of organic matter, the evolution of their

expression is in agreement with the overall decrease in POC concentration and expected decrease of labile organic carbon substrate with depth. Furthermore, their higher expression in small (1.2 ± 0.3 %) compared to large particle size-fractions (0.9 ± 0.3 %) implies higher organic resources within small particles.

With respect to respiratory cytochromes, the cytochrome *b6f* complex generates proton gradients necessary for photosynthetic energy storage (Hasan et al., 2013). Accordingly, transcripts related to the biogenesis of this cytochrome were the most abundant within the MLD (28 m), and especially in LSK, thus in agreement with the high expression of genes encoding for photosystem proteins at this depth.

Genes encoding for the biogenesis of cytochrome *c* oxidase, most commonly used in aerobic respiration, were the most expressed respiratory enzymes across all samples (0.20 ± 0.09 %). Genes involved in electron-donating reactions, including various respiratory complexes, such as NADH-quinone oxidoreductase, and sodium ion coupled energetics (oxaloacetate and glutaconyl-CoA decarboxylases), were also highly expressed in all samples, but were the highest for SSS, especially below the MLD. This further corroborates high expression levels of ATP synthases and intense remineralisation at this depth.

Cytochrome *cbb3* is a key respiratory protein exhibiting higher affinity with O_2, relative to cytochromes *a* and *c*, and is thus particularly important for aerobic bacteria in reduced oxygen conditions (Cotter et al., 1990). Genes encoding for the biogenesis of this cytochrome were more expressed in large particle size-fractions (0.029 ± 0.019 %), and especially in LSS samples. Though generally lower, expression was equally high in SSK in the upper-mesopelagic (128 m) (0.0053 %) and were absent altogether in SSS samples. Consistently, genes encoding for soluble cytochrome synthesis and functionally related electron-carriers were more expressed in LSS samples. Expression patterns of these genes strongly suggest reduced-O_2 conditions within large particles.

5.4.5.3 Implications for carbon remineralisation

Despite depth variations, the highest expression of genes involved in carbohydrates catabolism and respiration pathways was observed in SSS, followed by LSS and LSK, and their expression was the lowest in SSK, suggesting their relative importance in carbon remineralisation. Genes encoding for simple organic hydrolytic enzymes and aerobic respiratory pathways were highly expressed in SSS samples. Taken together, these findings suggest that free-living and small suspended particle-associated microbial communities carry out most of carbon remineralisation, especially below the MLD. This is congruent with the highest POC concentrations measured in suspended than in sinking particles at PAP (Riley et al., 2012; Baker et al., 2017). Additionally, this supports measurements combined in a model of sinking particle remineralisation in the North Atlantic (Collins et al., 2015). This model estimated that most of sinking particle organic matter is remineralised in the surrounding water column by either; (i) free-living microbes benefiting from sinking particle POM solubilisation and subsequent release of DOM in a plume (Shanks and Trent, 1979; Smith et al., 1992), or (ii) microbes associated with suspended particles originating from the disaggregation of sinking particles. This is corroborated by results from other oceanic regions suggesting suspended particles as a key carbon substrate for heterotrophs, especially in the mesopelagic (Baltar et al., 2009, 2010; Herndl and Reinthaler, 2013). Furthermore, these results are consistent with low microbial respiration rates measured on LSK at PAP (Belcher et al., 2016a), although further rate measurements in the other size-fractions are needed for a quantitative comparison of microbial remineralisation activities in particle-types and -sizes.

In general, microbial communities in large particle size-fractions had the highest expression of genes encoding for enzymes degrading complex organic compounds and generally showed an increase with depth. This agrees with increased detection of enzymes involved in aromatic compound catabolism with depth in the North Atlantic (Bergauer et al., 2018). Meanwhile, a decrease in organic matter lability with depth may

also occur within small particle size-fractions, as SSS also exhibited an increased expression of genes active in complex carbon compounds degradation with depth.

Genes encoding for the degradation of complex organic compounds and for fermentation were particularly highly expressed in LSS compared to LSK, especially below the MLD. This suggests that organic matter lability is lower in large suspended aggregates compared to their sinking counterparts in the mesopelagic. This is in correlation with what has been suggested based on colonisation patterns of the two particle-types by remineralising prokaryotic taxa in the Scotia Sea (Chapter 3), thereby LSK were favoured by r-strategists while K-strategists preferred the likely more refractory LSS.

Although microbes collected in SSS were more active and exhibited more diverse abilities for carbon remineralisation, those in SSK appeared to be more specialised in the carbon remineralisation pathways they carried out, which sometimes involved anaerobic processes. This finding could mean that, although free-living microbes would have been inadvertently collected in SSK, those samples were more likely to be dominated by microbial communities associated with true small sinking particles. This particle-type, sometimes referred to as slow-sinking particles in the literature, is important for POC flux at PAP (Baker et al., 2017) and exhibit higher microbial respiration rates than LSK (Cavan et al., 2017). Small sinking particles appeared to contain a very specific organic composition and their associated microbial communities seemed highly active in its remineralisation. Further investigation is required to understand the origin of small sinking particles and the roles they play within the remineralisation processes of large sinking aggregates.

Variations in the relative expression of organic carbon remineralisation genes across particle-fractions and depths suggest that microbial communities residing on different particle-types and sizes are adapted to the chemical composition of organic carbon available therein. This would be in agreement with changes of hydrolytic enzymatic rates associated with changes in organic matter composition of aggregates (Ziervogel et al.,

2010) and is to be expected considering changes in the nature of organic matter between sinking and suspended particles and its evolution with depth (Sheridan et al., 2002; Druffel et al., 1998).

5.4.6 Sources of cellular nitrogen

Ammonia (NH_3) is the first inorganic form of nitrogen released from the recycling of organic matter, but is also the primary form of nitrogen consumed by both autotrophic and heterotrophic microbes (Zehr and Ward, 2002). Therefore, it is taken up as soon as it is produced, leaving concentration in global oceans typically low to undetectable (Gruber, 2008). For this reason, the detection of highest expression for NH_3 transporters among other nitrogen transporters is unsurprising. Genes encoding for NH_3 transporters were highly expressed in small size-fractions (2.99 $\pm$ 2.86 %) and increased with depth. They were especially highly expressed in SSK, in which they represented up to 10.25 % at 500 m.

Nitrate (NO_3^-) assimilation requires more energy than NH_3 assimilation. However, as NO_3^- is generally much more abundant than NH_3 in the ocean, it is also largely taken up by most autotrophs and heterotrophs (Gruber, 2008). Genes encoding for the uptake of NO_3^- were the most expressed in large particle size-fractions (0.016 $\pm$ 0.012 %), although they were also detected in SSS below the MLD and in SSK above the MLD.

Apart from inorganic nitrogen forms, our data also revealed the active uptake of simple LMW organic nitrogen compounds. The ability to degrade urea with urease is widespread among phytoplankton (McCarthy, 1972), prokaryotes, including cyanobacteria (Valladares et al., 2002), and AOA (Alonso-Saez et al., 2012). Genes encoding for both urease and ABC urea transporters were detected, with the highest expression in SSS (0.116 $\pm$ 0.054 %), following by LSK (0.087 $\pm$ 0.042 %) and LSS (0.063 $\pm$ 0.019 %), and the lowest expression in SSK (0.042 $\pm$ 0.015 %). Accordingly, genes encoding for allantoin utilisation, used in the urea production pathway, were more highly expressed in SSS. Genes

encoding for the hydrolysis of cyanate, which is another by-product of the urea cycle, were more expressed in large (0.030 ± 0.019 %) rather than small size-fractions (0.010 ± 0.009 %), and showed a peak in expression below the MLD.

Our data also provided evidence for the uptake of other more complex forms of LMW organic nitrogen compounds and they are presented below in order of increasing complexity. Genes encoding for amino acids (glutamate and aspartate) assimilation were highly expressed in LSK, SSS and LSS (0.027 ± 0.019) and were the least expressed in SSK (0.009 ± 0.006 %). Genes encoding for branched amino acids were highly expressed in SSS (0.43 ± 0.08 %) and SSK (0.20 ± 0.09 %), and least expressed in LSK (0.07 ± 0.05 %) and LSS (0.04 ± 0.04 %). Genes encoding for dipeptides and oligopeptides transporters were highly expressed in SSS (0.33 ± 0.18 %) and large particle size-fractions (0. 17 ± 0.11 %) compared to SSK (0.07 ± 0.03 %). Genes encoding for peptides transporters were more expressed in large (0.017 ± 0.011 %) than small size-fractions (0.002 ± 0.003 %).

The active uptake of HMW organic nitrogen compounds was also evident, especially in large particle size-fractions. N-acetyl glucosamine or chitin is a biopolymer found in cell walls and crustacean exoskeletons and represents a source of nitrogen and carbon for heterotrophs capable of surface-attachment (Fontanez et al., 2015). Genes encoding for the utilisation of this compound were more expressed in large (0.116 ± 0.048 %) than small particle fraction size-fraction (0.039 ± 0.018 %). To some extent, this is congruent with larger proportion of crustaceans found in large particle size-fractions (Fig. C5A).

Nitrogen fixation, which is the reduction of dinitrogen gas into ammonia thereby fixating atmospheric nitrogen into a biologically available form, is the major nitrogen input into marine systems (Gruber, 2008). It is catalysed by the key enzyme nitrogenase (Zehr and Kudela, 2011). Genes encoding for nitrogenase were highly expressed in all samples, and especially LSK particles below the MLD, which corresponded to a peak in *Trichodesmium* abundance, as well as LSS and SSS. Nitrogen fixation is performed across the ocean and

throughout the water column. It can be carried by diazotrophic cyanobacteria, which can be free-living or in symbiosis with phytoplankton (Martínez-Pérez et al., 2016), and by certain heterotrophic gamma- and alphaproteobacterial taxa (Farnelid et al., 2011; Benavides and Voss, 2015; Benavides et al., 2015; Martínez-Pérez et al., 2018; Halm et al., 2011). Although the reason for nitrogenase activity in the mesopelagic zone, where concentrations of inorganic nitrogen are high, is unclear, the activity of nitrogen-fixing organisms has been associated with particle-associated diazotrophs (Benavides et al., 2015).

Similar to carbohydrate transport and degradation, there was a clear repartition between the expression of genes involved in cellular uptake of different nitrogen compounds between particle-types and size-fractions. SSK microbial communities were actively taking up the smallest forms of nitrogen compounds, mainly NH_3 and urea, while SSS communities were taking up a wide range of LMW nitrogen compounds. Genes for the uptake of urea, amino acids and branched amino acids, as well as oligo- and dipeptides were indeed highly expressed in SSS. Conversely, large particle size-fractions were actively taking up more complex sources of nitrogen, including oligo- and dipeptides but also peptide and chitin, also representing a source of organic carbon. Large sinking aggregates were particularly also active in nitrogen fixation.

5.4.7 Nitrogen cycling

5.4.7.1 Nitrification

Nitrification is the process whereby ammonia (NH_3) is oxidised to nitrite (NO_2^-) and subsequently to nitrate (NO_3^-) (Ward, 2008). The marker enzyme for the first step is ammonia monooxygenase (Francis et al., 2005; Alves et al., 2018; Norton et al., 2002), which catalyses the oxidation of NH_3 into NO_2^-. Genes encoding for this enzyme were expressed in all samples, reaching a peak below the MLD, especially in small (0.094 ± 0.083 %) compared to large particle size-fractions (0.007 ± 0.007 %). This is consistent

with previous observations that this process occurs at highest rates at the base of the mixed layer, where active remineralisation of POM releases copious amounts of ammonium (NH_4^+) and where competition with phytoplankton is minimal (Smith et al., 2014).

The peak in expression of ammonia monooxygenase gene below the MLD was congruent with that of ammonia-oxidising bacteria (AOB) *Nitrosomonas*, AOA *Nitrosopumilus* and nitrite oxidising bacteria (NOB) *Nitrospira*, which were all particularly abundant in small particle size-fractions. While AOA are usually free-living, AOB have been found to inhabit particles (Philips et al., 2002), and nitrification has been shown to occur on aggregates (Karl et al., 1984). The presence of AOA and AOB in small particle size-fractions provides further evidence that this particle size-fraction collected both free-living and ≤ 10 µm particle-associated microbial communities.

5.4.7.2 Nitrate reduction, denitrification and nitrite ammonification

Nitrate (NO_3^-) is the preferred alternative form of electron acceptor when oxygen concentrations are low, such as in oxygen minimum zones. It is first reduced to nitrite (NO_2^-) by the enzyme nitrate reductase as a stand-alone process, which can be followed by denitrification or dissimilatory nitrate reduction to ammonium (DNRA) that uses generated NO_2^- as substrate (Lam and Kuypers, 2011). Genes encoding for nitrate reductase were highly expressed in small (0.058 ± 0.040 %), except at 28 m, compared to large particle size-fractions (0.032 ± 0.026 %).

The second step of denitrification corresponds to the reduction of NO_2^- to nitric oxide (NO) which is catalysed by either a membrane-bound or a periplasmic form of nitrite reductase (Lam and Kuypers, 2011). Genes encoding for these enzymes were more expressed in SSK (0.460 ± 0.414 %) and SSS (0.361 ± 0.0481 %), except at 28 m, compared to large particle size-fractions (0.011 ± 0.011 %). Expression of these genes in both particle size-fractions reached maxima below the MLD. Anammox, or anaerobic ammonium oxidation,

is a chemolithoautotrophic pathway leading to nitrogen loss which was not detected in our samples.

The final two steps of denitrification correspond to the reduction of NO to nitrous oxide (N_2O), and subsequently to N_2, which are respectively catalysed by nitric oxide reductase and nitrous oxide reductase (Zehr and Kudela, 2011), the former being less oxygen-sensitive than the latter. Genes encoding for nitric oxide reductase were more expressed in large particle size-fractions (0.015 ± 0.011 %), except at 28 m, and in SSS below the MLD (0.013 ± 0.011 %). Finally, genes encoding for nitrous oxide reductase were highly expressed in LSK (0.007 ± 0.006 %) and LSS at 500 m, and were completely absent from small particle size-fractions.

The second step of DNRA is the reduction of NO_2^- to ammonium (NH_4^+) and is catalysed by the enzyme cytochrome *c* nitrite reductase (Simon et al., 2000), which is highly sensitive to oxygen. Genes encoding for this enzyme were more expressed in LSS (0.058 ± 0.011 %) and LSK (0.034 ± 0.020 %), and their expression increased with depth, compared to small particle size-fractions (0.007 ± 0.009 %). This is in agreement with the occurrence of the oxygen-sensitive final denitrification steps in large particle size-fractions.

In accordance with the observations for uptake and degradation of carbohydrates and nitrogen compounds, there was a distribution of the processes involved in the nitrogen cycle between particle-types. Such distribution likely reflected their oxygen sensitivity. None of these processes were detected at 28 m, where oxygen concentrations are the highest, which is consistent with the oxygen sensitivity of enzymes involved in these pathways (Zumft, 1997). Nonetheless, the reduction of NO_3^- is the least oxygen sensitive step, compared to those involved in DNRA and denitrification, and its occurrence has been observed in waters with oxygen concentration of 40 µM (Kalvelage et al., 2011). The second step of denitrification (NO_2^- to NO) is less oxygen sensitive than the final two steps of denitrification (NO to N_2O, and N_2O to N_2) and DNRA (NO_2^- to NH_4^+), which require very anaerobic settings (Lam and Kuypers, 2011). Accordingly, while the reduction of NO_2^-

appeared to occur mostly in small particle size-fractions, especially in small sinking particles, reductions of NO and N_2O and ammonification of NO_2^- were mainly detected in large particle size-fractions. This correlates with the existence of oxygen gradients in large aggregates (Alldredge and Cohen, 1987), which would allow oxygen reduced settings at the centre of the particle. A recent model of oxygen gradients in 10 µm-diameter aggregates indeed demonstrated that the oxygen deficiency created at the centre of particles is sufficient to sustain denitrification and sulphate reduction processes (Bianchi et al., 2018).

5.4.8 Sulphur metabolism

Similar to anaerobic nitrogen metabolism pathways, expression of genes associated with sulphate reduction and sulphur oxidation, both classically occurring in reduced oxygen settings, were also detected in our samples.

The presence of dissimilatory sulphate reduction, corresponding to the reduction of sulphate (SO_4^{2-}) to adenosine 5'-phosphosulfate to sulphite (SO_3^{2-}) coupled with its reduction to sulphide (HS^{2-}), was detected. The gene *dsrC* that encodes for a dissimilatory sulphite reductase used for SO_3^{2-} reduction to HS^{2-} (Santos et al., 2015) was expressed at 500 m in LSS and SSK (0.005 %), as well as at 28 m (0.005 %) and 70 m in SSS (0.011 %). SO_4^{2-} reduction processes normally occur in completely anoxic environments. However, its occurrence in the presence of oxygen has been shown in the so-called “cryptic sulphur cycle” such as found in oxygen minimum zones (Canfield et al., 2010). Our data suggests the potential occurrence of this cryptic cycle in oxygenated waters likely performed by microbial communities, even in small suspended particles.

Another source of reduced organic sulphur in the ocean is the breakdown of dimethylsulphoniopropionate (DMSP). DMSP is primarily produced by phytoplankton (Yoch, 2002) and degraded to dimethylsulphide (DMS) by the action of a DMSP lyase. DMS can then act as a source of reduced organic sulphur and carbon (Kiene and Linn, 2000). Some of the climatically active DMS gas produced is released to the atmospheres

(Lovelock et al., 1972). Similar to sulphate reduction, genes encoding for DMSP lyase were slightly more expressed in small (0.071 ± 0.026 %) than large particle size-fractions (0.022 ± 0.028 %). The produced DMS can then be oxidised to dimethyl-sulphoxide (DMSO) by a dimethylsulphide dehydrogenase (Reisch et al., 2011). Genes encoding for this enzyme were more expressed in large (0.0060 ± 0.0049 %) than small particle size-fractions, except in SSS at 28 m where their expression peaked at 0.0317 %.

Similar to both DMSP breakdown, SO_4^{2-} reduction produces reduced sulphur compounds that become available for sulphur oxidation. SO_3^{2-} produced by SO_4^{2-} reduction is generally oxidised at the oxic/anoxic interface in oxygen minimum zone settings (Canfield et al., 2010). Enzymes active in the oxidation of SO_3^{2-} can perform both reduction and oxidation of sulphur compounds (Wasmund et al., 2017). The genes *dsrMKJOP*, encoding for a reverse dissimilatory sulphite reductase (Grein et al., 2010) and *aprBA*, encoding for an adenylylsulphate reductase (Lampreia et al., 1994), were mostly abundant in SSS (0.042 ± 0.006 %) and SSK (0.015 ± 0.016 %) and almost absent in large particle size-fractions. The detection of sulphur oxidation in our samples is in agreement with increasing number of findings suggesting that this process can occur even in predominantly oxygenated waters (Xia et al., 2017; Anantharaman et al., 2013). This highlights the importance of sulphur-oxidising chemolithoautotrophy, especially in the mesopelagic (Swan et al., 2011).

The presence of oxygen-sensitive sulphur reduction and sulphur oxidation processes within small particle size-fractions, especially in SSS, is consistent with the detection of anaerobic nitrogen cycle pathways within small particles. Altogether, these findings serve as indicators of the presence of strong oxygen gradients within these particles, which consequently results in the creation of suboxic to anoxic micro-niches (Bianchi et al., 2018) with reduced compounds released and utilised within the vicinity of their production. The occurrence of sulphur oxidation, used in chemolithoautotrophic processes (Friedrich

et al., 2001), also points to the potential importance of particle microniches as hotspots for CO_2 fixation.

5.4.9 Chemolithoautotrophic carbon fixation

SUP05 is a ubiquitous gammaproteobacterial taxa, which displays adaptations for autotrophic sulphur oxidation and carbon fixation (Walsh et al., 2009; Swan et al., 2011; Glaubitz et al., 2013), that was detected in our samples. SUP05 uses sulphur oxidation as an energy source to fix CO_2 as a carbon source, using the Calvin–Benson–Bassham (CBB) cycle (Meier et al., 2017). Photosynthetic organisms also use the CBB cycle during photosynthesis. Genes involved in the CBB cycle (transketolase, glyceraldehyde-3-phosphate, and fructose-1,6-bisphosphatase) were less expressed in SSK (0.070 ± 0.007 %) than in other particle-types (0.132 ± 0.027 %).

Other sulphur-oxidising bacteria, such as *Sulfovorum* and *Sulfurimonas*, use the reductive tricarboxylic acid (rTCA) cycle for carbon fixation (Nakagawa and Takai, 2008). AOB and NOB, such as *Nitrosomonas* and *Nitrospira* that were detected in small particle size-fractions, use nitrification as an energy source and CO_2 fixation as a carbon source (Hooper et al., 1997) by performing the rTCA cycle (Lucker et al., 2010). Accordingly, genes encoding for the rTCA key enzymes fumarate reductase and 2-oxoglutarate dehydrogenase (Hügler and Sievert, 2011) were slightly more expressed in small particle (0.26 ± 0.08) than in large particle size-fractions (0.22 ± 0.04 %).

Sulphur-oxidising and AOA, such as *Sulfobulus* and *Nitrosopumilus* that were detected in the small particle size-fractions, respectively use the 3-hydroxypropionate/4-hydroxybutyrate (HP/HB) cycle (Berg et al., 2007) and an adaptation of this cycle, the dicarboxylate/4-hydroxybutarate cycle (Huber et al., 2008), to fix CO_2. Although expression of genes encoding for the propionyl-CoA carboxylase was detected, it is difficult to conclude with respect to the occurrence of which one of these cycles, as this

enzyme is also active in autotrophic carbon fixating 3-hydroxypropionate bicycle (Hügler and Sievert, 2011).

The Wood-Ljungdahl carbon fixation pathway is carried by anaerobic organisms that are growing under highly reducing conditions (Hügler and Sievert, 2011). Agreeing with the detection of sulphur reduction processes, genes encoding for the highly oxygen-sensitive CO dehydrogenase active in this cycle, were more expressed in small (0.062 ± 0.051 %) than large particle size-fractions (0.019 ± 0.018 %). This further corroborates the presence of anoxic conditions in particles ≤ 10 µm (Bianchi et al., 2018).

Overall, the detection of these chemolithoautotrophic pathways highlights the importance of these alternative CO_2 fixation processes, especially in small particles.

5.5 Implications and conclusions

This metatranscriptomics dataset is the first to display evidence on how activities involved in carbon, nitrogen and sulphur cycling are distributed among suspended and sinking particles of various sizes. The evolution of these activities with depth, and of their distribution among particle-types, could be related to modifications within associated microbial community structure. This suggests the prevalence of organic compounds exchanges between particle-types and/or the subsequent modification of microbial remineralisation functionalities. Our observations suggest a connectivity between small and large suspended and sinking particles that are likely induced by particle dynamics. Additionally, different particle-types also displayed specific gene expression patterns.

Microbes collected in the 0.22 – 10 µm suspended particle size-fraction (SSS) appeared to be the most active among all microbial communities investigated. SSS microbes were the most versatile in their ability to uptake and degrade small carbohydrates and nitrogen compounds (from inorganic to the simplest organic forms). On the other hand, elevated metabolic activity of microbes collected in the 0.22 – 10 µm sinking particle size-fraction (SSK) was evident, notably by their high ATP synthase genes expression. Nonetheless,

they appeared to be more specialised in their carbon and nitrogen demands. Unlike SSS, they exhibited limited abilities to degrade large range of carbohydrates and seemed adapted to competitive uptake of ammonia.

Our data provides further evidence that small particle-associated and free-living microbes carry out most of the carbon remineralisation processes, bearing in mind that small particle size-fractions did not allow the discrimination between these two entities. Future studies should seek to quantify the partition of organic matter remineralisation pathways between microbial communities associated with the different particle-types.

Microbes associated with large sinking (LSK) and large suspended (LSS) particles were characterised by their capabilities to degrade complex carbohydrates and to take up large nitrogen compounds. Generally, organic matter lability of large particle size-fractions appeared to decrease with depth, and even more so in suspended particles. Although microbes associated with LSK were more active, genes expressed by microbes in LSS suggest their ability to degrade more refractory organic matter. This is congruent with results presented in chapter 3 suggesting that organic matter of suspended particles in the upper-mesopelagic is more refractory than that of sinking particles. Microbes in SSS and SSK could benefit from degradation by-products of more complex organic matter contained in larger particles as they are disaggregated.

Our data provides evidence of the importance of chemolithoautotrophy fuelled by sulphur oxidation and nitrification, particularly in small particle size-fractions. Additionally, the detection of *dsrC*, encoding for a dissimilatory sulphite reductase that catalyses the reduction of sulphite to sulphide, suggests a possible involvement of small particles in cryptic sulphur cycling. These findings indicate the presence of highly reducing microenvironments within oxygenated waters, even within < 10 µm particles.

Overall, this dataset is in agreement with the consensus that microbial communities perform most remineralisation either; (i) if associated with small particles originating from the disaggregation of large sinking aggregates or, (ii) if free-living in the water column.

The pivotal role of large suspended particles was highlighted as carrier of complex carbon substrates, especially for mesopelagic microbes. The origin and roles carried by SSK remains to be elucidated, as they are clearly distinct from SSS. SSK are clearly of importance as they have been previously associated with high respiration rates (Cavan et al., 2017). The use of RT-qPCR to target key genes, such as *dsrC*, and direct rate measurements are required to provide further insights into the occurrence of these processes among individual particle-types.

Chapter 6: Synthesis and future work

6.1 Rationale, key findings and implications

The overall objective of this dissertation was to look at differences between prokaryotic and eukaryotic microbial communities associated with sinking and suspended particles, in terms of their diversity, structure and activities and how they may consequently differently influence the oceanic biological carbon pump (BCP).

The work presented in Chapters 3, 4 and 5 aimed to address research questions set out in Chapter 1 (section 1.5.1). How key findings of individual chapters (Fig. 6.1) answered each question is discussed below.

Are prokaryotic communities associated with suspended and sinking particles different? If so, what are the likely contributing factors to such distribution, and what are the implications on organic matter cycling?

Chapter 3 addressed these research questions using 16S rRNA gene amplicon sequencing on sinking and suspended particles collected from the mixed layer and upper-mesopelagic of four environmentally distinct stations in the Scotia Sea. Results indeed showed a niche partitioning between prokaryotic communities associated with suspended and sinking particles, with particle-associated heterotrophic taxa showing specific enrichments among particle-types. As these ubiquitous taxa exhibited a preference for either particle-type, previous assertions of their role as major remineralisers of presumably sinking particles might be inaccurate. In the mixed layer, differences between suspended and sinking particle-associated prokaryotic communities were lower than in the upper-mesopelagic. This higher connectivity with the two particle-pools suggests increased particle dynamics in the mixed layer, likely explained by more dynamic abiotic processes, such as surface wind mixing.

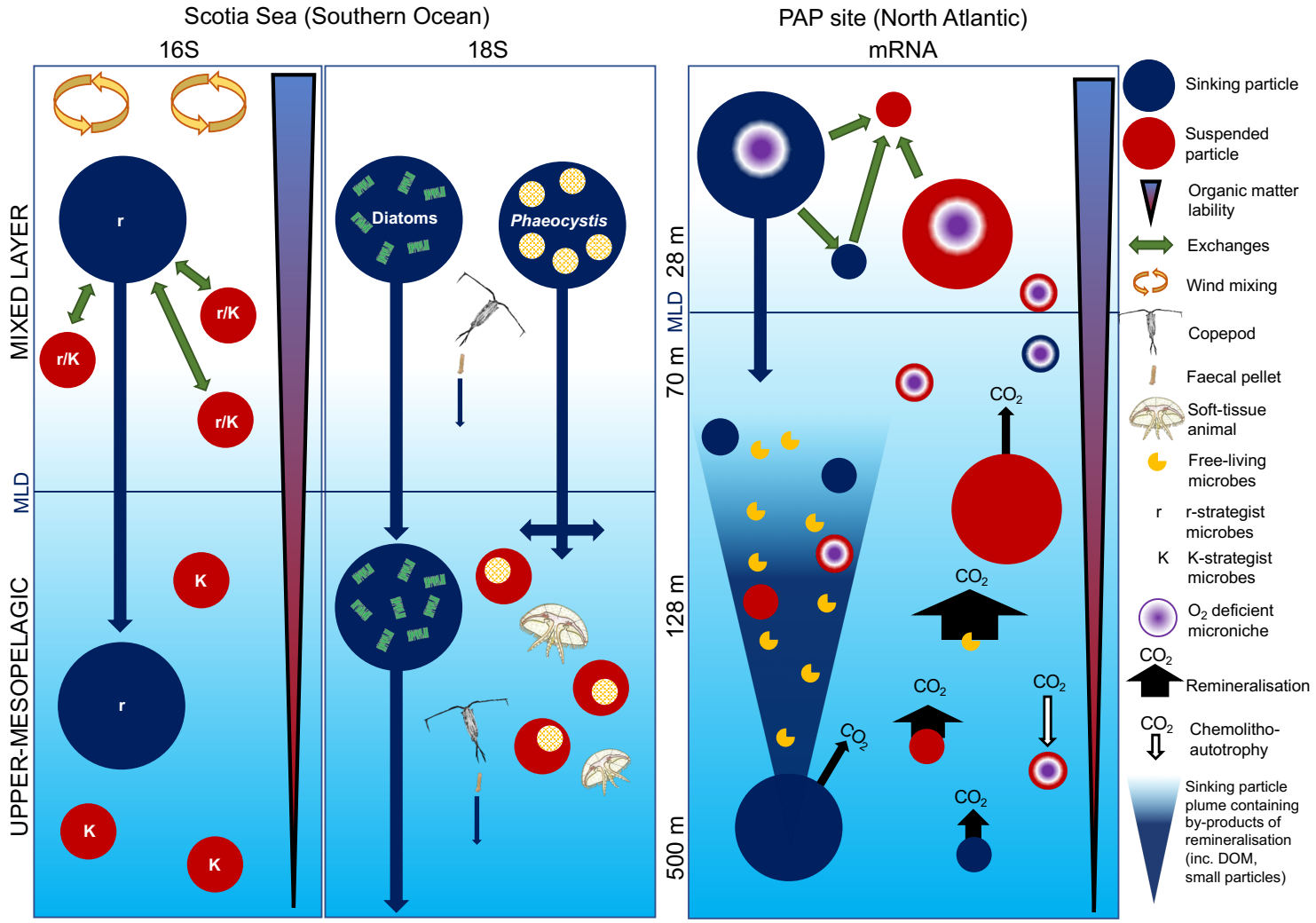

Figure 6.1. Summary schematic of key findings.

Notably, *Flavobacteriales* (*Bacteroidetes*) favoured suspended particles while the gammaproteobacterial *Pseudomonadales* and *Vibrionales*, and the alphaproteobacterial *Rhodobacterales* preferentially colonised sinking particles in the upper-mesopelagic. The latter are r-strategists presenting genetic abilities to degrade a wide variety of organic matter compounds. Conversely, *Flavobacteriales* are K-strategists that are specialised in the degradation of complex organic compounds. Physiological and genetic information of these notorious particle-associated remineralising taxa, coupled with their distribution among particle-types, suggests that while suspended particles are enriched in semi-labile organic compounds, organic matter in sinking particles has a more transient nature. Organic matter contained in sinking particles would indeed be more labile at shallower depths and would increase in complexity as particles sink and are increasingly remineralised. This agrees with our understanding of particle dynamics in the mesopelagic, where suspended particles originate from the disaggregation of sinking particles.

Activity rate measurements will provide insights into the nature of organic matter being degraded within each particle-types. Coupled with measurements of hydrolytic enzymatic activity for compounds of various lability (e.g., LAPase, CHIase, APase), these results would inform us if actual rates of organic matter degradation are different between particle-types, and if such differences have the potential to affect organic matter cycling, and hence, how they affect the BCP.

What are the eukaryotic contributions to particle export from the surface to mesopelagic ocean? Specifically:

- **Which phytoplankton taxa are the most efficient in carbon export?**
- **What metazoan and phytoplankton taxa influence sinking and suspended particles in the mesopelagic?**
- **Are heterotrophic and mixotrophic protists residing on mesopelagic sinking and suspended particles in the different? If so, how does their**

distribution impact organic matter remineralisation and particle attenuation?

Chapter 4 addressed these research questions using 18S rRNA gene amplicon sequencing on sinking and suspended particles collected at the same sites as in Chapter 3. Results showed that different phytoplankton taxa appeared to contribute to particle flux and to the composition of suspended particles in the upper-mesopelagic.

The diatom *Chaetoceros* appeared to compose most of particle export to the upper-mesopelagic. Even at the iron-depleted station, where the prymnesiophyte *Phaeocystis* dominated surface waters, *Chaetoceros* appeared to be the major carbon transporter to depth. In agreement with previous studies, this phytoplankton group was more efficient than *Phaeocystis* in the transfer of organic carbon to depth. *Chaetoceros* was likely assisted by mineral opal frustules acting as ballast, as well as by their chain-forming abilities. Both factors contribute to enhance sinking velocity of aggregates they constitute, thereby decreasing their susceptibility to disaggregation and remineralisation. On the other hand, *Phaeocystis* was abundant in suspended particles in the upper-mesopelagic, thereby suggesting that *Phaeocystis*-enriched sinking aggregates are more likely to break down into suspended particles. In other words, our data suggests that while both phytoplankton taxa contribute to particulate carbon export from the mixed layer to the upper-mesopelagic, *Phaeocystis*-enriched aggregates tend to disaggregate into suspended particles within the upper-mesopelagic. Therefore, these aggregates do not sink deeper into the dark ocean and contribute more to particle attenuation. In contrast, diatom-enriched aggregates tend to remain as sinking particles, thereby continuing their journey further into the deep ocean, translating to more efficient carbon sequestration at greater depth, and hence, longer carbon capture.

Different metazoan and hetero/mixotrophic protist signatures were detected on suspended and sinking particles from the upper-mesopelagic. Metazoan sequences recovered from sinking particles mostly belonged to copepods, while those in suspended particles

belonged to soft-tissue animals (such as ctenophores and tunicates). This agrees with the important contribution of copepod faecal pellets to particulate carbon export to the mesopelagic in this region. Our data highlights the potential for environmental DNA as a tool for determining the origin and composition of sinking and suspended particles as a complement to classic microscopy analyses, generally focusing on sinking particles.

Hetero- and mixotrophic protists largely dominated eukaryotic sequences collected in both suspended and sinking particles from the upper-mesopelagic. Bacterivorous ciliates and mixotrophic dinoflagellates were enriched on sinking particles, suggesting their major role in particle flux attenuation. These groups were also higher within suspended particles ≥ 10 µm. Additionally, the ciliate *Choreotrichia* was enriched in 10 – 100 µm suspended and sinking particles, and *Oligotrichia* in ≥ 100 µm suspended particles. The detection of parasitic *Syndiniales* in < 10 µm suspended particles, and of the *Rhizaria* supergroup in ≥ 100 µm suspended particles, is consistent with recent observations of their important to mesopelagic ecosystems.

Further work is required to quantify remineralisation activities carried out by heterotrophic protists and their subsequent impact on particle attenuation. Predatory pressures applied by these protists on prokaryotic communities associated with the two particle-types remain to be investigated. This would provide us with a more complete vision of syntrophy links, by connecting the different members of microbial communities residing on suspended and sinking particles.

Chapters 3 and 4 provided evidence of major compositional differences in microbial communities associated with suspended and sinking particles. This implies that the chemical nature and origin of organic matter bound to the two particle-types differ, which subsequently lead to their preferential colonisation by specific remineralising taxa. This appeared to be caused by; (i) influences of different phytoplankton and metazoan on suspended and sinking particles, and (ii) particle dynamics, caused by abiotic and biotic

processes defining the degree of connectivity between two particle-types, both of which varied with depth.

In order to confirm these observations, and to investigate biogeochemical cycling within the two particle-types, activities carried-out by microbial communities associated with small and large suspended and sinking particles from four depths of the Porcupine Abyssal Plain site were investigated using metatranscriptomics in Chapter 5.

Are there functional differences between sinking and suspended particle-associated microbial communities with respect to:

- **Carbon remineralisation?**
- **Biogeochemical cycling of other key elements, such as nitrogen and sulphur?**

While particle-size was the main driver differentiating activities of microbial communities residing in suspended and sinking particles, small and large particles from a same particle-type exhibited subtler, though distinguishable, differences that evolved with depth.

Free-living and small (< 10 µm) particle-associated microbes (referred to as small particle-associated microbes henceforth for simplicity) appeared to be more actively growing, and active in the remineralisation of low-molecular weight organic compounds compared to those residing in large particles (≥ 10 µm). The latter conversely appeared to be more active in the degradation of high-molecular weight organic compounds. Microbes residing in small suspended particles seemed to be remineralising a wide range of simple carbohydrates, compared to those in small sinking particles, which specialised on a small range of simple compounds. While also active in the degradation of simple carbohydrates in both large particle-types, microbial communities associated with large suspended particles were capable of degrading more complex refractory carbohydrates than those in sinking particles, providing further support for the r/K strategists colonisation patterns observed in Chapter 3.

Microbial communities exhibited similar behaviours with regards to cellular nitrogen uptake. Those residing in small sinking particles were capable of taking up the smallest forms of organic and inorganic molecules, while those in small suspended particles were capable of taking up a wider range of simple nitrogen-rich organic compounds. On the other hand, microbes associated with large particles were able to take up more complex forms of nitrogen.

Expression of genes involved in organic matter remineralisation suggested an overall decrease in organic matter lability with depth, especially within large particles. This suggests a more refractory state of organic matter bound to suspended particles than to sinking particles below the mixed layer depth, which is in accordance with our understanding of particle dynamics in the mesopelagic. In addition, expression of genes active in remineralisation suggested the transfer of organic compounds between large sinking particles and small particle size-fractions, which is consistent with the sinking particle plume theory, by which remineralisation processes taking place in the trailing plume are more active than on sinking particle themselves. Following this theory, microbes associated with large sinking particles degrade complex organic compounds, and although they partly benefit from hydrolysis products, most of the labile organic compounds produced are released in the trail following particles as they sink and/or are released within smaller sinking particles. Both of these fractions were collected in the small sinking particle size-fraction.

The origin of the small suspended particle pool remains unclear and is likely composed of materials from different origins (e.g., chemolithotrophic production and cells, disaggregation of larger suspended particles). Nevertheless, it was clear that microbial communities within these particles play major roles in organic matter remineralisation in the ocean.

The presence of actively expressed anaerobic processes corroborates recent suggestions that particles serve as important oxygen-deficient microniches. This agrees with the

growing number of reports on the occurrences of strictly anaerobic process-related genes in the oxic ocean. Microniches created within particles expand the occurrence of key anaerobic redox processes to the vast mesopelagic ocean, including chemolithoautotrophic CO_2 fixation via sulphur oxidation and the production of the greenhouse gas nitrous oxide. Particles, even those < 10 µm, would then have important implications for biogeochemical cycling and the budgeting of carbon, nitrogen and sulphur among other elements.

The distribution of processes involved in elemental biogeochemical cycling between particle-types provides further information on dynamics connecting suspended and sinking particle-pools together. Further work will better characterise these processes in order to assess the impact of such differences on oceanic system functioning. Notably, rates measurements coupled with RT-qPCR would allow the quantification of their occurrence in the two particle-types.

6.2 Future analyses and work

6.2.1 Nitrogen and carbon cycling activities in suspended and sinking particles

While metatranscriptomic analyses illustrate the potential occurrence of specific processes, activity rate measurements allow such processes to be quantified, thereby assessing biogeochemical implications. For this purpose, incubation experiments were conducted on DY032 to the Porcupine Abyssal Plain (PAP) in spring 2015. Isotopes of nitrogen (^{15}N) and carbon (^{13}C) labelled organic and inorganic compounds were set up (Table 6.1) with water collected from the upper and bottom part of the MSC. The future analysis of this data set will provide us with rate measurements of pathways active in; (i) nitrogen cycling, (ii) remineralisation processes and (iii) chemolithoautotrophy occurring within suspended and sinking particles.

Table 6.1. Label used for DY032 incubations on suspended and sinking particles and targeted pathways.

Label	Pathway targeted
$^{15}NH_4^+$ $H^{13}CO_3$	- Nitrification (NH_4^+ to NOx) - Chemolithoautotrophy (HCO_3 assimilation) - Assimilation
^{15}N-urea	- Remineralisation (ammonification) - Assimilation - Nitrification shortcut (urea uptake, intracellular deamination and direct oxidation to NO_2^-)
^{15}N and ^{13}C-phytoplankton POM	- POM remineralisation
^{15}N-amino acid	- Remineralisation - DON assimilation - Nitrification shortcut (urea uptake, intracellular deamination and oxidation to NO_2^-)
$^{15}NO_3^-$ $H^{13}CO_3$	- N assimilation - Chemolithoautotrophy (HCO_3 assimilation)

6.2.2 Quantitative analyses with epifluorescence microscopy and RT-qPCR

During the cruises JCR304 to the Scotia Sea in austral summer 2014 and DY032, samples were collected for microscopy to be analysed with the fluorescent catalysed reporter deposition in situ hybridisation (CARD-FISH) technique. These samples can be used to generate absolute counts of specific members of prokaryotic (e.g., *Alteromonadales*, *Rhodobacterales*, *Firmicutes*) and eukaryotic members (e.g., diatoms, dinoflagellates) associated with suspended and sinking particles (Fig 6.2). Microscopic analyses of eukaryotic members residing in suspended and sinking particles will also provide information on their physiological state (e.g., intact or burst cells). It is also a powerful tool to examine spatial associations between eukaryotic and prokaryotic cells, as well as the association of aggregated microbial cells.

While metatranscriptomic analyses have provided useful insights into the occurrence of biogeochemical cycling, measurements of processes using quantitative reverse transcription PCR (RT-qPCR) would provide more accurate comparison. This method can give quantitative information on the various processes taking place on suspended and sinking particles, as well as their distribution among particle-types and along depth. RNA extracts collected in suspended and sinking particles at PAP will be used as templates to

target specific genes active in remineralisation with RT-qPCR in order to provide an absolute quantification of gene expression. Notably, the detection of transcripts involved in sulphur reduction and oxidation on small suspended particles requires further investigation to determine the occurrence of a cryptic sulphur cycle. The genes *dsrC* and *dsrMKJOP* can be used as targets to investigate sulphur reduction and oxidation respectively.

Furthermore, high-sensitivity and high-resolution microscopy techniques, such as Raman atomic force microscopy, could also be used to look at single-cell processing of isotopically labelled metabolites such as sulphur compounds (e.g., Oren et al., 2015).

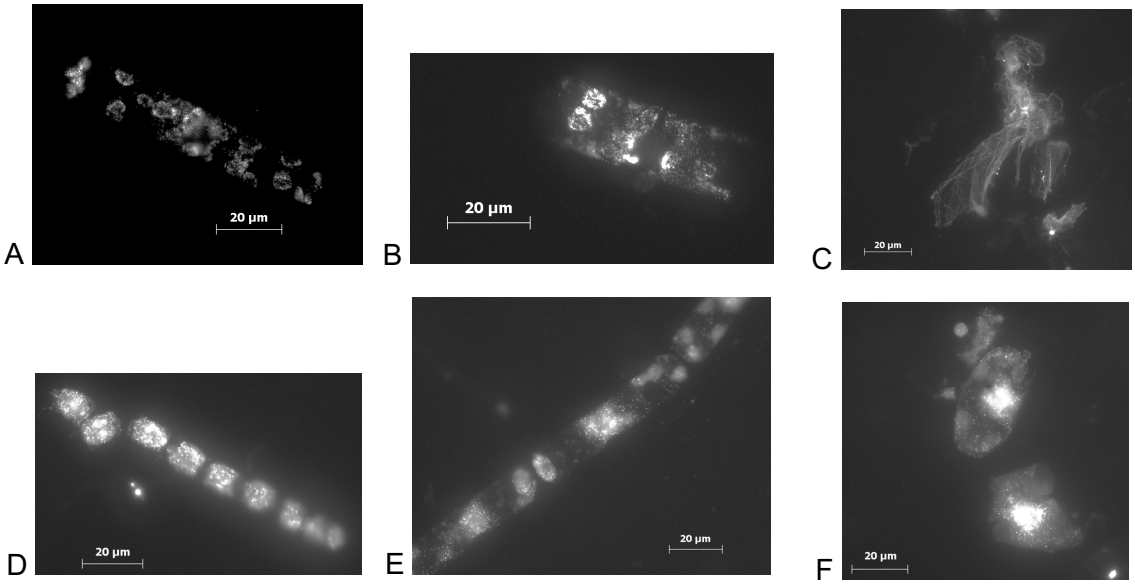

Figure 6.2. Example of images from CARD FISH hybridised cells. Images A, B and C present cells hybridised with the probe EUB338 (targeting all bacteria), images D and E cells hybridised with CF319a (targeting *Flavobacteriales*) and image F cells hybridised with ROS593 (targeting *Rhodobacterales*). Photographs were taken by Lucy Henshall as part of her integrated Master's project (University of Southampton).

6.2.3 Methodology comparison: CTD versus MSC for the accurate sampling of suspended and sinking particles

Size-fractionation of bulk seawater collected from CTD-attached Niskin bottles has been historically used to differentiate suspended from sinking particles – with the smaller fraction (1 – 60 µm) representing suspended particles and the larger fraction (≥ 60 µm)

representing sinking particles (e.g., Kellogg and Deming, 2009). However, chapter 5 has shown that solely using particle-size to differentiate suspended from sinking particles is not sufficient to capture particle diversity, as small and large size-fractions from the same particle type exhibit major differences.

Size-fractionated bulk seawater samples were collected during the JCR304 cruise from the same stations and depths as those presented in chapter 3. Amplicon sequencing of 16S rRNA data generated from samples collected with the MSC, upper part (MSCU) and bottom part (MSCB) (Fig. 2.1), will be compared with those collected using the classic bulk seawater size-fractionation.

Fig. 6.3 shows preliminary results as a non-metric multidimensional scaling (NMDS) plot based on Bray-Curtis dissimilarity of OTU composition. Large particles (10 – 100 µm) collected from Niskin bottles cluster closely to large particles collected from the MSCU. Similarly, small particles (0.22 – 10 µm) collected from Niskin bottles cluster closely to small particles collected from the MSCU. On the other hand, large particles collected from the MSCB form a separate group. These clustering patterns are apparent at both depths.

It seems that particles collected with Niskin bottles are largely dominated by suspended particles. This is in consistent with the literature investigating organic matter lability (e.g., Sheridan et al., 2002), which generally assimilate particles collected from Niskin-sampling to suspended particles. However, it is not in agreement with studies using size-fractionation of seawater collected from Niskin-bottles in order to separate suspended and sinking particles based on particle-size discrimination (i.e., large particles as sinking and smaller particles as suspended).

This piece of research will be the focus of a methodology paper that will test the following hypothesis:

(i) MSC sampling enables a more accurate characterisation of prokaryotic communities associated with sinking particles compared with Niskin-sampling.

(ii) Unlike Niskin-sampling, the MSC allows prokaryotic communities residing in sinking and suspended particles to be more reliably distinguished.

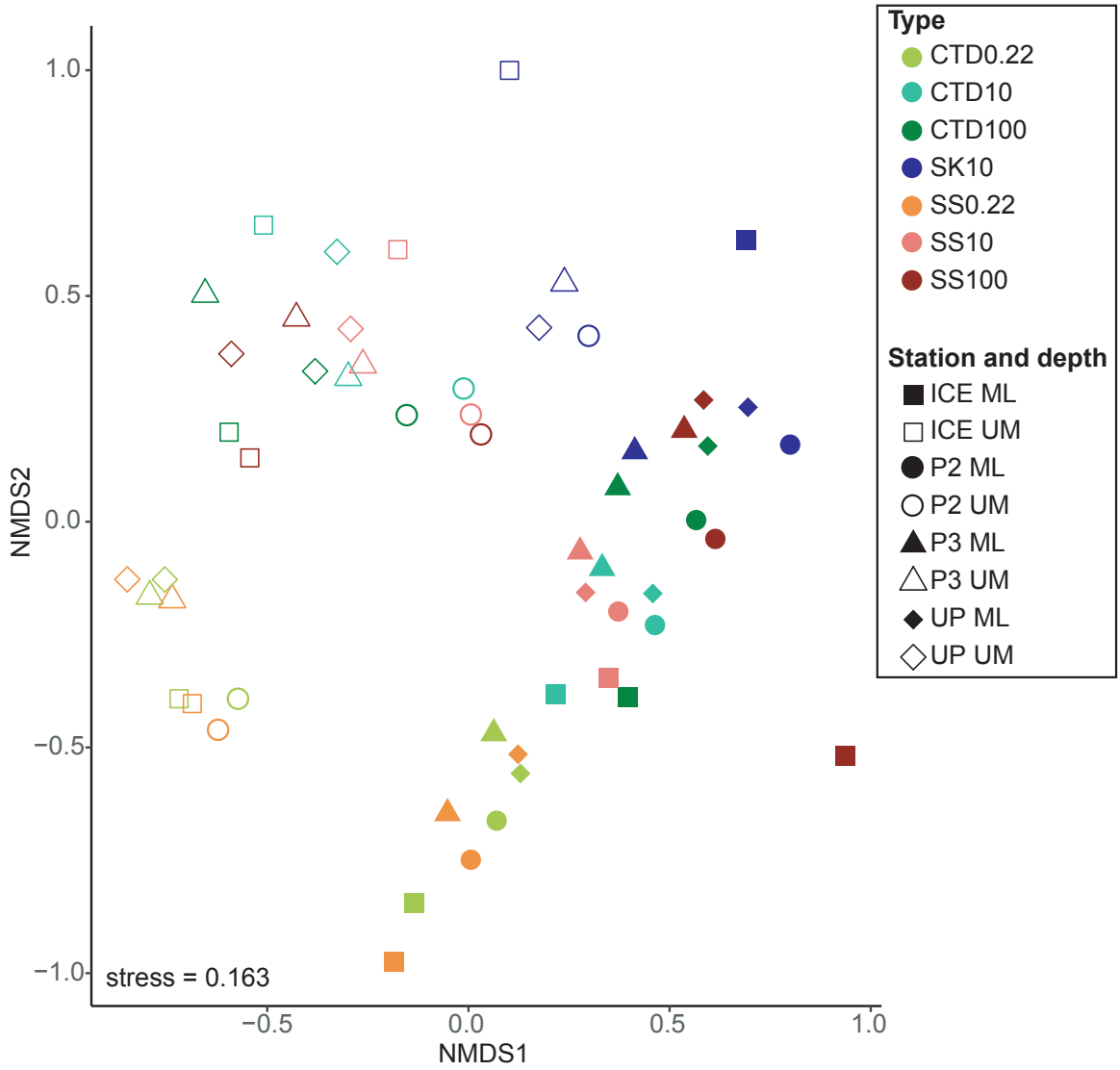

Figure 6.3. Non-metric multidimensional scaling plot of OTU composition. The NMDS was calculated with Bray-Curtis distance of the rarefied dataset. Samples "CTD" were collected from a Niskin bottle, "MSCU" from the upper part of the MSC and "MSCB" from the bottom part of the MSC. Water samples collected from Niskin bottles and MSCU were size-fractionated onto 100, 10 and 0.22 µm pore-size filters. Water samples collected from MSCB were filtered onto a 10 µm pore-size filter. ML = mixed layer; UM = upper-mesopelagic.

6.2.4 Further bioinformatics analyses

Other aspects of the data collected for this thesis work will be investigated using different bioinformatics analyses than those presented.

The 16S and 18S rRNA gene amplicon sequencing data from suspended and sinking particles collected in the Scotia Sea (presented in Chapters 3 and 4) will be analysed simultaneously in a network analysis. Network analyses can provide insights into microbial syntrophy (trophic interactions between members of the microbial community), interactions between microbes (as conducted for viral and bacterial communities by Chow et al., 2014) or with environmental parameters (as conducted with microbial eukaryotic communities between sites of different productivity by Lin et al., 2017). Such analyses have the potential to reveal differences in trophic, symbiotic and parasitic interactions between prokaryotic and eukaryotic members of microbial communities associated with suspended and sinking particles.

In order to gain further physiological information on the OTU recovered from 16S and 18S rRNA gene amplicon sequencing, sequences will be compared against the Tara Ocean database (http://ocean-microbiome.embl.de/companion.html). This database contains extensive physiological information on microbial communities collected from a variety of oceanic regions and, therefore, has to the potential to provide further insights into the roles of microbes collected from suspended and sinking particles in the Scotia Sea.

6.3 Concluding remarks

This thesis is the first to investigate differences between microbial communities associated with sinking and suspended particles as separate entities. This work has demonstrated that prokaryotic and eukaryotic microbes residing in the two particle-types are different, thereby adding another dimension of complexity to our understanding of marine microbial ecosystem structuring.

This work has also shown the distribution of various remineralisation processes and associated biogeochemical elemental cycling between suspended and sinking particles. Environmental nucleic acids generated during this work were used to characterise particle flux and dynamics in the water column, hence demonstrating the potential of this type of

dataset as an alternative to classic tools for the investigation of particle fluxes, such as microscopy observations.

This thesis highlights the potentially different biogeochemical implications of processes occurring on suspended and sinking particles and gives further insights into constraints shaping the biological carbon pump.

Similar work in other oceanic regions will provide us with information necessary to uncover the distribution of microbial roles among suspended and sinking particles, in order to provide insights into how particle dynamics and remineralisation activities vary spatially. Quantification of these processes will allow a greater understanding of the biogeochemical role and composition of the two particle types within the biological carbon pump and oceanic system.

Appendix A

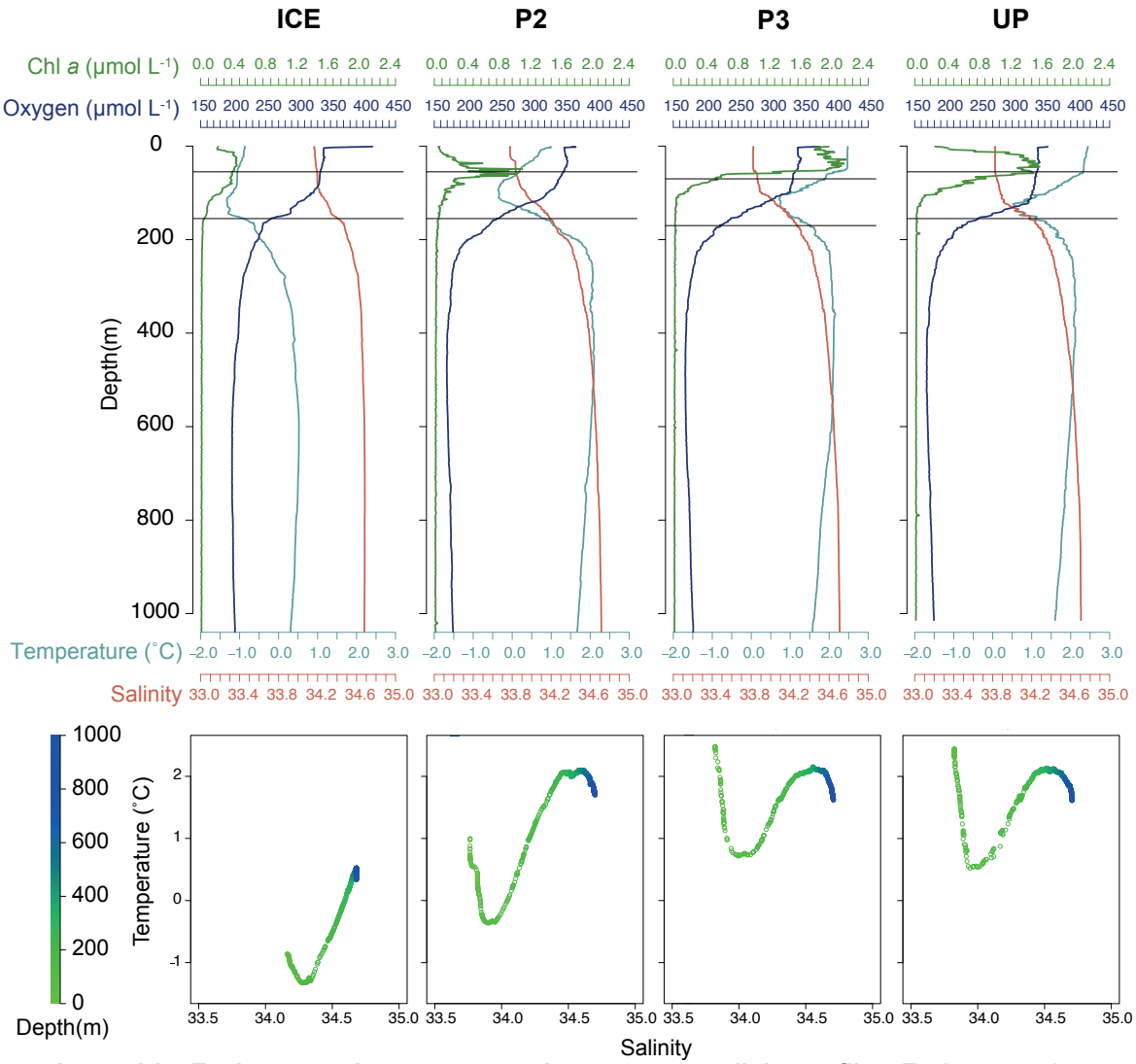

Annex A1. Environmental parameters and temperature-salinity profiles. Environmental parameters (upper panels) and temperature-salinity profiles (lower panels) at the four sampling stations constructed from CTD measurements of oxygen, fluorescence and POC concentrations and temperature. Horizontal black lines correspond to the sampling depths.

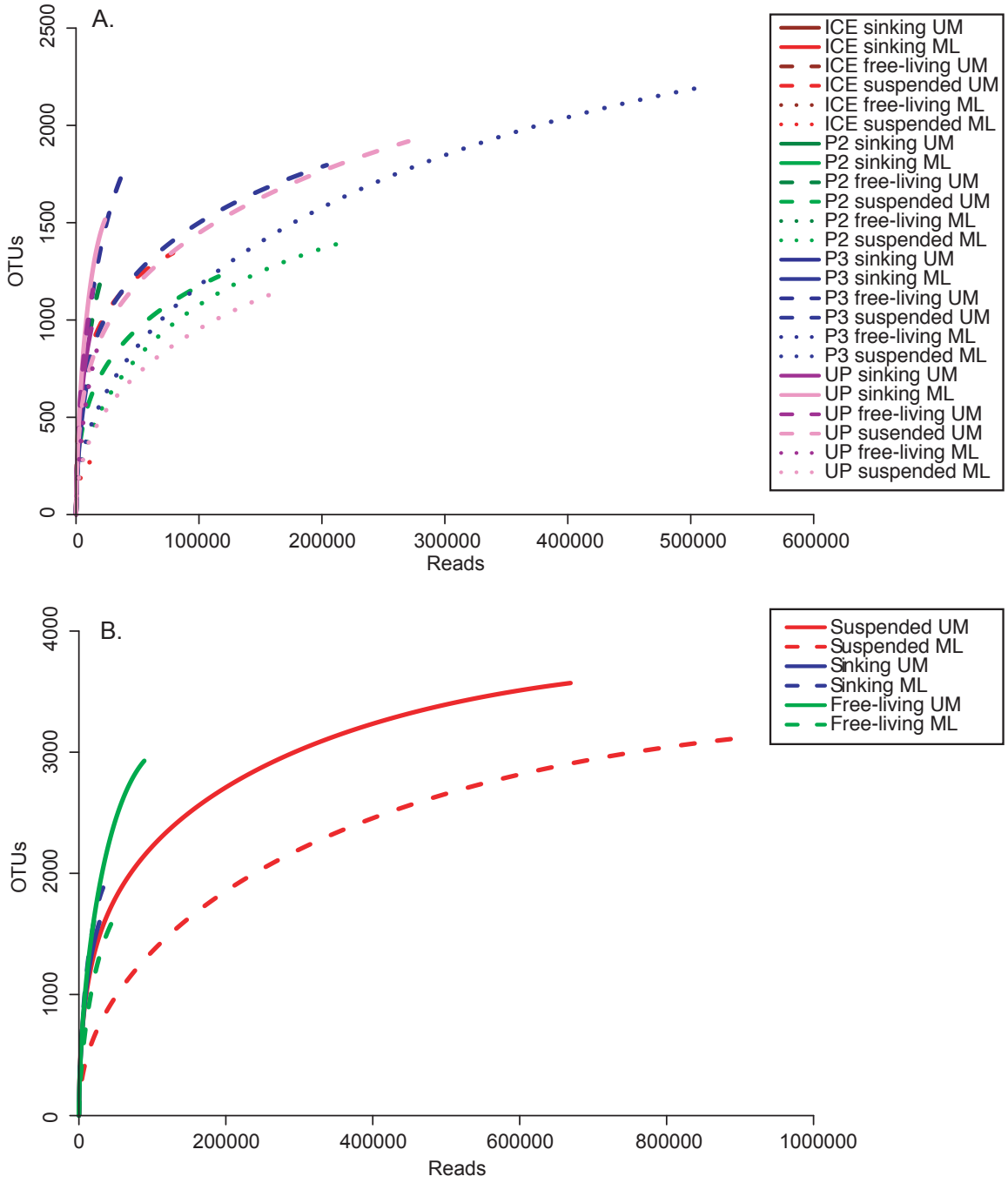

Annex A2. Rarefaction curves. Panel A shows the rarefaction curves for individual samples and panel B shows the rarefaction curves for samples pooled by particle-type (suspended, sinking and free-living) from all stations. ML = mixed layer, UM = upper-mesopelagic.

Annex A3. Dissimilarity values from similarity percentages analyses. Table A shows the dissimilarity between sinking and suspended particle-associated. Table B shows the dissimilarity between communities at different stations. Dissimilarity values were calculated on the rarefied dataset based on results from a SIMPER analyses that are presented in Annex A9. S. D.: standard deviation.

A - Overall dissimilarity (%)

MIXED LAYER		U-MESOPELAGIC	
Average	*36.8%*	Average	*48.1%*
S.D.	*15.3%*	S.D.	*12.9%*
ICE	60.1%	ICE	63.9%
P2	36.0%	P2	54.7%
P3	17.3%	P3	44.6%
UP	33.8%	UP	29.1%

B - Overall dissimilarity (%)

MIXED LAYER

	ICE	P2	P3	UP
ICE		76.5%	78.0%	77.0%
P2			52.5%	55.2%
P3				39.3%
UP				

UPPER-MESOPELAGIC

	ICE	P2	P3	UP
ICE		80.6%	82.0%	82.0%
P2			65.3%	59.7%
P3				48.5%
UP				

Annex A4. Permutational multivariate analysis of variance of environmental parameters. Table A displays the PERMANOVA results for sample collection-related factors (including station and depth – which are an integration of all environmental parameters – and particle-type). Table B displays the PERMANOVA results for environmental parameters. Factors highlighted with an asterisk (*) were significantly affecting the OTU composition variability. SS: sums of squares; MS: means of squares; F.Model: F-tests results; R2: effect size; Pr: p-value.

A - Sample collection						
	Df	**SS**	**MS**	**F.Model**	**R2**	**Pr**
Station*	3	0.968	0.323	2.304	15%	0.002
Depth*	1	1.264	1.264	9.017	20%	0.001
Particle-type*	2	1.722	0.861	6.143	27%	0.001
Residuals	*17*	*2.382*	*0.140*	*NA*	*38%*	*NA*
Total	*23*	*6.336*	*NA*	*NA*	*100%*	*NA*

B - Envrionmental parameters						
	Df	**SS**	**MS**	**F.Model**	**R2**	**Pr**
Temperature*	1	0.637	0.637	3.351	10%	0.001
Oxygen*	1	1.297	1.297	6.824	20%	0.001
Fluorescence	1	0.137	0.137	0.723	2%	0.687
POC*	1	0.655	0.655	3.444	10%	0.003
Residuals	*19*	*3.610*	*0.190*	*NA*	*57%*	*NA*
Total	*23*	*6.336*	*NA*	*NA*	*100%*	*NA*

Annex A5. Detailed proportions of shared/unique OTU and affiliated sequences. This table is associated with Fig. 3.3.

MIXED LAYER		*Mean*	*S.D.*	ICE	P2	P3	UP
% unique OTU	Suspended	*11.8*	*3.5*	14.8	15.6	9.7	7.2
	Sinking	*38.5*	*8.1*	47.2	29.0	31.8	46.0
	Free-living	*27.2*	*4.9*	23.6	31.7	32.2	21.1
% shared OTU	Suspended - sinking	*5.1*	*2.0*	2.5	7.0	7.2	3.8
	Suspended - free-living	*3.7*	*1.0*	5.4	3.2	3.4	2.7
	Sinking - free-living	*5.1*	*2.8*	2.3	5.4	3.3	9.6
	All	*8.5*	*2.9*	4.2	8.1	12.3	9.6
% unique sequence	Suspended	*11.0*	*10.3*	27	13	2	2
	Sinking	*27.5*	*23.2*	64	31	9	6
	Free-living	*14.3*	*8.0*	17	26	9	5
% suspended sequence shared with	Sinking	*4.0*	*2.2*	5	7	3	1
	Free-living	*5.3*	*4.4*	11	8	1	1
	All	*79.8*	*16.2*	57	72	94	96
% sinking sequence shared with	Suspended	*12.8*	*5.7*	20	14	13	4
	Free-living	*4.5*	*3.2*	2	9	1	6
	All	*52.8*	*25.4*	14	46	77	74
% free-living sequence shared with	Suspended	*5.5*	*4.7*	12	8	1	1
	Sinking	*3.3*	*2.3*	2	7	1	3
	Free-living	*77.0*	*13.9*	68	59	89	92

UPPER-MESOPELAGIC		*Mean*	*S.D.*	ICE	P2	P3	UP
% unique OTU	Suspended	*17.5*	*3.3*	22.1	16.6	18.6	12.9
	Sinking	*23.4*	*1.6*	21.9	25.5	21.7	24.6
	Free-living	*33.0*	*1.9*	30.6	35.7	32.3	33.6
% shared OTU	Suspended - sinking	*6.7*	*0.3*	6.7	7.0	6.3	6.9
	Suspended - free-living	*7.1*	*1.7*	9.3	5.2	8.3	5.6
	Sinking - free-living	*2.9*	*0.7*	2.7	2.0	3.0	4.0
	All	*9.3*	*2.1*	6.7	8.1	9.8	12.5
% unique sequence	Suspended	*13.0*	*5.7*	21	13	13	5
	Sinking	*22.5*	*11.1*	39	26	15	10
	Free-living	*18.8*	*2.2*	22	19	18	16
% suspended sequence shared with	Sinking	*11.5*	*3.6*	14	16	8	8
	Free-living	*10.0*	*6.0*	19	5	12	4
	All	*65.5*	*13.1*	46	66	67	83
% sinking sequence shared with	Suspended	*13.3*	*3.8*	17	17	9	10
	Free-living	*3.8*	*3.1*	9	1	3	2
	All	*60.8*	*16.5*	36	56	73	78
% free-living sequence shared with	Suspended	*12.3*	*8.3*	26	8	11	4
	Sinking	*3.8*	*0.4*	4	4	3	4
	Free-living	*65.3*	*10.4*	48	69	68	76

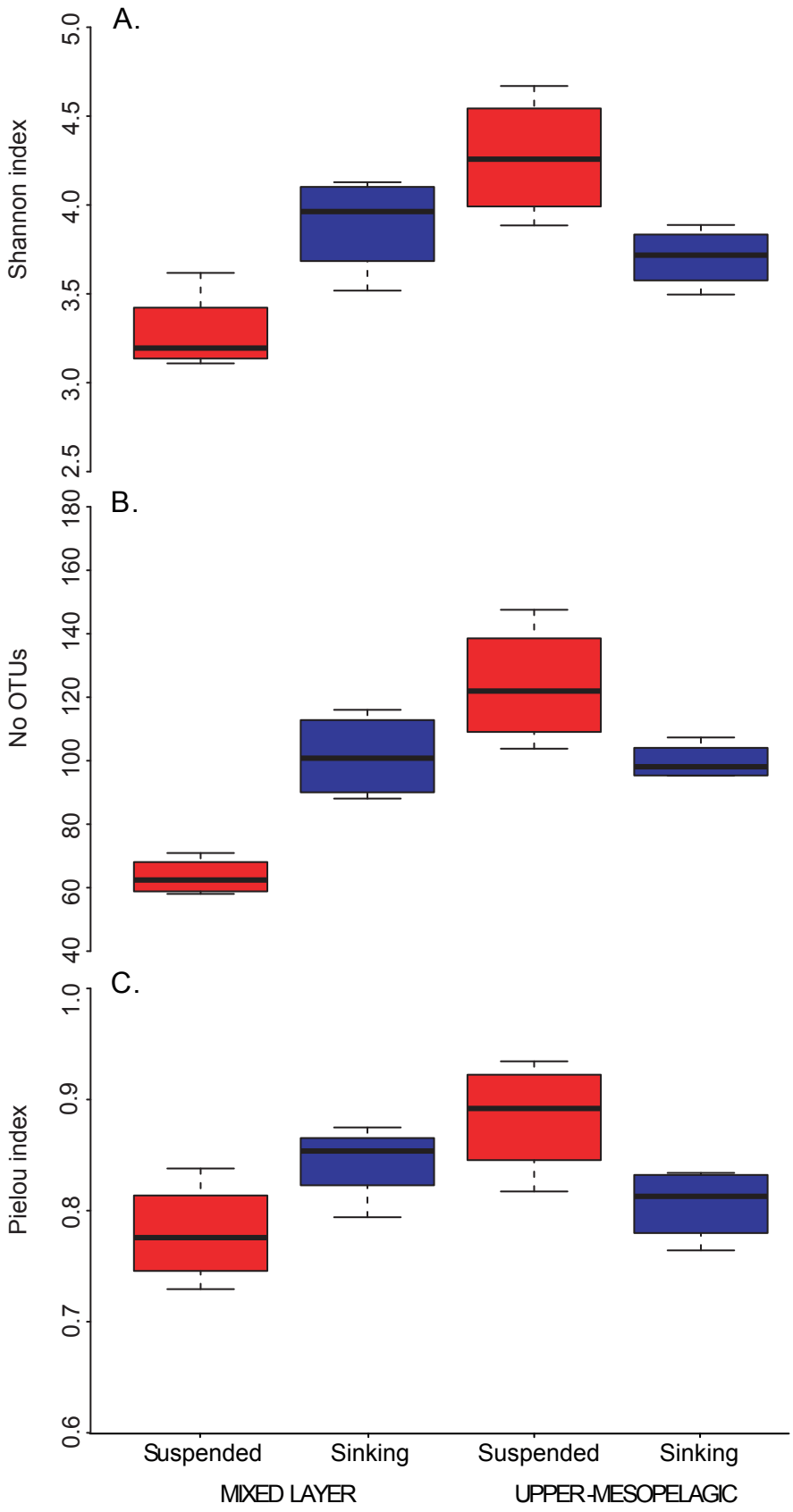

Annex A6. Alpha-diversity plots. Panel A shows Shannon's index, panel B shows the unbiased number of OTU and panel C shows Pielou's index. Indices were calculated on the rarefied dataset and were pooled by particle-type (suspended and sinking) from all stations.

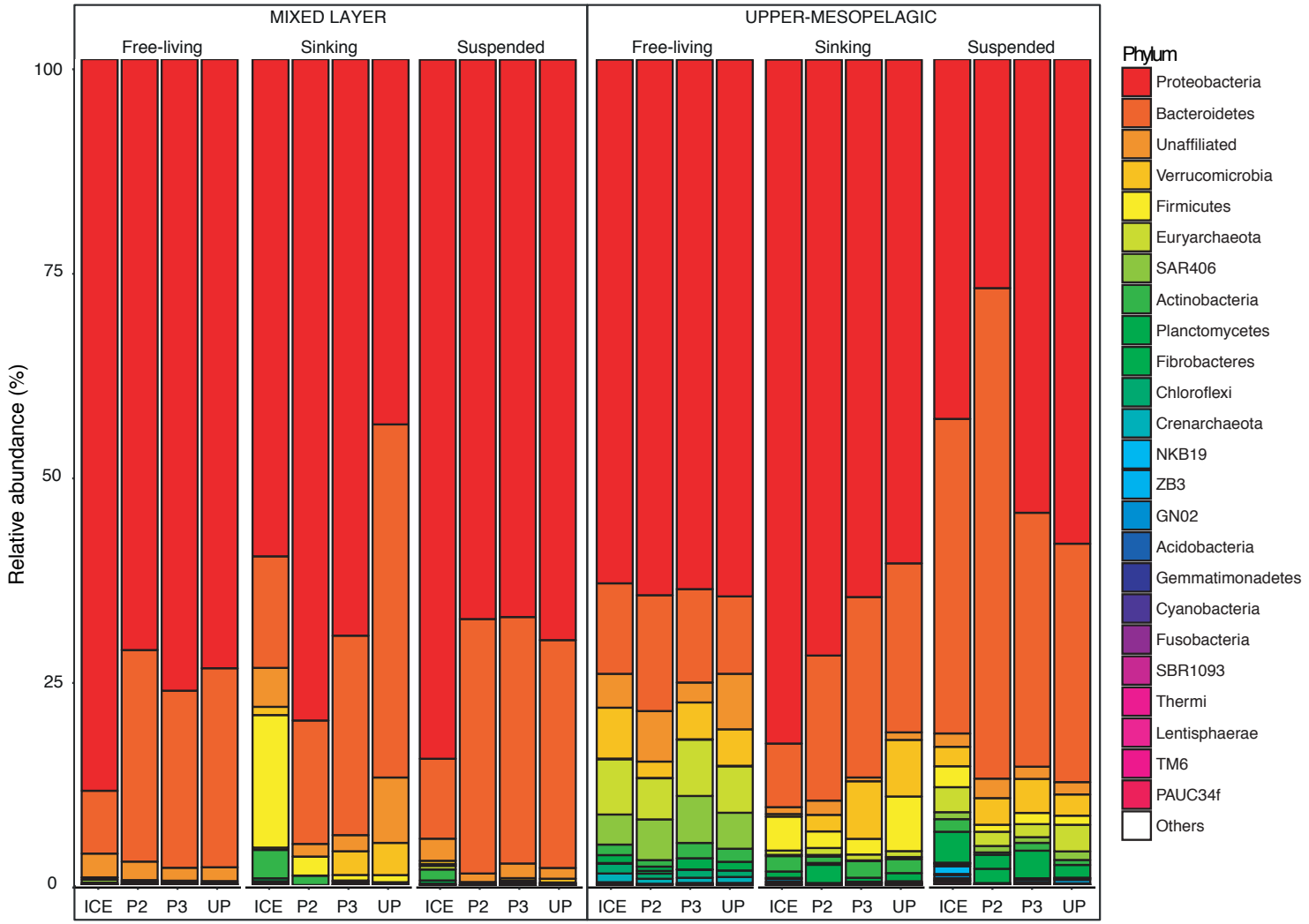

Annex A7-A. Taxonomic phylum composition. The category "Others" corresponds to the pooled abundance of remaining less abundant phyla.

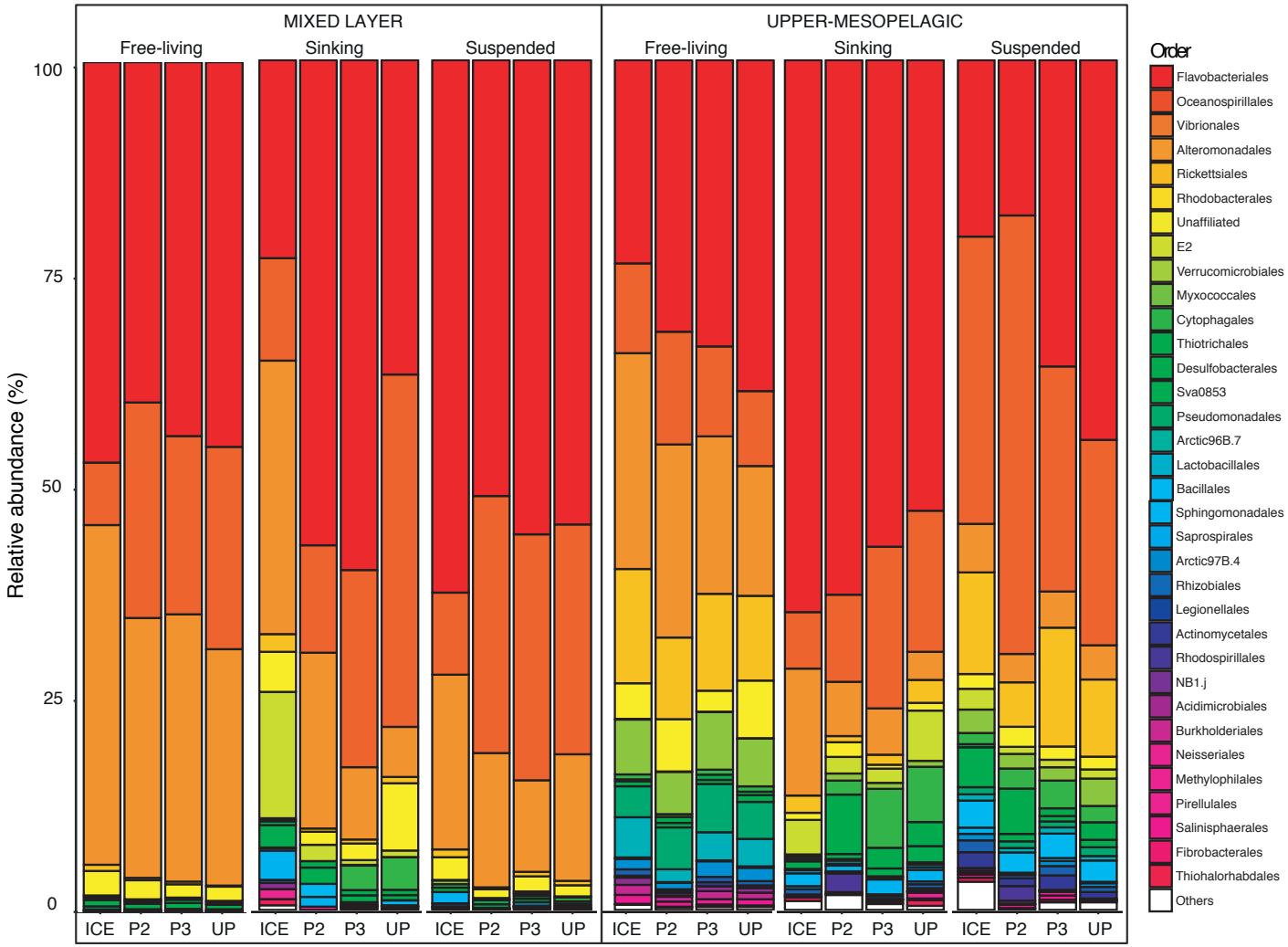

Annex A7-B. Taxonomic order composition. The category “Others” corresponds to the pooled abundance of remaining less abundant orders.

Annex A8. Similarity percentages analyses details. Table A displays results from ICE, B from P2, C from P3 and D from UP (see following pages). Dissimilarities were calculated with the Bray-Curtis index based on the taxonomic family composition of the rarefied dataset. Taxonomic families are showed in decreasing order of importance regarding dissimilarities between the two particle-associated communities. Relative abundances of families are indicated and "Av. cum. sum" is the cumulative sum of average relative abundance within the two communities. Percentages in red are the overall dissimilarity between the two communities calculated with the Bray-Curtis index based on the OTU composition.

ICE - Mixed layer	Sinking	Suspendec	Av. cum. Sum
Oceanospirillaceae	1.7%	21.4%	0.16
Vibrionaceae	0.0%	9.7%	0.24
Unaffiliated	20.3%	11.3%	0.32
Streptococcaceae	7.9%	0.0%	0.38
Rhodobacteraceae	17.2%	11.1%	0.44
Alteromonadaceae	3.8%	9.0%	0.48
Pseudomonadaceae	5.2%	0.5%	0.52
Colwelliaceae	0.2%	4.6%	0.56
Flavobacteriaceae	7.6%	3.2%	0.59
Pelagibacteraceae	2.0%	6.3%	0.63
Cryomorphaceae	1.0%	5.2%	0.66
HTCC2188	0.3%	4.3%	0.70
Planococcaceae	3.6%	0.0%	0.73
Pseudoalteromonadaceae	3.9%	0.7%	0.75
Halomonadaceae	1.4%	3.4%	0.77
Gemellaceae	1.5%	0.0%	0.78
Dietziaceae	0.0%	1.5%	0.79
Methylobacteriaceae	1.6%	0.2%	0.81
Neisseriaceae	1.4%	0.0%	0.82
Corynebacteriaceae	1.4%	0.0%	0.83
Micrococcaceae	1.2%	0.0%	0.84
Pasteurellaceae	1.2%	0.0%	0.85
Staphylococcaceae	0.9%	0.0%	0.86
Hyphomonadaceae	0.9%	0.0%	0.86
NS9	1.3%	0.5%	0.87
Piscirickettsiaceae	0.8%	0.0%	0.88
Sphingomonadaceae	1.0%	0.2%	0.88
Enterobacteriaceae	0.8%	0.0%	0.89
Paraprevotellaceae	0.7%	0.0%	0.90
Rhodospirillaceae	0.1%	0.7%	0.90
Oxalobacteraceae	0.7%	0.1%	0.91
Brucellaceae	0.0%	0.6%	0.91
Nitrospinaceae	0.1%	0.6%	0.92
Veillonellaceae	0.5%	0.0%	0.92
Francisellaceae	0.5%	0.0%	0.93
Salinisphaeraceae	0.5%	0.0%	0.93
Rickettsiaceae	0.5%	0.0%	0.93
Moraxellaceae	0.5%	0.0%	0.94
Rhizobiaceae	0.5%	0.0%	0.94
Geodermatophilaceae	0.1%	0.5%	0.94
Marine group II	0.2%	0.5%	0.95
Shewanellaceae	0.4%	0.0%	0.95
Microbacteriaceae	0.4%	0.0%	0.95
Carnobacteriaceae	0.4%	0.0%	0.96
Bradyrhizobiaceae	0.2%	0.5%	0.96
Verrucomicrobiaceae	0.2%	0.5%	0.96
Idiomarinaceae	0.4%	0.1%	0.96
Pirellulaceae	0.4%	0.6%	0.97
Comamonadaceae	0.1%	0.4%	0.97
Alcanivoracaceae	0.3%	0.5%	0.97
Desulfobacteraceae	0.0%	0.3%	0.97
Tissierellaceae	0.3%	0.0%	0.98
Burkholderiaceae	0.3%	0.0%	0.98
Oleiphilaceae	0.0%	0.3%	0.98
SAR324	0.2%	0.0%	0.98
OM60	0.1%	0.3%	0.98
Kiloniellaceae	0.0%	0.2%	0.98
Rhodocyclaceae	0.2%	0.0%	0.99
Xanthomonadaceae	0.2%	0.0%	0.99
Clostridiaceae	0.2%	0.0%	0.99
Cytophagaceae	0.2%	0.0%	0.99
Leptotrichiaceae	0.2%	0.0%	0.99
Dermabacteraceae	0.2%	0.0%	0.99
mb2424	0.2%	0.0%	0.99
Flammeovirgaceae	0.2%	0.1%	1.00

ICE - Upper- mesopelagic	Sinking	Suspendec	Av. cum. Sum
Alteromonadaceae	27.9%	2.6%	0.20
Unaffiliated	10.3%	24.2%	0.31
Idiomarinaceae	14.2%	0.6%	0.41
NS9	0.2%	10.0%	0.49
Rhodobacteraceae	7.6%	1.0%	0.54
Cryomorphaceae	0.7%	7.0%	0.59
Flavobacteriaceae	4.8%	9.5%	0.63
Halomonadaceae	6.5%	2.9%	0.66
Piscirickettsiaceae	4.9%	1.7%	0.68
Salinisphaeraceae	3.3%	0.1%	0.71
Saprospiraceae	0.3%	3.3%	0.73
Comamonadaceae	0.1%	3.1%	0.75
Marine group II	0.3%	2.4%	0.77
Alcanivoracaceae	2.6%	0.5%	0.78
JTB38	0.4%	2.5%	0.80
OM27	0.1%	2.0%	0.82
Pelagibacteraceae	0.3%	2.1%	0.83
Syntrophobacteraceae	0.1%	1.4%	0.84
Planococcaceae	1.6%	0.3%	0.85
Nitrospinaceae	0.1%	1.0%	0.86
OM60	0.8%	1.7%	0.86
Pirellulaceae	0.5%	1.4%	0.87
Verrucomicrobiaceae	0.3%	1.1%	0.88
Legionellaceae	0.0%	0.7%	0.88
SAR324	0.0%	0.6%	0.89
Pseudoalteromonadaceae	0.8%	0.3%	0.89
Erythrobacteraceae	0.6%	0.1%	0.90
Colwelliaceae	0.2%	0.8%	0.90
Desulfobacteraceae	0.0%	0.5%	0.90
Oxalobacteraceae	0.0%	0.5%	0.91
Sphingomonadaceae	0.2%	0.7%	0.91
Oceanospirillaceae	0.5%	0.9%	0.91
Rhizobiaceae	0.4%	0.0%	0.92
Ectothiorhodospiraceae	0.2%	0.6%	0.92
Enterobacteriaceae	0.1%	0.5%	0.92
Vibrionaceae	0.0%	0.4%	0.93
Microbacteriaceae	0.4%	0.0%	0.93
A714017	0.1%	0.5%	0.93
Methylophilaceae	0.0%	0.4%	0.94
Rickettsiaceae	0.5%	0.2%	0.94
Pseudomonadaceae	0.4%	0.1%	0.94
Moritellaceae	0.0%	0.3%	0.94
Haliangiaceae	0.0%	0.3%	0.95
Campylobacteraceae	0.0%	0.3%	0.95
HTCC2188	0.1%	0.4%	0.95
Marine group III	0.0%	0.3%	0.95
SUP05	0.0%	0.3%	0.96
Aerococcaceae	0.3%	0.0%	0.96
Cenarchaeaceae	0.0%	0.3%	0.96
Neisseriaceae	0.7%	1.0%	0.96
Puniceicoccaceae	0.0%	0.3%	0.96
Geodermatophilaceae	0.2%	0.0%	0.97
Helicobacteraceae	0.0%	0.2%	0.97
Staphylococcaceae	0.2%	0.0%	0.97
Dietziaceae	0.2%	0.0%	0.97
Rhodocyclaceae	0.0%	0.2%	0.97
Nocardioidaceae	0.2%	0.0%	0.97
AEGEAN_185	0.0%	0.2%	0.97
wb1_P06	0.3%	0.5%	0.98
Synechococcaceae	0.2%	0.0%	0.98
Bacillaceae	0.0%	0.2%	0.98
Carnobacteriaceae	0.1%	0.0%	0.98
Psychromonadaceae	0.0%	0.1%	0.98
SB-1	0.0%	0.2%	0.98
Desulfobulbaceae	0.1%	0.2%	0.98
Mycobacteriaceae	0.0%	0.1%	0.98
Pasteurellaceae	0.2%	0.1%	0.98
Hyphomonadaceae	0.1%	0.0%	0.99
Fusobacteriaceae	0.1%	0.0%	0.99
Paraprevotellaceae	0.1%	0.0%	0.99
NS11-12	0.0%	0.1%	0.99
Prevotellaceae	0.1%	0.0%	0.99
Peptostreptococcaceae	0.0%	0.1%	0.99
Xenococcaceae	0.0%	0.1%	0.99
Arctic95B-10	0.1%	0.0%	0.99
Balneolaceae	0.0%	0.1%	0.99
Shewanellaceae	0.0%	0.0%	0.99
Clostridiaceae	0.0%	0.0%	0.99
Phyllobacteriaceae	0.1%	0.0%	0.99
Endoecteinascidiaceae	0.0%	0.0%	0.99
Desulfuromonadaceae	0.0%	0.0%	0.99
Coriobacteriaceae	0.0%	0.0%	0.99
JTB36	0.0%	0.0%	0.99
Nitrospiraceae	0.0%	0.0%	0.99
Sinobacteraceae	0.0%	0.0%	0.99
Planctomycetaceae	0.1%	0.1%	0.99
Micrococcaceae	0.2%	0.2%	0.99
Methylobacteriaceae	0.2%	0.2%	0.99
Rhodospirillaceae	0.0%	0.1%	0.99
Francisellaceae	0.1%	0.0%	0.99
ZA3409c	0.0%	0.0%	1.00

A.

Appendix A

P2 - Mixed layer	Sinking	Suspended	Av. cum. Sum
Oceanospirillaceae	10.7%	24.1%	0.19
Pseudoalteromonadaceae	29.9%	18.4%	0.35
Flavobacteriaceae	8.8%	19.2%	0.49
Methylobacteriaceae	5.7%	0.4%	0.56
Cryomorphaceae	1.9%	6.5%	0.63
Alteromonadaceae	10.3%	6.1%	0.69
Pelagibacteraceae	5.0%	8.8%	0.74
Rhodobacteraceae	4.2%	6.5%	0.77
Sphingomonadaceae	1.9%	0.0%	0.80
Rhizobiaceae	1.5%	0.0%	0.82
Chitinophagaceae	1.5%	0.0%	0.84
Halomonadaceae	1.9%	0.8%	0.86
Planococcaceae	1.1%	0.0%	0.87
Neisseriaceae	1.1%	0.0%	0.89
Rickettsiaceae	1.1%	0.4%	0.90
Comamonadaceae	0.8%	0.0%	0.91
Nitrospinaceae	0.4%	0.0%	0.91
Idiomarinaceae	0.4%	0.0%	0.92
Colwelliaceae	0.0%	0.4%	0.93
Pseudomonadaceae	0.4%	0.0%	0.93
SUP05	0.4%	0.0%	0.94
Vibrionaceae	0.0%	0.4%	0.94
Rhodospirillaceae	0.4%	0.0%	0.95
Puniceicoccaceae	0.0%	0.4%	0.95
Enterobacteriaceae	0.4%	0.0%	0.96
Veillonellaceae	0.4%	0.0%	0.96
Microbacteriaceae	0.4%	0.0%	0.97
Bradyrhizobiaceae	0.4%	0.0%	0.97
Bacillaceae	0.4%	0.0%	0.98
Hyphomicrobiaceae	0.0%	0.4%	0.98
mitochondria	0.4%	0.0%	0.99
Thermomonosporaceae	0.4%	0.0%	0.99
NS9	1.9%	1.5%	1.00

P2 - Upper- mesopelagic	Sinking	Suspended	Av. cum. Sum
Pseudoalteromonadaceae	41.8%	2.2%	0.36
NS9	2.8%	29.8%	0.61
Flavobacteriaceae	4.4%	11.9%	0.68
Cryomorphaceae	2.1%	6.9%	0.72
Unaffiliated	8.4%	12.4%	0.76
Francisellaceae	4.5%	0.9%	0.79
OM27	0.1%	2.3%	0.81
Saprospiraceae	0.2%	2.4%	0.83
Flammeovirgaceae	7.0%	5.2%	0.85
JTB38	0.0%	1.6%	0.86
Helicobacteraceae	1.6%	0.0%	0.88
Rhodobacteraceae	2.6%	1.1%	0.89
Oceanospirillaceae	2.6%	1.6%	0.90
Idiomarinaceae	1.5%	0.6%	0.91
OM60	0.3%	0.9%	0.91
Piscirickettsiaceae	1.0%	0.5%	0.92
Verrucomicrobiaceae	1.6%	2.2%	0.92
Pelagibacteraceae	1.4%	1.0%	0.93
Alteromonadaceae	5.8%	6.2%	0.93
Neisseriaceae	0.1%	0.4%	0.93
A714017	0.2%	0.5%	0.94
Colwelliaceae	0.7%	0.4%	0.94
Staphylococcaceae	0.3%	0.0%	0.94
Halomonadaceae	2.0%	2.2%	0.94
Marine group II	0.8%	1.1%	0.95
Planococcaceae	0.6%	0.4%	0.95
Syntrophobacteraceae	0.1%	0.3%	0.95
Coxiellaceae	0.2%	0.4%	0.95
Methylobacteriaceae	0.2%	0.0%	0.96
Pirellulaceae	0.1%	0.3%	0.96
Salinisphaeraceae	0.4%	0.2%	0.96
Alcanivoracaceae	0.3%	0.0%	0.96
Nitrospinaceae	0.1%	0.3%	0.96
SUP05	0.0%	0.2%	0.97
Bacteriovoracaceae	0.0%	0.2%	0.97
Comamonadaceae	0.2%	0.1%	0.97
Geodermatophilaceae	0.2%	0.0%	0.97
SAR324	0.3%	0.5%	0.97
Rhizobiaceae	0.1%	0.0%	0.97
Erythrobacteraceae	0.1%	0.0%	0.97
Moritellaceae	0.0%	0.1%	0.98
Haliangiaceae	0.1%	0.0%	0.98
Hyphomicrobiaceae	0.1%	0.0%	0.98
Streptococcaceae	0.5%	0.4%	0.98
Cenarchaeaceae	0.1%	0.2%	0.98
Marine group III	0.1%	0.1%	0.98
Pasteurellaceae	0.1%	0.0%	0.98
Enterobacteriaceae	0.1%	0.0%	0.98
Paraprevotellaceae	0.0%	0.1%	0.98
Burkholderiaceae	0.1%	0.0%	0.98
Enterococcaceae	0.0%	0.1%	0.99
Fusobacteriaceae	0.1%	0.0%	0.99
Shewanellaceae	0.1%	0.0%	0.99
Methylophilaceae	0.1%	0.1%	0.99
Rickettsiaceae	0.0%	0.1%	0.99
Moraxellaceae	0.1%	0.0%	0.99
Micrococcaceae	0.1%	0.1%	0.99
Puniceicoccaceae	0.0%	0.1%	0.99
Oxalobacteraceae	0.2%	0.2%	0.99
Corynebacteriaceae	0.1%	0.0%	0.99
Carnobacteriaceae	0.1%	0.0%	0.99
Ectothiorhodospiraceae	0.1%	0.0%	0.99
Kiloniellaceae	0.1%	0.0%	0.99
Nocardioidaceae	0.1%	0.0%	0.99
Cerasicoccaceae	0.0%	0.1%	0.99
Prevotellaceae	0.1%	0.0%	0.99
HTCC2188	0.1%	0.2%	0.99
Pseudomonadaceae	0.1%	0.1%	0.99
Vibrionaceae	0.1%	0.0%	0.99
AEGEAN_185	0.0%	0.1%	0.99
Gemellaceae	0.0%	0.0%	0.99
Veillonellaceae	0.0%	0.0%	0.99
Microbacteriaceae	0.1%	0.0%	1.00

B.

C.

P3 - Mixed layer	Sinking	Suspended	Av. cum. Sum
Shewanellaceae	7.3%	0.1%	0.21
Oceanospirillaceae	6.4%	12.0%	0.37
Rhodobacteraceae	1.6%	4.6%	0.46
Flavobacteriaceae	19.2%	22.1%	0.54
Verrucomicrobiaceae	2.9%	0.3%	0.62
Cryomorphaceae	2.6%	5.1%	0.69
Pelagibacteraceae	4.5%	5.9%	0.73
Alteromonadaceae	8.0%	6.9%	0.76
Pseudoalteromonadaceae	30.4%	29.3%	0.80
OM60	1.8%	0.7%	0.83
Methylobacteriaceae	0.9%	0.0%	0.85
Unaffiliated	5.1%	5.9%	0.88
Saprospiraceae	0.2%	0.5%	0.89
Flammeovirgaceae	0.6%	0.3%	0.89
Rickettsiaceae	0.4%	0.1%	0.90
Moraxellaceae	0.4%	0.1%	0.91
Pseudomonadaceae	0.5%	0.3%	0.92
Rhizobiaceae	0.2%	0.0%	0.92
Oxalobacteraceae	0.3%	0.1%	0.93
Comamonadaceae	0.2%	0.0%	0.93
Bacteriovoracaceae	0.2%	0.0%	0.94
Planococcaceae	0.3%	0.1%	0.94
Vibrionaceae	0.1%	0.0%	0.95
Rhodospirillaceae	0.2%	0.3%	0.95
NS9	0.5%	0.6%	0.95
Idiomarinaceae	0.0%	0.1%	0.95
Streptococcaceae	0.1%	0.0%	0.96
Bacillaceae	0.1%	0.0%	0.96
Veillonellaceae	0.1%	0.0%	0.96
Neisseriaceae	0.1%	0.0%	0.96
SAR324	0.1%	0.1%	0.96
Nitrospinaceae	0.0%	0.0%	0.96
Alcanivoracaceae	0.0%	0.1%	0.97
Micrococcaceae	0.1%	0.0%	0.97
Pasteurellaceae	0.0%	0.0%	0.97
Microbacteriaceae	0.0%	0.0%	0.97
Piscirickettsiaceae	0.0%	0.0%	0.97
Staphylococcaceae	0.0%	0.0%	0.97
Chitinophagaceae	0.0%	0.0%	0.97
Bradyrhizobiaceae	0.0%	0.0%	0.97
NS11-12	0.1%	0.1%	0.97
Xanthomonadaceae	0.0%	0.0%	0.98
Cyclobacteriaceae	0.0%	0.0%	0.98
Colwelliaceae	0.4%	0.3%	0.98
HTCC2188	0.1%	0.1%	0.98
Francisellaceae	0.1%	0.1%	0.98
OM27	0.0%	0.0%	0.98
Gemellaceae	0.0%	0.0%	0.98
Enterobacteriaceae	0.0%	0.0%	0.98
Carnobacteriaceae	0.0%	0.0%	0.98
Hyphomonadaceae	0.0%	0.0%	0.98
Rhodocyclaceae	0.0%	0.0%	0.98
mitochondria	0.0%	0.0%	0.98
Thermomonosporaceae	0.0%	0.0%	0.98
Synechococcaceae	0.0%	0.0%	0.99
Phyllobacteriaceae	0.0%	0.0%	0.99
Psychromonadaceae	0.0%	0.0%	0.99
SC3-41	0.0%	0.0%	0.99
Peptostreptococcaceae	0.0%	0.0%	0.99
Marine group II	0.1%	0.1%	0.99
SUP05	0.0%	0.0%	0.99
Sphingomonadaceae	0.0%	0.0%	0.99
Chromatiaceae	0.1%	0.2%	0.99
Halomonadaceae	2.9%	2.8%	0.99
A714017	0.0%	0.0%	0.99
Salinisphaeraceae	0.0%	0.0%	0.99
ZA3409c	0.0%	0.0%	0.99
Syntrophobacteraceae	0.0%	0.0%	0.99
Thiohalorhabdaceae	0.0%	0.0%	0.99
Coxiellaceae	0.0%	0.0%	0.99
Helicobacteraceae	0.0%	0.0%	0.99
Erythrobacteraceae	0.0%	0.0%	0.99
Moritellaceae	0.0%	0.0%	1.00

P3 - Upper- mesopelagic	Sinking	Suspended	Av. cum. Sum
Pseudoalteromonadaceae	35.0%	15.0%	0.22
NS9	0.7%	9.5%	0.32
Unaffiliated	4.1%	12.8%	0.42
OM27	0.1%	7.0%	0.50
Flavobacteriaceae	15.9%	11.1%	0.55
Verrucomicrobiaceae	6.9%	3.3%	0.59
Pseudomonadaceae	3.2%	0.4%	0.62
Saprospiraceae	0.2%	2.8%	0.65
JTB38	0.3%	2.6%	0.68
Cryomorphaceae	1.7%	3.8%	0.70
Shewanellaceae	2.1%	0.1%	0.72
Piscirickettsiaceae	2.8%	0.9%	0.75
OM60	1.7%	3.3%	0.76
Colwelliaceae	1.6%	3.1%	0.78
Rhodobacteraceae	2.1%	0.6%	0.80
Flammeovirgaceae	2.3%	0.9%	0.81
Marine group II	0.7%	1.7%	0.82
Alteromonadaceae	4.3%	5.2%	0.83
Francisellaceae	0.4%	1.2%	0.84
Moraxellaceae	0.8%	0.1%	0.85
Syntrophobacteraceae	0.1%	0.8%	0.86
Cystobacterineae	0.0%	0.7%	0.87
Oceanospirillaceae	1.3%	0.7%	0.87
Pirellulaceae	0.3%	0.9%	0.88
Coxiellaceae	0.1%	0.6%	0.89
Nocardioidaceae	0.4%	0.0%	0.89
A714017	0.1%	0.5%	0.89
SAR324	0.0%	0.4%	0.90
Geodermatophilaceae	0.3%	0.0%	0.90
Chromatiaceae	0.0%	0.3%	0.90
Veillonellaceae	0.1%	0.4%	0.91
Planococcaceae	0.3%	0.0%	0.91
Halomonadaceae	1.9%	1.6%	0.91
Paraprevotellaceae	0.0%	0.3%	0.92
Helicobacteraceae	0.2%	0.0%	0.92
Erythrobacteraceae	0.3%	0.1%	0.92
Comamonadaceae	0.2%	0.0%	0.93
Sphingomonadaceae	0.5%	0.3%	0.93
Neisseriaceae	0.2%	0.5%	0.93
SUP05	0.1%	0.3%	0.93
Hyphomonadaceae	0.0%	0.2%	0.94
Planctomycetaceae	0.0%	0.2%	0.94
ZA3409c	0.1%	0.3%	0.94
Pelagibacteraceae	0.8%	1.0%	0.94
Micrococcaceae	0.2%	0.0%	0.94
Methylophilaceae	0.3%	0.1%	0.95
Intrasporangiaceae	0.2%	0.0%	0.95
Cerasicoccaceae	0.0%	0.2%	0.95
Xanthomonadaceae	0.2%	0.0%	0.95
AEGEAN_185	0.0%	0.1%	0.95
Rhizobiaceae	0.2%	0.0%	0.96
Haliangiaceae	0.1%	0.2%	0.96
Methylobacteriaceae	0.2%	0.1%	0.96
Salinisphaeraceae	0.1%	0.0%	0.96
Enterobacteriaceae	0.1%	0.2%	0.96
Alcanivoracaceae	0.1%	0.0%	0.96
Marine group III	0.0%	0.1%	0.96
Kiloniellaceae	0.0%	0.1%	0.96
JdFBGBact	0.1%	0.0%	0.97
Dietziaceae	0.1%	0.0%	0.97
TK06	0.0%	0.1%	0.97
Weeksellaceae	0.1%	0.0%	0.97
Streptococcaceae	0.7%	0.5%	0.97
Rhodospirillaceae	0.1%	0.2%	0.97
Cenarchaeaceae	0.0%	0.1%	0.97
HTCC2188	0.0%	0.1%	0.97
Oxalobacteraceae	0.1%	0.0%	0.98
Gemellaceae	0.1%	0.1%	0.98
wb1_P06	0.0%	0.1%	0.98
Cytophagaceae	0.1%	0.0%	0.98
Moritellaceae	0.2%	0.3%	0.98
Idiomarinaceae	0.1%	0.0%	0.98
Corynebacteriaceae	0.1%	0.0%	0.98
Desulfuromonadaceae	0.0%	0.1%	0.98
Amoebophilaceae	0.1%	0.0%	0.98
Thiohalorhabdaceae	0.1%	0.0%	0.98
Phormidiaceae	0.1%	0.0%	0.98
Clostridiaceae	0.1%	0.0%	0.99
Chitinophagaceae	0.1%	0.0%	0.99
Bacteriovoracaceae	0.2%	0.2%	0.99
Bradyrhizobiaceae	0.0%	0.1%	0.99
Legionellaceae	0.0%	0.1%	0.99
Psychromonadaceae	0.1%	0.0%	0.99
Fusobacteriaceae	0.0%	0.1%	0.99
Porphyromonadaceae	0.0%	0.1%	0.99
Paenibacillaceae	0.1%	0.0%	0.99
Gemmataceae	0.0%	0.1%	0.99
Ectothiorhodospiraceae	0.0%	0.1%	0.99
Phyllobacteriaceae	0.1%	0.0%	0.99
Bacillaceae	0.0%	0.0%	0.99
Propionibacteriaceae	0.0%	0.0%	0.99
Enterococcaceae	0.0%	0.1%	0.99
Synechococcaceae	0.0%	0.0%	0.99
Erysipelotrichaceae	0.0%	0.0%	0.99
Pseudanabaenaceae	0.0%	0.0%	0.99
Vibrionaceae	0.1%	0.1%	0.99
Rickettsiaceae	0.1%	0.1%	1.00

Appendix A

UP - Mixed layer	Sinking	Suspended	Av. cum. Sum
Flavobacteriaceae	38.0%	22.8%	0.22
Oceanospirillaceae	7.4%	22.4%	0.45
Pelagibacteraceae	3.6%	10.1%	0.54
Pseudoalteromonadaceae	13.1%	19.2%	0.63
Unaffiliated	10.6%	5.3%	0.71
Alteromonadaceae	10.6%	6.5%	0.77
Verrucomicrobiaceae	3.8%	0.4%	0.82
Rhodobacteraceae	1.3%	4.4%	0.87
OM60	2.1%	0.3%	0.89
Halomonadaceae	1.2%	2.6%	0.91
Colwelliaceae	0.6%	0.1%	0.92
Shewanellaceae	0.4%	0.0%	0.93
Bacteriovoracaceae	0.4%	0.0%	0.93
Pseudomonadaceae	0.5%	0.1%	0.94
Flammeovirgaceae	0.6%	0.3%	0.94
Planococcaceae	0.4%	0.0%	0.95
NS9	0.3%	0.6%	0.95
Chromatiaceae	0.1%	0.4%	0.96
Saprospiraceae	0.6%	0.3%	0.96
Rickettsiaceae	0.3%	0.1%	0.97
Cryomorphaceae	2.4%	2.6%	0.97
Methylophilaceae	0.4%	0.1%	0.97
Rhodospirillaceae	0.0%	0.2%	0.97
Alcanivoracaceae	0.0%	0.1%	0.98
SAR324	0.0%	0.1%	0.98
Streptococcaceae	0.1%	0.0%	0.98
Staphylococcaceae	0.1%	0.0%	0.98
HTCC2188	0.0%	0.1%	0.98
Moraxellaceae	0.1%	0.1%	0.98
Neisseriaceae	0.1%	0.0%	0.99
Francisellaceae	0.2%	0.1%	0.99
Marine group II	0.0%	0.1%	0.99
Comamonadaceae	0.1%	0.0%	0.99
mitochondria	0.0%	0.0%	0.99
Oxalobacteraceae	0.1%	0.0%	0.99
HTCC2089	0.0%	0.0%	0.99
Veillonellaceae	0.0%	0.0%	0.99
Idiomarinaceae	0.0%	0.0%	0.99
Micrococcaceae	0.0%	0.0%	0.99
Piscirickettsiaceae	0.0%	0.0%	0.99
Methylobacteriaceae	0.0%	0.0%	0.99
NS11-12	0.0%	0.0%	0.99
Rhizobiaceae	0.0%	0.0%	0.99
Bacteroidaceae	0.0%	0.0%	0.99
Hyphomonadaceae	0.0%	0.0%	0.99
Tissierellaceae	0.0%	0.0%	0.99
Actinomycetaceae	0.0%	0.0%	0.99
Lachnospiraceae	0.0%	0.0%	0.99
Carnobacteriaceae	0.0%	0.0%	1.00

UP - Upper- mesopelagic	Sinking	Suspended	Av. cum. Sum
NS9	1.6%	10.3%	0.15
Verrucomicrobiaceae	6.5%	2.0%	0.23
Unaffiliated	7.1%	11.4%	0.30
Flavobacteriaceae	12.1%	8.1%	0.37
Pseudoalteromonadaceae	34.6%	30.6%	0.44
Marine group II	0.7%	3.3%	0.48
OM27	0.6%	2.9%	0.52
Saprospiraceae	0.3%	2.3%	0.56
Cryomorphaceae	1.6%	3.4%	0.59
Planococcaceae	1.9%	0.2%	0.62
OM60	3.0%	1.3%	0.65
Oceanospirillaceae	2.4%	0.7%	0.68
Streptococcaceae	2.1%	0.5%	0.71
Pseudomonadaceae	2.1%	1.1%	0.72
Methylophilaceae	1.0%	0.1%	0.74
Colwelliaceae	2.0%	1.2%	0.75
JTB38	0.7%	1.5%	0.77
Flammeovirgaceae	2.8%	2.1%	0.78
Halomonadaceae	0.8%	1.4%	0.79
SAR324	0.2%	0.8%	0.80
Cystobacterineae	0.1%	0.7%	0.81
Pelagibacteraceae	1.1%	1.6%	0.82
Pasteurellaceae	0.6%	0.0%	0.83
A714017	0.2%	0.7%	0.84
Paraprevotellaceae	0.5%	0.0%	0.85
Rhodobacteraceae	1.0%	0.6%	0.85
SUP05	0.1%	0.6%	0.86
Piscirickettsiaceae	0.6%	1.0%	0.87
Veillonellaceae	0.4%	0.0%	0.88
Nitrospinaceae	0.1%	0.5%	0.88
Shewanellaceae	0.4%	0.1%	0.89
Coxiellaceae	0.1%	0.4%	0.89
Francisellaceae	1.0%	0.7%	0.90
Syntrophobacteraceae	0.1%	0.4%	0.91
Staphylococcaceae	0.4%	0.0%	0.91
Gemellaceae	0.3%	0.0%	0.92
Sphingomonadaceae	0.2%	0.5%	0.92
Tissierellaceae	0.2%	0.0%	0.93
Moraxellaceae	0.5%	0.3%	0.93
AEGEAN_185	0.0%	0.2%	0.93
Ectothiorhodospiraceae	0.0%	0.2%	0.94
Alteromonadaceae	2.5%	2.3%	0.94
Micrococcaceae	0.3%	0.1%	0.94
Haliangiaceae	0.0%	0.2%	0.95
wb1_P06	0.0%	0.1%	0.95
Lactobacillaceae	0.1%	0.0%	0.95
Rhizobiaceae	0.1%	0.0%	0.95
Weeksellaceae	0.1%	0.0%	0.95
Propionibacteriaceae	0.1%	0.0%	0.95
Chromatiaceae	0.0%	0.1%	0.96
Actinomycetaceae	0.1%	0.0%	0.96
Deinococcaceae	0.1%	0.0%	0.96
Rickettsiaceae	0.1%	0.1%	0.96
Corynebacteriaceae	0.1%	0.0%	0.96
Thiohalorhabdaceae	0.1%	0.0%	0.96
Porphyromonadaceae	0.1%	0.0%	0.96
HTCC2188	0.2%	0.1%	0.97
Cenarchaeaceae	0.0%	0.1%	0.97
Pirellulaceae	0.4%	0.5%	0.97
Moritellaceae	0.3%	0.3%	0.97
Prevotellaceae	0.1%	0.0%	0.97
Bifidobacteriaceae	0.1%	0.0%	0.97
Bacteriovoracaceae	0.2%	0.2%	0.97
Dietziaceae	0.1%	0.0%	0.97
Erythrobacteraceae	0.1%	0.0%	0.97
TK06	0.0%	0.1%	0.97
Geodermatophilaceae	0.1%	0.0%	0.98
Rhodocyclaceae	0.1%	0.0%	0.98
Alcanivoracaceae	0.1%	0.0%	0.98
ZA3409c	0.2%	0.2%	0.98
Nitrosomonadaceae	0.0%	0.1%	0.98
Hyphomonadaceae	0.0%	0.1%	0.98
Planctomycetaceae	0.0%	0.1%	0.98
Nocardioidaceae	0.0%	0.0%	0.98
NS11-12	0.0%	0.0%	0.98
Carnobacteriaceae	0.2%	0.3%	0.98
Vibrionaceae	0.0%	0.0%	0.98
Microbacteriaceae	0.0%	0.0%	0.98
Bradyrhizobiaceae	0.0%	0.0%	0.99
Desulfuromonadaceae	0.0%	0.0%	0.99
Oxalobacteraceae	0.1%	0.1%	0.99
Comamonadaceae	0.1%	0.1%	0.99
Helicobacteraceae	0.0%	0.0%	0.99
Xanthomonadaceae	0.0%	0.0%	0.99
Clostridiaceae	0.0%	0.0%	0.99
Aerococcaceae	0.0%	0.0%	0.99
Leptotrichiaceae	0.0%	0.0%	0.99
Neisseriaceae	0.6%	0.7%	0.99
Idiomarinaceae	0.0%	0.0%	0.99
Salinisphaeraceae	0.0%	0.0%	0.99
Puniceicoccaceae	0.0%	0.0%	0.99
Pelagicoccaceae	0.0%	0.0%	0.99
Campylobacteraceae	0.0%	0.0%	0.99
Cerasicoccaceae	0.0%	0.0%	0.99
Brevibacteriaceae	0.0%	0.0%	0.99
Methylococcaceae	0.0%	0.0%	0.99
Rhodospirillaceae	0.1%	0.0%	0.99
Halobacteriaceae	0.0%	0.0%	0.99
Burkholderiaceae	0.0%	0.0%	1.00

D.

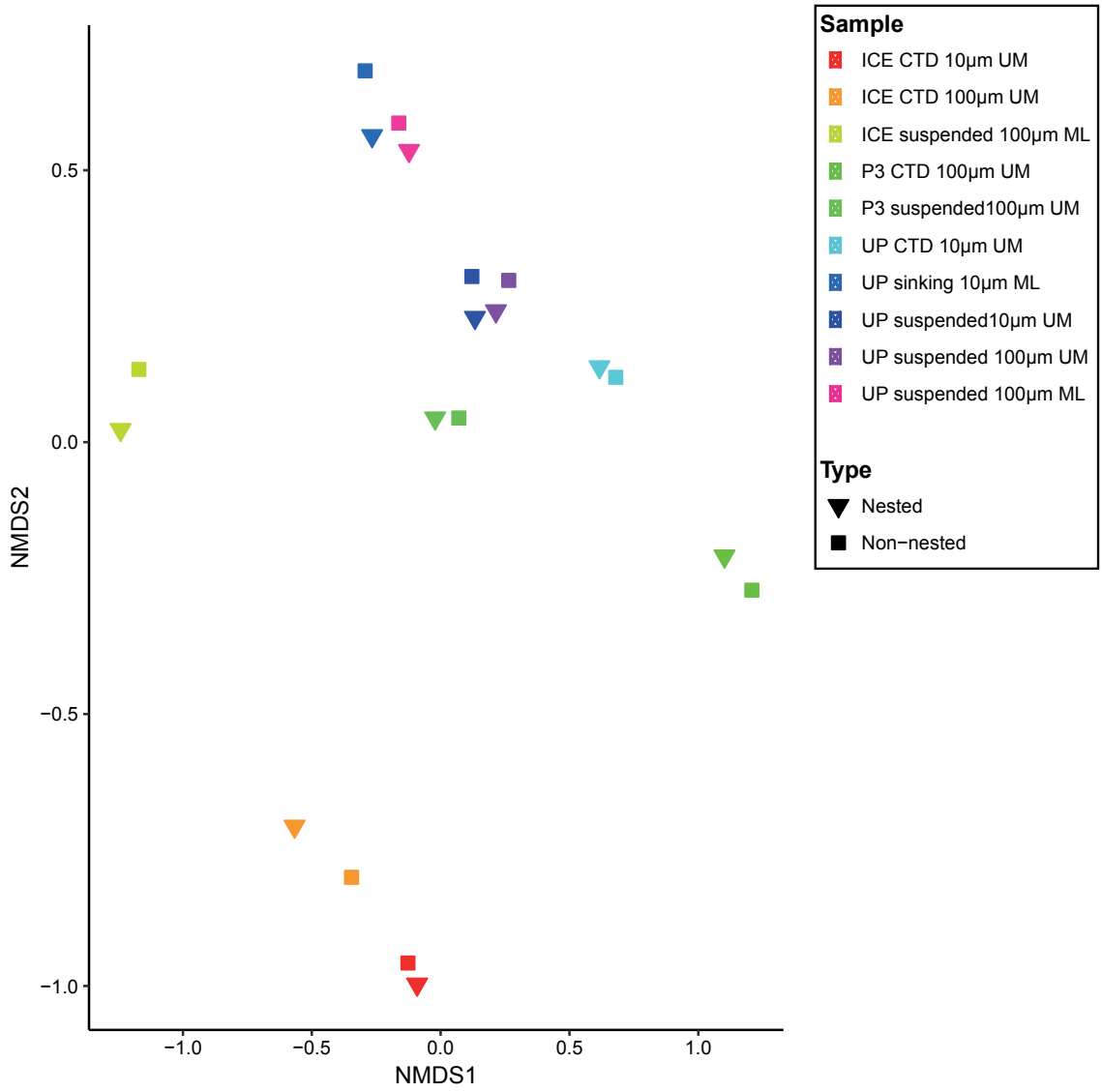

Stress = 0.1713764

Annex A9-A. Non-metric multidimensional scaling plot of OTU composition from nested-PCR amplified samples. The NMDS was calculated with the Bray-Curtis distance of the rarefied dataset. It compares the OTU composition of samples amplified with a nested-PCR (triangle) to their composition when amplified with a classic PCR (square). ML = mixed layer, UM = upper-mesopelagic.

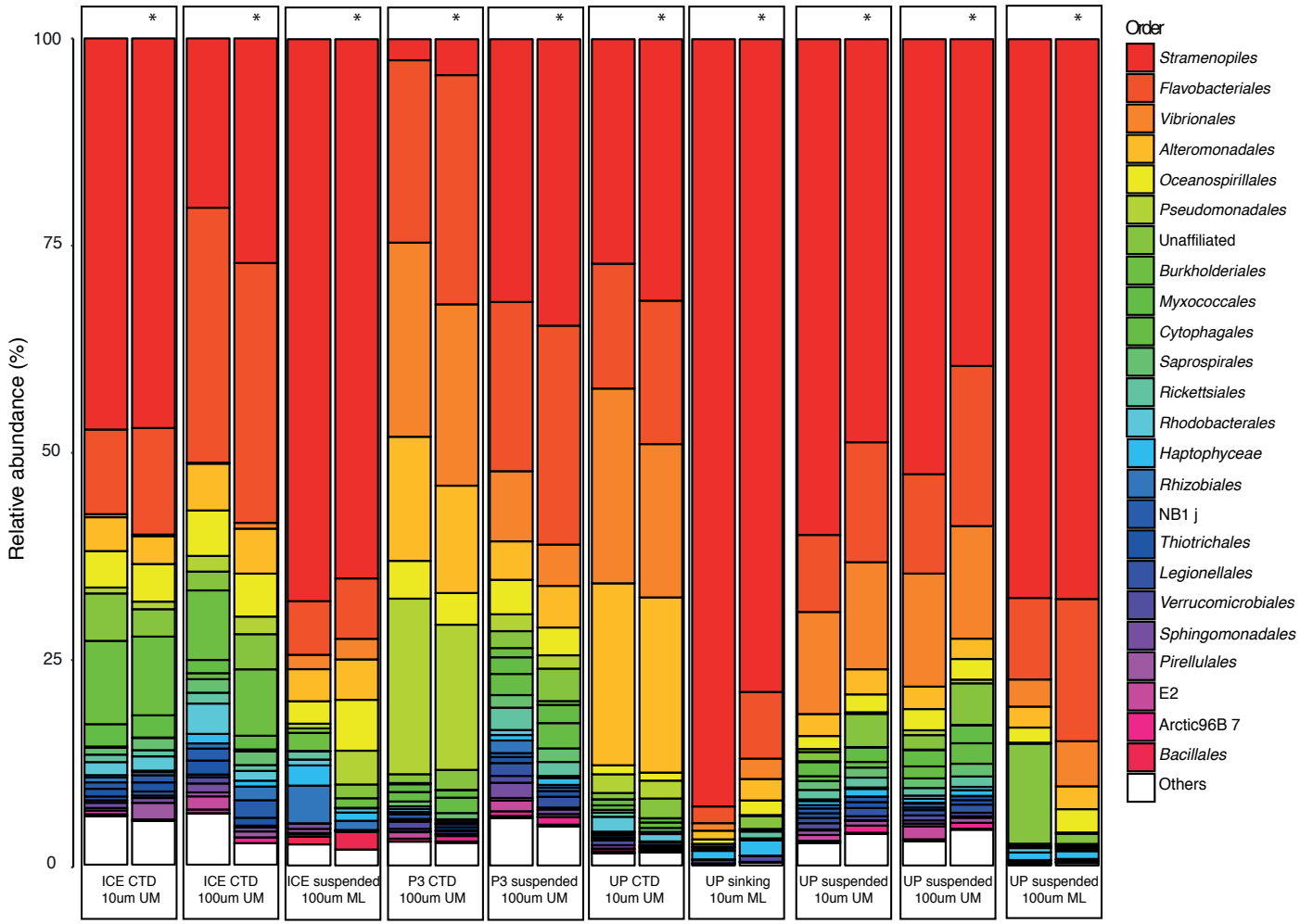

Annex A9-B. Taxonomic order composition of nested-PCR amplified samples. These bar charts compare the composition of samples amplified with a nested-PCR, marked with an asterisk (*) to their composition when amplified with a classic PCR. ML = mixed layer, UM = upper-mesopelagic.

Appendix B

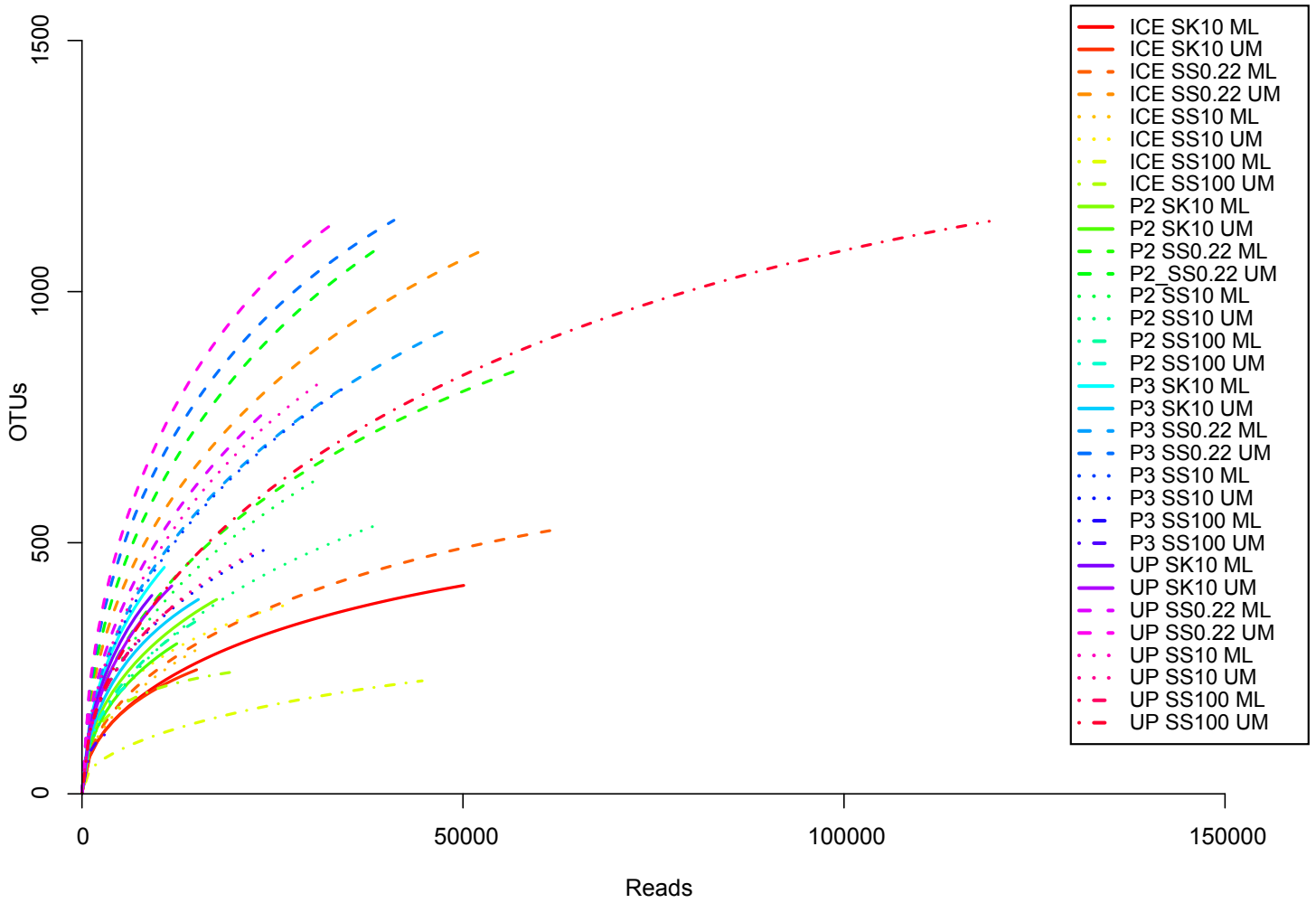

Annex B1. Rarefaction curves. ML = mixed layer, UM = upper-mesopelagic; SS0.22 = suspended particles 0.22 – 10 µm; SS10 = suspended particles 10 – 100 µm; SS100 = suspended particles ≥ 100 µm; (SS100), SK10 = sinking particles ≥ 10 µm.

Annex B2. Sequence counts tables. ML = mixed layer, UM = upper-mesopelagic; SS0.22 = suspended particles 0.22 – 10 µm; SS10 = suspended particles 10 – 100 µm; SS100 = suspended particles ≥ 100 µm; (SS100), SK10 = sinking particles ≥ 10 µm.

Station	Depth	Particle type	**Total reads**	Protists & Unaffiliated reads	%	Metazoa reads	%	Phytoplankton reads	%	HM reads	%
ICE	ML	SK10	**52714**	50100	95%	2578	5%	518	1%	49181	93%
P2	ML	SK10	**64085**	17679	28%	46318	72%	1553	2%	15297	24%
P3	ML	SK10	**40472**	10804	27%	29619	73%	595	1%	9715	24%
UP	ML	SK10	**44056**	9169	21%	34820	79%	554	1%	8338	19%
ICE	ML	SS0.22	**61402**	61399	100%	0	0%	28775	47%	32061	52%
P2	ML	SS0.22	**61310**	57583	94%	3720	6%	12367	20%	42251	69%
P3	ML	SS0.22	**49746**	48152	97%	1586	3%	4097	8%	41446	83%
UP	ML	SS0.22	**35048**	23684	68%	11350	32%	2553	7%	19330	55%
ICE	ML	SS10	**16127**	16123	100%	4	0%	1982	12%	13581	84%
P2	ML	SS10	**38790**	31150	80%	7610	20%	3742	10%	23546	61%
P3	ML	SS10	**41797**	35191	84%	6588	16%	3695	9%	28929	69%
UP	ML	SS10	**39264**	31512	80%	7721	20%	4404	11%	24358	62%
ICE	ML	SS100	**44868**	44641	99%	227	1%	3198	7%	39837	89%
P2	ML	SS100	**41798**	15219	36%	26560	64%	1649	4%	9233	22%
P3	ML	SS100	**25974**	7706	30%	18247	70%	553	2%	6354	24%
UP	ML	SS100	**42060**	14188	34%	27805	66%	1295	3%	10515	25%
ICE	UM	SK10	**30672**	15044	49%	6047	20%	406	1%	8836	29%
P2	UM	SK10	**37045**	12446	34%	24561	66%	170	0%	12135	33%
P3	UM	SK10	**44546**	15275	34%	29234	66%	238	1%	14582	33%
UP	UM	SK10	**40702**	11785	29%	28786	71%	154	0%	11150	27%
ICE	UM	SS0.22	**55381**	52118	94%	3240	6%	10336	19%	39868	72%
P2	UM	SS0.22	**40468**	38842	96%	1626	4%	2100	5%	35937	89%
P3	UM	SS0.22	**45121**	40941	91%	4177	9%	511	1%	39092	87%
UP	UM	SS0.22	**37019**	32800	89%	4211	11%	417	1%	31382	85%
ICE	UM	SS10	**32158**	26749	83%	5362	17%	541	2%	22842	71%
P2	UM	SS10	**41621**	38299	92%	3311	8%	514	1%	36563	88%
P3	UM	SS10	**31649**	24244	77%	7401	23%	222	1%	22314	71%
UP	UM	SS10	**28937**	23113	80%	5793	20%	282	1%	21268	73%
ICE	UM	SS100	**20811**	20431	98%	314	2%	851	4%	16362	79%
P2	UM	SS100	**29119**	5841	20%	23271	80%	138	0%	5366	18%
P3	UM	SS100	**6055**	3976	66%	2078	34%	4	0%	3067	51%
UP	UM	SS100	**312451**	119058	38%	193054	62%	2700	1%	110131	35%

Annex B3. Permutational multivariate analysis of variance of environmental parameters. Table A displays the PERMANOVA results for phytoplankton community and table B for hetero/mixotrophic protist community. Factors highlighted with an asterisk (*) were significantly affecting the OTU composition variability. SS: sums of squares; MS: means of squares; F.Model: F-tests results; R2: effect size; Pr: p-value.

A - Phytoplankton						
	Df	**SumsOfSqs**	**MeanSqs**	**F.Model**	**R2**	**Pr(>F)**
Temperature*	1	0.815	0.815	4.444	17%	0.001
Oxygen	1	0.254	0.254	1.383	5%	0.137
Fluorescence*	1	0.471	0.471	2.570	10%	0.003
POC	1	0.232	0.232	1.262	5%	0.228
Type*	3	0.931	0.310	1.692	19%	0.014
Residuals	*12*	*2.202*	*0.183*	*NA*	*45%*	*NA*
Total	*19*	*4.906*	*NA*	*NA*	*1*	*NA*

B - Hetero/mixotrophic protist						
	Df	**SumsOfSqs**	**MeanSqs**	**F.Model**	**R2**	**Pr(>F)**
Temperature*	1	0.431	0.431	2.759	11%	0.001
Oxygen*	1	0.379	0.379	2.428	9%	0.002
Fluorescence*	1	0.270	0.270	1.729	7%	0.023
POC*	1	0.349	0.349	2.234	9%	0.004
Type*	3	0.752	0.251	1.604	19%	0.010
Residuals	*12*	*1.875*	*0.156*	*NA*	*46%*	*NA*
Total	*19*	*4.057*	*NA*	*NA*	*1*	*NA*

Annex B4. Higher resolution taxonomic composition of phytoplankton, metazoan and hetero/mixotrophic protist communities (following three pages). Panel A shows the taxonomic family composition of phytoplankton communities, panel B the taxonomic order composition of metazoan communities and panel C the taxonomical family composition of hetero/mixotrophic protist communities. ML = mixed layer, UM = upper-mesopelagic; SS0.22 = suspended particles 0.22 – 10 µm; SS10 = suspended particles 10 – 100 µm; SS100 = suspended particles ≥ 100 µm; (SS100), SK10 = sinking particles ≥ 10 µm

A.

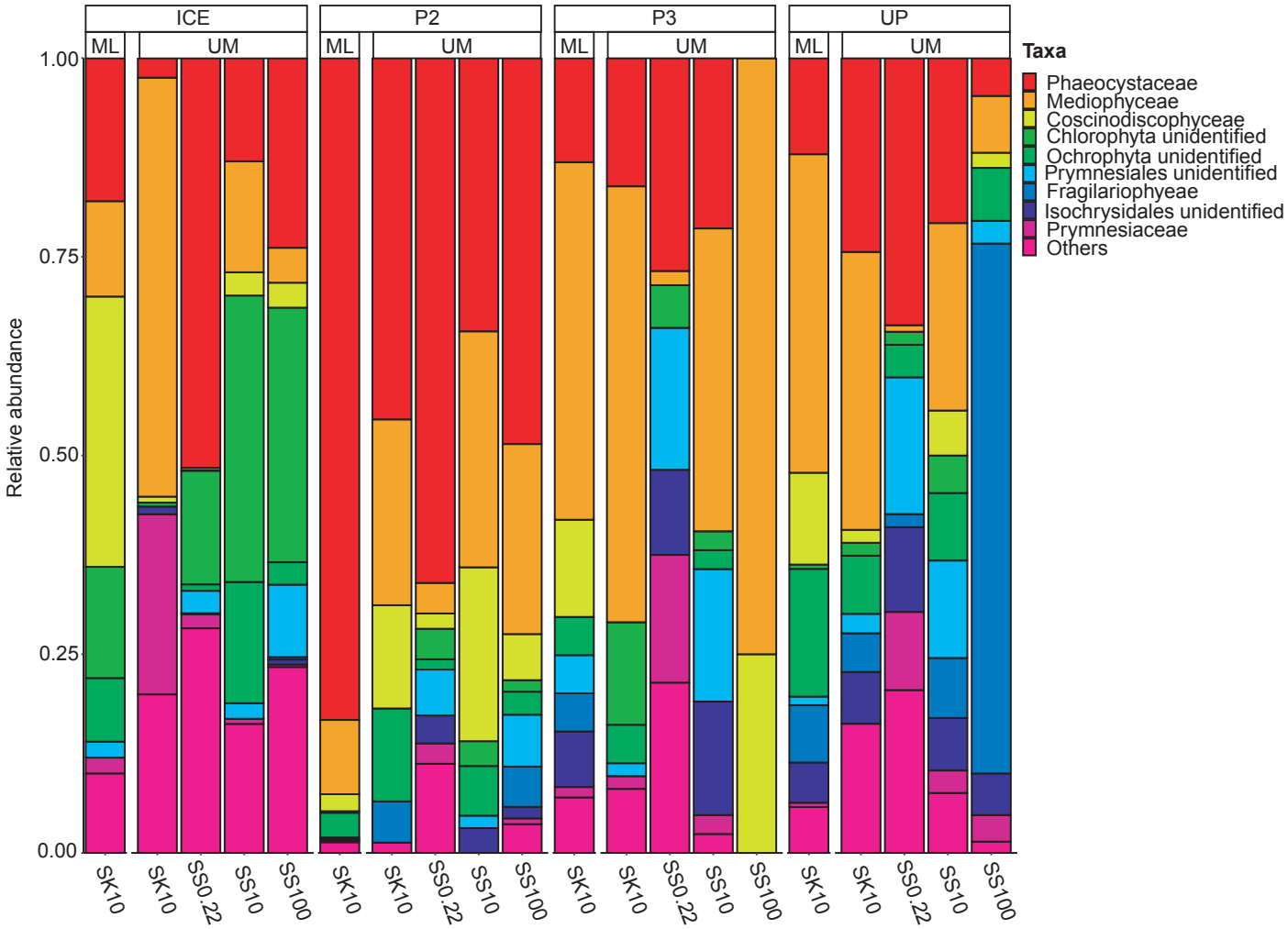
ICE
P2
P3
UP
ML
UM
Relative abundance
1.00
0.75
0.50
0.25
0.00
SK10
SS0.22
SS10
SS100
Taxa
Phaeocystaceae
Mediophyceae
Coscinodiscophyceae
Chlorophyta unidentified
Ochrophyta unidentified
Prymnesiales unidentified
Fragilariophyeae
Isochrysidales unidentified
Prymnesiaceae
Others

Appendix B

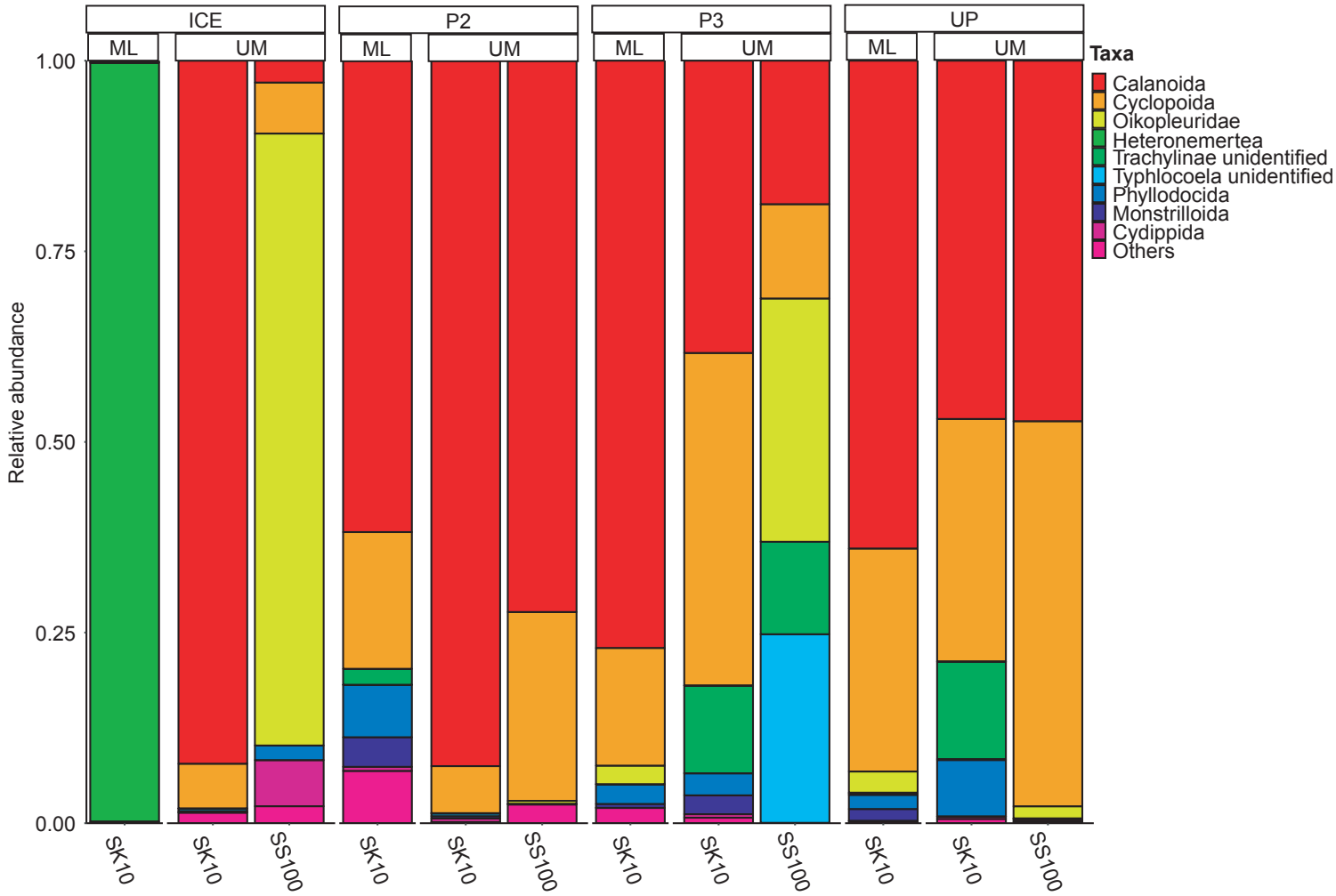
ICE
P2
P3
UP
ML
UM
1.00
0.75
0.50
0.25
0.00
Relative abundance
SK10
SS100
Taxa
Calanoida
Cyclopoida
Oikopleuridae
Heteronemertea
Trachylinae unidentified
Typhlocoela unidentified
Phyllodocida
Monstrilloida
Cydippida
Others

B.

C.

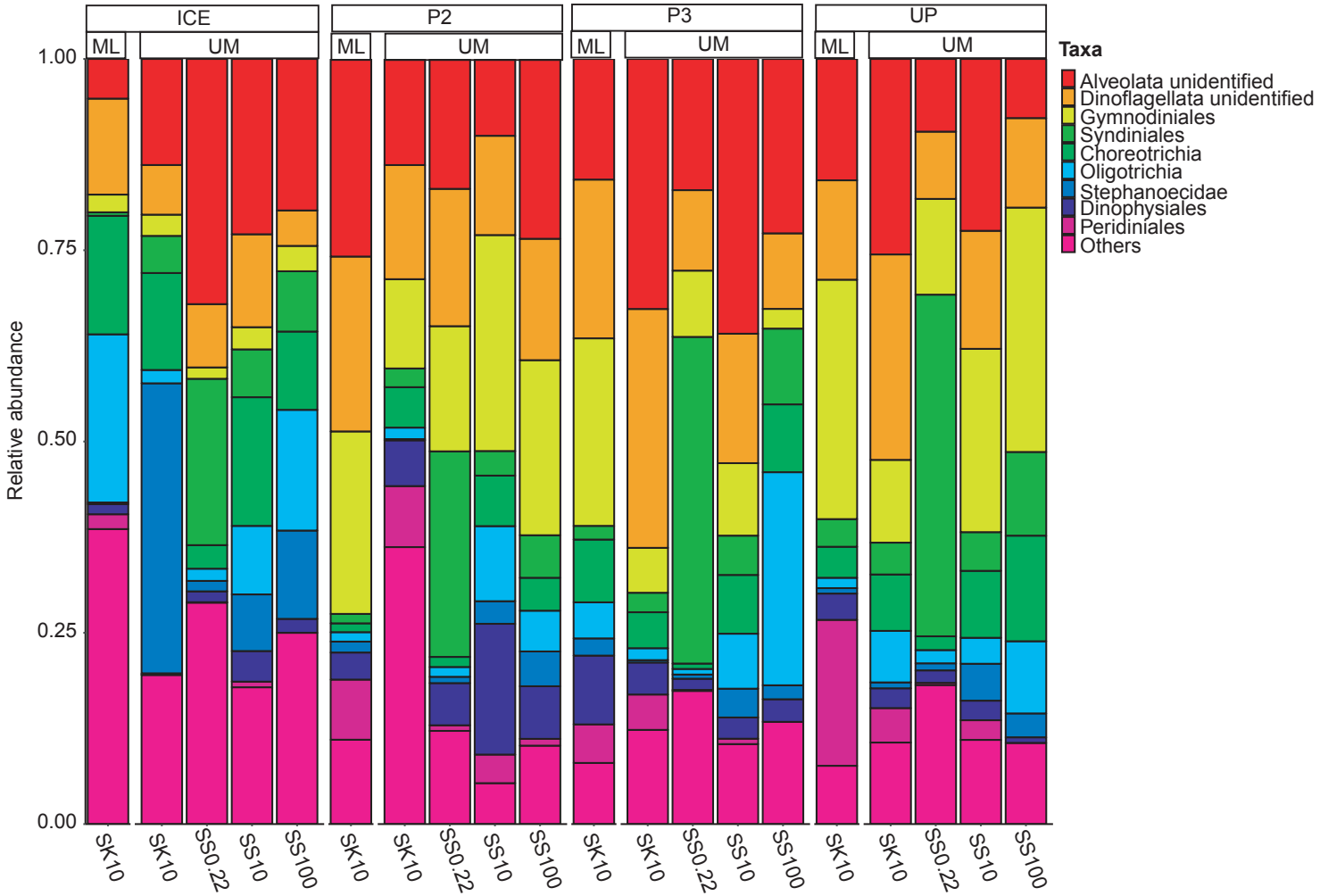
ICE
P2
P3
UP
ML
UM
Relative abundance
1.00
0.75
0.50
0.25
0.00
SK10
SS0.22
SS10
SS100
Taxa
Alveolata unidentified
Dinoflagellata unidentified
Gymnodiniales
Syndiniales
Choreotrichia
Oligotrichia
Stephanoecidae
Dinophysiales
Peridiniales
Others

Annex B5. Dissimilarity values from similarity percentages analyses of hetero/mixotrophic protist community. Dissimilarity between particle-types in the upper-mesopelagic were calculated on rarefied dataset based on results from a SIMPER analyses.

ICE

	SK10	SS100	SS10	SS0.22
SK10		95.7%	89.3%	88.9%
SS100			44.0%	53.5%
SS10				54.8%
SS0.22				

P2

	SK10	SS100	SS10	SS0.22
SK10		52.2%	57.1%	63.4%
SS100			37.5%	49.9%
SS10				56.2%
SS0.22				

P3

	SK10	SS100	SS10	SS0.22
SK10		62.9%	43.5%	62.6%
SS100			52.7%	64.5%
SS10				57.5%
SS0.22				

UP

	SK10	SS100	SS10	SS0.22
SK10		56.6%	34.9%	63.3%
SS100			41.5%	62.3%
SS10				59.8%
SS0.22				

Annex B6. Proportions of shared/unique hetero/mixotrophic protist OTU and affiliated sequences. The proportions of shared/unique OTU were calculated on the rarefied dataset. The "shared" values correspond to the proportion of OTU shared among all particle types in the upper-mesopelagic and to the proportion of affiliated sequences within every particle-type.

	ICE		P2		P3		UP	
	% OTU	% sequence	% OTU	% sequence	% OTU	% sequence	% OTU	% sequence
unique SK10	50.8	7.0	39.3	5.2	37.9	9.6	35.3	3.6
unique SS100	20.0	0.8	20.3	0.9	25.9	2.8	44.2	2.9
unique SS10	34.5	2.9	35.1	1.6	28.3	2.7	23.7	1.0
unique SS0.22	61.1	8.0	58.4	11.8	62.8	17.4	60.3	12.6
shared SK10	4.6	78.9	7.1	88.2	5.2	72.4	6.8	79.4
shared SS100		43.8		88.4		66.3		90.1
shared SS10		40.0		90.9		73.3		85.7
shared SS0.22		26.6		64.5		42.3		69.5

Appendix C

Appendix C

Annex C1. Sequence counts tables. LSK = large sinking particles (≥ 10 µm); LSS = large suspended particles; SSK = small sinking particles (0.22 – 10 µm); SSS = small suspended particles.

Particle-type	Depth (m)	Raw read	mRNA reads	rRNA reads	RefSeq affiliated transcript	SEED affiliated transcript
LSK	28	1,310,288	478,252	832,036	103,597	23,359
LSK	70	1,312,640	571,708	740,932	96,496	36,505
LSK	128	1,329,885	918,948	410,937	125,886	32,232
LSK	500	1,198,780	1,092,376	106,404	202,158	70,329
LSS	28	1,470,365	661,192	809,173	166,096	35,572
LSS	70	1,318,730	580,436	738,294	136,410	50,660
LSS	128	1,041,002	575,328	465,674	101,746	26,187
LSS	500	1,540,115	1,007,426	532,689	156,073	49,943
SSK	28	1,200,296	177,588	1,022,708	108,788	54,391
SSK	70	1,256,006	165,266	1,090,740	119,407	61,980
SSK	128	1,843,755	302,140	1,541,615	155,610	83,715
SSK	500	1,655,612	232,190	1,423,422	139,863	76,595
SSS	28	1,220,403	240,858	979,545	128,381	60,629
SSS	70	1,399,629	345,578	1,054,051	174,826	87,944
SSS	128	1,608,462	1,075,224	533,238	490,299	226,409
SSS	500	1,465,853	1,248,740	217,113	659,520	314,437

Annex C2. Dissimilarity values from similarity percentages analyses. Dissimilarity between particle-types were calculated on rarefied dataset based on results from a SIMPER analyses using taxonomic affiliations from Refseq (A) and functional annotations from SEED (B).

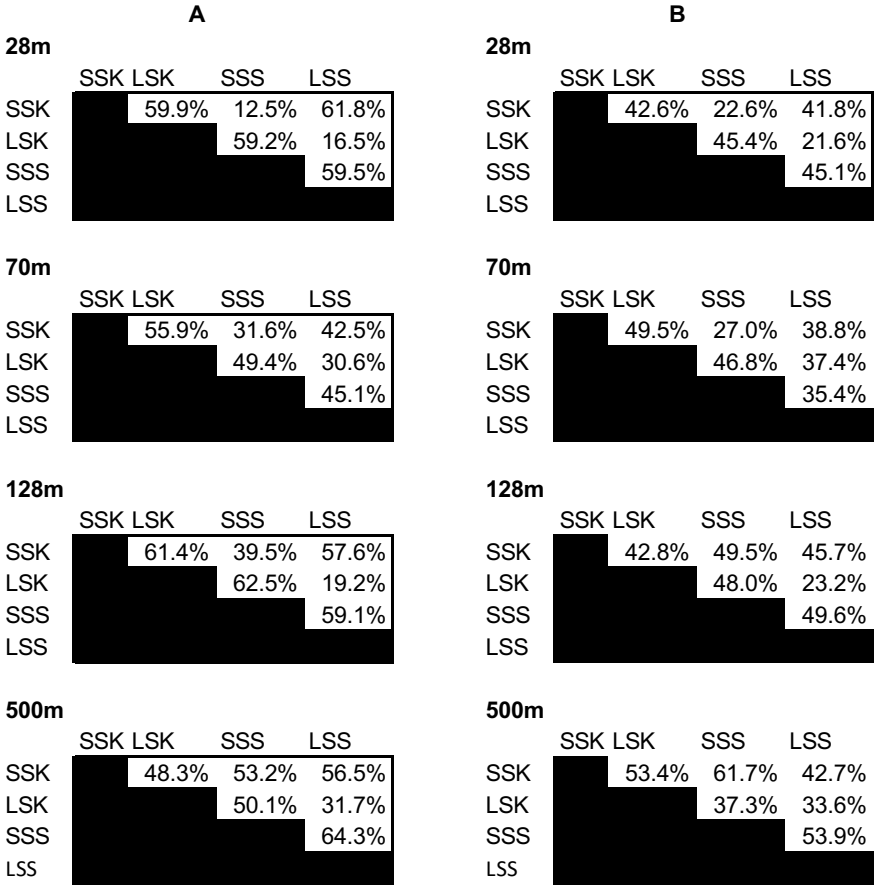

Annex C3. Permutational multivariate analysis of variance of environmental parameters. Table A displays the PERMANOVA results for sample collection-related factors (including particle-size and particle-type) based on taxonomic affiliations from Refseq. Table B displays PERMANOVA results for sample collection-related factors (a) and for environmental parameters (b) based on functional annotations from SEED. Factors highlighted with an asterisk (*) were significantly affecting the transcript composition variability. SS: sums of squares; MS: means of squares; F.Model: F-tests results; R2: effect size; Pr: p-value.

A - RefSeq						
	Df	**SumsO**	**MeanSqs**	**F.Model**	**R2**	**Pr(>F)**
Size*	1	0.824	0.824	12.651	47%	0.001
Type	1	0.097	0.097	1.483	5%	0.201
Residuals	*13*	*0.847*	*0.065*	*NA*	*48%*	*NA*
Total	*15*	*1.767*	*NA*	*NA*	*100%*	*NA*

B - SEED						
	Df	**SumsO**	**MeanSqs**	**F.Model**	**R2**	**Pr(>F)**
Size*	1	0.354	0.354	5.321	27%	0.001
Type	1	0.114	0.114	1.715	9%	0.11
Residuals	*13*	*0.866*	*0.067*	*NA*	*65%*	*NA*
Total	*15*	*1.335*	*NA*	*NA*	*100%*	*NA*

Annex C4. Proportions of shared/unique transcripts. The proportions of shared/unique transcripts were calculated on the rarefied dataset. Table A displays the proportion of shared and unique transcripts based on the family level of taxonomic affiliations from Refseq. Table B displays the shared and unique transcripts based on functional annotations from SEED. LSK = large sinking particles (≥ 10 µm); LSS = large suspended particles; SSK = small sinking particles (0.22 – 10 µm); SSS = small suspended particles.

A

		28 m	70 m	128 m	500 m
% unique transcripts	**SSK**	3.6	3.2	3.8	3.6
	LSK	3.6	7.9	9.1	6.2
	SSS	3.2	2.0	1.9	2.2
	LSS	4.2	5.6	7.1	6.3
% unique sequences	**SSK**	0.03	0.02	0.04	0.03
	LSK	0.07	0.06	0.11	0.05
	SSS	0.02	0.02	0.02	0.01
	LSS	0.03	0.05	0.07	0.09

% shared transcripts

28 m	LSS	SSS	LSK	SSK	All
LSS		81.9	82.0	82.0	70.2
SSS			80.2	86.7	
LSK				80.6	
SSK					

70 m	LSS	SSS	LSK	SSK	All
LSS		83.7	79.5	80.5	69.2
SSS			82.3	83.4	
LSK				80.2	
SSK					

128 m	LSS	SSS	LSK	SSK	All
LSS		83.9	79.9	80.3	69.0
SSS			82.0	86.2	
LSK				77.5	
SSK					

500 m	LSS	SSS	LSK	SSK	All
LSS		82.0	84.3	80.5	70.2
SSS			84.6	83.5	
LSK				81.1	
SSK					

B

		28 m	70 m	128 m	500 m
% unique transcripts	**SSK**	12.1	8.4	9.1	5.6
	LSK	14.4	17.4	13.8	14.6
	SSS	12.9	12.1	19.4	13.2
	LSS	26.5	20.4	19.4	20.4
% unique sequences	**SSK**	1.55	0.90	0.97	0.52
	LSK	1.80	2.73	2.13	3.11
	SSS	1.79	1.55	4.12	2.41
	LSS	4.12	4.19	3.50	4.66

% shared transcripts

28 m	LSS	SSS	LSK	SSK	All
LSS		44.9	40.9	44.5	22.9
SSS			42.3	58.2	
LSK				42.9	
SSK					

70 m	LSS	SSS	LSK	SSK	All
LSS		49.3	51.1	45.0	24.6
SSS			47.4	48.7	
LSK				43.3	
SSK					

128 m	LSS	SSS	LSK	SSK	All
LSS		47.7	50.6	41.0	23.6
SSS			48.8	46.3	
LSK				43.2	
SSK					

500 m	LSS	SSS	LSK	SSK	All
LSS		46.7	54.9	38.3	23.3
SSS			55.6	42.3	
LSK				40.5	
SSK					

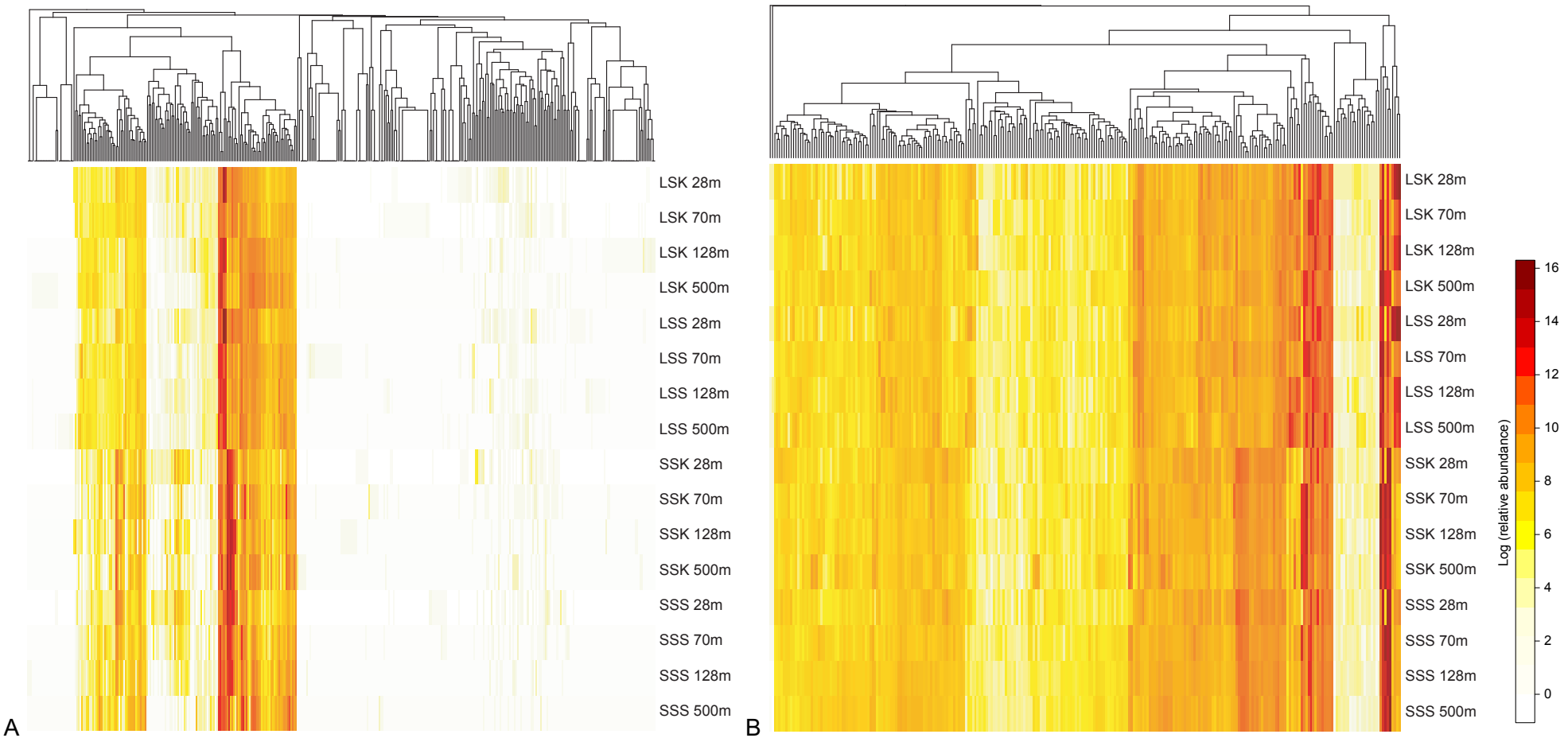

Annex C5. Heatmap of taxonomic family composition. The heatmap represents the log(relative abundance) of the rarefied dataset. Heatmap A displays transcripts affiliated with eukaryotic families and heatmap B affiliated with prokaryotic families based on taxonomic affiliations from Refseq. LSK = large sinking particles (≥ 10 µm); LSS = large suspended particles; SSK = small sinking particles (0.22 – 10 µm); SSS = small suspended particles.

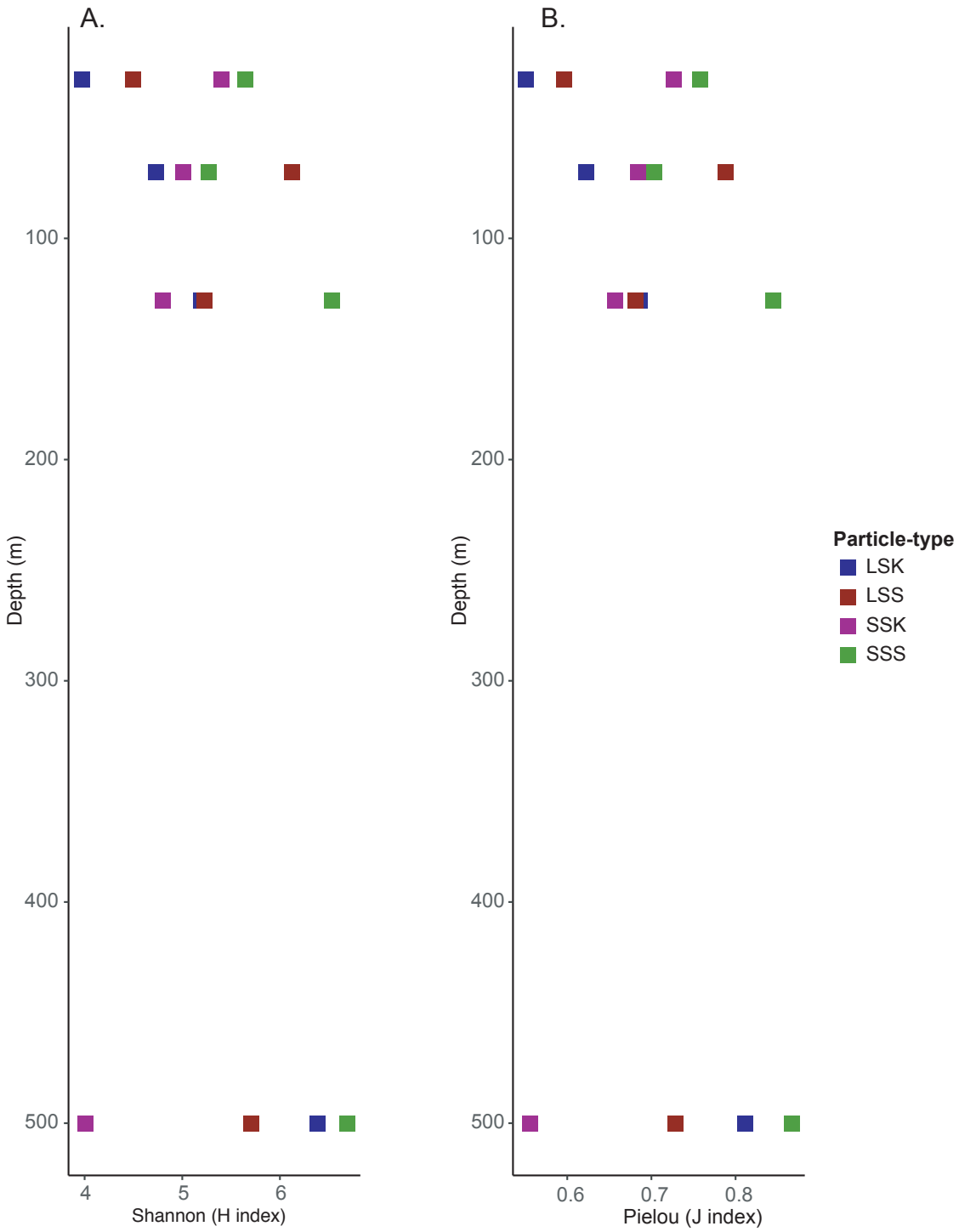

Annex C6. Alpha-diversity plots. Panel A shows Shannon's index and panel B Pielou's index. Indices were calculated on the rarefied dataset and are based functional annotations of transcripts with SEED.

Annex C7. Detailed table of the relative abundance for genes of interest (following pages). LSK = large sinking particles (≥ 10 µm); LSS = large suspended particles; SSK = small sinking particles (0.22 – 10 µm); SSS = small suspended particles.

Group	Function	LSK_28m	LSK_70m	LSK_128m
C catabolism	Lactose_and_Galactose_Uptake_and_Utilization	0.00032	0.00153	0.00116
	Maltose_and_Maltodextrin_Utilization	0.00042	0.00116	0.00159
	Beta-Glucoside_Metabolism	0.00011	0.00048	0.00042
	Fructooligosaccharides(FOS)_and_Raffinose_Utilization	0.00011	0.00032	0.00016
	Trehalose_Biosynthesis	0.00016	0.00021	0.00079
	Sucrose_utilization	0.00000	0.00000	0.00011
	Trehalose_Uptake_and_Utilization	0.00000	0.00016	0.00000
	Sucrose_utilization_Shewanella	0.00000	0.00000	0.00000
	Lactose_utilization	0.00000	0.00000	0.00005
	Fermentations:_Mixed_acid	0.00053	0.00101	0.00116
	Acetone_Butanol_Ethanol_Synthesis	0.00101	0.00101	0.00153
	Acetoin,_butanediol_metabolism	0.00021	0.00053	0.00021
	Acetyl-CoA_fermentation_to_Butyrate	0.00000	0.00026	0.00011
	Fermentations:_Lactate	0.00011	0.00011	0.00016
	Butanol_Biosynthesis	0.00000	0.00000	0.00000
	Chitin_and_N-acetylglucosamine_utilization	0.00058	0.00085	0.00111
	(GlcNAc)2_Catabolic_Operon	0.00011	0.00011	0.00005
	N-Acetyl-Galactosamine_and_Galactosamine_Utilization	0.00000	0.00000	0.00000
	Glycogen_metabolism	0.00011	0.00053	0.00042
	Cellulosome	0.00042	0.00011	0.00085
	Alpha-Amylase_locus_in_Streptocococcus	0.00000	0.00000	0.00005
	Unknown_carbohydrate_utilization_containing_Fructose-bisphosphate_aldolase	0.00000	0.00000	0.00000
	Deoxyribose_and_Deoxynucleoside_Catabolism	0.00069	0.00085	0.00164
	Mannose_Metabolism	0.00026	0.00026	0.00095
	L-rhamnose_utilization	0.00005	0.00026	0.00021
	D-Galacturonate_and_D-Glucuronate_Utilization	0.00042	0.00053	0.00048
	D-gluconate_and_ketogluconates_metabolism	0.00021	0.00058	0.00042
	D-ribose_utilization	0.00000	0.00032	0.00000
	D-galactarate,_D-glucarate_and_D-glycerate_catabolism	0.00005	0.00000	0.00021
	L-fucose_utilization_temp	0.00005	0.00032	0.00000
	Xylose_utilization	0.00000	0.00000	0.00005
	Fructose_utilization	0.00000	0.00016	0.00005
	L-fucose_utilization	0.00005	0.00005	0.00000
	L-Arabinose_utilization	0.00000	0.00005	0.00000
	D-galactonate_catabolism	0.00000	0.00011	0.00000
	D-Sorbitol(D-Glucitol)_and_L-Sorbose_Utilization	0.00000	0.00000	0.00000
	L-ascorbate_utilization_(and_related_gene_clusters)	0.00000	0.00021	0.00000
	D-Tagatose_and_Galactitol_Utilization	0.00000	0.00021	0.00005
	2-Ketogluconate_Utilization	0.00000	0.00000	0.00000
	Glyoxylate_bypass	0.00291	0.00296	0.00307
	Pyruvate_metabolism_II:_acetyl-CoA,_acetogenesis_from_pyruvate	0.00116	0.00217	0.00365
	Pyruvate_metabolism_I:_anaplerotic_reactions,_PEP	0.00127	0.00201	0.00265
	Dehydrogenase_complexes	0.00148	0.00275	0.00349
	Glycolysis_and_Gluconeogenesis	0.00243	0.00201	0.00328
	Entner-Doudoroff_Pathway	0.00143	0.00227	0.00212
	Isocitrate dehydrogenase	0.00058	0.00106	0.00153
	Glycolysis_and_Gluconeogenesis,_including_Archaeal_enzymes	0.00132	0.00063	0.00042
	Pentose_phosphate_pathway	0.00058	0.00095	0.00063
	Fumarate hydratase	0.00032	0.00079	0.00101
	Malate dehydrogenase	0.00026	0.00016	0.00090
	2-oxoglutarate dehydrogenase	0.00048	0.00042	0.00079
	Pyruvate_Alanine_Serine_Interconversions	0.00011	0.00021	0.00005
	Glycolate,_glyoxylate_interconversions	0.00000	0.00021	0.00011
	Methylglyoxal_Metabolism	0.00000	0.00016	0.00005
	Ethylmalonyl-CoA_pathway_of_C2_assimilation	0.00000	0.00011	0.00021
	Pyruvate:ferredoxin_oxidoreductase	0.00000	0.00000	0.00000
	Succinyl-CoA ligase	0.00011	0.00000	0.00005
	Dihydroxyacetone_kinases	0.00000	0.00005	0.00011
	Peripheral_Glucose_Catabolism_Pathways	0.00000	0.00000	0.00000
	Aconitate hydratase	0.00000	0.00000	0.00000
	Serine-glyoxylate_cycle	0.00386	0.00587	0.00587
	One-carbon_metabolism_by_tetrahydropterines	0.00016	0.00005	0.00021
	Methanogenesis	0.00000	0.00000	0.00000
	Formaldehyde_assimilation:_Ribulose_monophosphate_pathway	0.00000	0.00016	0.00000
	Methanogenesis_from_methylated_compounds	0.00000	0.00000	0.00000
	Propionate-CoA_to_Succinate_Module	0.00074	0.00148	0.00143
	Propionyl-CoA_to_Succinyl-CoA_Module	0.00032	0.00069	0.00190
	Methylcitrate_cycle	0.00000	0.00005	0.00011
	Lactate_utilization	0.00005	0.00021	0.00011
	Glycerate_metabolism	0.00000	0.00021	0.00011
	2-methylcitrate_to_2-methylaconitate_metabolism_cluster	0.00000	0.00005	0.00000
	Isobutyryl-CoA_to_Propionyl-CoA_Module	0.00000	0.00011	0.00000
	Malonate_decarboxylase	0.00000	0.00000	0.00000
	Tricarballylate_Utilization	0.00000	0.00000	0.00000
	Alpha-acetolactate_operon	0.00000	0.00000	0.00000
	Glycerol_and_Glycerol-3-phosphate_Uptake_and_Utilization	0.00021	0.00111	0.00063
	Inositol_catabolism	0.00016	0.00026	0.00021
	Mannitol_Utilization	0.00016	0.00011	0.00021
	Propanediol_utilization	0.00000	0.00000	0.00011
	Ethanolamine_utilization	0.00000	0.00016	0.00005
	Erythritol_utilization	0.00005	0.00000	0.00000
	Glycerol_fermenation_to_1,3-propanediol	0.00000	0.00000	0.00000
	Protocatechuate_branch_of_beta-ketoadipate_pathway	0.00005	0.00011	0.00074
	Homogentisate_pathway_of_aromatic_compound_degradation	0.00021	0.00048	0.00042
	Catechol_branch_of_beta-ketoadipate_pathway	0.00000	0.00016	0.00026
	Central_meta-cleavage_pathway_of_aromatic_compound_degradation	0.00005	0.00016	0.00000
	N-heterocyclic_aromatic_compound_degradation	0.00000	0.00005	0.00005
	4-Hydroxyphenylacetic_acid_catabolic_pathway	0.00000	0.00026	0.00000
	Salicylate_and_gentisate_catabolism	0.00000	0.00000	0.00005
	p-cymene_degradation	0.00000	0.00000	0.00000
	n-Phenylalkanoic_acid_degradation	0.00090	0.00116	0.00116
	Biphenyl_Degradation	0.00000	0.00032	0.00032
	Phenylpropanoid_compound_degradation	0.00005	0.00011	0.00005
	Quinate_degradation	0.00000	0.00000	0.00000
	Benzoate_catabolism	0.00005	0.00000	0.00000
	Benzoate_degradation	0.00000	0.00032	0.00000
	Naphtalene_and_antracene_degradation	0.00000	0.00016	0.00000
	p-Hydroxybenzoate_degradation	0.00000	0.00000	0.00011
	Salicylate_ester_degradation	0.00000	0.00005	0.00011
	Chloroaromatic_degradation_pathway	0.00011	0.00000	0.00005
	Phenol_hydroxylase	0.00000	0.00000	0.00000
	Toluene_degradation	0.00000	0.00000	0.00000
	Anaerobic_benzoate_metabolism	0.00164	0.00132	0.00259
	Anaerobic_toluene_and_ethylbenzene_degradation	0.00000	0.00000	0.00000

Appendix C

Group	Function	SSK_28m	SSK_70m	SSK_128m
C catabolsm	Lactose_and_Galactose_Uptake_and_Utilization	0.00090	0.00026	0.00042
	Maltose_and_Maltodextrin_Utilization	0.00037	0.00011	0.00032
	Beta-Glucoside_Metabolism	0.00048	0.00011	0.00016
	Fructooligosaccharides(FOS)_and_Raffinose_Utilization	0.00026	0.00026	0.00032
	Trehalose_Biosynthesis	0.00011	0.00000	0.00005
	Sucrose_utilization	0.00000	0.00032	0.00005
	Trehalose_Uptake_and_Utilization	0.00000	0.00016	0.00005
	Sucrose_utilization_Shewanella	0.00000	0.00016	0.00000
	Lactose_utilization	0.00000	0.00000	0.00000
	Fermentations:_Mixed_acid	0.00111	0.00106	0.00058
	Acetone_Butanol_Ethanol_Synthesis	0.00106	0.00090	0.00058
	Acetoin,_butanediol_metabolism	0.00074	0.00069	0.00042
	Acetyl-CoA_fermentation_to_Butyrate	0.00026	0.00053	0.00053
	Fermentations:_Lactate	0.00000	0.00000	0.00000
	Butanol_Biosynthesis	0.00000	0.00000	0.00000
	Chitin_and_N-acetylglucosamine_utilization	0.00048	0.00026	0.00005
	(GlcNAc)2_Catabolic_Operon	0.00000	0.00016	0.00000
	N-Acetyl-Galactosamine_and_Galactosamine_Utilization	0.00000	0.00000	0.00000
	Glycogen_metabolism	0.00042	0.00016	0.00000
	Cellulosome	0.00005	0.00021	0.00016
	Alpha-Amylase_locus_in_Streptocococcus	0.00000	0.00005	0.00000
	Unknown_carbohydrate_utilization_containing_Fructose-bisphosphate_aldolase	0.00000	0.00000	0.00000
	Deoxyribose_and_Deoxynucleoside_Catabolism	0.00079	0.00053	0.00058
	Mannose_Metabolism	0.00079	0.00042	0.00026
	L-rhamnose_utilization	0.00201	0.00042	0.00042
	D-Galacturonate_and_D-Glucuronate_Utilization	0.00074	0.00032	0.00016
	D-gluconate_and_ketogluconates_metabolism	0.00016	0.00032	0.00042
	D-ribose_utilization	0.00032	0.00000	0.00026
	D-galactarate,_D-glucarate_and_D-glycerate_catabolism	0.00063	0.00011	0.00000
	L-fucose_utilization_temp	0.00021	0.00005	0.00005
	Xylose_utilization	0.00016	0.00005	0.00000
	Fructose_utilization	0.00021	0.00011	0.00011
	L-fucose_utilization	0.00032	0.00005	0.00016
	L-Arabinose_utilization	0.00016	0.00011	0.00005
	D-galactonate_catabolism	0.00000	0.00000	0.00000
	D-Sorbitol(D-Glucitol)_and_L-Sorbose_Utilization	0.00011	0.00005	0.00011
	Hexose_Phosphate_Uptake_System	0.00000	0.00000	0.00000
	L-ascorbate_utilization_(and_related_gene_clusters)	0.00000	0.00000	0.00000
	D-Tagatose_and_Galactitol_Utilization	0.00000	0.00000	0.00000
	2-Ketogluconate_Utilization	0.00000	0.00000	0.00000
	Glyoxylate_bypass	0.00360	0.01635	0.00397
	Pyruvate_metabolism_II:_acetyl-CoA,_acetogenesis_from_pyruvate	0.00423	0.00175	0.00164
	Pyruvate_metabolism_I:_anaplerotic_reactions,_PEP	0.00391	0.00397	0.00217
	Dehydrogenase_complexes	0.00413	0.00190	0.00217
	Glycolysis_and_Gluconeogenesis	0.00222	0.00138	0.00132
	Entner-Doudoroff_Pathway	0.00159	0.00026	0.00058
	Isocitrate dehydrogenase	0.00132	0.00111	0.00053
	Glycolysis_and_Gluconeogenesis,_including_Archaeal_enzymes	0.00106	0.00063	0.00058
	Pentose_phosphate_pathway	0.00085	0.00074	0.00037
	Fumarate hydratase	0.00069	0.00074	0.00032
	Malate dehydrogenase	0.00058	0.00148	0.00053
	2-oxoglutarate dehydrogenase	0.00074	0.00127	0.00042
	Pyruvate_Alanine_Serine_Interconversions	0.00037	0.00048	0.00085
	Glycolate,_glyoxylate_interconversions	0.00037	0.00011	0.00000
	Methylglyoxal_Metabolism	0.00026	0.00026	0.00011
	Ethylmalonyl-CoA_pathway_of_C2_assimilation	0.00037	0.00000	0.00005
	Pyruvate:ferredoxin_oxidoreductase	0.00000	0.00048	0.00005
	Succinyl-CoA ligase	0.00000	0.00016	0.00000
	Dihydroxyacetone_kinases	0.00000	0.00000	0.00000
	Peripheral_Glucose_Catabolism_Pathways	0.00000	0.00005	0.00005
	Aconitate hydratase	0.00000	0.00000	0.00000
	Serine-glyoxylate_cycle	0.00973	0.00550	0.00492
	One-carbon_metabolism_by_tetrahydropterines	0.00026	0.00021	0.00016
	Methanogenesis	0.00011	0.00005	0.00000
	Formaldehyde_assimilation:_Ribulose_monophosphate_pathway	0.00000	0.00005	0.00011
	Methanogenesis_from_methylated_compounds	0.00005	0.00000	0.00000
	Propionate-CoA_to_Succinate_Module	0.00169	0.00196	0.00079
	Propionyl-CoA_to_Succinyl-CoA_Module	0.00079	0.00021	0.00005
	Methylcitrate_cycle	0.00042	0.00005	0.00005
	Lactate_utilization	0.00000	0.00011	0.00005
	Glycerate_metabolism	0.00011	0.00000	0.00000
	2-methylcitrate_to_2-methylaconitate_metabolism_cluster	0.00011	0.00000	0.00000
	Isobutyryl-CoA_to_Propionyl-CoA_Module	0.00005	0.00000	0.00000
	Malonate_decarboxylase	0.00005	0.00000	0.00005
	Tricarballylate_Utilization	0.00000	0.00000	0.00000
	Alpha-acetolactate_operon	0.00000	0.00000	0.00000
	Glycerol_and_Glycerol-3-phosphate_Uptake_and_Utilization	0.00095	0.00085	0.00063
	Inositol_catabolism	0.00074	0.00021	0.00026
	Mannitol_Utilization	0.00011	0.00037	0.00011
	Propanediol_utilization	0.00005	0.00000	0.00005
	Ethanolamine_utilization	0.00000	0.00000	0.00005
	Erythritol_utilization	0.00000	0.00005	0.00000
	Glycerol_fermenation_to_1,3-propanediol	0.00000	0.00000	0.00000
	Protocatechuate_branch_of_beta-ketoadipate_pathway	0.00021	0.00026	0.00021
	Homogentisate_pathway_of_aromatic_compound_degradation	0.00005	0.00011	0.00011
	Catechol_branch_of_beta-ketoadipate_pathway	0.00016	0.00005	0.00016
	Central_meta-cleavage_pathway_of_aromatic_compound_degradation	0.00005	0.00005	0.00000
	N-heterocyclic_aromatic_compound_degradation	0.00011	0.00011	0.00000
	4-Hydroxyphenylacetic_acid_catabolic_pathway	0.00005	0.00000	0.00005
	Salicylate_and_gentisate_catabolism	0.00000	0.00000	0.00000
	p-cymene_degradation	0.00000	0.00000	0.00000
	n-Phenylalkanoic_acid_degradation	0.00122	0.00058	0.00079
	Biphenyl_Degradation	0.00011	0.00000	0.00011
	Phenylpropanoid_compound_degradation	0.00000	0.00000	0.00011
	Quinate_degradation	0.00032	0.00005	0.00000
	Benzoate_catabolism	0.00005	0.00000	0.00000
	Benzoate_degradation	0.00000	0.00005	0.00005
	Naphtalene_and_antracene_degradation	0.00005	0.00005	0.00000
	p-Hydroxybenzoate_degradation	0.00011	0.00005	0.00000
	Salicylate_ester_degradation	0.00005	0.00000	0.00000
	Chloroaromatic_degradation_pathway	0.00000	0.00000	0.00000
	Phenol_hydroxylase	0.00000	0.00000	0.00000
	Toluene_degradation	0.00000	0.00000	0.00000
	Anaerobic_benzoate_metabolism	0.00212	0.00085	0.00085
	Anaerobic_toluene_and_ethylbenzene_degradation	0.00011	0.00000	0.00000

Group	Function	LSK_28m	LSK_70m	LSK_128m
Respiration	F0F1-type_ATP_synthase	0.01201	0.00720	0.00778
	V-Type_ATP_synthase	0.00037	0.00042	0.00037
	Biogenesis_of_cbb3-type_cytochrome_c_oxidases	0.00005	0.00011	0.00000
	Biogenesis_of_c-type_cytochromes	0.00148	0.00111	0.00116
	Biogenesis_of_cytochrome_c_oxidases	0.00016	0.00074	0.00058
	Cytochrome_B6-F_complex	0.00175	0.00069	0.00021
N uptake	Ammonia_assimilation	0.00206	0.00349	0.00323
	nitrate_transporter	0.00000	0.00021	0.00026
	Urea ABC transporter, urea binding protein	0.00011	0.00005	0.00000
	Urea ABC transporter, ATPase protein UrtD	0.00016	0.00000	0.00011
	Urea ABC transporter, permease protein UrtC	0.00011	0.00011	0.00016
	Urea ABC transporter, permease protein UrtB	0.00011	0.00011	0.00005
	Urea ABC transporter, ATPase protein UrtE	0.00000	0.00000	0.00005
	Urea carboxylase-related ABC transporter, ATPase protein	0.00005	0.00005	0.00000
	Eukaryotic-type low-affinity urea transporter	0.00000	0.00000	0.00000
	Urea carboxylase-related ABC transporter, periplasmic substrate-binding protein	0.00000	0.00000	0.00000
	Urea carboxylase-related ABC transporter, permease protein	0.00000	0.00000	0.00000
	Urea channel UreI	0.00000	0.00000	0.00000
	Glutamate_and_Aspartate_uptake_in_Bacteria	0.00005	0.00011	0.00032
	ABC_transporter_branched-chain_amino_acid(TC_3.A.1.4.1)	0.00016	0.00058	0.00042
	ABC_transporter_oligopeptide(TC_3.A.1.5.1)	0.00011	0.00048	0.00069
	ABC_transporter_dipeptide(TC_3.A.1.5.2)	0.00005	0.00026	0.00122
	ABC_transporter_peptide(TC_3.A.1.5.5)	0.00011	0.00000	0.00011
	Nitrogenase	0.00000	0.00011	0.00000
Nitrification	Ammonia monooxygenase	0.00000	0.00000	0.00005
Ntrate reduction	nitrate_reductase	0.00011	0.00042	0.00005
Denitrification	nitrite_reductase	0.00000	0.00000	0.00005
	nitric_oxide_reductase	0.00000	0.00011	0.00011
	nitrous_oxide_reductase	0.00005	0.00005	0.00000
DNRA	nitrite_reductase	0.00021	0.00021	0.00069
S reduction	Sulfite reductase, dissimilatory-type gamma subunit (EC 1.8.99.3)	0.00000	0.00000	0.00000
	Sulfite reductase alpha subunit (EC 1.8.99.1)	0.00000	0.00000	0.00000
	DMSP_breakdown	0.00021	0.00000	0.00005
	Anaerobic dimethyl sulfoxide reductase chain B (EC 1.8.99.-)	0.00000	0.00005	0.00000
	Anaerobic dimethyl sulfoxide reductase chain C (EC 1.8.99.-)	0.00000	0.00000	0.00005
	Sulfite reductase beta subunit (EC 1.8.99.1)	0.00000	0.00000	0.00000
	Sulfite reduction-associated complex DsrMKJOP protein DsrK (=HmeD)	0.00000	0.00000	0.00000
	Sulfite reduction-associated complex DsrMKJOP iron-sulfur protein DsrO (=HmeA)	0.00000	0.00000	0.00000
	Sulfite reduction-associated complex DsrMKJOP protein DsrM (= HmeC)	0.00000	0.00000	0.00000
	Adenylylsulfate reductase beta-subunit (EC 1.8.99.2)	0.00000	0.00000	0.00000
CBB	Transketolase (EC 2.2.1.1)	0.00048	0.00079	0.00037
	Transketolase, C-terminal section (EC 2.2.1.1)	0.00032	0.00011	0.00048
	Transketolase, N-terminal section (EC 2.2.1.1)	0.00005	0.00011	0.00053
	NAD-dependent glyceraldehyde-3-phosphate dehydrogenase (EC 1.2.1.12)	0.00058	0.00058	0.00095
	NADPH-dependent glyceraldehyde-3-phosphate dehydrogenase (EC 1.2.1.13)	0.00011	0.00005	0.00026
	NAD(P)-dependent glyceraldehyde 3-phosphate dehydrogenase archaeal (EC 1.2.1.59)	0.00000	0.00000	0.00000
	Fructose-1,6-bisphosphatase, type I (EC 3.1.3.11)	0.00032	0.00063	0.00032
	Fructose-1,6-bisphosphatase, GlpX type (EC 3.1.3.11)	0.00000	0.00000	0.00011
	Fructose-1,6-bisphosphatase, type V, archaeal (EC 3.1.3.11)	0.00000	0.00000	0.00000
	Fructose-1,6-bisphosphatase, Bacillus type (EC 3.1.3.11)	0.00000	0.00000	0.00000
rTCA	fumarate reductase/succinate dehydrogenase flavoprotein, N-terminal:FAD dependent oxidoreductase	0.00011	0.00000	0.00000
	Fumarate reductase subunit C	0.00000	0.00000	0.00000
	Fumarate reductase flavoprotein subunit (EC 1.3.99.1)	0.00000	0.00000	0.00000
	Fumarate and nitrate reduction regulatory protein	0.00000	0.00000	0.00000
	2-oxoglutarate dehydrogenase E1 component (EC 1.2.4.2)	0.00063	0.00106	0.00106
	Dihydrolipoamide succinyltransferase component (E2) of 2-oxoglutarate dehydrogenase complex (EC 2.3.1.61)	0.00048	0.00042	0.00079
	Dihydrolipoamide dehydrogenase of 2-oxoglutarate dehydrogenase (EC 1.8.1.4)	0.00037	0.00042	0.00063
HP/HB	Propionyl-CoA carboxylase carboxyl transferase subunit (EC 6.4.1.3)	0.00005	0.00005	0.00016
	Propionyl-CoA carboxylase biotin-containing subunit (EC 6.4.1.3)	0.00000	0.00000	0.00005
	Propionyl-CoA carboxylase beta chain (EC 6.4.1.3)	0.00000	0.00005	0.00000
W-L	Carbon-monoxide dehydrogenase form II, large subunit (EC 1.2.99.2)	0.00000	0.00000	0.00000
	CO dehydrogenases maturation factor, CoxF family	0.00000	0.00000	0.00000
	carbon monoxide dehydrogenase operon C protein	0.00000	0.00000	0.00000

Appendix C

Group	Function	SSK_28m	SSK_70m	SSK_128m
Respiration	F0F1-type_ATP_synthase	0.01153	0.01725	0.01212
	V-Type_ATP_synthase	0.00021	0.00011	0.00042
	Biogenesis_of_cbb3-type_cytochrome_c_oxidases	0.00005	0.00005	0.00016
	Biogenesis_of_c-type_cytochromes	0.00132	0.00085	0.00032
	Biogenesis_of_cytochrome_c_oxidases	0.00048	0.00016	0.00005
	Cytochrome_B6-F_complex	0.00042	0.00026	0.00016
N uptake	Ammonia_assimilation	0.00831	0.02116	0.02598
	nitrate_transporter	0.00005	0.00005	0.00000
	Urea ABC transporter, urea binding protein	0.00005	0.00021	0.00005
	Urea ABC transporter, ATPase protein UrtD	0.00005	0.00016	0.00000
	Urea ABC transporter, permease protein UrtC	0.00000	0.00000	0.00000
	Urea ABC transporter, permease protein UrtB	0.00000	0.00000	0.00000
	Urea ABC transporter, ATPase protein UrtE	0.00000	0.00000	0.00000
	Urea carboxylase-related ABC transporter, ATPase protein	0.00000	0.00000	0.00000
	Eukaryotic-type low-affinity urea transporter	0.00000	0.00000	0.00000
	Urea carboxylase-related ABC transporter, periplasmic substrate-binding protein	0.00000	0.00000	0.00000
	Urea carboxylase-related ABC transporter, permease protein	0.00000	0.00000	0.00000
	Urea channel UreI	0.00000	0.00000	0.00000
	Glutamate_and_Aspartate_uptake_in_Bacteria	0.00011	0.00011	0.00000
	ABC_transporter_branched-chain_amino_acid(TC_3.A.1.4.1)	0.00354	0.00106	0.00159
	ABC_transporter_oligopeptide(TC_3.A.1.5.1)	0.00058	0.00042	0.00026
	ABC_transporter_dipeptide(TC_3.A.1.5.2)	0.00048	0.00000	0.00016
	ABC_transporter_peptide(TC_3.A.1.5.5)	0.00000	0.00005	0.00005
	Nitrogenase	0.00000	0.00000	0.00000
Nitrification	Ammonia monooxygenase	0.00000	0.00206	0.00138
Nitrate reduction	nitrate_reductase	0.00000	0.00037	0.00090
Denitrification	nitrite_reductase	0.00000	0.01132	0.00376
	nitric_oxide_reductase	0.00005	0.00000	0.00000
	nitrous_oxide_reductase	0.00000	0.00000	0.00000
DNRA	nitrite_reductase	0.00005	0.00000	0.00026
S reduction	Sulfite reductase, dissimilatory-type gamma subunit (EC 1.8.99.3)	0.00000	0.00000	0.00000
	Sulfite reductase alpha subunit (EC 1.8.99.1)	0.00005	0.00000	0.00000
	DMSP_breakdown	0.00106	0.00016	0.00016
	Anaerobic dimethyl sulfoxide reductase chain B (EC 1.8.99.-)	0.00005	0.00000	0.00000
	Anaerobic dimethyl sulfoxide reductase chain C (EC 1.8.99.-)	0.00000	0.00000	0.00000
	Sulfite reductase beta subunit (EC 1.8.99.1)	0.00000	0.00000	0.00000
	Sulfite reduction-associated complex DsrMKJOP protein DsrK (=HmeD)	0.00000	0.00000	0.00000
	Sulfite reduction-associated complex DsrMKJOP iron-sulfur protein DsrO (=HmeA)	0.00000	0.00000	0.00000
	Sulfite reduction-associated complex DsrMKJOP protein DsrM (= HmeC)	0.00000	0.00000	0.00000
	Adenylylsulfate reductase beta-subunit (EC 1.8.99.2)	0.00005	0.00000	0.00005
CBB	Transketolase (EC 2.2.1.1)	0.00053	0.00058	0.00021
	Transketolase, C-terminal section (EC 2.2.1.1)	0.00021	0.00000	0.00016
	Transketolase, N-terminal section (EC 2.2.1.1)	0.00005	0.00000	0.00005
	NAD-dependent glyceraldehyde-3-phosphate dehydrogenase (EC 1.2.1.12)	0.00063	0.00063	0.00026
	NADPH-dependent glyceraldehyde-3-phosphate dehydrogenase (EC 1.2.1.13)	0.00026	0.00032	0.00048
	NAD(P)-dependent glyceraldehyde 3-phosphate dehydrogenase archaeal (EC 1.2.1.59)	0.00005	0.00000	0.00000
	Fructose-1,6-bisphosphatase, type I (EC 3.1.3.11)	0.00011	0.00026	0.00005
	Fructose-1,6-bisphosphatase, GlpX type (EC 3.1.3.11)	0.00021	0.00000	0.00000
	Fructose-1,6-bisphosphatase, type V, archaeal (EC 3.1.3.11)	0.00000	0.00005	0.00000
	Fructose-1,6-bisphosphatase, Bacillus type (EC 3.1.3.11)	0.00000	0.00000	0.00000
rTCA	fumarate reductase/succinate dehydrogenase flavoprotein, N-terminal:FAD dependent oxidoreductase	0.00000	0.00000	0.00000
	Fumarate reductase subunit C	0.00000	0.00000	0.00000
	Fumarate reductase flavoprotein subunit (EC 1.3.99.1)	0.00011	0.00000	0.00000
	Fumarate and nitrate reduction regulatory protein	0.00000	0.00016	0.00005
	2-oxoglutarate dehydrogenase E1 component (EC 1.2.4.2)	0.00175	0.00090	0.00127
	Dihydrolipoamide succinyltransferase component (E2) of 2-oxoglutarate dehydrogenase complex (EC 2.3.1.61)	0.00074	0.00127	0.00042
	Dihydrolipoamide dehydrogenase of 2-oxoglutarate dehydrogenase (EC 1.8.1.4)	0.00111	0.00005	0.00021
HP/HB	Propionyl-CoA carboxylase carboxyl transferase subunit (EC 6.4.1.3)	0.00011	0.00005	0.00005
	Propionyl-CoA carboxylase biotin-containing subunit (EC 6.4.1.3)	0.00021	0.00000	0.00000
	Propionyl-CoA carboxylase beta chain (EC 6.4.1.3)	0.00005	0.00000	0.00016
W-L	Carbon-monoxide dehydrogenase form II, large subunit (EC 1.2.99.2)	0.00005	0.00000	0.00000
	CO dehydrogenases maturation factor, CoxF family	0.00000	0.00000	0.00000
	carbon monoxide dehydrogenase operon C protein	0.00000	0.00005	0.00000

References

Abramson L, Lee C, Liu Z, Wakeham SG, Szlosek J. (2010). Exchange between suspended and sinking particles in the northwest Mediterranean as inferred from the organic composition of in situ pump and sediment trap samples. Limnol Oceanogr 55: 725–739.

Agarwala R, Barrett T, Beck J, Benson DA, Bollin C, Bolton E, et al. (2017). Database Resources of the National Center for Biotechnology Information. Nucleic Acids Res 45: D12–D17.

Alldredge AL, Cohen Y. (1987). Can microscale chemical patches persist in the sea? Microelectrode study of marine snow, fecal sellets. Science (80-) 235: 689–691.

Alldredge AL, Passow U, Logan BE. (1993). The abundance and significance of a class of large, transparent organic particles in the ocean. Deep Res Part I 40: 1131–1140.

Alldredge AL, Silver MW. (1988). Characteristics, dynamics and significance of marine snow. Prog Oceanogr 20: 41–82.

Allen AE, Allen LZ, McCrow JP. (2013). Lineage specific gene family enrichment at the microscale in marine systems. Curr Opin Microbiol 16: 605–617.

Allen LZ, Allen EE, Badger JH, McCrow JP, Paulsen IT, Elbourne LD, et al. (2012). Influence of nutrients and currents on the genomic composition of microbes across an upwelling mosaic. ISME J 6: 1403–1414.

Allers E, Gómez-Consarnau L, Pinhassi J, Gasol JM, Šimek K, Pernthaler J. (2007). Response of *Alteromonadaceae* and *Rhodobacteriaceae* to glucose and phosphorus manipulation in marine mesocosms. Environ Microbiol 9: 2417–2429.

Alonso-González IJ, Arístegui J, Vilas JC, Hernández-Guerra A. (2009). Lateral POC transport and consumption in surface and deep waters of the Canary Current region: A box model study. Global Biogeochem Cycles 23: 1–12.

Alonso-Saez L, Waller AS, Mende DR, Bakker K, Farnelid H, Yager PL, et al. (2012). Role for urea in nitrification by polar marine *Archaea*. Proc Natl Acad Sci 109: 17989–17994.

Alves RJE, Minh BQ, Urich T, von Haeseler A, Schleper C. (2018). Unifying the global phylogeny and environmental distribution of ammonia-oxidising archaea based on *amoA* genes. Nat Commun 9: 1517.

Anantharaman K, Breier JA, Sheik CS, Dick GJ. (2013). Evidence for hydrogen oxidation and metabolic plasticity in widespread deep-sea sulfur-oxidizing bacteria. Proc Natl Acad Sci 110: 330–335.

Andersen KH, Berge T, Gonçalves RJ, Hartvig M, Heuschele J, Hylander S, et al. (2016). Characteristic sizes of life in the oceans, from bacteria to whales. Ann Rev Mar Sci 8: 217–241.

Anderson L a, Sarmiento JL. (1994). Redfield ratios of remineralization determined by nutrient data analysis. Global Biogeochem Cycles 8: 65–80.

Bibliography

Anderson R, Wylezich C, Glaubitz S, Labrenz M, Jürgens K. (2013). Impact of protist grazing on a key bacterial group for biogeochemical cycling in Baltic Sea pelagic oxic/anoxic interfaces. Environ Microbiol 15: 1580–1594.

Anderson TR, Tang KW. (2010). Carbon cycling and POC turnover in the mesopelagic zone of the ocean: Insights from a simple model. Deep Res Part II Top Stud Oceanogr 57: 1581–1592.

Arístegui J, Gasol JM, Duarte CM, Herndl GJ. (2009). Microbial oceanography of the dark ocean's pelagic realm. Limnol Oceanogr 54: 1501–1529.

Armstrong R a., Lee C, Hedges JI, Honjo S, Wakeham SG. (2002). A new, mechanistic model for organic carbon fluxes in the ocean based on the quantitative association of POC with ballast minerals. Deep Res Part II Top Stud Oceanogr 49: 219–236.

Arnosti C. (2011). Microbial extracellular enzymes and the marine carbon cycle. Ann Rev Mar Sci 3: 401–425.

Arnosti C, Steen AD. (2013). Patterns of extracellular enzyme activities and microbial metabolism in an Arctic fjord of Svalbard and in the northern Gulf of Mexico: contrasts in carbon processing by pelagic microbial communities. Front Microbiol 4: 1–9.

Arrigo KR. (1999). Phytoplankton Community structure and the drawdown of nutrients and CO_2 in the Southern Ocean. Science (80-) 283: 365–367.

Atkinson A, Whitehouse MJ, Priddle J, Cripps GC, Ward P, Brandon MA. (2001). South Georgia, Antarctica: A productive, cold water, pelagic ecosystem. Mar Ecol Prog Ser 216: 279–308.

Azam F, Fenchel T, Field J, Gray J, Meyer-Reil L, Thingstad F. (1983). The ecological role of water-column microbes in the sea. Mar Ecol Prog Ser 10: 257–263.

Azam F, Hodson R. (1977). Size distribution and activity of marine microheterotrophs. Limnol Oceanogr 22: 492–501.

Azam F, Malfatti F. (2007). Microbial structuring of marine ecosystems. Nat Rev Microbiol 5: 782–791.

Bach LT, Riebesell U, Sett S, Febiri S, Rzepka P, Schulz KG. (2012). An approach for particle sinking velocity measurements in the 3-400 µm size range and considerations on the effect of temperature on sinking rates. Mar Biol 159: 1853–1864.

Bacon MP, Huh CA, Fleer AP, Deuser WG. (1985). Seasonality in the flux of natural radionuclides and plutonium in the deep Sargasso Sea. Deep Sea Res Part A, Oceanogr Res Pap 32: 273–286.

Baker CA, Henson SA, Cavan EL, Giering SLC, Yool A, Gehlen M, et al. (2017). Slow-sinking particulate organic carbon in the Atlantic Ocean: magnitude, flux and potential controls. Global Biogeochem Cycles 1–15.

Baltar F, Arístegui J, Gasol JM, Sintes E, Herndl GJ. (2009). Evidence of prokaryotic metabolism on suspended particulate organic matter in the dark waters of the subtropical North Atlantic. Limnol Oceanogr 54: 182–193.

Baltar F, Arístegui J, Sintes E, Gasol JM, Reinthaler T, Herndl GJ. (2010). Significance of non-sinking particulate organic carbon and dark CO_2 fixation to heterotrophic carbon demand in the mesopelagic northeast Atlantic. Geophys Res Lett 37: 1–6.

Baltar F, Morán XAG, Lønborg C. (2017). Warming and organic matter sources impact the proportion of dissolved to total activities in marine extracellular enzymatic rates. Biogeochemistry 133: 307–316.

Bannon CC, Campbell DA. (2017). Sinking towards destiny: High throughput measurement of phytoplankton sinking rates through time-resolved fluorescence plate spectroscopy. PLoS One 12: 1–16.

Bauer M, Kube M, Teeling H, Richter M, Lombardot T, Allers E, et al. (2006). Whole genome analysis of the marine *Bacteroidetes Gramella forsetii* reveals adaptations to degradation of polymeric organic matter. Environ Microbiol 8: 2201–2213.

Belcher A, Iversen M, Giering S, Riou V, Henson S, Sanders R. (2016a). Depth-resolved particle associated microbial respiration in the northeast Atlantic. Biogeosciences Discuss 1–31.

Belcher A, Iversen M, Manno C, Henson SA, Tarling GA, Sanders R. (2016b). The role of particle associated microbes in remineralization of fecal pellets in the upper mesopelagic of the Scotia Sea, Antarctica. Limnol Oceanogr 61: 1049–1064.

Benavides M, H. Moisander P, Berthelot H, Dittmar T, Grosso O, Bonnet S. (2015). Mesopelagic N_2 fixation related to organic matter composition in the Solomon and Bismarck Seas (Southwest Pacific). PLoS One 10: 1–19.

Benavides M, Voss M. (2015). Five decades of N_2 fixation research in the North Atlantic Ocean. Front Mar Sci 2: 1–20.

Benoiston A-S, Ibarbalz FM, Bittner L, Guidi L, Jahn O, Dutkiewicz S, et al. (2017). The evolution of diatoms and their biogeochemical functions. Philos Trans R Soc B Biol Sci 372: 20160397.

Berg IA, Kockelkorn D, Buckel W, Fuchs G. (2007). A 3-hydroxypropionate/4-hydroxybutyrate autotrophic carbon dioxide assimilation pathway in archaea. Science (80-) 318: 1782–1786.

Bergauer K, Fernandez-Guerra A, Garcia JAL, Sprenger RR, Stepanauskas R, Pachiadaki MG, et al. (2018). Organic matter processing by microbial communities throughout the Atlantic water column as revealed by metaproteomics. Proc Natl Acad Sci 115: E400–E408.

Berger WH. (1971). Sedimentation of planktonic foraminifera. Mar Geol 11: 325–358.

Bettarel Y, Motegi C, Weinbauer MG, Mari X. (2016). Colonization and release processes of viruses and prokaryotes on artificial marine macroaggregates. FEMS Microbiol Lett 363: fnv216.

Bianchi D, Weber TS, Kiko R, Deutsch C. (2018). Global niche of marine anaerobic metabolisms expanded by particle microenvironments. Nat Geosci 2018 1.

Biard T, Stemmann L, Picheral M, Mayot N, Vandromme P, Hauss H, et al. (2016). *In situ* imaging reveals the biomass of giant protists in the global ocean. Nature 532: 504–507.

Bibliography

Biddanda B, Benner R. (1997). Carbon, nitrogen, and carbohydrate fluxes during the production of particulate and dissolved organic matter by marine phytoplankton. Limnol Oceanogr 42: 506–518.

Bishop, J.K.B., Edmond, J.M., Ketten, D.R., Bacon, M.P., and Silker, W.B. (1977) The chemistry, biology, and vertical flux of particulate matter from the upper 400 m of the equatorial Atlantic Ocean. Deep Sea Res. 24: 511–548.

Bižić-Ionescu M, Zeder M, Ionescu D, Orlić S, Fuchs BM, Grossart H-P, et al. (2014). Comparison of bacterial communities on limnic versus coastal marine particles reveals profound differences in colonization. Environ Microbiol 1–36.

Bjornsen PK. (1988). Phytoplankton exudation of organic matter - Why do healthy cells do it. Limnol Oceanogr 33: 151–154.

Blackburn N, Fenchel T. (1999). Influence of bacteria, diffusion and shear on micro-scale nutrient patches, and implications for bacterial chemotaxis. Mar Ecol Prog Ser 189: 1–7.

Bochdansky AB, van Aken HM, Herndl GJ. (2010). Role of macroscopic particles in deep-sea oxygen consumption. Proc Natl Acad Sci U S A 107: 8287–8291.

Bochdansky AB, Clouse MA, Herndl GJ. (2017). Eukaryotic microbes, principally fungi and labyrinthulomycetes, dominate biomass on bathypelagic marine snow. ISME J 11: 362–373.

Boyd PW, Sherry ND, Berges JA, Bishop JKB, Calvert SE, Charette MA, et al. (1999). Transformations of biogenic particulates from the pelagic to the deep ocean realm. Deep Res Part II Top Stud Oceanogr 46: 2761–2792.

Bratbak G, Egge JK, Heldal M. (1993). Viral mortality of the marine alga *Emiliania huxleyi* (*Haptophyceae*) and termination of algal blooms. Mar Ecol Prog Ser 93: 39–48.

Brinkhoff T, Giebel HA, Simon M. (2008). Diversity, ecology, and genomics of the *Roseobacter* clade: A short overview. Arch Microbiol 189: 531–539.

Brown M V., Bowman JP. (2001). A molecular phylogenetic survey of sea-ice microbial communities (SIMCO). FEMS Microbiol Ecol 35: 267–275.

Brum JR, Hurwitz BL, Schofield O, Ducklow HW, Sullivan MB. (2015). Seasonal time bombs: dominant temperate viruses affect Southern Ocean microbial dynamics. ISME J 10: 1–13.

Buchan A, González JM, Moran MA. (2005). Overview of the marine *Roseobacter* lineage. Appl Environ Microbiol 71: 5665–5677.

Buchan A, LeCleir GR, Gulvik C a, González JM. (2014). Master recyclers: features and functions of bacteria associated with phytoplankton blooms. Nat Rev Microbiol 12: 686–698.

Buesseler KO. (1998). The decoupling of production and particle export in the surface ocean. Global Biogeochem Cycles 12: 297–310.

Buesseler KO, Antia AN, Chen M, Fowler SW, Gardner WD, Gustafsson O, et al. (2007a). An assessment of the use of sediment traps for estimating upper ocean particle fluxes. J Mar Res 65: 345–416.

Buesseler KO, Boyd PW. (2009). Shedding light on processes that control particle export and flux attenuation in the twilight zone of the open ocean. Limnol Oceanogr 54: 1210–1232.

Buesseler KO, Lamborg CH, Boyd PW, Lam PJ, Trull TW, Bidigare RR, et al. (2007b). Revisiting carbon flux through the ocean's twilight zone. Science 316: 567–570.

Burd AB, Jackson GA. (2009). Particle aggregation. Ann Rev Mar Sci 1: 65–90.

Burge SW, Daub J, Eberhardt R, Tate J, Barquist L, Nawrocki EP, et al. (2013). Rfam 11.0: 10 years of RNA families. Nucleic Acids Res 41: D226–D232.

Calbet A, Landry MR. (2004). Phytoplankton growth, microzooplankton grazing, and carbon cycling in marine systems. Limnol Oceanogr 49: 51–57.

Canfield DE, Stewart FJ, Thamdrup B, De Brabandere L, Dalsgaard T, Delong EF, et al. (2010). A cryptic sulfur cycle in oxygen-minimum-zone waters off the Chilean coast. Science 330: 1375–1378.

Caporaso JG, Lauber CL, Walters WA, Berg-lyons D, Lozupone CA, Turnbaugh PJ, et al. (2010). Global patterns of 16S rRNA diversity at a depth of millions of sequences per sample. Proc Natl Acad Sci U S A 108: 4516–4522.

Capriulo GM, Smith G, Troy R, Wikfors GH, Pellet J, Yarish C. (2002). The planktonic food web structure of a temperate zone estuary, and its alteration due to eutrophication. Hydrobiologia 475–476: 263–333.

Carlson CA. (2002). Production and Removal Processes. In: Biogeochemistry of Marine Dissolved Organic Matter. Elsevier, pp 91–151.

Caron DA. (2017). Acknowledging and incorporating mixed nutrition into aquatic protistan ecology, finally. Environ Microbiol Rep 9: 41–43.

Caron DA., Davis PG, Madin LP, Sieburth JM. (1986). Enrichment of microbial populations in macroaggregates (marine snow) from surface waters of the North Atlantic. J Mar Res 44: 543–565.

Caron DA, Alexander H, Allen AE, Archibald JM, Armbrust EV, Bachy C, et al. (2017). Probing the evolution, ecology and physiology of marine protists using transcriptomics. Nat Rev Microbiol 15: 6–20.

Caron DA, Countway PD, Jones AC, Kim DY, Schnetzer A. (2012). Marine protistan diversity. Ann Rev Mar Sci 4: 467–493.

Caron DA, Davis PG, Madin LP, Sieburth JM. (1982). Heterotrophic bacteria and bacterivorous protozoa in oceanic macroaggregates. Science (80-) 218: 795–797.

Caron DA, Gast RJ, Garneau MÈ. (2016). Sea ice as a habitat for micrograzers. Sea Ice Third Ed 370–393.

Cassar N, Wright SW, Thomson PG, Trull TW, Westwood KJ, De Salas M, et al. (2015). Global biogeochemical cycles composition in the Southern Ocean. Global Biogeochem Cycles 1–17.

Cavan EL, Henson SA, Belcher A, Sanders R. (2016). Role of zooplankton in determining the efficiency of the biological carbon pump. Biogeosciences Discuss 1–25.

Cavan EL, Trimmer M, Shelley F, Sanders R. (2017). Remineralization of particulate organic carbon in an ocean oxygen minimum zone. Nat Commun 8: 1–9.

Chen B, Laws EA. (2017). Is there a difference of temperature sensitivity between marine phytoplankton and heterotrophs? Limnol Oceanogr 62: 806–817.

Cho BC, Azam F. (1988). Major role of bacteria in biogeochemical fluxes in the ocean's interior. Nature 332: 441–443.

Chow CET, Kim DY, Sachdeva R, Caron DA, Fuhrman JA. (2014). Top-down controls on bacterial community structure: Microbial network analysis of bacteria, T4-like viruses and protists. ISME J 8: 816–829.

Cole J, Findlay S, Pace M. (1988). Bacterial production in fresh and saltwater ecosystems: a cross-system overview. Mar Ecol Prog Ser 43: 1–10.

Collins JR, Edwards BR, Thamatrakoln K, Ossolinski JE, DiTullio GR, Bidle KD, et al. (2015). The multiple fates of sinking particles in the North Atlantic Ocean. Global Biogeochem Cycles 29: 1471–1494.

Cotter PA, Chepuri V, Gennis RB, Gunsalus RP. (1990). Cytochrome *o* (*cyoABCDE*) and *d* (*cydAB*) oxidase gene expression in *Escherichia coli* is regulated by oxygen, pH, and the *fnr* gene product. J Bacteriol 172: 6333–6338.

Cottrell MT, Kirchman DL. (2000). Natural assemblages of marine *Proteobacteria* and members of the *Cytophaga-Flavobacter* cluster consuming low- and high-molecular-weight dissolved organic matter. Appl Environ Microbiol 66: 1692–1697.

Crespo BG, Pommier T, Fernández-Gómez B, Pedrós-Alió C. (2013). Taxonomic composition of the particle-attached and free-living bacterial assemblages in the Northwest Mediterranean Sea analyzed by pyrosequencing of the 16S rRNA. Microbiologyopen 2: 541–552.

Crump BC, Baross JA, Simenstad CA. (1998). Dominance of particle-attached bacteria in the Columbia River estuary, USA. Aquat Microb Ecol 14: 7–18.

Crump BC, Crump BC, Armbrust EV, Armbrust EV, Baross J a, Baross J a. (1999). Phylogenetic analysis of particle-attached and free-living bacterial communities in the Columbia River, its estuary, and the adjacent coastal ocean. Appl Environ Microbiol 65: 3192–3204.

Crump BC, Peranteau C, Beckingham B, Cornwell JC. (2007). Respiratory succession and community succession of bacterioplankton in seasonally anoxic estuarine waters. Appl Environ Microbiol 73: 6802–6810.

D'Ambrosio L, Ziervogel K, Macgregor B, Teske A, Arnosti C. (2014). Composition and enzymatic function of particle-associated and free-living bacteria: a coastal/offshore comparison. ISME J 1–13.

Dall'Olmo G, Mork KA. (2014). Carbon export by small particles in the Norwegian Sea. Geophys Res Lett 41: 2921–2927.

Dang H, Lovell CR. (2016). Microbial surface colonization and biofilm development in marine environments. Microbiol Mol Biol Rev 80: 91–138.

Datta MS, Sliwerska E, Gore J, Polz M, Cordero OX. (2016). Microbial interactions lead to rapid micro-scale successions on model marine particles. Nat Commun 7: 11965.

Decelle J, Martin P, Paborstava K, Pond DW, Tarling G, Mahé F, et al. (2013). Diversity, ecology and biogeochemistry of cyst-forming *Acantharia* (*Radiolaria*) in the oceans. PLoS One 8: e53598.

Delong EF, Franks DG, Alldredge AL. (1993). Phylogenetic diversity of aggregate-attached vs. free-living marine bacterial assemblages. Limnol Oceanogr 38: 924–934.

DiTullio GR, Grebmeier JM, Arrigo KR, Lizotte MP, Robinson DH, Leventer A, et al. (2000). Rapid and early export of *Phaeocystis antarctica* blooms in the Ross Sea, Antarctica. Nature 404: 595–598.

Djurhuus A, Pitz K, Sawaya NA, Rojas-Márquez J, Michaud B, Montes E, et al. (2018). Evaluation of marine zooplankton community structure through environmental DNA metabarcoding. Limnol Oceanogr Methods 209–221.

Druffel ERM, Griffin S, Bauer JE, Wolgast DM, Wang XC. (1998). Distribution of particulate organic carbon and radiocarbon in the water column from the upper slope to the abyssal NE Pacific Ocean. Deep Res Part II Top Stud Oceanogr 45: 667–687.

Ducklow HW, Steinberg DK, Buesseler KO. (2001). Upper ocean carbon export and the biological pump. Oceanography 14: 50–58.

Dugdale RC, Goering JJ. (1967). Uptake of new and regenerated forms of nitrogen in primary productivity. Limnol Oceanogr 12: 196–206.

Duret MT, Pachiadaki MG, Stewart FJ, Sarode N, Christaki U, Monchy S, et al. (2015). Size-fractionated diversity of eukaryotic microbial communities in the Eastern Tropical North Pacific oxygen minimum zone. FEMS Microbiol Ecol 91: fiv037-fiv037.

Eberlein K, Leal M, Hammer K, Hickel W. (1985). Dissolved organic substances during a *Phaeocystis pouchetii* bloom in the German Bight (North Sea). Mar Biol 316: 311–316.

Ebersbach F, Trull TW. (2008). Sinking particle properties from polyacrylamide gels during KEOPS: controls on carbon export in an area of persistent natural iron inputs in the Southern Ocean. Limnol Ocean 53: 212–224.

Ebersbach F, Trull TW, Davies DM, Bray SG. (2011). Controls on mesopelagic particle fluxes in the Sub-Antarctic and Polar Frontal Zones in the Southern Ocean south of Australia in summer-Perspectives from free-drifting sediment traps. Deep Res Part II Top Stud Oceanogr 58: 2260–2276.

Edgcomb V, Orsi W, Bunge J, Jeon S, Christen R, Leslin C, et al. (2011). Protistan microbial observatory in the Cariaco Basin, Caribbean. I. Pyrosequencing vs Sanger insights into species richness. ISME J 5: 1344–56.

Edgcomb VP. (2016). Marine protist associations and environmental impacts across trophic levels in the twilight zone and below. Curr Opin Microbiol 31: 169–175.

Eloe E a., Shulse CN, Fadrosh DW, Williamson SJ, Allen EE, Bartlett DH. (2010). Compositional differences in particle-associated and free-living microbial assemblages from an extreme deep-ocean environment. Environ Microbiol Rep 3: 449–458.

Emerson JB, Adams RI, Román CMB, Brooks B, Coil DA, Dahlhausen K, et al. (2017). Schrödinger's microbes: Tools for distinguishing the living from the dead in microbial ecosystems. Microbiome 5: 86.

Farnelid H, Andersson AF, Bertilsson S, Al-Soud WA, Hansen LH, Sørensen S, et al. (2011). Nitrogenase gene amplicons from global marine surface waters are dominated by genes of non-cyanobacteria. PLoS One 6. e-pub ahead of print, doi: 10.1371/journal.pone.0019223.

Fernandez E, Serret P, De Madariaga I, Harbour DS, Davies AG. (1992). Photosynthetic carbon metabolism and biochemical composition of spring phytoplankton assemblages enclosed in microcosms: the diatom-*Phaeocystis* sp. succession. Mar Ecol Prog Ser 90: 89–102.

Field CB, Behrenfeld MJ, Randerson JT, Falkowski P. (1998). Primary productivity of the biosphere: an integration of terrestrial and oceanic components. Science (80-) 281: 237–240.

Fontanez KM, Eppley JM, Samo TJ, Karl DM, DeLong EF. (2015). Microbial community structure and function on sinking particles in the North Pacific Subtropical Gyre. Front Microbiol 6: 1–14.

Francis CA, Roberts KJ, Beman JM, Santoro AE, Oakley BB. (2005). Ubiquity and diversity of ammonia-oxidizing archaea in water columns and sediments of the ocean. Proc Natl Acad Sci 102: 14683–14688.

Francois R, Honjo S, Krishfield R, Manganini S. (2002). Factors controlling the flux of organic carbon to the bathypelagic zone of the ocean. Global Biogeochem Cycles 16: 34-1-34–20.

Friedrich CG, Rother D, Quentmeier A, Fischer J, Bardischewsky F. (2001). Oxidation of reduced Inorganic sulfur compounds by bacteria: Emergence of a common mechanism ? Appl Environ Microbiol 67: 2873–2882.

Fuchs BM, Zubkov M V., Sahm K, Burkill PH, Amann R. (2000). Changes in community composition during dilution cultures of marine bacterioplankton as assessed by flow cytometric and molecular biological techniques. Environ Microbiol 2: 191–201.

Fuchsman CA., Kirkpatrick JB, Brazelton WJ, Murray JW, Staley JT. (2011). Metabolic strategies of free-living and aggregate-associated bacterial communities inferred from biologic and chemical profiles in the Black Sea suboxic zone. FEMS Microbiol Ecol 78: 586–603.

Fuhrman JA, Azam F. (1982). Thymidine incorporation as a measure of heterotrophic bacterioplankton production in marine surface waters: Evaluation and field results. Mar Biol 66: 109–120.

Fuhrman JA, Comeau DE, Hagström A, Chan AM. (1988). Extraction from natural planktonic microorganisms of DNA suitable for molecular biological studies. Appl Environ Microbiol 54: 1426–9.

Ganesh S, Bristow L a, Larsen M, Sarode N, Thamdrup B, Stewart FJ. (2015). Size-fraction partitioning of community gene transcription and nitrogen metabolism in a marine oxygen minimum zone. ISME J 9: 1–15.

Ganesh S, Parris DJ, DeLong EF, Stewart FJ. (2014). Metagenomic analysis of size-fractionated picoplankton in a marine oxygen minimum zone. ISME J 8: 187–211.

García-Martínez J, Acinas SG, Massana R, Rodríguez-Valera F. (2002). Prevalence and microdiversity of *Alteromonas macleodii*-like microorganisms in different oceanic regions. Environ Microbiol 4: 42–50.

Garrison DL, Gibson A, Coale SL, Gowing MM, Okolodkov YB, Fritsen CH, et al. (2005). Sea-ice microbial communities in the Ross Sea: Autumn and summer biota. Mar Ecol Prog Ser 300: 39–52.

Garzio LM, Steinberg DK, Erickson M, Ducklow HW. (2013). Microzooplankton grazing along the Western Antarctic Peninsula. Aquat Microb Ecol 70: 215–232.

Georges C, Monchy S, Genitsaris S, Christaki U. (2014). Protist community composition during early phytoplankton blooms in the naturally iron-fertilized Kerguelen area (Southern Ocean). Biogeosciences Discuss 11: 11179–11215.

Ghiglione JF, Mevel G, Pujo-Pay M, Mousseau L, Lebaron P, Goutx M. (2007). Diel and seasonal variations in abundance, activity, and community structure of particle-attached and free-living bacteria in NW Mediterranean Sea. Microb Ecol 54: 217–231.

Giering SLC, Sanders R, Lampitt RS, Anderson TR, Tamburini C, Boutrif M, et al. (2014). Reconciliation of the carbon budget in the ocean's twilight zone. Nature 507: 480–483.

Giering SLC, Sanders R, Martin AP, Henson SA, Riley JS, Marsay CM, et al. (2017). Particle flux in the oceans: Challenging the steady state assumption. Global Biogeochem Cycles 31: 159–171.

Giesecke R, González HE, Bathmann U. (2010). The role of the chaetognath *Sagitta gazellae* in the vertical carbon flux of the Southern Ocean. Polar Biol 33: 293–304.

Giovannoni SJ, Cameron Thrash J, Temperton B. (2014). Implications of streamlining theory for microbial ecology. ISME J 8: 1–13.

Givskov M, Eberl L, Molin S. (1997). Control of exoenzyme production, motility and cell differentiation in *Serratia liquefaciens*. FEMS Microbiol Lett 148: 115–122.

Glaubitz S, Kießlich K, Meeske C, Labrenz M, Jürgens K. (2013). SUP05 Dominates the gammaproteobacterial sulfur-oxidizer assemblages in pelagic redoxclines of the central Baltic and Black Seas. Appl Environ Microbiol 79: 2767–2776.

Gloeckler K, Choy CA, Hannides CCS, Close HG, Goetze E, Popp BN, et al. (2017). Stable isotope analysis of micronekton around Hawaii reveals suspended particles are an important nutritional source in the lower mesopelagic and upper bathypelagic zones. Limnol Oceanogr 0. e-pub ahead of print, doi: 10.1002/lno.10762.

Gómez-Pereira PR, Schüler M, Fuchs BM, Bennke C, Teeling H, Waldmann J, et al. (2012). Genomic content of uncultured *Bacteroidetes* from contrasting oceanic provinces in the North Atlantic Ocean. Environ Microbiol 14: 52–66.

Gowing MM, Silver MW. (1985). Minipellets: A new and abundant size class of marine fecal pellets. J Mar Res 43: 395–418.

Gram L, Grossart H, Schlingloff A, Kiørboe T. (2002). Possible quorum sensing in marine snow bacteria: Production of acylated homoserine lactones by *Roseobacter* strains isolated from marine snow. Appl Environ Microbiol 68: 4111–4116.

Grattepanche J-D, Santoferrara LF, McManus GB, Katz LA. (2016). Unexpected biodiversity of ciliates in marine samples from below the photic zone. Mol Ecol 25: 3987–4000.

Grein F, Pereira IAC, Dahl C. (2010). Biochemical characterization of individual components of the *Allochromatium vinosum DsrMKJOP* transmembrane complex aids understanding of complex function *in vivo*. J Bacteriol 192: 6369–6377.

Grossart HP, Tang KW, Kiørboe T, Ploug H. (2007). Comparison of cell-specific activity between free-living and attached bacteria using isolates and natural assemblages. FEMS Microbiol Lett 266: 194–200.

Gruber N. (2008). The marine nitrogen cycle: Overview and challenges. Nitrogen Mar Environ 1–50.

Guidi L, Chaffron S, Bittner L, Eveillard D, Larhlimi A, Roux S, et al. (2016). Plankton networks driving carbon export in the oligotrophic ocean. Nature 532: 465–470.

Guidi L, Stemmann L, Jackson G a., Ibanez F, Claustre H, Legendre L, et al. (2009). Effects of phytoplankton community on production, size, and export of large aggregates: A world-ocean analysis. Limnol Oceanogr 54: 1951–1963.

Guillou L, Viprey M, Chambouvet A, Welsh RM, Kirkham AR, Massana R, et al. (2008). Widespread occurrence and genetic diversity of marine parasitoids belonging to *Syndiniales* (*Alveolata*). Environ Microbiol 10: 3349–3365.

Hadziavdic K, Lekang K, Lanzen A, Jonassen I, Thompson EM, Troedsson C. (2014). Characterization of the 18S rRNA gene for designing universal eukaryote specific. PLoS One 9: e87624.

Hagström A, Larsson U, Hörstedt P, Normark S. (1979). Frequency of dividing cells, a new approach to the determination of bacterial growth rates in aquatic environments. Appl Environ Microbiol 37: 805–12.

Halm H, Lam P, Ferdelman TG, Lavik G, Dittmar T, Laroche J, et al. (2011). Heterotrophic organisms dominate nitrogen fixation in the south pacific gyre. ISME J 6: 1238–1249.

Hansen HP, Koroleff F. (1983). Determination of nutrients. In: Vol. 7. Methods of Seawater Analysis. Wiley-VCH Verlag GmbH: Weinheim, Germany, pp 159–228.

Hasan SS, Yamashita E, Baniulis D, Cramer WA. (2013). Quinone-dependent proton transfer pathways in the photosynthetic cytochrome *b6f* complex. Proc Natl Acad Sci 110: 4297–4302.

Henson SA, Sanders R, Madsen E. (2012). Global patterns in efficiency of particulate organic carbon export and transfer to the deep ocean. Global Biogeochem Cycles 26: 1–14.

Herbold CW, Pelikan C, Kuzyk O, Hausmann B, Angel R, Berry D, et al. (2015). A flexible and economical barcoding approach for highly multiplexed amplicon sequencing of diverse target genes. Front Microbiol 6: 731.

Herndl GJ, Reinthaler T. (2013). Microbial control of the dark end of the biological pump. Nat Geosci 6: 718–724.

Holmes RM, Aminot A, Kérouel R, Hooker B a, Peterson BJ. (1999). A simple and precise method for measuring ammonium in marine and freshwater ecosystems. Can J Fish Aquat Sci 56: 1801–1808.

Hong Y, Smith WO, White A-M. (1997). Studies on Transparent Exopolymer Particles (TEP) produced in the Ross Sea (Antarctica) and by *Phaeocystis Antarctica* (*Prymnesiophyceae*). J Phycol 33: 368–376.

Hooper AB, Vannelli T, Bergmann DJ, Arciero DM. (1997). Enzymology of the oxidation of ammonia to nitrate by bacteria. Antonie Van Leeuwenhoek 71: 59–67.

Huber H, Gallenberger M, Jahn U, Eylert E, Berg IA, Kockelkorn D, et al. (2008). A dicarboxylate/4-hydroxybutyrate autotrophic carbon assimilation cycle in the hyperthermophilic archaeum *Ignicoccus hospitalis*. Proc Natl Acad Sci 105: 7851–7856.

Huber JA, Mark Welch DB, Morrison HG, Huse SM, Neal PR, Butterfield DA, et al. (2007). Microbial population structures in the deep marine biosphere. Sci (New York, NY) 318: 97–100.

Hügler M, Sievert SM. (2011). Beyond the Calvin cycle: autotrophic carbon fixation in the ocean. Ann Rev Mar Sci 3: 261–289.

Hwang J, Druffel ERM. (2003). Lipid-like material as the source of the uncharacterized organic carbon in the ocean? Science (80-) 299: 881–884.

Iversen MH, Ploug H. (2010). Ballast minerals and the sinking carbon flux in the ocean: Carbon-specific respiration rates and sinking velocity of marine snow aggregates. Biogeosciences 7: 2613–2624.

Jacques G. (1983). Some ecophysiological aspects of the Antarctic phytoplankton. Polar Biol 2: 27–33.

Janouškovec J, Tikhonenkov D V., Burki F, Howe AT, Kolísko M, Mylnikov AP, et al. (2015). Factors mediating plastid dependency and the origins of parasitism in apicomplexans and their close relatives. Proc Natl Acad Sci 112: 10200–10207.

Jeandel C, Rutgers van der Loeff M, Lam PJ, Roy-Barman M, Sherrell RM, Kretschmer S, et al. (2015). What did we learn about ocean particle dynamics in the GEOSECS-JGOFS era? Prog Oceanogr 133: 6–16.

Jiao N, Herndl GJ, Hansell D a, Benner R, Kattner G, Wilhelm SW, et al. (2010). Microbial production of recalcitrant dissolved organic matter: long-term carbon storage in the global ocean. Nat Rev Microbiol 8: 593–599.

Jin. X, Gruber N, Dune JP, Sarmiento JL, Armstrong RA. (2006). Diagnosing the contributions of phytoplankton functional groups to the production and export of particulate organic carbon, CaCO3, and opal from global nutrient and alkalinity distributions. Global Biogeochem Cycles 20: 1–17.

Kabisch A, Otto A, König S, Becher D, Albrecht D, Schüler M, et al. (2014). Functional characterization of polysaccharide utilization loci in the marine *Bacteroidetes Gramella forsetii* KT0803. ISME J 8: 1492–1502.

Kalvelage T, Jensen MM, Contreras S, Revsbech NP, Lam P, Günter M, et al. (2011). Oxygen sensitivity of anammox and coupled N-cycle processes in oxygen minimum zones. PLoS One 6: e29299.

Karl DM, Knauer G a. (1984). Vertical distribution, transport, and exchange of carbon in the northeast Pacific Ocean: evidence for multiple zones of biological activity. Deep Sea Res Part A Oceanogr Res Pap 31: 221–243.

Karl DM, Knauer G a., Martin JH. (1988). Downward flux of particulate organic matter in the ocean: a particle decomposition paradox. Nature 332: 438–441.

Karl DM, Knauer G a., Martin JH, Ward BB. (1984). Bacterial chemolithotrophy in the ocean is associated with sinking particles. Nature 309: 54–56.

Kellogg CTE, Deming JW. (2009). Comparison of free-living, suspended particle, and aggregate-associated bacterial and archaeal communities in the Laptev Sea. Aquat Microb Ecol 57: 1–18.

Kiene RP, Linn LJ. (2000). Distribution and turnover of dissolved DMSP and its relationship with bacterial production and dimethylsulfide in the Gulf of Mexico. Limnol Oceanogr 45: 849–861.

Kiørboe T, Grossart H-P, Ploug H, Tang K. (2002). Mechanisms and rates of bacterial colonization of sinking aggregates. Appl Environ Microbiol 68: 3996–4006.

Kiørboe T, Jackson G a. (2001). Marine snow, organic solute plumes, and optimal chemosensory behavior of bacteria. Limnol Oceanogr 46: 1309–1318.

Kirchman DL. (2008). Microbial ecology of the oceans. John Wiley & Sons, Inc.: Hoboken, NJ, USA.

Klaas C, Archer DE. (2002). Association of sinking organic matter with various types of mineral ballast in the deep sea: Implications for the rain ratio. Global Biogeochem Cycles 16: 63-1-63–14.

Knefelkamp B, Carstens K, Wiltshire KH. (2007). Comparison of different filter types on chlorophyll-*a* retention and nutrient measurements. J Exp Mar Bio Ecol 345: 61–70.

Korb RE, Whitehouse MJ, Ward P, Gordon M, Venables HJ, Poulton AJ. (2012). Regional and seasonal differences in microplankton biomass, productivity, and structure across the Scotia Sea: Implications for the export of biogenic carbon. Deep Res Part II Top Stud Oceanogr 59–60: 67–77.

Krupke A, Hmelo LR, Ossolinski JE, Mincer TJ, Van Mooy BAS. (2016). Quorum sensing plays a complex role in regulating the enzyme hydrolysis activity of microbes associated with sinking particles in the ccean. Front Mar Sci 3. e-pub ahead of print, doi: 10.3389/fmars.2016.00055.

Krupovic M, Forterre P. (2011). Microviridae goes temperate: Microvirus-related proviruses reside in the genomes of *Bacteroidetes*. PLoS One 6: e19893.

Kwon EY, Primeau F, Sarmiento JL. (2009). The impact of remineralization depth on the air–sea carbon balance. Nat Geosci 2: 630–635.

De La Rocha CL, Passow U. (2007). Factors influencing the sinking of POC and the efficiency of the biological carbon pump. Deep Res Part II Top Stud Oceanogr 54: 639–658.

Lam P, Jensen MM, Kock A, Lettmann KA, Plancherel Y, Lavik G, et al. (2011). Origin and fate of the secondary nitrite maximum in the Arabian Sea. Biogeosciences 8: 1565–1577.

Lam P, Kuypers MMM. (2011). Microbial nitrogen cycling processes in oxygen minimum zones. Ann Rev Mar Sci 3: 317–345.

Lam PJ, Marchal O. (2015). Insights into particle cycling from thorium and particle data. Ann Rev Mar Sci 7: 159–184.

Lampitt RS, Wishner KF, Turley CM, Angel M V. (1993). Marine snow studies in the Northeast Atlantic Ocean: distribution, composition and role as a food source for migrating plankton. Mar Biol 116: 689–702.

Lampreia J, Pereira AS, Moura JGBT-M in E. (1994). Adenylylsulfate reductases from sulfate-reducing bacteria. In: Vol. 243. Inorganic microbial sulfur metabolism. Academic Press, pp 241–260.

Lauro FM, McDougald D, Thomas T, Williams TJ, Egan S, Rice S, et al. (2009). The genomic basis of trophic strategy in marine bacteria. Proc Natl Acad Sci U S A 106: 15527–33.

Leblanc K, Quéguiner B, Diaz F, Cornet V, Michel-Rodriguez M, Durrieu De Madron X, et al. (2018). Nanoplanktonic diatoms are globally overlooked but play a role in spring blooms and carbon export. Nat Commun 9: 1–12.

Lecleir GR, Debruyn JM, Maas EW, Boyd PW, Wilhelm SW. (2014). Temporal changes in particle-associated microbial communities after interception by nonlethal sediment traps. FEMS Microbiol Ecol 87: 153–163.

Legendre L, Rivkin RB, Weinbauer MG, Guidi L, Uitz J. (2015). The microbial carbon pump concept: Potential biogeochemical significance in the globally changing ocean. Prog Oceanogr 134: 432–450.

Lin Y, Cassar N, Marchetti A, Moreno C, Ducklow H, Li Z. (2017). Specific eukaryotic plankton are good predictors of net community production in the Western Antarctic Peninsula. Sci Rep 7: 1–11.

Liu S, Wawrik B, Liu Z. (2017). Different bacterial communities involved in peptide decomposition between normoxic and hypoxic coastal waters. Front Microbiol 8: 1–17.

Logue JB, Stedmon CA, Kellerman AM, Nielsen NJ, Andersson AF, Laudon H, et al. (2016). Experimental insights into the importance of aquatic bacterial community composition to the degradation of dissolved organic matter. ISME J 10: 533–545.

López-García P, Rodrguez-Valera F, Pedrós-Alió C, Moreira D. (2002). Unexpected diversity of small eukaryotes in deep-sea Antarctic plankton. Nature 409: 603–606.

López-Pérez M, Kimes NE, Haro-Moreno JM, Rodriguez-Valera F. (2016). Not all particles are equal: The selective enrichment of particle-associated bacteria from the Mediterranean Sea. Front Microbiol 7. e-pub ahead of print, doi: 10.3389/fmicb.2016.00996.

Lovelock J. E, Maggs RJ, Rasmussen RA. (1972). Atmospheric dimethyl sulfide and the natural sulfur cycle. Nature 237: 452–453.

Lucker S, Wagner M, Maixner F, Pelletier E, Koch H, Vacherie B, et al. (2010). A *Nitrospira* metagenome illuminates the physiology and evolution of globally important nitrite-oxidizing bacteria. Proc Natl Acad Sci 107: 13479–13484.

Lyons MM, Dobbs FC. (2012). Differential utilization of carbon substrates by aggregate-associated and water-associated heterotrophic bacterial communities. Hydrobiologia 686: 181–193.

Magoč T, Salzberg SL. (2011). FLASH: Fast length adjustment of short reads to improve genome assemblies. Bioinformatics 27: 2957–2963.

Malfatti F, Azam F. (2010). Atomic force microscopy reveals microscale networks and possible symbioses among pelagic marine bacteria. Aquat Microb Ecol 58: 1–14.

Malfatti F, Samo TJ, Azam F. (2010). High-resolution imaging of pelagic bacteria by Atomic Force Microscopy and implications for carbon cycling. ISME J 4: 427–439.

Marchant HJ. (1985). Choanoflagellates in the Antarctic marine food chain. In: Vol. 0. Antarctic nutrient cycles and food webs. Springer Berlin Heidelberg: Berlin, Heidelberg, pp 271–276.

Mari X, Passow U, Migon C, Burd AB, Legendre L. (2017). Transparent exopolymer particles: Effects on carbon cycling in the ocean. Prog Oceanogr 151: 13–37.

Martin JH, Knauer G a., Karl DM, Broenkow WW. (1987). VERTEX: carbon cycling in the northeast Pacific. Deep Sea Res Part A Oceanogr Res Pap 34: 267–285.

Martínez-Pérez C, Mohr W, Löscher CR, Dekaezemacker J, Littmann S, Yilmaz P, et al. (2016). The small unicellular diazotrophic symbiont, UCYN-A, is a key player in the marine nitrogen cycle. Nat Microbiol 1: 16163.

Martínez-Pérez C, Mohr W, Schwedt A, Dürschlag J, Callbeck CM, Schunck H, et al. (2018). Metabolic versatility of a novel N_2-fixing Alphaproteobacterium isolated from a marine oxygen minimum zone. Environ Microbiol 20: 755–768.

Masella AP, Bartram AK, Truszkowski JM, Brown DG, Neufeld JD. (2012). PANDAseq: PAired-eND Assembler for Illumina sequences. BMC Bioinformatics 13: 31.

Mason OU, Hazen TC, Borglin S, Chain PSG, Dubinsky EA, Fortney JL, et al. (2012). Metagenome, metatranscriptome and single-cell sequencing reveal microbial response to Deepwater Horizon oil spill. ISME J 6: 1715–1727.

Mayali X, Stewart B, Mabery S, Weber PK. (2015). Temporal succession in carbon incorporation from macromolecules by particle-attached bacteria in marine microcosms. Environ Microbiol Rep 8: 68–75.

Mayor DJ, Sanders R, Giering SLC, Anderson TR. (2014). Microbial gardening in the ocean's twilight zone: Detritivorous metazoans benefit from fragmenting, rather than ingesting, sinking detritus: Fragmentation of refractory detritus by zooplankton beneath the euphotic zone stimulates the harvestable production. Bioessays 1132–1137.

McCarren J, Becker JW, Repeta DJ, Shi Y, Young CR, Malmstrom RR, et al. (2010). Microbial community transcriptomes reveal microbes and metabolic pathways associated with dissolved organic matter turnover in the sea. Proc Natl Acad Sci U S A 107: 16420–7.

McCarthy JJ. (1972). The uptake of urea by natural populations of marine phytoplankton. Limnol Oceanogr 17: 738–748.

McDonnell AMP, Boyd PW, Buesseler KO. (2015a). Effects of sinking velocities and microbial respiration rates on the attenuation of particulate carbon fluxes through the mesopelagic zone. Global Biogeochem Cycles 29: 175–193.

McDonnell AMP, Lam PJ, Lamborg CH, Buesseler KO, Sanders R, Riley JS, et al. (2015b). The oceanographic toolbox for the collection of sinking and suspended marine particles. Prog Oceanogr 133: 17–31.

Meier D V, Pjevac P, Bach W, Hourdez S, Girguis PR, Vidoudez C, et al. (2017). Niche partitioning of diverse sulfur-oxidizing bacteria at hydrothermal vents. ISME J 11: 1545–1558.

Mestre M, Borrull E, Sala Mm, Gasol JM. (2017). Patterns of bacterial diversity in the marine planktonic particulate matter continuum. ISME J 1–12.

Meyer F, Paarmann D, D'Souza M, Olson R, Glass E, Kubal M, et al. (2008). The metagenomics RAST server – a public resource for the automatic phylogenetic and functional analysis of metagenomes. BMC Bioinformatics 9: 386.

Milici M, Deng Z-L, Tomasch J, Decelle J, Wos-Oxley ML, Wang H, et al. (2016). Co-occurrence analysis of microbial taxa in the Atlantic Ocean reveals high connectivity in the free-living bacterioplankton. Front Microbiol 7: 1–20.

Monier A, Larsen JB, Sandaa RA, Bratbak G, Claverie JM, Ogata H. (2008). Marine *Mimivirus* relatives are probably large algal viruses. Virol J 5: 1–8.

Moran MA, Kujawinski EB, Stubbins A, Fatland R, Aluwihare LI, Buchan A, et al. (2016). Deciphering ocean carbon in a changing world. Proc Natl Acad Sci 113: 3143–3151.

Nakagawa S, Takai K. (2008). Deep-sea vent chemoautotrophs: Diversity, biochemistry and ecological significance. FEMS Microbiol Ecol 65: 1–14.

Needham DM, Sachdeva R, Fuhrman JA. (2017). Ecological dynamics and co-occurrence among marine phytoplankton, bacteria and myoviruses shows microdiversity matters. ISME J 11: 1614–1629.

Norton JM, Alzerreca JJ, Suwa Y, Klotz MG. (2002). Diversity of ammonia monooxygenase operon in autotrophic ammonia-oxidizing bacteria. Arch Microbiol 177: 139–149.

Not F, Gausling R, Azam F, Heidelberg JF, Worden AZ. (2007). Vertical distribution of picoeukaryotic diversity in the Sargasso Sea. Environ Microbiol 9: 1233–1252.

Oren A, Mana L, Jehlicka J. (2015). Probing single cells of purple sulfur bacteria with Raman spectroscopy: carotenoids and elemental sulfur. FEMS Microbiol Lett 1–13.

Orsi W, Song YC, Hallam S, Edgcomb V. (2012). Effect of oxygen minimum zone formation on communities of marine protists. ISME J 6: 1586–1601.

Orsi WD, Smith JM, Wilcox HM, Swalwell JE, Carini P, Worden AZ, et al. (2015). Ecophysiology of uncultivated marine euryarchaea is linked to particulate organic matter. ISME J 1–17.

Overbeek R, Olson R, Pusch GD, Olsen GJ, Davis JJ, Disz T, et al. (2014). The SEED and the Rapid Annotation of microbial genomes using Subsystems Technology (RAST). Nucleic Acids Res 42: 206–214.

Padilla CC, Ganesh S, Gantt S, Huhman A, Parris DJ, Sarode N, et al. (2015). Standard filtration practices may significantly distort planktonic microbial diversity estimates. Front Microbiol 6: 1–10.

Painter SC, Lucas MI, Stinchcombe MC, Bibby TS, Poulton AJ. (2010). Summertime trends in pelagic biogeochemistry at the Porcupine Abyssal Plain study site in the northeast Atlantic. Deep Res Part II Top Stud Oceanogr 57: 1313–1323.

Parris DJ, Ganesh S, Edgcomb VP, DeLong EF, Stewart FJ. (2014). Microbial eukaryote diversity in the marine oxygen minimum zone off northern Chile. Front Microbiol 5: 1–11.

Passow U, Carlson CA. (2012). The biological pump in a high CO_2 world. Mar Ecol Prog Ser 470: 249–271.

Passow U, Shipe RF, Murray A, Pak DK, Brzezinski MA, Alldredge AL. (2001). The origin of transparent exopolymer particles (TEP) and their role in the sedimentation of particulate matter. Cont Shelf Res 21: 327–346.

Pelve EA, Fontanez KM, DeLong EF. (2017). Bacterial succession on sinking particles in the ocean's interior. Front Microbiol 8: 1–15.

Pernice MC, Forn I, Gomes A, Lara E, Alonso-Sáez L, Arrieta JM, et al. (2014). Global abundance of planktonic heterotrophic protists in the deep ocean. ISME J 9: 782–792.

Pernice MC, Giner CR, Logares R, Perera-Bel J, Acinas SG, Duarte CM, et al. (2015). Large variability of bathypelagic microbial eukaryotic communities across the world's oceans. ISME J 945–958.

Pernthaler J. (2005). Predation on prokaryotes in the water column and its ecological implications. Nat Rev Microbiol 3: 537.

Philips S, Laanbroek HJ, Verstraete W. (2002). Origin, causes and effects of increased nitrite concentrations in aquatic environments. Rev Environ Sci Bio/Technology 1: 115–141.

Pinhassi J, Berman T. (2003). Differential growth response of colony-forming alpha- and gamma-proteobacteria in dilution culture and nutrient addition experiments from Lake Kinneret (Israel), the eastern Mediterranean Sea, and the Gulf of Eilat. Appl Environ Microbiol 69: 199–211.

Pinhassi J, Havskum H, Peters F, Malits A. (2004). Changes in Bacterioplankton Composition under Different Phytoplankton Regimens. Appl Environ Microbiol 70: 6753–6766.

Ploug H, Grossart H-P. (2000). Bacterial growth and grazing on diatom aggregates: Respiratory carbon turnover as a function of aggregate size and sinking velocity. Limnol Oceanogr 45: 1467–1475.

Ploug H, Grossart H-P, Azam F, Jorgensen BB. (1999). Photosynthesis, respiration, and carbon turnover in sinking marine snow from surface waters of Southern California Bight: implications for the carbon cycle in the ocean. Mar Ecol Prog Ser 179: 1–11.

Ploug H, Iversen MH, Fischer G. (2008). Ballast, sinking velocity, and apparent diffusivity within marine snow and zooplankton fecal pellets: Implications for substrate turnover by attached bacteria. Limnol Oceanogr 53: 1878–1886.

Polz MF, Hunt DE, Preheim SP, Weinreich DM. (2006). Patterns and mechanisms of genetic and phenotypic differentiation in marine microbes. Philos Trans R Soc B Biol Sci 361: 2009–2021.

Pomeroy LR. (1974). The ocean's food web, a changing paradigm. Bioscience 24: 499–504.

Pomeroy LR, Wiebe WJ. (1988). Energetics of microbial food webs. Hydrobiologia 159: 7–18.

Poulsen LK, Iversen MH. (2008). Degradation of copepod fecal pellets: Key role of protozooplankton. Mar Ecol Prog Ser 367: 1–13.

Poulton REK, Whitehouse MJ, Gordon M, Ward P, A.J. (2010). Summer microplankton community structure across the Scotia Sea: implications for biological carbon export. Biogeosciences 7: 343–346.

Quast C, Pruesse E, Yilmaz P, Gerken J, Schweer T, Yarza P, et al. (2013). The SILVA ribosomal RNA gene database project: Improved data processing and web-based tools. Nucleic Acids Res 41: 590–596.

Raoult D. (2004). The 1.2-megabase genome sequence of *Mimivirus*. Science (80-) 306: 1344–1350.

Reinfelder JR. (2011). Carbon concentrating mechanisms in eukaryotic marine phytoplankton. Ann Rev Mar Sci 3: 291–315.

Reinthaler T, van Aken H, Veth C, Arístegui J, Robinson C, Williams PJ le B, et al. (2006). Prokaryotic respiration and production in the meso- and bathypelagic realm of the eastern and western North Atlantic basin. Limnol Oceanogr 51: 1262–1273.

Reintjes G, Arnosti C, Fuchs BM, Amann R. (2017). An alternative polysaccharide uptake mechanism of marine bacteria. ISME J 11: 1640–1650.

Reisch CR, Moran MA, Whitman WB. (2011). Bacterial catabolism of dimethylsulfoniopropionate (DMSP). Front Microbiol 2: 1–12.

Rembauville M, Manno C, Tarling GA, Blain S, Salter I. (2016). Strong contribution of diatom resting spores to deep-sea carbon transfer in naturally iron-fertilized waters downstream of South Georgia. Deep Sea Res Part I Oceanogr Res Pap 115: 22–35.

Repeta DJ, Gagosian RB. (1984). Transformation reactions and recycling of carotenoids and chlorins in the Peru upwelling region (15°S, 75°W). Geochim Cosmochim Acta 48: 1265–1277.

Rhodes CJ, Martin AP. (2010). The influence of viral infection on a plankton ecosystem undergoing nutrient enrichment. J Theor Biol 265: 225–237.

Van Rijssel M, Janse I, Noordkamp DJB, Gieskes WWC. (2000). An inventory of factors that affect polysaccharide production by *Phaeocystis globosa*. J Sea Res 43: 297–306.

Riley JS, Sanders R, Marsay C, Le Moigne FAC, Achterberg EP, Poulton AJ. (2012). The relative contribution of fast and slow sinking particles to ocean carbon export. Global Biogeochem Cycles 26: 1–10.

Rodríguez-Marconi S, De La Iglesia R, Díez B, Fonseca CA, Hajdu E, Trefault N, et al. (2015). Characterization of bacterial, archaeal and eukaryote symbionts from Antarctic sponges reveals a high diversity at a three-domain level and a particular signature for this ecosystem. PLoS One 10: 1–19.

Ryther JH. (1969). Photosynthesis and fish production in the sea. The production of organic matter and its conversion to higher forms of life vary throughout the world ocean. Science (80-) 166: 72–76.

Sabine CL, Feely RA, Gruber N, Key RM, Lee K, Bullister JL, et al. (2004). The oceanic sink for anthropogenic CO_2. Science (80-) 305: 367–371.

Salazar G, Cornejo-Castillo FM, Benítez-Barrios V, Fraile-Nuez E, Álvarez-Salgado XA, Duarte CM, et al. (2016). Global diversity and biogeography of deep-sea pelagic prokaryotes. ISME J 10: 596–608.

Santos AA, Venceslau SS, Grein F, Leavitt WD, Dahl C, Johnston DT, et al. (2015). A protein trisulfide couples dissimilatory sulfate reduction to energy conservation. Science (80-) 350: 1541–1545.

Sarmiento JL, Dunne J, Gnanadesikan A, Key RM, Matsumoto K, Slater R. (2002). A new estimate of the $CaCO_3$ to organic carbon export ratio. Global Biogeochem Cycles 16: 54-1-54–12.

Sarmiento JL, Gruber N. (2006). Introduction. In: Sarmiento JL, Gruber N (eds). Ocean Biogeochemical Dynamics. Princeton University Press, pp 1–18.

Satinsky BM, Crump BC, Smith CB, Sharma S, Zielinski BL, Doherty M, et al. (2014). Microspatial gene expression patterns in the Amazon River Plume. Proc Natl Acad Sci 111: 11085–90.

Schmoker C, Hernández-León S, Calbet A. (2013). Microzooplankton grazing in the oceans: Impacts, data variability, knowledge gaps and future directions. J Plankton Res 35: 691–706.

Sedwick PN, Ditullio GR. (1997). Regulation of algal blooms in Antarctic shelf waters by the release of iron from melting sea ice. Geophys Res Lett 24: 2515–2518.

Seiler C, van Velzen E, Neu TR, Gaedke U, Berendonk TU, Weitere M. (2017). Grazing resistance of bacterial biofilms: a matter of predators' feeding trait. FEMS Microbiol Ecol 93: 1–9.

Seitz KW, Lazar CS, Hinrichs K-U, Teske AP, Baker BJ. (2016). Genomic reconstruction of a novel, deeply branched sediment archaeal phylum with pathways for acetogenesis and sulfur reduction. ISME J 1–10.

Servinsky MD, Terrell JL, Tsao C-Y, Wu H-C, Quan DN, Zargar A, et al. (2015). Directed assembly of a bacterial quorum. ISME J 10: 1–12.

Shanks AL, Trent JD. (1979). Marine snow: Microscale nutrient patches. Limnol Oceanogr 24: 850–854.

Shanks AL, Trent JD. (1980). Marine snow: Sinking rates and potential role in vertical flux. Deep Res Part a-Oceanographic Res Pap 27: 137–143.

Sheik AR, Brussaard CPD, Lavik G, Lam P, Musat N, Krupke A, et al. (2014). Responses of the coastal bacterial community to viral infection of the algae *Phaeocystis globosa*. ISME J 8: 212–25.

Sheridan CC, Lee C, Wakeham SG, Bishop JKB. (2002). Suspended particle organic composition and cycling in surface and midwaters of the equatorial Pacific Ocean. Deep Res Part I Oceanogr Res Pap 49: 1983–2008.

Sherr EB, Sherr BF. (2007). Heterotrophic dinoflagellates: A significant component of microzooplankton biomass and major grazers of diatoms in the sea. Mar Ecol Prog Ser 352: 187–197.

Sherr EB, Sherr BF. (2002). Significance of predation by protsts. Antonie Van Leeuwenhoek 81: 293–308.

Shi L, Huang Y, Zhang M, Shi X, Cai Y, Gao S, et al. (2018). Large buoyant particles dominated by cyanobacterial colonies harbor distinct bacterial communities from small suspended particles and free-living bacteria in the water column. Microbiologyopen e00608.

Siegenthaler U, Sarmiento JL. (1993). Atmospheric carbon dioxide and the ocean. Nature 365: 119–125.

Simon HM, Smith MW, Herfort L. (2014). Metagenomic insights into particles and their associated microbiota in a coastal margin ecosystem. Front Microbiol 5: 1–10.

Simon J, Gross R, Einsle O, Kroneck PMH, Kröger A, Klimmek O. (2000). A *NapC/NirT*-type cytochrome *c* (*NrfH*) is the mediator between the quinone pool and the cytochrome *c* nitrite reductase of Wolinella succinogenes. Mol Microbiol 35: 686–696.

Simon M, Grossart HP, Schweitzer B, Ploug H. (2002). Microbial ecology of organic aggregates in aquatic ecosystems. Aquat Microb Ecol 28: 175–211.

Smith DC, Simon M, Alldredge AL, Azam F. (1992). Intense hydrolytic enzyme activity on marine aggregates and implications for rapid particle dissolution. Nature 359: 139–142.

Smith JM, Chavez FP, Francis CA. (2014). Ammonium uptake by phytoplankton regulates nitrification in the sunlit ocean. PLoS One 9: e108173.

Smith MW, Allen LZ, Allen AE, Herfort L, Simon HM. (2013). Contrasting genomic properties of free-living and particle-attached microbial assemblages within a coastal ecosystem. Front Microbiol 4: 1–20.

Smith WO, Shields AR, Dreyer JC, Peloquin JA, Asper V. (2011). Interannual variability in vertical export in the Ross Sea: Magnitude, composition, and environmental correlates. Deep Res Part I Oceanogr Res Pap 58: 147–159.

Smythe-Wright D, Boswell S, Kim YN, Kemp A. (2010). Spatio-temporal changes in the distribution of phytopigments and phytoplanktonic groups at the Porcupine Abyssal Plain (PAP) site. Deep Res Part II Top Stud Oceanogr 57: 1324–1335.

Sogin ML, Morrison HG, Huber JA, Welch DM, Huse SM, Neal PR, et al. (2006). Microbial diversity in the deep sea and the underexplored 'rare biosphere'. Proc Natl Acad Sci 103: 12115–12120.

Sperling M, Piontek J, Engel A, Wiltshire KH, Niggemann J, Gerdts G, et al. (2017). Combined carbohydrates support rich communities of particle-associated marine bacterioplankton. Front Microbiol 8: 1–14.

Stahl DA, de la Torre JR. (2012). Physiology and diversity of ammonia-oxidizing archaea. Annu Rev Microbiol 66: 83–101.

Stamieszkin K, Poulton N, Pershing A. (2017). Zooplankton grazing and egestion shifts particle size distribution in natural communities. Mar Ecol Prog Ser 575: 43–56.

Steen AD, Ziervogel K, Arnosti C. (2010). Comparison of multivariate microbial datasets with the Shannon index: An example using enzyme activity from diverse marine environments. Org Geochem 41: 1019–1021.

Steinberg DK, Carlson CA, Bates NR, Goldthwait SA, Madin LP, Michaels AF. (2000). Zooplankton vertical migration and the active transport of dissolved organic and inorganic carbon in the Sargasso Sea. Deep Res Part I Oceanogr Res Pap 47: 137–158.

Steinberg DK, Landry MR. (2017). Zooplankton and the ocean carbon cycle. Ann Rev Mar Sci 9: 413–444.

Steinberg DK, Van Mooy B a. S, Buesseler KO, Boyd PW, Kobari T, Karl DM. (2008). Bacterial vs. zooplankton control of sinking particle flux in the ocean's twilight zone. Limnol Oceanogr 53: 1327–1338.

Stemmann L, Boss E. (2012). Plankton and particle size and packaging: From determining optical properties to driving the biological pump. Ann Rev Mar Sci 4: 263–290.

Stewart FJ, Dalsgaard T, Young CR, Thamdrup B, Revsbech NP, Ulloa O, et al. (2012). Experimental incubations elicit profound changes in community transcription in OMZ bacterioplankton. PLoS One 7: e37118.

Stocker R, Seymour JR, Samadani A, Hunt DE, Polz MF. (2008). Rapid chemotactic response enables marine bacteria to exploit ephemeral microscale nutrient patches. Proc Natl Acad Sci U S A 105: 4209–4214.

Stoecker DK, Hansen PJ, Caron DA, Mitra A. (2017). Mixotrophy in the marine plankton. Ann Rev Mar Sci 9: 311–335.

Strom SL, Benner R, Ziegler S, Dagg MJ. (1997). Planktonic grazers are a potentially important source of marine dissolved organic carbon. Linmol Ocean 42: 1364–1374.

Suter EA, Pachiadaki M, Taylor GT, Astor Y, Edgcomb VP. (2018). Free-living chemoautotrophic and particle-attached heterotrophic prokaryotes dominate microbial assemblages along a pelagic redox gradient. Environ Microbiol 20: 693–712.

Suttle CA. (1994). The significance of viruses to mortality in aquatic microbial communities. Microb Ecol 28: 237–243.

Suttle CA. (2005). Viruses in the sea. Nature 437: 356–361.

Suttle C a. (2007). Marine viruses - major players in the global ecosystem. Nat Rev Microbiol 5: 801–812.

Swan BK, Martinez-Garcia M, Preston CM, Sczyrba A, Woyke T, Lamy D, et al. (2011). Potential for chemolithoautotrophy among ubiquitous bacteria lineages in the dark ocean. Science 333: 1296–1300.

Swanberg NR, Caron DA. (1991). Patterns of sarcodine feeding in epipelagic oceanic plankton. J Plankton Res 13: 287–312.

Takahashi S, Tomita J, Nishioka K, Hisada T, Nishijima M. (2014). Development of a prokaryotic universal primer for simultaneous analysis of *Bacteria* and *Archaea* using next-generation sequencing. PLoS One 9: e105592.

Tang K, Jiao N, Liu K, Zhang Y, Li S. (2012). Distribution and functions of *tonb*-dependent transporters in marine bacteria and environments: Implications for dissolved organic matter utilization. PLoS One 7. e-pub ahead of print, doi: 10.1371/journal.pone.0041204.

Taylor BW, Keep CF, Hall RO, Koch BJ, Tronstad LM, Flecker AS, et al. (2007). Improving the fluorometric ammonium method: matrix effects, background fluorescence, and standard additions. J North Am Benthol Soc 26: 167–177.

Taylor GT. (1982). The role of pelagic heterotrophic protozoa in nutrient recycling: a review. Ann Inst Oceanogr 58: 227–241.

Taylor GT, Sullivan CW. (2008). Vitamin B_{12} and cobalt cycling among diatoms and bacteria in Antarctic sea ice microbial communities. Limnol Oceanogr 53: 1862–1877.

Teeling H, Fuchs BM, Becher D, Klockow C, Gardebrecht A, Bennke CM, et al. (2012). Substrate-controlled succession of marine bacterioplankton populations induced by a phytoplankton bloom. Science (80-) 336: 608–611.

Thiele S, Fuchs BM, Amann R, Iversen MH. (2015). Colonization in the photic zone and subsequent changes during sinking determine bacterial community composition in marine snow. Appl Environ Microbiol 81: 1463–1471.

Thomas T, Evans FF, Schleheck D, Mai-Prochnow A, Burke C, Penesyan A, et al. (2008). Analysis of the *Pseudoalteromonas tunicata* genome reveals properties of a surface-associated life style in the marine environment. PLoS One 3: 1–11.

Thomsen H a., Buck KR, Bolt P a., Garrison DL. (1991). Fine structure and biology of *Cryothecomonas* gen. nov. (Protista incertae sedis) from the ice biota. Can J Zool 69: 1048–1070.

Tréguer P, Bowler C, Moriceau B, Dutkiewicz S, Gehlen M, Aumont O, et al. (2018). Influence of diatom diversity on the ocean biological carbon pump. Nat Geosci 11: 27–37.

Turner JT. (2015). Zooplankton fecal pellets, marine snow, phytodetritus and the ocean's biological pump. Prog Oceanogr 130: 205–248.

Valladares A, Montesinos ML, Herrero A, Flores E. (2002). An ABC-type, high-affinity urea permease identified in cyanobacteria. Mol Microbiol 43: 703–715.

de Vargas C, Audic S, Henry N, Decelle J, Mahé F, Logares R, et al. (2015). Ocean plankton. Eukaryotic plankton diversity in the sunlit ocean. Science 348: 1261605.

Verdugo P, Alldredge AL, Azam F, Kirchman DL, Passow U, Santschi PH. (2004). The oceanic gel phase: A bridge in the DOM-POM continuum. Mar Chem 92: 67–85.

Volk T, Hoffert MI. (1985). Ocean carbon pumps: Analysis of relative strengths and efficiencies in ocean-driven atmospheric CO_2 changes. In: Vol. 32. Geophysical Monograph Se. pp 99–110.

Wakeham SG, Canuel E a. (1988). Organic geochemistry of particulate matter in the eastern tropical North Pacific Ocean: Implications for particle dynamics. J Mar Res 46: 183–213.

Wakeham SG, Lee C. (1989). Organic geochemistry of particulate matter in the ocean: The role of particles in oceanic sedimentary cycles. Org Geochem 14: 83–96.

Wakeham SG, Lee C, Peterson ML, Liu Z, Szlosek J, Putnam IF, et al. (2009). Organic biomarkers in the twilight zone - Time series and settling velocity sediment traps during MedFlux. Deep Sea Res Part II Top Stud Oceanogr 56: 1437–1453.

Walker BD, Beaupré SR, Guilderson TP, McCarthy MD, Druffel ERM. (2016). Pacific carbon cycling constrained by organic matter size, age and composition relationships. Nat Geosci 9: 888–891.

Walsh D a, Zaikova E, Howes CG, Song YC, Wright JJ, Tringe SG, et al. (2009). Metagenome of a versatile chemolithoautotroph from expanding oceanic dead zones. Science 326: 578–582.

Ward BB. (2008). Nitrification in marine systems. In: Nitrogen in the marine environment. Elsevier, pp 199–261.

Wasmund K, Mußmann M, Loy A. (2017). The life sulfuric: Microbial ecology of sulfur cycling in marine sediments. Environ Microbiol Rep 1–44.

Weinbauer MG, Chen F, Wilhelm SW. (2011). Virus-mediated redistribution and partitioning of carbon in the global oceans. Microb Carbon Pump Ocean 54–56.

Wells ML, Goldberg ED. (1994). The distribution of colloids in the North Atlantic and Southern Oceans. Limnol Oceanogr 39: 286–302.

Westreich ST, Korf I, Mills DA, Lemay DG. (2016). SAMSA: A comprehensive metatranscriptome analysis pipeline. BMC Bioinformatics 17: 1–12.

Whitehead NA, Barnard AML, Slater H, Simpson NJL, Salmond GPC. (2001). Quorum-sensing in Gram-negative bacteria. FEMS Microbiol Rev 25: 365–404.

Wilke A, Bischof J, Gerlach W, Glass E, Harrison T, Keegan KP, et al. (2016). The MG-RAST metagenomics database and portal in 2015. Nucleic Acids Res 44: D590–D594.

Williams TJ, Wilkins D, Long E, Evans F, Demaere MZ, Raftery MJ, et al. (2013). The role of planktonic Flavobacteria in processing algal organic matter in coastal East Antarctica revealed using metagenomics and metaproteomics. Environ Microbiol 15: 1302–1317.

Woebken D, Fuchs BM, Kuypers MMM, Amann R. (2007). Potential interactions of particle-associated anammox bacteria with bacterial and archaeal partners in the Namibian upwelling system. Appl Environ Microbiol 73: 4648–4657.

Worden AZ, Follows MJ, Giovannoni SJ, Wilken S, Zimmerman AE, Keeling PJ. (2015). Rethinking the marine carbon cycle: Factoring in the multifarious lifestyles of microbes. Science (80-) 347: 1257594–1257594.

Wright JJ, Konwar KM, Hallam SJ. (2012). Microbial ecology of expanding oxygen minimum zones. Nat Rev Microbiol 10: 381–394.

Xia Y, Lü C, Hou N, Xin Y, Liu J, Liu H, et al. (2017). Sulfide production and oxidation by heterotrophic bacteria under aerobic conditions. ISME J 1–13.

Yamada Y, Fukuda H, Tada Y, Kogure K, Nagata T. (2016). Bacterial enhancement of gel particle coagulation in seawater. Aquat Microb Ecol 77: 11–22.

Yawata Y, Cordero OX, Menolascina F, Hehemann J-H, Polz MF, Stocker R. (2014). Competition-dispersal tradeoff ecologically differentiates recently speciated marine bacterioplankton populations. Proc Natl Acad Sci U S A 111: 5622–7.

Yawata Y, Nguyen J, Stocker R, Rusconi R. (2016). Microfluidic studies of biofilm formation in dynamic environments. J Bacteriol JB.00118-16.

Yoch DC. (2002). Dimethylsulfoniopropionate: Its sources, role in the marine food web, and biological degradation to dimethylsulfide. Appl Environ Microbiol 68: 5804–5815.

Yung C, Ward CS, Davis KM, Johnson ZI, Hunt DE. (2016). Insensitivity of diverse and temporally variable particle-associated microbial communities to bulk seawater environmental parameters. Appl Environ Microbiol 82: 3431–3437.

Zehr JP, Kudela RM. (2011). Nitrogen cycle of the open ocean: from genes to ecosystems. Ann Rev Mar Sci 3: 197–225.

Zehr JP, Ward BB. (2002). Nitrogen cycling in the ocean: New perspectives on processes and paradigms. Appl Environ Microbiol 68: 1015–1024.

Zhang CL, Xie W, Martin-Cuadrado AB, Rodriguez-Valera F. (2015). Marine Group II Archaea, potentially important players in the global ocean carbon cycle. Front Microbiol 6. e-pub ahead of print, doi: 10.3389/fmicb.2015.01108.

Ziervogel K, Arnosti C. (2008). Polysaccharide hydrolysis in aggregates and free enzyme activity in aggregate-free seawater from the North-Eastern Gulf of Mexico. Environ Microbiol 10: 289–299.

Ziervogel K, Steen AD, Arnosti C. (2010). Changes in the spectrum and rates of extracellular enzyme activities in seawater following aggregate formation. Biogeosciences 7: 1007–1015.

Zoccarato L, Pallavicini A, Cerino F, Fonda Umani S, Celussi M. (2016). Water mass dynamics shape Ross Sea protist communities in mesopelagic and bathypelagic layers. Prog Oceanogr 149: 16–26.

Zumft WG. (1997). Cell biology and molecular basis of denitrification. Microbiol Mol Biol Rev 61: 533–616.